

https://dspace.org/

Open-cast mine slope deformation and failure mechanisms interpreted from slope radar monitoring

Osasan, Kayode Stephen

2013-07-22
http://hdl.handle.net/10539/12867

Downloaded from a DSpace repository. https://dspace.org/

OPEN-CAST MINE SLOPE DEFORMATION AND FAILURE MECHANISMS INTERPRETED FROM SLOPE RADAR MONITORING

Kayode Stephen Osasan

Doctor of Philosophy

A thesis submitted to the Faculty of Engineering and the Built Environment, University of the Witwatersrand, Johannesburg, in fulfilment of the requirements for the degree of Doctor of Philosophy.

Johannesburg, 2012

DECLARATION

I declare that this thesis is my own work. It is being submitted for the Degree of Doctor of Philosophy at the University of the Witwatersrand, Johannesburg. It has not been submitted before for any other degree or examination at any other University

_____

October, 2012

ABSTRACT

The monitoring of open-pit mine slopes using radar systems is becoming more and more common. The output from radar monitoring is the displacement of the full slope surface after each radar scan, allowing displacements, velocities and acceleration to be determined. The displacement trends obtained from radar monitoring are a representation of the deformation taking place within the mine slope. The research deals with the analysis of the displacement trends in order to understand the slope deformation behaviour. The main objectives of this research work were:

- To interpret the deformation behaviour and failure mechanisms of open-cast mine slopes based primarily on displacement data from radar monitoring; and
- To develop a method using the radar displacement data for predicting the time to failure of open-cast mine slopes.

The research established that slope failure is preceded by the gradual accumulation of deformation within the slope. Identifying where the deformation is taking place, the magnitudes and state of the deformation is crucial in understanding and interpreting the slope deformation and failure mechanisms. The main accomplishments of the research include:

- The interpretation of deformation and failure mechanisms from radar displacement data of both stable and unstable open-cast mine slopes. The interpretation of deformation was used in classifying the deformation behaviour of unstable open-cast mine slopes into five main stages, consisting of three pre-failure stages and two post-failure stages. From the displacement data, two types of deformation behaviour of stable slopes were also identified;
- The development of a simple model for estimating the threshold values for the cumulative rate of displacement. The cumulative rate of displacement threshold determines when mine personnel and equipment must evacuate the unstable area of the slope. The model can also be used to effectively identify the deformation state of open-cast mine slopes; and
- The development of a Slope Failure Prediction Model (SFPM) for estimating the time to failure of open-cast mine slopes. The model was effective in predicting the time to failure when validated with four case examples of open cast mine slope failures. The development of the SFPM is a novel approach which provides an automated prediction of time to failure.

To my lovely and wonderful wife, Oluwakemi Osasan, and my amazing children, Anjola and Darasimi Osasan

ACKNOWLEDGEMENTS

I return all glory to the almighty God, the Alpha and Omega for His benevolence, divine grace and wisdom granted unto me to successfully complete this research work. I appreciate His protection during my numerous trips in course of conducting this study.

I acknowledge my family and my in-laws for their unwavering love, support and understanding in all seasons. I especially appreciate my wonderful wife, Oluwakemi Osasan for her love, care of the children and tremendous encouragement, specifically in the course of my study and in my life in general. Special recognition goes to my lovely daughters, Anjola and Darasimi Osasan for the pains they endured while I was away studying.

To my supervisor, Professor T. R. Stacey, I am grateful for your kindness and fatherly support. Your technical expertise, guidance and the time taken to painstakingly read this thesis are priceless. I equally recognise the contributions of the other members of staff of the School of Mining Engineering, University of the Witwatersrand for their love and support.

I am grateful for the support that I received from members of staff of Anglo Coal Kleinkopje Colliery, South Africa. The following members of staff deserve special mention: Mr. Gift Makusha, Mr. Godfrey Mottie and Mr. Meaker. For the technical support given by members of staff of Reutech, South Africa, a big thank you goes to Mr. Jan de Beer, Mr. Emile Rossouw, Mr. Jaco and Mr. A. Joubert. I also recognise the assistance of Mr. Thapelo Agus in the development of the prediction model.

Finally, the Centennial Trust Fund in the School of Mining Engineering, University of the Witwatersrand was tremendously helpful in bearing the financial burden involved in conducting this research.

TABLE OF CONTENTS

DECLARATION ii
ABSTRACT iii
ACKNOWLEDGEMENTS v
TABLE OF CONTENTS vi
LIST OF FIGURES xiii
ABBREVIATIONS xx
LIST OF SYMBOLS xxii
CHAPTER ONE 1
INTRODUCTION 1
1.1. Background to the Research 1
1.2. Problem Statement 2
1.3. Research Questions 3
1.4. Aims and Objectives of the Research 3
1.5. Research Approach and Thesis Structure 4
1.6. Limitations of the Research 5
CHAPTER TWO 7
REVIEW OF ROCK SLOPE DEFORMATION PROCESSES 7
2.1. Introduction 7
2.2. Surface Mine 7
2.3. Rock Deformation 9
2.3.1. Definitions 10
2.4. Causes of Slope Failure/Slope Failure Triggers 13
2.5. Modes and Mechanisms of Slope Failure in Rock Mass 14
2.5.1. Plane Failure 15
2.5.2. Rotational/Circular Failure 16
2.5.3. Wedge Failure 18
2.5.4. Toppling Failure 19

2.6. Complex Failure Mechanism 24
2.7. Deformation and Displacement Behaviour of Surface Mine Slope with Time 26
2.7.1. Initial Response 27
2.7.2. Regressive Failure/ Progressive Failure 27
2.8. Post Collapse and Post Mining Behaviour Mode (Stage 4 and 5) 30
2.9. Long Term Horizontal and Vertical (Downwards) Creep Deformation (Relaxation) Resulting from Excavation: 31
2.11. Slope Movement (Velocity) Scale 32
2.12. Summary 32
CHAPTER THREE 33
MONITORING SLOPE STABILITY 33
3.1 Introduction 33
3.2 Slope Monitoring Steps 34
3.3 Slope Monitoring System 35
3.4. Visual Monitoring 36
3.5. Surface Measurement 37
3.5.1. Survey Network 37
3.5.2. Tension Crack Mapping 38
3.5.3 Global Positioning System (GPS) 39
3.6 Subsurface Measurement 39
3.6.1 Piezometers 39
3.6.2. Inclinometers 39
3.6.3 Seismic Monitoring 41
3.7. Remote Monitoring Technologies 42
3.7.1. Time Domain Reflectometry (TDR) 42
3.7.2. Laser Scanner 43
3.8. Radar 44
3.8.1. Introduction 44

3.8.2. Basic Operation of Radar 45
3.8.3. Types of Radar....45
3.8.4. Synthetic Aperture Radar 45
3.8.5. Slope Stability Radar (SSR) 46
3.8.6. Movement and Surveying Radar (MSR)....49
3.8.7. IBIS-M Slope Monitoring Radar....52
3.9. Conventional Slope Monitoring versus Radar Monitoring....53
3.10. Summary 54
CHAPTER FOUR....58
OPEN-CAST COAL MINE USED FOR CASE STUDIES....58
4.1. Introduction....58
4.2. Organisation of the Chapter 59
4.3. Kleinkopje Open-Cast Mine....59
4.3.1. Introduction 59
4.3.2. Geology of the Mine Area....60
4.3.3. Mine Groundwater....63
4.3.4. Mine Slope Stability Problems....64
4.3.4.1. Bord and Pillar Collapse....65
4.3.4.2 Spontaneous Combustion 65
4.3.4.3. Low-Wall (Spoil) Failure 66
4.3.4.4. High-Wall Failure....66
4.3.5. Mine Slope Displacement Monitoring 67
4.3.6. Kleinkopje Open-Cast Mine Slope Failure Case Study 67
4.4. Landau Open-Cast Coal Mine....68
4.4.1. Introduction 68
4.4.2. Geology of the Mine Area....70
4.4.2.1. Introduction 70
4.4.2.2. Kromdraai Open-cast Mine 73

4.4.2.3. Mine Groundwater....74
4.4.2.4. Schoongezicht/ Umlalazi (Navigation) Open-cast....74
4.4.2.5. Mine Groundwater....75
4.4.2.6. Mine Slope Stability Problems at Landau Open-Cast Mine....75
4.4.2.7. High-wall Failure....75
4.4.2.8. Low-wall (spoil) Failure....76
4.4.2.9. Spontaneous Combustion....76
4.4.2.10. Bord and Pillar Collapse....76
4.4.2.11. Mine Slope Displacement Monitoring at Landau....77
4.4.2.12. Landau Open Cast Mine Case Study....77
4.5. New Vaal Open-Cast Coal Mine....78
4.5.1. Introduction....78
4.5.2. Geology of the mine area....79
4.5.3. Geological structures....81
4.5.4. Mine Groundwater....82
4.5.5. Mine Slope Stability Problems at New Vaal....83
4.5.5.1. Soft Overburden and Spoils (Low-wall) Failure....83
4.5.5.2. High-wall Failure....84
4.5.5.3. Bord and Pillar Collapse....84
4.5.5.4. Spontaneous Combustion....85
4.5.6. Mine Slope Displacement Monitoring....85
4.5.7. New Vaal Open Cast Mine Case Studies....85
4.5.7.1. Case Study 1....85
4.5.7.3. Case Study 2....87
4.5.7.5. Case Study 3....89
4.6. Summary....90
CHAPTER FIVE....91
DEFORMATION BEHAVIOUR OF MINE SLOPES CASE STUDIES....91

5.1. MSR and Deformation Behaviour Terminology 91
5.2. Deformation Behaviour of Stable Slopes 93
5.3. Deformation Behaviour of Unstable Slopes 95
5.3.1. Case Example 1 (High-wall Failure) 95
5.3.1.1. Locating the Area of Failure 96
5.3.1.2. Description of Case Example 1 Slope Failure 97
5.3.2. Case Example 2 (Ramp 0 Low-Wall Failure) 103
5.3.2.1. Locating the Area of Failure 103
5.3.2.2. Description of Ramp 0 Slope Failure 104
5.3.3. Case Example 3 (Ramp 5 High-wall Failure) 107
5.3.3.1. Locating the Area of failure 108
5.3.3.2. Description of Ramp 5 Failure 109
5.3.4. Case Example 4 (Ramp 11 High-wall Failure) 113
5.3.4.1. Locating the Area of Failure 113
5.3.4.2. Description of Ramp 11 Failure 115
5.3.5. Case Example 5 (Ramp 12 High-wall Failure) 120
5.3.5.1. Locating the Area of Failure 120
5.3.5.2. Description of Ramp 12 Slope Failure 121
5.4.6. Case Example 6 (High-wall Failure) 124
5.4.6.1. Locating the Area of Failure 125
5.4.6.2. Description of Case Example 6 Slope Failure 127
5.5. Discussion on Slope Failure Mechanisms Based on Displacement Records 130
5.5.1. Surface Displacement Trend 131
5.5.2. Deformation Propagation 134
5.6. Validity of Commonly Recognised Slope Failure Mechanisms 138
5.7. Summary 141
CHAPTER SIX 144

DEVELOPMENT OF AN EMPIRICAL THRESHOLD MODEL AND A SLOPE FAILURE PREDICTION MODEL....144
6.1. Predicting Time of failure of a Mine Slope....144
6.2. Determination of a Threshold Value for the Cumulative Rate of Displacement....150
6.3. Development of Slope Failure Prediction Model (SFPM)....153
6.3.1. Introduction....153
6.3.2. STEP 1: Inverse Rate of Displacement (RD) Calculation....153
6.3.3. Effects of Data Filtering on Rate of Displacement Calculation....154
6.3.4. STEP 2: Simple Linear Regression....160
6.3.5. STEP3: Regression Line....160
6.3.6. STEP 4: Coefficient of Regression....161
6.4. Prediction of the Time of Failure from the Most Active Points....162
6.5. SFPM Home Page....163
6.6. Validation of the Slope Failure Prediction Model (SFPM)....165
6.6.1. Validation Test 1 (Copper Mine)....166
6.6.2. Validation Test 2 (Ramp 12 High-wall Failure, New Vaal Open-Cast Coal Mine)....170
6.6.3. Validation Test 3 (Ramp 5 High-wall Failure, Landau Open-Cast Coal Mine)...173
6.6.4. Validation Test 4 (Mine Name Unknown)....176
6.7. Summary....179
CHAPTER SEVEN....182
CONCLUSIONS AND RECOMMENDATIONS....182
7.1. Conclusions....182
7.2. Recommendations for Further Research....186
References....187
APPENDICES....203
APPENDIX 1....203
Kleinkopje Open-cast Coal Mine....203
APPENDIX 2....208

New Vaal Open-cast Coal Mine 208

APPENDIX 3 211

Mine Slope Displacement Records Used for Validation Tests 211

APPENDIX 4 222

Slope Failure Prediction Model (SFPM) 222

LIST OF FIGURES

Figure 2.1: Open pit slope geometry showing relationship between overall slope angle, inter-ramp angle and bench (After Williams, et al. 2009). 8

Figure 2.2: Open cast coal mine slope geometry. 9

Figure 2.3: (a) Strain-softening stress-strain curve. (b) Strain-hardening stress-strain curve (After Brady and Brown, 2006). 11

Figure 2.4: Types of slope failure in open-pit mines: (a) Large-scale wedge failure (b) Large-scale plane failure (C) Small-scale local failure (d) Circular failure of intensely fractured and weathered rock. Modified from Deere and Patton (1971) by Gayer, et al. (1995). 12

Figure 2.5: (a) Plane failure mode (b) Kinematic analysis of plane failure. 16

Figure 2.6: (a) Rotational failure mode (b) Circular failure mode, according to Hoek and Bray (1981). 17

Figure 2.7: Circular failure at New Vaal Coal mine. 17

Figure 2.8: Failure stages for circular (rock mass) shear failure slope (After Sjoberg, 2000). 18

Figure 2.9: (a) Wedge failure mode (Piteau and Martin, 1982) (b) Kinematic analysis of wedge failure. 19

Figure 2.10: Large-scale wedge failure disrupting the entire mine slope (After Lorig, et al. 2009). 19

Figure 2.11: (a) Toppling failure mode. (b) Potential toppling failure when the vertical weight component, W, is outside the pivot point (After Kliche, 1999). 21

Figure 2.12: Block toppling example (After Goodman and Bray, 1976). 21

Figure 2.13: Bench-scale block toppling on joints in ganodiorite (After Lorig, et al. 2009). .22

Figure 2.14: (a) Flexural toppling example (After Goodman and Bray, 1976) (b) Flexural toppling with a sliding movement between the faces of the toppling columns (After Hoek and Bray, 1981). 22

Figure 2.15: Bench-scale flexural toppling on cleavage in sericitic phyllite (After Lorig, et al. 2009). 23

Figure 2.16: Failure stages for large-scale toppling failure in a slope (After Sjoberg, 2000). 23

Figure 2.17: Complex failure mechanisms with multiple step-path failure (After Eberhardt, et al. 2004a and Stead, et al. 2006) 25

Figure 2.18: Complex failure mechanisms with deep-seated multi-block failure. Modified from Eberhardt, et al (2004a) and Stead, et al (2006).....25

Figure 2.19: Toppling with circular failure (After Alejano, et al. 2010).....26

Figure 2.20: Typical regressive/progressive stage displacement curves (Broadbent and Zavodni, 1982).....28

Figure 2.21: Generalised time and event dependent rock mass deformation model (After Mercer, 2006).....29

Figure 2.22. Generalised time and event dependent rock mass deformation model showing post collapse and post mining behaviour modes (Mercer, 2006).....31

Figure 3.1: Slope monitoring strategy at PPRust open pit, Limpopo, South Africa (After Little, 2006a).....35

Figure 3.2: Slope monitoring system.....36

Figure 3.3: Portable borehole inclinometer system (Abramson, et al. 2002).....40

Figure 3.4: Proper inclinometer placement in a slope (Abramson, et al. 2002).....41

Figure 3.5: Riegel LPM-2K SiteMonitor by 3-D Laser Mapping Ltd U.K (Hunter, 2007).....44

Figure 3.6: Slope Stability Radar (After Hawley, et al. 2009).....48

Figure 3.7: Work Area Monitoring (WAM) (GroundProbe, 2011b).....49

Figure 3.8: Movement and Surveying Radar, MSR-300 (Reutech, 2008).....50

Figure 3. 9: Movement and Surveying Radar, MSR-060 V (Reutech, 2011).....51

Figure 3.10: (a) First phase measurement of the MSR (b) Second phase measurement of the MSR (Reutech, 2006b).....52

Figure 3.11: The IBIS-M Slope Monitoring Radar (Ingegneria Dei Sistemi, 2011).....53

Figure 4.1: Location of Kleinkopje open-cast mine (Kleinkopje Colliery, 2009).....60

Figure 4.2: Typical borehole stratigraphy of Kleinkopje open-cast mine (Kleinkopje Colliery, 2009).....62

Figure 4.3: Typical geological cross section of Kleinkoje open-cast mine (Kleinkopje Colliery, 2009).....63

Figure 4.4: Trend plot of Kleinkopje open cast mine low-wall failure (Mottie, 2008).....68

Figure 4.5: Locality plan of Landau open cast mine (Landau Colliery, 2009).....70

Figure 4.6: The Karoo basin in Southern Africa (Landau Colliery, 2009). 71

Figure 4.7: Typical borehole stratigraphy of Landau open cast mine (Landau Colliery, 2009). 72

Figure 4.8: Typical geological cross section of Landau open cast mine (Landau Colliery, 2009). 73

Figure 4.9: Failed high-wall at Landau open-cast mine (Landau Colliery, 2009). 78

Figure 4.10: Map showing location of the New Vaal open-cast mine (New Vaal Colliery, 2009a). 79

Figure 4.11: Typical stratigraphy column for New Vaal open cast mine (New Vaal Colliery, 2009a). 81

Figure 4.12: MSR trend plots and synthetic map of the scanned low-wall (New Vaal Colliery, 2009b). 86

Figure 4.13: Unstable low-wall before failure (New Vaal Colliery, 2009b). 87

Figure 4.14: High-wall before and after failure (Zindela, 2008). 88

Figure 4.15: MSR trend plot of the high-wall displacement (Zindela, 2008) 88

Figure 4.16: MSR synthetic map and trend plots of low-wall displacement (Zindela, 2008). 89

Figure 5. 1: Negative-positive regressive behaviour of stable slope at Landau open cast mine (Type I). 94

Figure 5. 2: Negative regressive behaviour of stable slope at Landau open-cast mine (Type I). 94

Figure 5.3: The scanned region of case example 1 slope 96

Figure 5.4: Relative range (Displacement, mm) of sections 1-9 of case example 1 slope. 96

Figure 5.5: Cumulative rate of displacement (mm/hr) of sections 1- 9 of case example 1 slope. 97

Figure 5.6: Failure section showing the locations of ten selected points in case example 1 slope. 98

Figure 5.7: Relative range (Displacement, mm) of 10 points in the failure section of case example 1 slope 99

Figure 5.8: Cumulative rates of displacement, (mm/hr) of 10 points in section 7 of case example 1 slope 100

Figure 5.9: The scanned region of ramp 0 slope. 103
Figure 5.10: Relative range (Displacement, mm) of sections 1-7 of ramp 0 slope. 104
Figure 5.11: Cumulative rate of displacement (mm/hr) of sections 1-7 of ramp 0 slope. 105
Figure 5.12: The scanned region of ramp 5 slope. 108
Figure 5.13: Relative range (Displacement, mm) of sections 1-10 of ramp 5 slope. 108
Figure 5.14: Cumulative rate of displacement (mm/hr) of sections 1-10 of ramp 5 slope. ... 109
Figure 5.15: Failure section of ramp 5 showing the locations of eleven selected points. 109
Figure 5.16: Relative range (Displacement, mm) of eleven points in ramp 5 failure region. 110
Figure 5.17: Cumulative rate of displacement (mm/hr) of eleven points in ramp 5 failure region. 111
Figure 5.18: The scanned region of ramp 11 slope. 114
Figure 5.19: Relative range (Displacement, mm) of sections 1-8 of ramp 11 slope. 114
Figure 5.20: Cumulative rate of displacement (mm/hr) of sections 1-8 of ramp 11 slope. ... 115
Figure 5.21: Failure section of ramp 11 slope failure showing the locations of ten selected points. 115
Figure 5.22: Relative range (Displacement, mm) of 10 points in ramp 11 failure sections. . 116
Figure 5.23: Cumulative rate of displacement (mm/hr) of 10 points in ramp 11 failure sections. 117
Figure 5.24: The scanned region of ramp 12 slope. 120
Figure 5.25: Relative range (Dispalcement, mm) of sections 1-9 of ramp 12 slope. 121
Figure 5.26: Cumulative rate of displacement (mm/hr) of sections 1-9 of ramp 12 slope. ... 122
Figure 5.27: The scanned region of case example 6 slope. 125
Figure 5.28: Relative range (Displacement, mm) of sections 1-11 of case example 6. 126
Figure 5.29: Cumulative rate of displacement (mm/hr) of sections 1-11 of case example 6. 126
Figure 5.30: Failure section of case example 6 showing the locations of ten selected points. 127
Figure 5.31: Relative range (Displacement, mm) of 10 points in the failure section of case example 6. 127

Figure 5.32: Cumulative rate of displacement (mm/hr) of 10 points in the failure section of case example 6. 128

Figure 5.33: Post-failure class 1 type I displacement behaviour. 135

Figure 5.34: Post-failure class 1 type II and class 2 type I displacement behaviour. 136

Figure 5.35: Post-failure class 1 type III dispalcement behaviour.....137

Figure 6.1: Displacement rate curve and failure collapse prediction (After Zavodni and Broadbent, 1980).....146

Figure 6.2: Inverse velocity versus time relationships preceding slope failure (After Fukuzono, 1985). 148

Figure 6.3: Point area monitoring with the MSR (Area ABCD, AB = 133m, BC = 75m). ..152

Figure 6.4: Cumulative rate of displacement (mm/hr) threshold determination based on point monitoring for the New Vaal coal mine. 153

Figure 6.5: Inverse rates of displacement at 1 data interval (4 minutes). 155

Figure 6.6: Inverse rates of displacement at 2 data interval (8 minutes). 156

Figure 6.7: Inverse rates of displacement at 5 data interval (20 minutes). 156

Figure 6.8: Inverse rates of displacement at 10 data interval (40 minutes). 157

Figure 6.9: Inverse rates of displacement at 15 data interval (60 minutes). 157

Figure 6.10: Inverse rates of displacement at 20 data interval (80 minutes). 158

Figure 6.11: Inverse rates of displacement at 25 data interval (100 minutes). 158

Figure 6. 12: Inverse rates of displacement at 2, 5 and 10 data interval (8, 20 and 40 minutes). 159

Figure 6.13: Inverse rates of displacement at 15, 20 and 25 data interval (60, 80 and 100 minutes).....159

Figure 6.14: SFPM flow chart. 163

Figure 6.15: SFPM home page without results.....164

Figure 6.16: SFPM home page with results.....164

Figure 6.17: Graphical illustration of predictions from the active points.....165

Figure 6.18: Failed first prediction of validation test 1. 167

Figure 6.19: Second prediction of validation test 1. 168

Figure 6.20: Graphical illustration of the five most active points of validation test 1. 169
Figure 6.21: Predictions with three most active points of validation test 1. 169
Figure 6.22: Relative range (Displacement, mm) of 10 points used for validation test 2. 170
Figure 6.23: Third predictions of validation test 2. 172
Figure 6.24: Graphical illustration of the five most active points of validation test 2. 172
Figure 6.25: Predictions with three most active points of validation test 2. 173
Figure 6.26: Sixth prediction of validation test 3. 175
Figure 6.27: Graphical illustration of the five most active points of validation test 3. 175
Figure 6.28: Predictions with the three most active points of validation test 3. 176
Figure 6.29: Relative range (Displacement, mm) of 6 points used for validation test 4. 177
Figure 6.30: Eighth prediction of validation test 4. 178
Figure 6.31: Graphical illustration of the two most active points of validation test 4.....179

LIST OF TABLES

Table 2.1: Slope Movement Scale (After Varnes, 1978).....32

Table 3.1: Bye's Fault Tree Analysis (Bye, 2009). 53

Table 3.2: Slope Monitoring System 56

Table 4.1: Pit Geometry of Kleinkopje open cast mine (Kleinkopje Colliery, 2009). 59

Table 4.2: Summary of failure at Kleinkopje mine between March 2003–July, 2007. 67

Table 6.1: Summary of prediction results of validation test 1 conducted at 20:07 on 5th August, 2008. 170

Table 6.2: Summary of prediction results of validation test 2 conducted at 15:09 on 13th March, 2008. 173

Table 6.3: Summary of prediction results of validation test 3 conducted at 14:25 on 21st October, 2007.....176

Table 6.4: Summary of prediction results of validation test 4 conducted at 08:38 on 13th February, 2011. 179

ABBREVIATIONS

ADT	Automatic Detection and Tracking
AOL	Anglo Operations limited
BHHW	Base Horizon of Hard Weathering
BHWE	Base Horizon of Weathering
CCD	Charge Couple Device
CV	Calorific Value
DEM	Digital Elevation Models
DIANE	Discontinuous, Inhomogeneous, Anisotropic and Non-Elastic
FLAC	Fast Lagrangian Analysis of Continua
FM-CW	Frequency Modulated – Continuous Wave radar
FOG	Fall Of Ground
FS	Full Scale
GEOMOS	Geodetic Monitoring System
GPS	Global Positioning System
GMAS	GPS Multiple-Antenna Switch
IFSAR	Interferometry Synthetic Aperture Radar
ISAR	Inverse Synthetic Sperture Radar
MSR	Movement and Surveying Radar
MTI	Moving Target Indication
NASA	National Aeronautics and Space Administration
PALS	Personal Alerts
PPRust	Potgietersrust Platinum
RADAR	Radio Detection and Ranging
RD	Rate of Displacement
SAR	Synthetic Aperture Radar (SAR)
SFPM	Slope Failure Prediction Model
SLAR	Sidelooking Airborne Radar

SSR	Slope Stability Radar
STT	Single Target Tracker
TDR	Time Domain Reflectometry
TF_a	Actual Time of Failure
TF_P	Predicted Time to Failure
TFP	Time of Failure Prediction
TTF	Time o Failure
TWS	Track-While-Scan
WAM	Work Area Monitoring

LIST OF SYMBOLS

σ'	Effective stress
σ	Total stress acting on the plane
u	Pore pressure.
R^i	Rate of movement
t_f	Time of failure
Ω^i	Rate of displacement
V_0	Velocity at onset of progressive displacement stage
V_{mp}	Velocity at mid-point of the progressive displacement stage
V	Velocity
C	Intercept of the line on the time axis
e	Base of natural logarithm
S	Slope of the line on the time axis
t	Time
V_{col}	Velocity at collapse
Ω^{ii}	Change in rate of displacement
$\Omega^i{}_f$	Velocity at the time of failure
t_0	Initial time
$\Omega^i{}_0$	Initial velocity
t_i	Recent time
u_i	Recent displacement
n	*n*th observation
a	Intercept of a straight line graph
b	Slope of a straight line graph
R^2	Coefficient of regression
y_i	Observed or recorded value
x_i	Predictor variable
$\bar{y}$	Mean of all observed or recorded values
$\bar{x}$	Mean of all values of the predictor variable
e_i	Residual

CHAPTER ONE

INTRODUCTION

1.1. Background to the Research

With the increasing depths of open-pit and open-cast mines, prediction of the behaviour of the rock mass is necessary in order to design mine slopes that are safe, both for the workers and the equipment. Geological structures, rock mass properties, such as shear strength and hydrogeological conditions, engineering common sense, and good blast design are among the many factors that must be considered in the design of a stable and safe mine slope. Unfortunately, even with advanced slope design techniques, and utilising the best available computer software, unexpected slope failures are still prevalent today. Why has it been impossible to prevent slopes from failing unexpectedly? Behind every slope, whether in open-pit mining or in civil engineering situations, is the natural, variable geological rock mass whose physical and engineering properties, and boundary conditions, cannot be established or defined through a manufacturing process like metals and plastic materials. Harrison and Hudson (2000) described rock masses as largely Discontinuous, Inhomogeneous, Anisotropic and Non-Elastic (DIANE)

According to Hoek, et al (2000) rock slope deformation and failure are events controlled by natural physical processes. Although, various researchers have investigated numerous ways of predicting the mechanism of failure of mine slopes, there is still no universally acceptable model for failure, and the mechanisms behind large scale failure are not well known, particularly in hard and strong rocks (Stacey, 2007). Consequently, proper understanding of the peculiarity of each rock formation and the underlying mechanisms driving instability is essential in analysing and predicting deformation and failure mechanisms.

Various techniques have been advanced in understanding and analysing mine slope deformation and failure mechanisms. Conventional methods of slope stability analysis involve the use of kinematic analysis, limit equilibrium analysis and rockfall simulation (Coggan et al, 1998). These methods are, however, not adequate to capture complexities, such as the complex interactions between joints, the slope hydrological conditions, slope geometry, non-linear behaviour and various boundary conditions influencing slope stability or instability. Computer-based numerical methods classified as continuum modelling (finite

element and finite difference), discontinuum modelling (distinct-element and discrete-element) and hybrid/coupled modelling have proved to have the capabilities of analysing and simulating complex rock slope deformation.

Surface and underground mining operations result in ground movement, which could be detrimental to mining operations and personnel. Fortunately, slope failures usually give advance warning before failing, if these can be accurately detected. Through proper knowledge of the deformation behaviour, mine slope hazards can be greatly reduced.

The quest for a more effective system of slope management in mines has resulted in the development of various slope monitoring techniques to monitor the deformation of the slope. The use of radar for slope monitoring was pioneered by GroundProbe (Pty) Ltd, Australia with the introduction of the Slope Stability Radar (SSR) in June 2003. An alternative radar monitoring system called the Movement and Surveying Radar (MSR 200) was introduced into the market in January, 2006 by Reutech Radar System (Pty) Ltd, South Africa. These techniques are dealt with in more detail later in this thesis.

1.2. Problem Statement

"Whether on the surface or underground, unanticipated movement of the ground can pose hazardous conditions which may lead to accidents, destruction of equipment, loss of ore reserves and closure of the mine" (Girard and McHugh, 2000). Girard and McHugh (2000) suggested the following ways of reducing the occurrence of slope failures resulting from mining operations:

1) good geotechnical design;
2) slope dewatering;
3) slope support and rock fall catchment systems;
4) monitoring systems to identify mechanisms of rock mass and slope behaviour and for advance warning of impending failures; and
5) cutting back of slopes to more stable angles.

The research proposed will focus on aspect 4, and with minor focus on aspect 1.

Radar slope monitoring is now widely used across the world, for example, the MSR is currently in use in several Anglo Coal mines and other surface mines around the world.

However, the effectiveness of this radar in notifying mine personnel of an impending slope failure is not fully realised. In order to solve this problem, a good knowledge of the mechanism of slope failure in open-cast mines is necessary. What the proposed research aims to do is to determine the intrinsic and extrinsic factors, and their interactions in causing slope instability and failure from time/displacement information gathered from the radar monitoring. To achieve these objectives, the history of failures in some Anglo Coal mines and other surface mines will be studied using the MSR records. The aim will be to develop a predictive or representative model of the deformation behaviour of the open-cast slopes. A detailed study of the past time/displacement information from the radar monitoring should allow the derivation of empirical threshold parameters for the MSR. The research will also attempt to derive a model for predicting time to failure (TTF) using information from the time/displacement records.

1.3. Research Questions

The research should be able to address or answer the following questions:

1) What are the possible mechanisms of failure at the open-cast mines?
2) What are the triggering factors responsible for slope failures in the mines and the mechanisms involved in the failure?
3) How effective is the MSR in monitoring slope failure?
4) Apart from giving warning of when the slope will fail, can the MSR be effectively used to determine failure mechanisms?
5) How can failure, and time to failure, be effectively predicted utilising the time/displacement data from the radar monitoring system?

1.4. Aims and Objectives of the Research

The aims and objectives of the research contained in this thesis are:

1) To determine the nature and magnitude of slope movements or deformation using the MSR;
2) To determine the modes and mechanisms of slope instability at the critical areas of instability;
3) To investigate factors tending to initiate instability.

4) To determine accurate threshold limits of slope displacements, such as rates and/or accelerations, at which the slope radar monitoring system should recommend an alarm; and
5) To develop, if possible, a method using the MSR data that can confidently predict the time to failure of an open-cast mine slope.

1.5. Research Approach and Thesis Structure

A range of equipment has been produced to investigate the problem of surface mine slope failure through appropriate slope monitoring, the latest of which is the slope monitoring radar. To understand the processes involved in mine slope failure, a review of the various failure modes and deformation behaviours of surface mine slopes was done. The various techniques available for slope monitoring were also reviewed. This was followed by four months of field work in some Anglo Coal open-cast mines, and five days training on the use of the MSR at Reutech (Pty) Ltd, South Africa. At Reutech, displacement records of slope failures in other surface mines where the MSR is operating were collected. The experience gained in the field work was combined with the displacement data obtained from the MSR to develop two models as follows: one for the determination of a threshold value for the cumulative rate of displacement and the other for time to failure prediction. The thesis is divided into seven chapters with the content of each chapter explained, as follows:

Chapter 1 contains an introduction to the problem of surface mine slope failure, the statement of the problem, research questions and the objectives of the research.

Chapter 2 presents a review of mine slope behaviour processes, as obtained from the literature. Further specific reviews of work done by several authors on the displacement behaviour of mine slopes were also carried out.

Chapter 3 entails a detailed review of the conventional slope monitoring techniques. The Movement and Surveying Radar (MSR)**,** the Slope Stability Radar (SSR), the Work Area Monitoring (WAM), the IBIS-M slope monitoring radar, which are the known slope monitoring radar systems available, are reviewed. The shortcomings of some of the conventional monitoring techniques are also highlighted.

Chapter 4 presents the detailed geology of the open-cast mines visited in course of the research. The slope stability challenges faced by each mine are reviewed. This chapter also contains a review of some documented slope failures which have occurred in mines and were monitored with MSR. Other mine slope failures not monitored with the MSR, but which were documented by the geotechnical staff, are also reviewed.

Chapter 5 is divided into three sections. Section one analyses the deformation behaviour of stable slopes. Section two analyses the deformation behaviour of unstable slopes utilising the displacement data obtained from the MSR, while in section three, the slope deformation mechanisms based on the displacement trend and deformation propagation are discussed. The outcome of the analysis resulted in the classification of the different stages of failure.

Chapter 6 contains a brief review of some of the existing methods of predicting the time to failure of mine slopes. A review of the inverse velocity method, which was adopted in this research, can also be found in this chapter. In chapter 6, the failure data from different mines were analysed with the objective of developing a model for the determination of a threshold value for the cumulative rate of displacement. The threshold model is based on point monitoring of mine slopes. In this chapter, the development of a model called the Slope Failure Prediction Model (SFPM) to predict the time to failure of mine slopes is also described. The model was tested and proved to be effective with four case examples of unstable slopes.

Chapter 7 contains the conclusion drawn from the research and recommendations for further research.

1.6. Limitations of the Research

The objectives of this research were achieved through a comprehensive analysis of the displacement data obtained from the MSR. However, the research work encountered some limitations. First, only six case studies were analyzed for the deformation behaviour of open-cast mine slopes while the SFPM was validated with four case studies. This is due to the lack of adequate slope failure database for research purposes since slope radar monitoring is a relatively new technology. Mining companies with records of slope failure monitored with the radar are not willing to release them. Second, the research was limited to displacement

data from the MSR. This situation prevented the analysis of displacement data from other slope monitoring system other than the radar. A combination of displacement data from other slope monitoring system would have provided more insight into the deformation behaviour of open-cast mine slopes. Lastly, numerical modelling, probabilistic analysis and detailed study of the mathematics of the radar are not included in the scope of the research.

CHAPTER TWO

REVIEW OF ROCK SLOPE DEFORMATION PROCESSES

2.1. Introduction

The first aspect of literature review relevant to the concept of slope deformation is presented in chapter 2. The section contains a review of the following pertinent subjects:

- Surface mine, namely open-pit and open-cast surface mines;
- Deformation terminologies;
- Common slope failure modes and the causes of slope failure; and
- Deformation and displacement behaviour of surface mine slopes.

2.2. Surface Mine

Before mining, the natural deformation within the rock mass is contained through confinement by the surrounding rock materials. The excavation process exposes the inherent geological weaknesses in the rock mass by removing the confinement. The onset of excavation for mineral recovery through both underground and surface mining results in the creation of openings in the ground. These openings become the free space for the deformed rock to be displaced into. The disturbance produced by mining through excavation also disturbs and redistributes the in-situ stress field causing further deformation in the rock mass. Xu et al (2011) utilised seismic monitoring to establish a strong correlation between excavation and formation of micro-cracks in deep rock mass. Excavation-induced fractures in a shallow high-quality granite rock were also confirmed by Stacey (2007).

The process of excavating ore bodies, which are close to the surface, either by open-pit or open-cast surface mining methods results in the creation of pit with series of benches referred to as high-walls (Reutech, 2006b). For economic reasons, the slope angle of the benches cannot be made too flat because of the cost of waste materials to be removed. Hence, mining companies are caught in a dilemma of designing a slope that is not too flat for economic gains, and not too steep for safety concerns. The features of a typical open pit slope are shown in figure 2.1, where the overall pit slope angle (slope crest to slope toe), the inter-ramp

angles and the face angle of each bench are the three main features of an open-pit slope (Wyllie and Mah, 2004). The overall pit slope, which incorporates all inter-ramp areas, haulage roads and benches, is steeper in competent rocks than in weak rocks, sometimes with varying slope angles within the same mine. The maximum inter-ramp angle is a function of the bench face angle, the bench height and width, and these are all governed by the geomechanical properties of the slopes and operational factors. Consequently, the overall slope angle becomes a function of the bench angles and widths inter-ramp angle and width and the total number of haulage roads (Sjoberg, 1996).

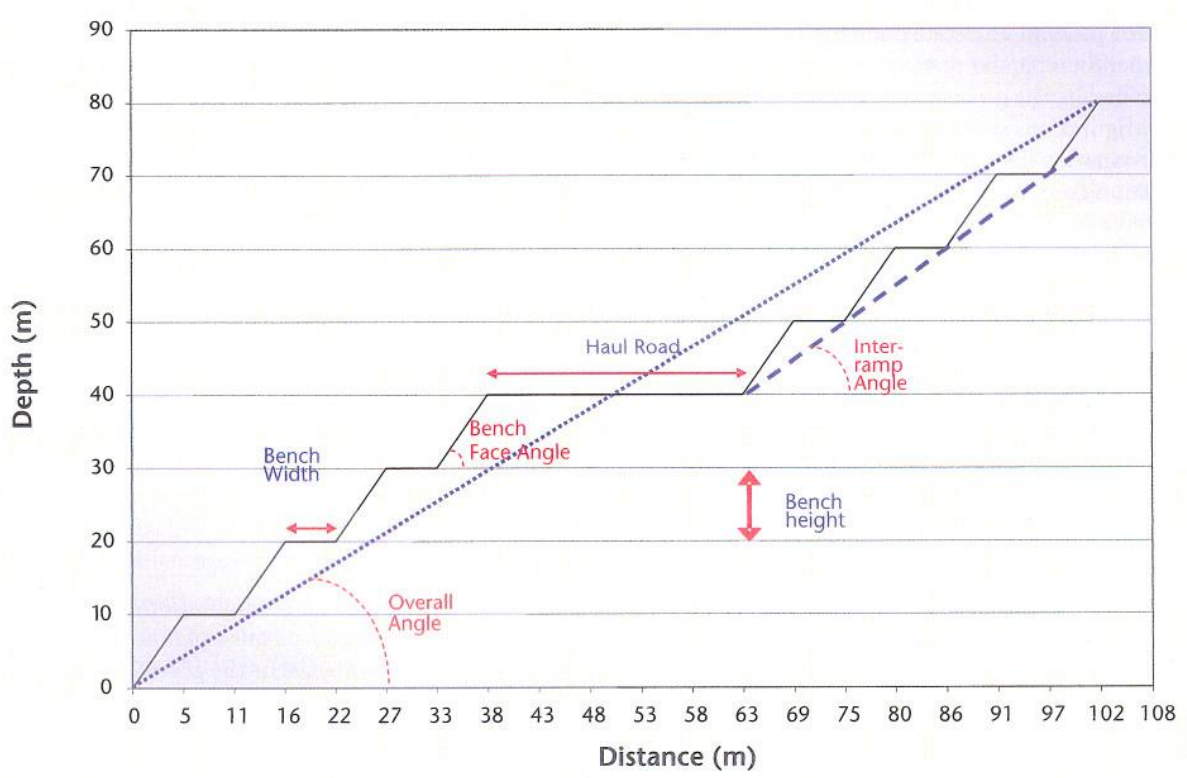


Figure 2.1: Open pit slope geometry showing relationship between overall slope angle, inter-ramp angle and bench (After Williams, et al. 2009).

The bench configuration in an open-cast coal mine as seen in figure 2.2 differs significantly from that of an open-pit mine. In an open-cast mine, mining is done in strips, with the dragline positioned on the high-wall for overburden removal. The overburden overlying the ore body is removed and placed in the mined-out area, creating a stack of waste which is referred to as low-wall or spoil. The strip geometry is determined by both operational parameters and safety considerations, with important design considerations given to both the

high-wall and the low-wall. Okagbue (1987), Ulusay et al. (2001) and Kasmer et al. (2006) have reported several examples of spoil, or low-wall failure in open-cast mines. These large-scale spoil failures and their consequences on production and safety have given attention to the stability of spoil piles as much as high-wall stability (Kasmer, et al. 2006). In a study conducted by Okagbue (1987), it was confirmed that the major slope stability problem in a number of open-cast coal mines is spoil instability, particularly, where the spoil consists largely of loose sand with insufficient waste rock to support the low strength soil. The high-walls of open-cast coal mines on the other hand are not as complex as those of open-pit mines. The geology is straightforward and the rock mass strength is fairly similar from mine to mine, because the same rock types are usually found (Seegmiller, 2000). The high-wall of open cast coal mines are designed to generally be steep when compared to the high-wall of most open-pit mines. This is because the lifespan of open-cast coal mine high-walls is short as compared to that of an open-pit mine where the high-wall is expected to be stable throughout the lifespan of the mine.

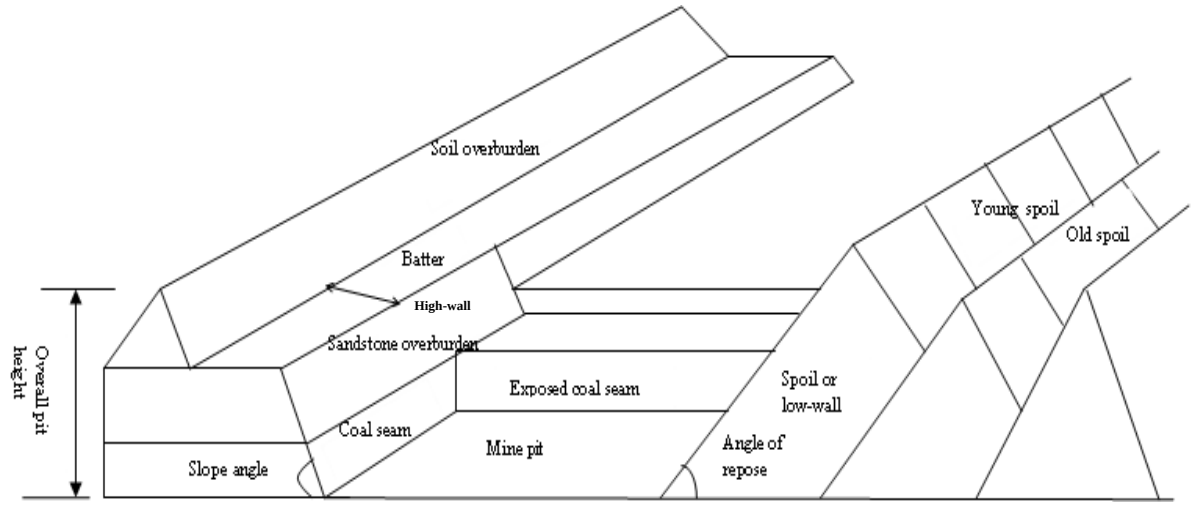


Figure 2.2: Open cast coal mine slope geometry.

2.3. Rock Deformation

Some terminologies used in this study, which are peculiar to the subject of slope monitoring and management, are briefly explained in the following sections. This is necessary to avoid any ambiguity that may exist in the use of some of the terms.

2.3.1. Definitions

Deformation: This occurs when there is a change in structure or formation of displacement in rocks under the influence of external forces. Deformation always precedes failure during the process of slope failure. In this study it is expressed in terms of displacement magnitudes and cumulative rates of displacement.

Fracture: This occurs when the bonds between the rock material breaks with the creation of planes of separation. Fracture does not always results in rock failure.

Strength or Peak Strength: This is the maximum stress averaged over a plane, which the rock can sustain under a specified set of conditions (Brady and Brown, 2006). In figure 2.3a, point B stands for the peak strength. The residual strength that is reached only after significant post-peak deformation is given as point C in Figure 2.3a (Brady and Brown, 2006).

Brittle Deformation: This occurs when the stress exceeds the rock strength and there is an abrupt loss of strength with fracture on a rock plane without significant preceding plastic deformation (Brady and Brown, 2006). As shown in figure 2.3a, it is usually associated with strain-softening or strain-weakening behaviour of the rock (Brady and Brown, 2006). In brittle deformation, the strain is irreversible.

Ductile Deformation: This occurs when the stress exceeds the rock strength but it can accommodate further permanent deformation without breaking as seen in figure 2.3b. In ductile deformation, the strain is irreversible.

Yield: This is the stress at the end of elastic behaviour, represented by point A in figure 2.3a. The yield stress, σ_y, depicted in figure 2.3, is the onset of permanent and irreversible deformation (Brady and Brown, 2006). During slope monitoring, the yield point corresponds to the beginning of progressive displacement behaviour, which is often times the same as the on-set of failure point.

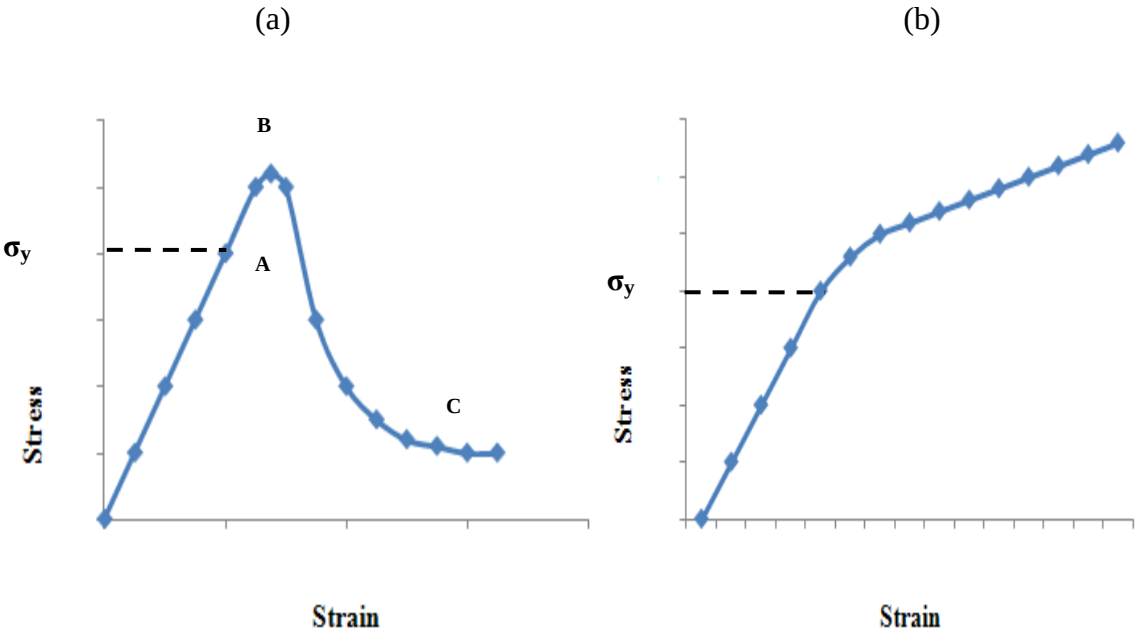


Figure 2.3: (a) Strain-softening stress-strain curve. (b) Strain-hardening stress-strain curve (After Brady and Brown, 2006).

Failure: Failure occurs when the load or stresses acting on the rock material exceed the strength of the rock. Failure occurs or initiates at the peak strength (Jaeger and Cook, 1979). Failure and collapse are used interchangeably in open-cast mine slopes (Stacey, 2009).

Functional Failure: This is defined as a situation where a slope cannot perform the function for which it was designed. This implies that it does not necessarily involve overall collapse, although localised sections of the structure may have collapsed (Goldberg and Frizzell, 1989).

Operational Slope Failure: Call (1982) defined operational slope failure as a condition where the rate of displacement exceeds the rate at which the slide material can be safely mined.

Slope Collapse/Slope Failure: Sjoberg (1996) defined slope collapse as a situation where the consequences of the developing failure render the slope impossible to mine. Local scale slope collapse involves one or a few benches while global scale slope collapse involves the entire slope (Sjoberg, 1996). Deere and Patton (1971) classified slope collapse/slope failure, as seen in figure 2.4, into three categories:

Type 1 – Small scale local failure involving a single bench.

Type 2 – Large-scale wedge failures involving a number of benches.

Type 3 – Circular failure in sheared/fractured and weathered rock which may involve several benches.

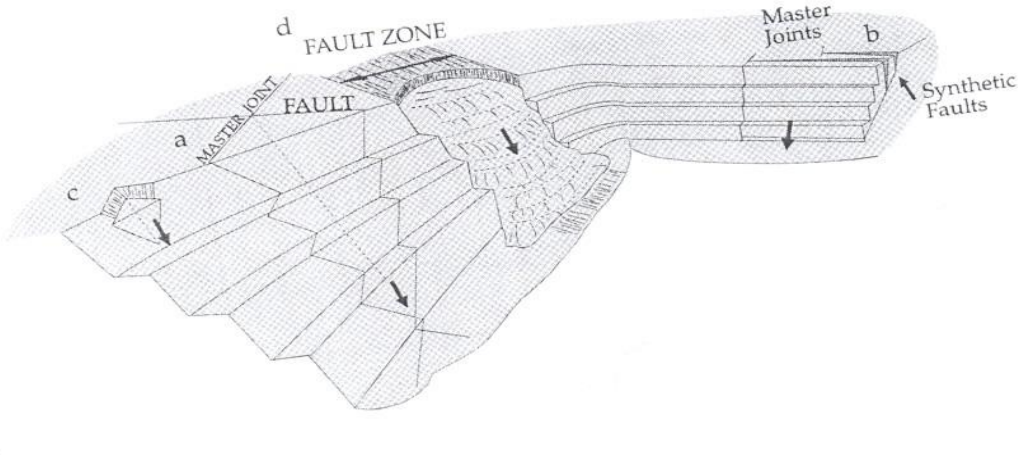


Figure 2.4: Types of slope failure in open-pit mines: (a) Large-scale wedge failure (b) Large-scale plane failure (C) Small-scale local failure (d) Circular failure of intensely fractured and weathered rock. Modified from Deere and Patton (1971) by Gayer, et al. (1995).

Failure Mechanism: This is a description of the physical process that occur in the rock mass as the stress increases and failure initiates and propagates within the rock mass (Sjoberg, 1996).

Failure Kinematics: Failure kinematics is simply a geometrical description of the motion or movements, which result from a failure (Meriam, 1980).

Failure Kinetics: This relates the action of forces and loads on the slope to the resulting motions, and is therefore closely linked to failure mechanism (Meriam, 1980).

Effective Stress: The effective stress is a function of the total applied stress and the pressure of the fluid in the pores of the rock, referred to as the pore pressure or pore-water pressure (Brady and Brown, 2006). Effective stress governs the gross mechanical response of jointed rock mass (Brady and Brown, 2006).

The effective stress is given as:

$$\sigma^i = \boldsymbol{\sigma} - \mu \quad 2.1$$

Where:

σ^i = effective stress;

σ = total stress acting on the plane; and

μ = Pore pressure.

2.4. Causes of Slope Failure/Slope Failure Triggers

Several combinations of factors are responsible for slope failure, whether in rock or in soil. It is uncommon that a given failure can be attributed to any single cause (Kliche, 1999). Call (1982) stated that a rock mass does not move unless there is a change in forces acting on it. Usually a number of factors subsist simultaneously to eventually trigger the slope failure. Varnes (1978) grouped these factors into two major categories.

1) Factors that contribute to increased shear stress: One of the factors contributing to an increase in shear stress of natural slopes is the removal of lateral support from erosion by streams and rivers, and wave actions on lakes and glaciers (Varnes, 1978). Call (1982) found that the removal of lateral support by excavation is one of the major causes of slope failure in open pit mines. The high-wall failure at a coal mine in the Bowen Basin, Queensland was caused by the removal of lateral support (Kelso, 2011). Another factor is the addition of surcharge by rain, hail, snow or water. Surcharge from rain has been a main triggering factor to many slope failures, for example, the waste dump failure at Arcturus Gold mines in Zimbabwe (Shakesby and Whitlow, 1991) and the Himmetoglu coal mine failure (Ulusay, et al. 2001).

Other causes of increased shear stresses are transitory earth stresses, such as vibrations from earthquakes, blasting, heavy machinery, traffic, vibratory compactor, lateral pressure from water in pore spaces, cracks or cavities, tectonic activities, which may alter the stress fields on a very large scale causing an increase or shift in the direction of geostatic stresses (Varnes, 1978). Wesseloo and Dight (2009) reported that change in stress in mine slopes resulting from mining is the driver behind rock fracture. The North Wall failure at Palabora mine was

triggered by the alteration of the stress field caused by caving operations (Vyazmensky et al. 2010).

2) Factors that contribute to low or reduced shear strength: These are factors resulting from initial state or inherent characteristics of the material. These factors include texture and gross structure, material composition and slope geometry, that is, slope orientation, the presence and orientation of discontinuities (Varnes, 1978). With regards to the geometry of open-cast coal mines, slopes are designed to be as steep as possible resulting in over steepening of the high-wall, which is a major cause of slope failure in open-cast coal mines (Simmons and Simpson, 2006).

Weathering and other physiochemical reactions may also cause a great reduction in shear strength of the rock mass (Deere and Patton, 1971, Varnes, 1978). These changes can include softening of fissured clays, physical disintegration of granular rocks caused by frost or thermal expansion and contraction, removal of cement within discontinuities by solution (Varnes, 1978). Changes in intergranular forces due to water content and pressure in fractures and pores, is a major cause of shear strength reduction in many mine slopes (Varnes, 1978; Mandzic, 1992; Atkinson, 2000; Call, et al. 2000; Stacey, et al. 2003).

2.5. Modes and Mechanisms of Slope Failure in Rock Mass

Sjoberg (1996) defines the failure mode of rock mass as a macroscopic description of the way in which failure occurs, for example, the shape and appearance of the resulting failure surface. It encompasses the mechanisms, kinematics and kinetics of the failure. As classified by Wyllie and Mah (2004), the four primary modes of slope failure that exist in rock mass are:

1) Plane failure;
2) Rotational/circular failure;
3) Wedge failure; and
4) Toppling failure.

Other secondary modes of failure include rock falls, rock or earth spread, rock or earth flow and buckling of dipping thin beds. Complex failure mechanisms occur when slope failure involves more than one failure mode.

The four primary mode of failure outlined above are based on the assumption that slope failure occurs on identified or interpreted failure surfaces. Therefore, identifying the critical failure surface and the acting forces becomes the base of limit equilibrium analysis of slopes stability. However, in studies conducted by Sjoberg (2000) and Stacey (2006), they suggested that there are other possible failure modes in mine slopes, which do not correspond with the established mechanisms, particularly in high stress and hard rock conditions. These unknown and poorly investigated mechanisms prompted the following questions from Stacey (2006):

1) Does failure actually take place on the selected failure surface?
2) Is the selected failure surface a unique failure surface or does failure take place on more than one failure surface?
3) Does failure take place on multiple failure surfaces, and in several locations within the slope?
4) Are back-analysed strength parameters of this failure surface representative of the 'strength' of the rock slope?
5) What about the three-dimensional geometry of the failure?

In light of the above questions, the four primary failure modes are reviewed in this section. Also, with the failure mechanisms observed from the MSR displacement data, an attempt will be made to respond to questions 1- 4 in chapter 5 of this study.

2.5.1. Plane Failure

Plane failure, as shown in figure 2.5, involves the movement of the rock block downward and outward along a gently undulating release surface (Hoek and Bray, 1981; Kliche, 1999). The movement is usually controlled structurally by surface weakness, such as joints, faults and bedding planes (Kliche, 1999).

For plane failure to occur, the strike of the plane of weakness must be within $\pm\ 20^0$ of the strike of the crest of the slope (Hoek and Bray, 1981). The toe of the failure plane must daylight between the toe and the crest of the slope, where daylight means "to intersect the face of the excavation above the toe level." In addition, Hoek and Bray (1981) stated that the dip of the failure plane must be less than the dip of the slope face, and greater than the angle of internal friction of the failure plane.

(a) (b)

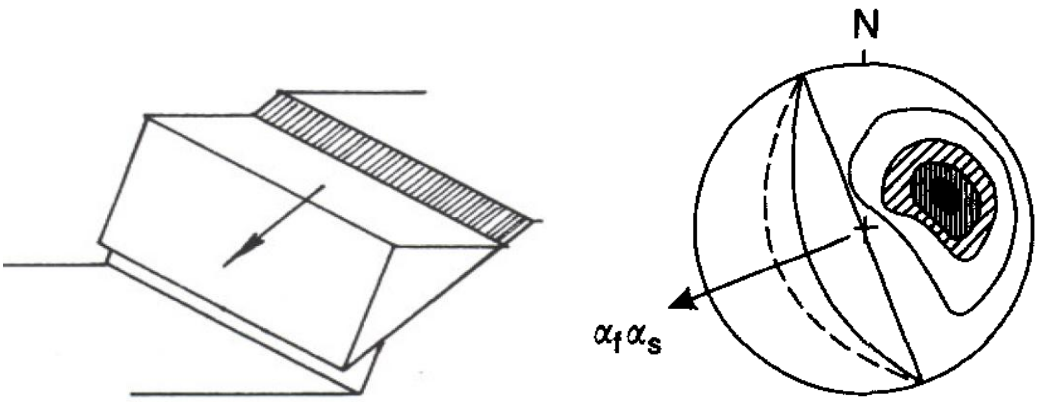


Figure 2.5: (a) Plane failure mode (b) Kinematic analysis of plane failure.

2.5.2. Rotational/Circular Failure

As classified by Coates (1977, 1981), the other type of failure mode is rotational shear failure, and this is illustrated in figure 2.6a. Hoek and Bray (1981) refer to this type of failure as circular failure as shown in figure 2.6b and 2.7. It occurs in soil when the material is very weak, especially when the weakness is aggravated by water intrusion. Rotational failures occur mostly in homogenous materials, such as constructed embankments, fills and highly jointed or fractured rock slopes (Kliche, 1999).

A model study of circular failure conducted by Sjoberg (2000) showed that typically failure occurs in stages. Figure 2.8 demonstrates the first stage and it involves elastic displacement, caused by removal of rock material by mining. This is followed by yielding, which begins at the toe and spreads upwards as more materials are removed. Yielding then leads to strain accumulation at the toe of the slope and progresses upward. When this occurs, the slope will start showing some displacements, which can be tracked if a good slope monitoring system is in place. As soon as the yielding reaches the crest, a failure surface is formed and the slope may fail with time.

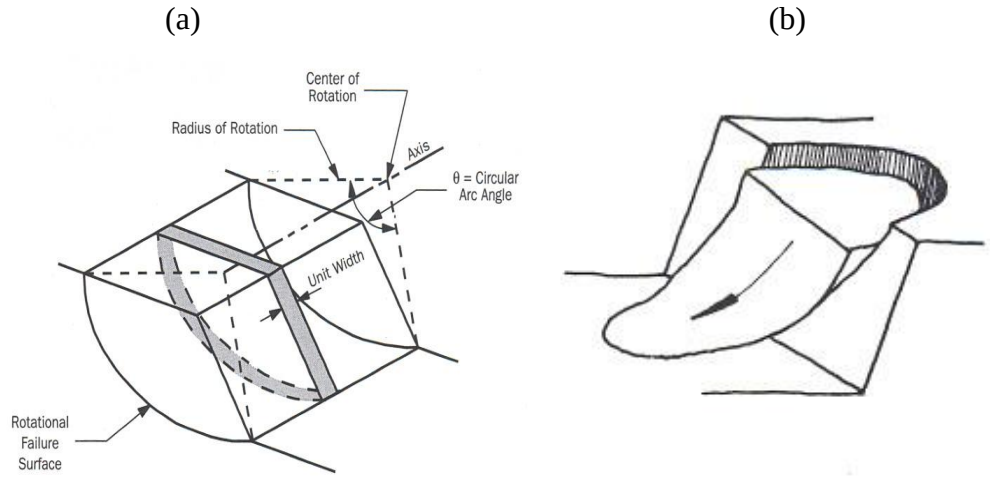


Figure 2.6: (a) Rotational failure mode (b) Circular failure mode, according to Hoek and Bray (1981).



Figure 2.7: Circular failure at New Vaal Coal mine.

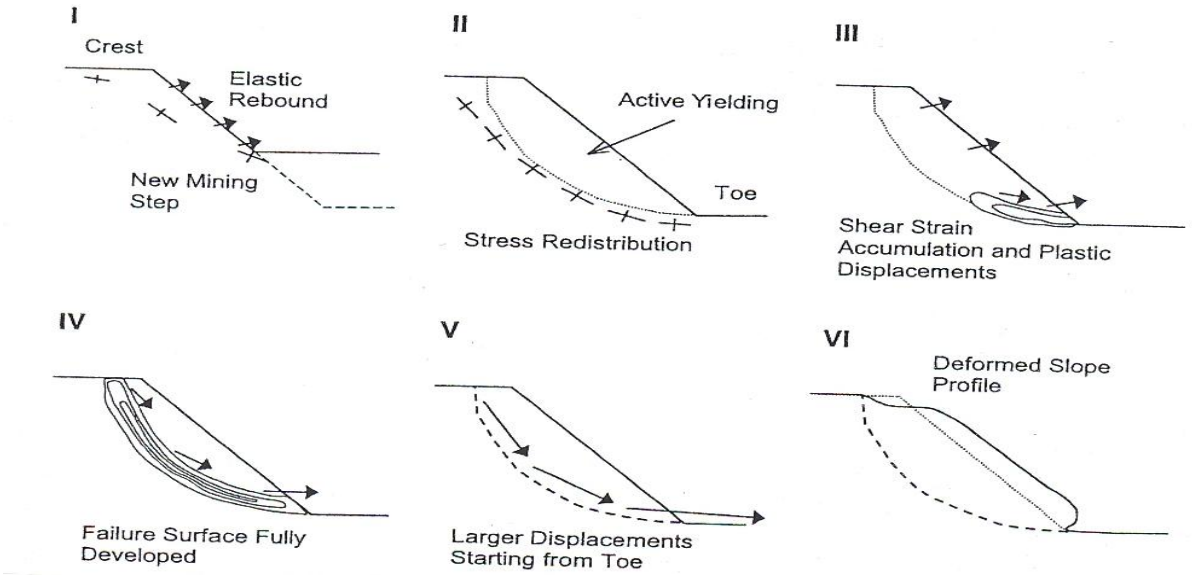


Figure 2.8: Failure stages for circular (rock mass) shear failure slope (After Sjoberg, 2000).

2.5.3. Wedge Failure

As depicted in Figure 2.9, when two discontinuities represented by plane A and B, strike obliquely across the slope face and their line of intersection daylights in the slope face, the wedge of rock resting on these discontinuities will slide down the line of intersection if the inclination of this line is considerably greater than the internal angle of friction along the discontinuities (Hoek and Bray, 1981: Kliche, 1999). For wedge failure to occur, the plunge of the line of intersection of plane A and B, namely ψ_i, must also be less than the dip of the slope face namely ψ_f, measured in the direction of sliding, that is, $\psi_i < \psi_f$ (Hoek and Bray, 1981). A large scale wedge failure is shown in figure 2.10.

(a) (b)

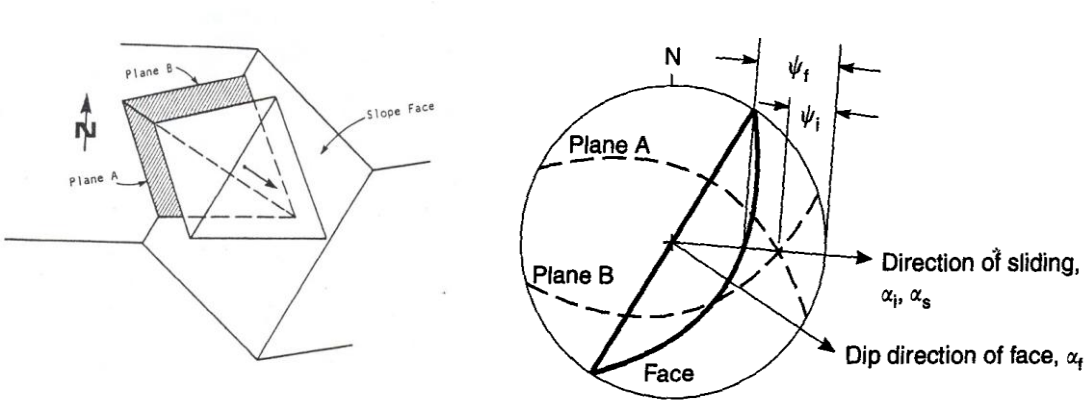


Figure 2.9: (a) Wedge failure mode (Piteau and Martin, 1982) (b) Kinematic analysis of wedge failure.



Figure 2.10: Large-scale wedge failure disrupting the entire mine slope (After Lorig, et al. 2009).

2.5.4. Toppling Failure

As illustrated in figure 2.11a and 2.11b, when the weight vector of a block of rock resting on an inclined plane falls outside the base of the block, toppling failure occurs (Kliche, 1999). Toppling refers to overturning of columns of rock formed by steeply dipping discontinuities

and sub-horizontal cross points or primary toppling. It could also be initiated by crushing of the slope toe, which is termed secondary toppling (Hoek and Bray, 1981; Glawe 1991). Goodman and Bray (1976) described the different toppling instability mechanisms shown in figure 2.12, 2.13 and 2.14 as Block toppling, Block-flexure toppling and Flexural toppling respectively. Flexural toppling, shown in figure 2.14 and 2.15 is more likely on a bench scale, since it requires very continuous pre-existing discontinuities. Adhikary and Dyskin (2007) stated that during flexural toppling, tensile stresses are induced when rock layers bend into the excavation, the tensile stresses may initiate tensile fractures in the rock layers located in areas of maximum bending moments.

Secondary toppling failure mechanisms, as classified by Goodman and Bray (1976) are Slide head toppling, Slide base toppling, Slide toe toppling, Tension crack toppling and Toppling and slumping. These instability phenomena are induced by a toe weakening caused by natural events, such as erosion or human activity such as mining or civil excavation works.

Sjoberg (2000) claimed in a model that toppling failure develops in various identifiable stages similar to circular failure as shown in figure 2.16. An elastic rebound occurs after the mining cut is made followed by slip along the steeply dipping joints in the slope. The slip, which begins at the slope toe and then progresses towards the crest, while redistributing stresses around the region of the slip. This results in the compression of rock columns, which creates the space for a slight rotation of the columns starting at the toe. In a high slope, the elastic deformations of the rock mass can cause a small rotation. This is followed by tensile bending failure at the base of the rotating column, which progresses to the crest, therefore causing base failure surface on which the failed rock can slide (Sjoberg, 2000).

(a) (b)

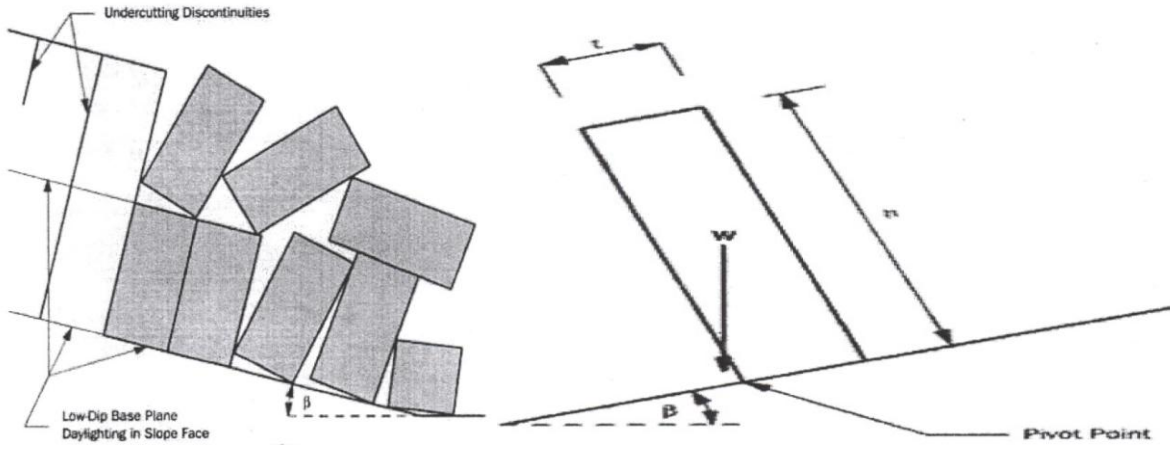


Figure 2.11: (a) Toppling failure mode. (b) Potential toppling failure when the vertical weight component, W, is outside the pivot point (After Kliche, 1999).

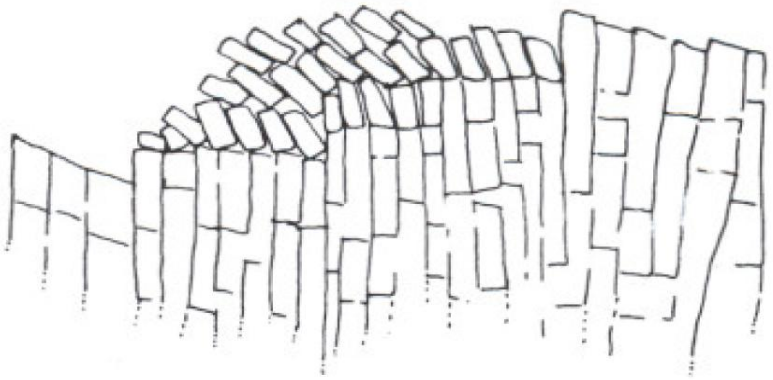


Figure 2.12: Block toppling example (After Goodman and Bray, 1976).



Figure 2.13: Bench-scale block toppling on joints in ganodiorite (After Lorig, et al. 2009).

(a) (b)

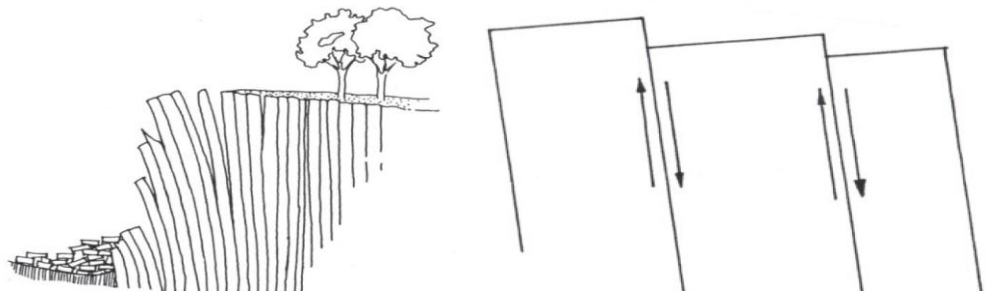


Figure 2.14: (a) Flexural toppling example (After Goodman and Bray, 1976) (b) Flexural toppling with a sliding movement between the faces of the toppling columns (After Hoek and Bray, 1981).



Figure 2.15: Bench-scale flexural toppling on cleavage in sericitic phyllite (After Lorig, et al. 2009).

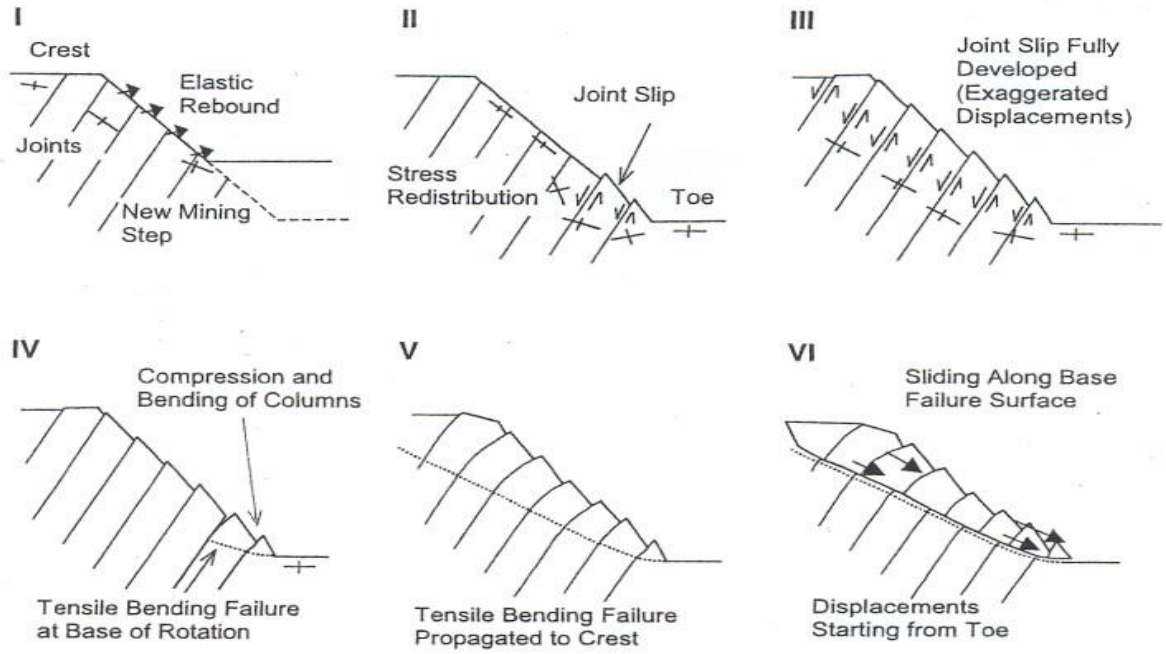


Figure 2.16: Failure stages for large-scale toppling failure in a slope (After Sjoberg, 2000).

2.6. Complex Failure Mechanism

A combination of two or more of the four primary failure mechanisms, or of other secondary failure mechanisms, constitutes what could be referred to as complex failure mechanism. Complex failure mechanisms may occur in weathered rock materials, where low shear strength permit failure through the rock material, rather than only along discontinuities (Vaziri et al. 2010). The slope failure shown in figure 2.17 involves multiple step-paths failure and intact rock fracture through gradual strength degradation along non-persistent sliding surfaces (Kemeny, 2003). The complex failure mechanism illustrated in figure 2.18 involves multi-block failure with internal shearing and strength reduction on sliding surfaces (Stead et al. 2006). In figure 2.18, the concept of damage zones within the active section of the 1963 Vaiont slide was introduced by Mencl (1966) to explain the complex failure along sliding surfaces. The concept was further developed by Martin and Kaiser (1984) to demonstrate that internal shearing and the resulting dilation of the rock mass during deformation are necessary for movement on the sliding surfaces.

Vaziri, et al. (2010) recorded toppling failure at the toe of a failure zone, with circular or planar sliding failure in the upper part of the failure. In a back-analysis of a slope failure in excess of 17.8 million tons at Cassiar Mine in British Columbia Canada, Martin (1993) referred to one of such complex failure mechanism as, "ratchet mechanisms." Analysis of the failure mechanisms conducted using geological mapping and prism monitoring showed that groundwater recharge of several steeply dipping cracks resulted in a ratchet mechanism of displacement rates. Alejano, et al (2010) reported a complex toppling-circular failure mode in an open-pit mine caused by forces exerted by limestone slabs with toppling tendency on the weaker sedimentary sequence in the lower part of the slope. This can be seen in figure 2.19. Thus, the sedimentary parts of the slope experience a circular failure resulting from a combination of forces from the limestone slab and water surcharge.

Complex failure mechanisms were also described in Simmons and Simpson (2006). In their study, they concluded that complex failure mechanisms are very difficult to predict, rapid and often occur without warning. Other complex failure mechanisms are active-passive sliding blocks (Calder and Blackwell, 1980), laccolith slides (Stewart and Reid, 1988), slide toppling mechanisms (Sijing, 1981) and wedge toppling (Seegmiller, 2000). In high and hard rock

slopes, failure mechanisms are more complex than common planar, wedge, circular and toppling failure mechanisms (Stacey, 2007).

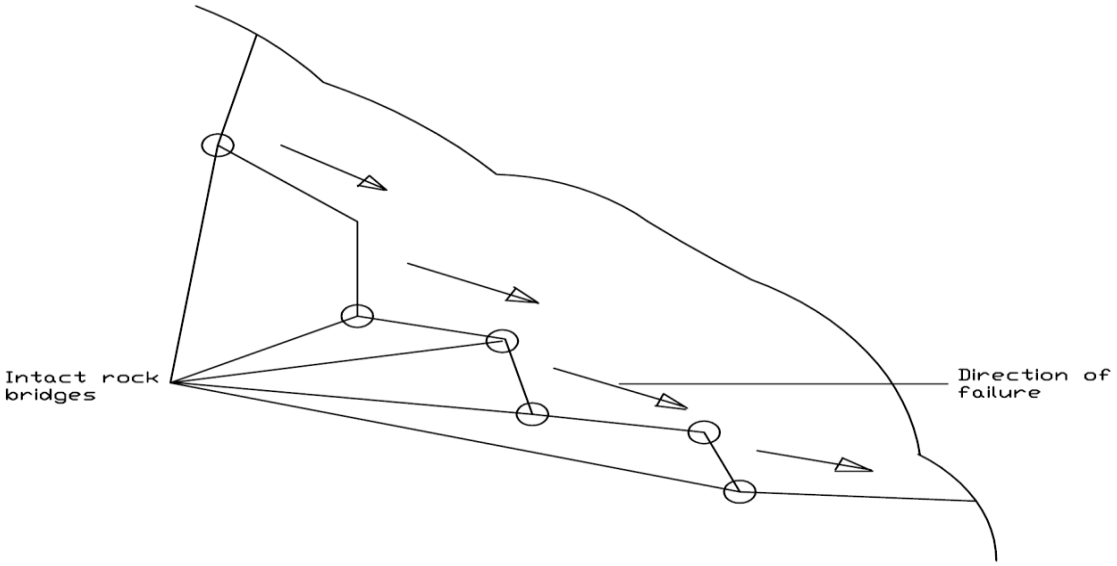


Figure 2.17: Complex failure mechanisms with multiple step-path failure (After Eberhardt, et al. 2004a and Stead, et al. 2006)

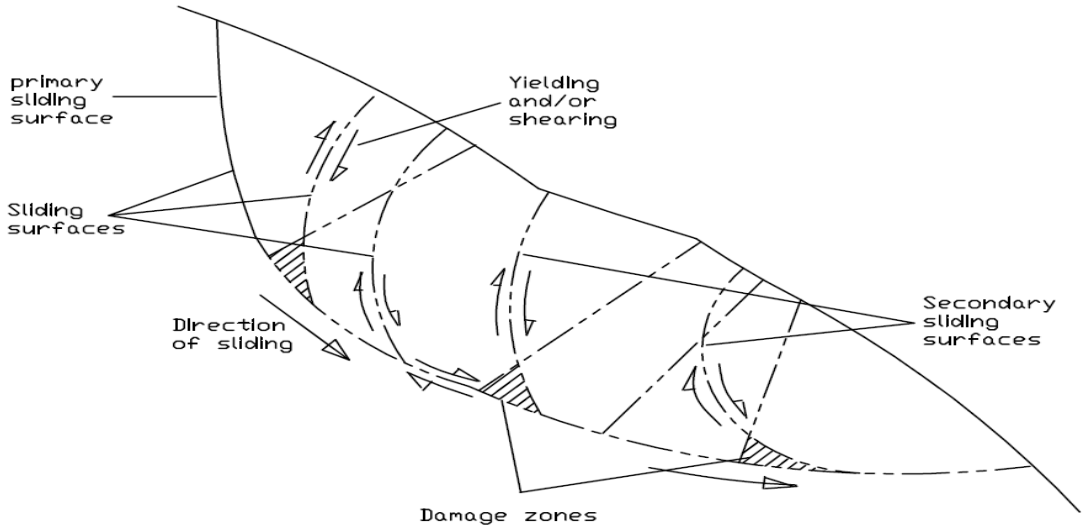


Figure 2.18: Complex failure mechanisms with deep-seated multi-block failure. Modified from Eberhardt, et al (2004a) and Stead, et al (2006)

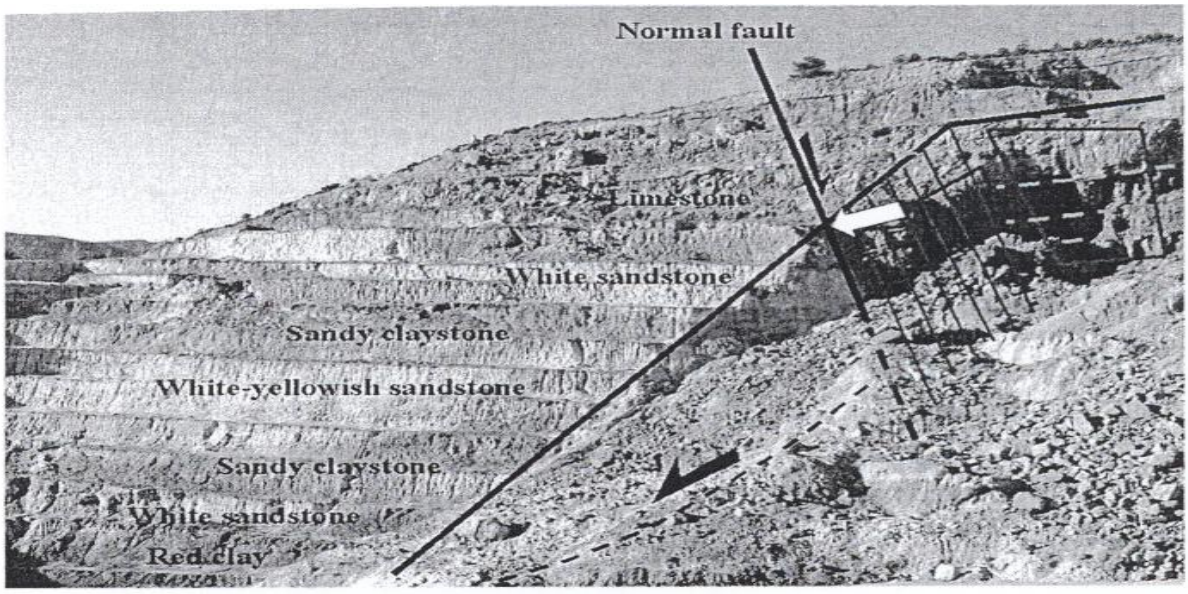


Figure 2.19: Toppling with circular failure (After Alejano, et al. 2010).

2.7. Deformation and Displacement Behaviour of Surface Mine Slope with Time

According to Lajtai and Schmidtke (1986) and Lajtai and Bielus (1986), the knowledge of time dependent behaviour of rock mass is important in understanding and predicting the long-term stability and deformation of rock slopes. Although the time-dependent deformation of rock is assumed to be small except with ductile salt rocks. However, with prolonged constant stress loading, most rocks experience about 50% reduction in strength (Lajtai and Schmidtke, 1986; Lajtai and Bielus, 1986). The time-dependent response to excavation is a function of the mechanical properties of the rock mass, structural geology, slope geometry, excavation rate, the failure mechanism and the effect of external forces such as groundwater pressures, seismic activity and in-situ stresses (Zavodni, 2000). Eberhardt, et al (2004a) in a model of the Rand Rockslide suggested that, in the absence of any triggering event, the main contributing factor to the landslide was brittle strength degradation and progressive failure resulting from time-dependent mechanisms. The Pandemonium creek rockslide in western Canada was caused by gradual long-term reduction in rock mass strength (Eberhardt, et al. 2004a).

Zavodni (2000) stated that rock slopes experience three different phases of time-dependent deformation behaviour as follows:

Phase I - Initial response;

Phase II- Regressive failure stage, which is short-term decelerating displacement; and

Phase III- Progressive failure stage, which is strain-softening and large-scale deformation leading to failure.

2.7.1. Initial Response

Zavodni (2000) stated that all slopes experience a stage of initial response as a result of elastic rebound, relaxation and dilation of the rock mass due to changes in stresses caused by excavation. However, initial response of slope to excavation is rarely reflected in monitoring data since monitoring only starts long after the first excavation (Zavodni, 2000). The initial deformation occurs without the development of a defined failure surface or failure mechanism with movement in the range of 0.1 to 4mm/day (Martin, 1993, Zavodni, 2000).

2.7.2. Regressive Failure/ Progressive Failure

A regressive failure occurs when the slope shows short-term decelerating displacement cycles if disturbing events external to the rock are removed from the slope environment. A progressive failure on the other hand occurs when the slope displaces at an accelerating rate, usually an algebraically predictable rate to the point of failure, unless effective control measures are taken (Zavodni 2000).

It is important to determine its regressive or progressive state of a slope to enable effective correction efforts the moment a failure situation is recognised. To correct a regressive displacement condition, the external cause must be removed, examples of such control measures include, dewatering, control blasting, and buttressing. On the other hand, a progressive failure requires immediate planning to avoid the consequences of possible collapse (Zavodni 2000).

Figure 2.20 shows regressive/progressive displacement stage and the different stages in the curves. Curve A is considered a regressive curve, because of the deceleration of each cycle between external stimuli at points 1, 2 and 3. Curve B shows the progressive stage, which display an accelerating state. Curve C shows the transition from regressive to progressive stage (Zavodni, 2000).

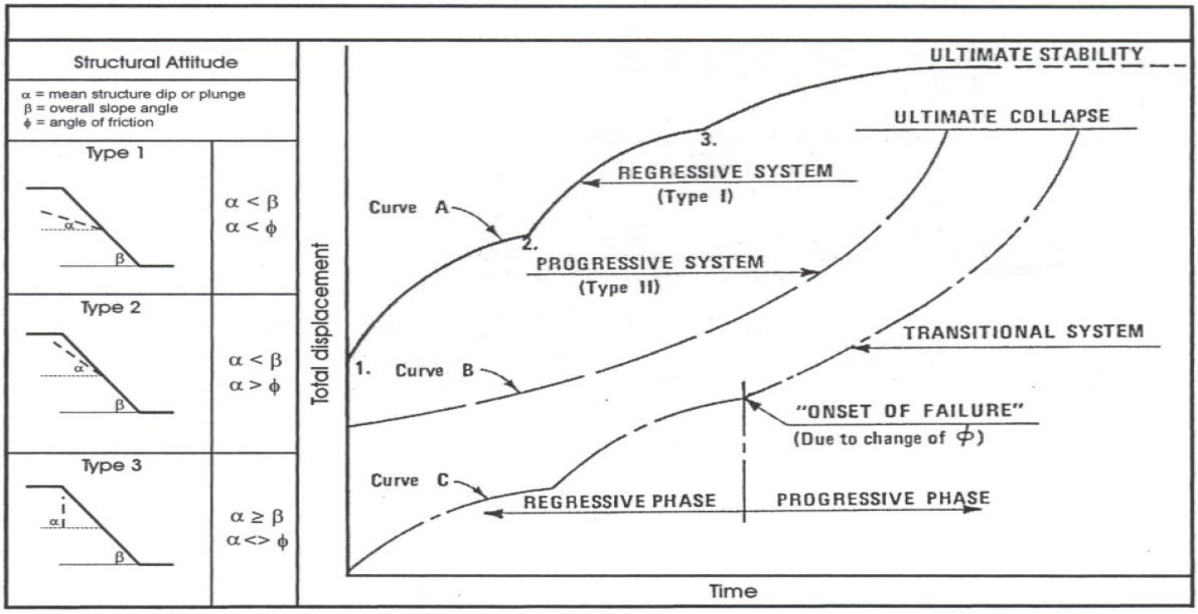


Figure 2.20: Typical regressive/progressive stage displacement curves (Broadbent and Zavodni, 1982).

As illustrated in figure 2.20, the geological conditions that may lead to progressive failure are discontinuities that dip out of the face at a steeper angle than the friction angle (Type II). Progressive failure may also occur when the shear strength of a slide surface gradually reduces with displacement. Zavodni and Broadbent (1980) specified that the duration of the progressive stage of failure is between 4 days to 45 days.

After an extensive review of various slope failures in different mines around the world, Mercer (2006) further divided the situation before the onset-of-failure in the Broadbent and Zavodni model, as shown in figure 2.20, into two categories, namely category 1 and 2. According to him, category 1, pre-onset-of failure deformation behaviour is driven by continuous period of specific, macro event such as mining and they are therefore event driven. Mercer (2006) further stated that category 2, pre-onset-of-failure deformation, does not involve a continuous period of a specific macro event such as mining, and that the onset-of-failure can occur with little or no prior warning, this means that the deformation patterns can be attributed to micro events, such as crack propagation within the rock.

Mercer (2006) in his work illustrated in figure 2.21, classified the stages in the deformation of a mine slope into:

Stage 1 - Pre-collapse, primary rock mass creep modes;

Stage 2 – Pre-collapse, secondary rock mass creep modes;

Stage 3 – Onset of failure to collapse behaviour modes;

Stage 4 – Post-collapse behaviour modes; and

Stage 5 – Post-mining/recovery behaviour modes.

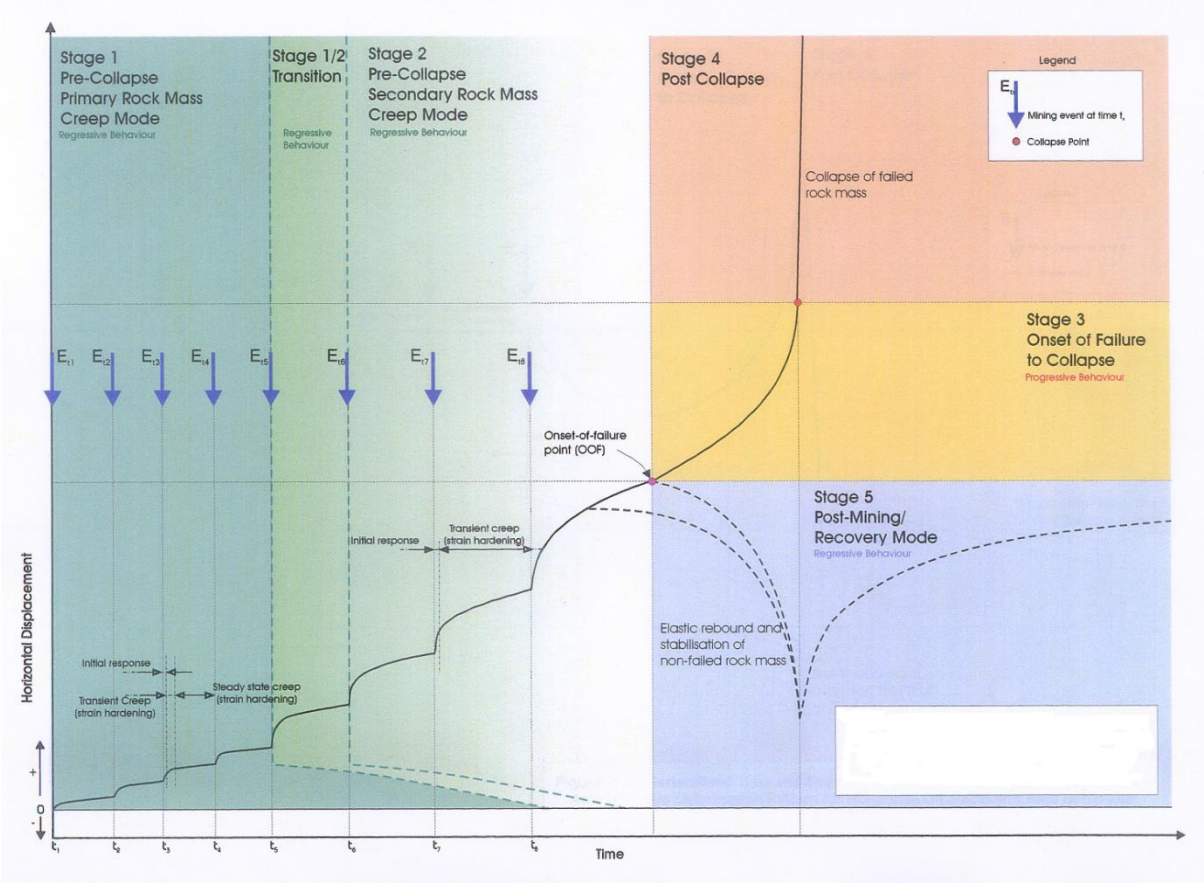


Figure 2.21: Generalised time and event dependent rock mass deformation model (After Mercer, 2006).

The pre-collapse primary rock mass creep mode namely stage 1 of Mercer's model, represents the regressive stage (type I, figure 2.20) in Zavodni's model. The pre-collapse secondary rock mass creep mode, stage 2, is equivalent to the progressive system (type II, figure 2.20). The onset of failure to collapse behaviour mode, stage 3, is the same as the transitional system, where-in the slope experiences a transition from progressive displacement to failure. The most significant difference in the two models is the inclusion of the post-collapse behaviour of mine slopes classified as stage 4 and stage 5 in Mercer's model, which is illustrated in section 2.8.

2.8. Post Collapse and Post Mining Behaviour Mode (Stage 4 and 5)

Stage 4 constitutes the progressive displacement behaviour of the slope immediately after failure while stage 5 is the post-mining behaviour of the slope. Mercer (2006) identified six principal post collapse deformation modes, as seen in figure 2.22, in the post collapse stages which are named as:

$S_{4\text{-type }1}$: Disintegration;
$S_{4\text{-type }2}$: Partial recovery and gradual deceleration to creeping;
$S_{4\text{-type }3}$: Full recovery, velocity almost completely stops;
$S_{4\text{-type }4}$: Partial recovery followed by another final collapse;
$S_{4\text{-type }5}$: Ratchet mechanism; and
$S_{4\text{-type }6}$: High creeping rate and probably accelerating.

Mercer (2006) stated that a complex deformation mode may occur if the failed slope alternates between types 2 to 6, and could be in a matter of minutes to years. The deformation mode can also change from a progressive state to a regressive state depending on transient factors such as changing phreatic surface, seismicity and changing geometry (Mercer, 2006). The post-mining state involves the long-term stabilisation of the rock mass, although transition from stage 5 back to stages 3 and 4 may occur based on long-term creep theory. At stage 5, the slope is in a regressive state of recovery (Mercer, 2006).

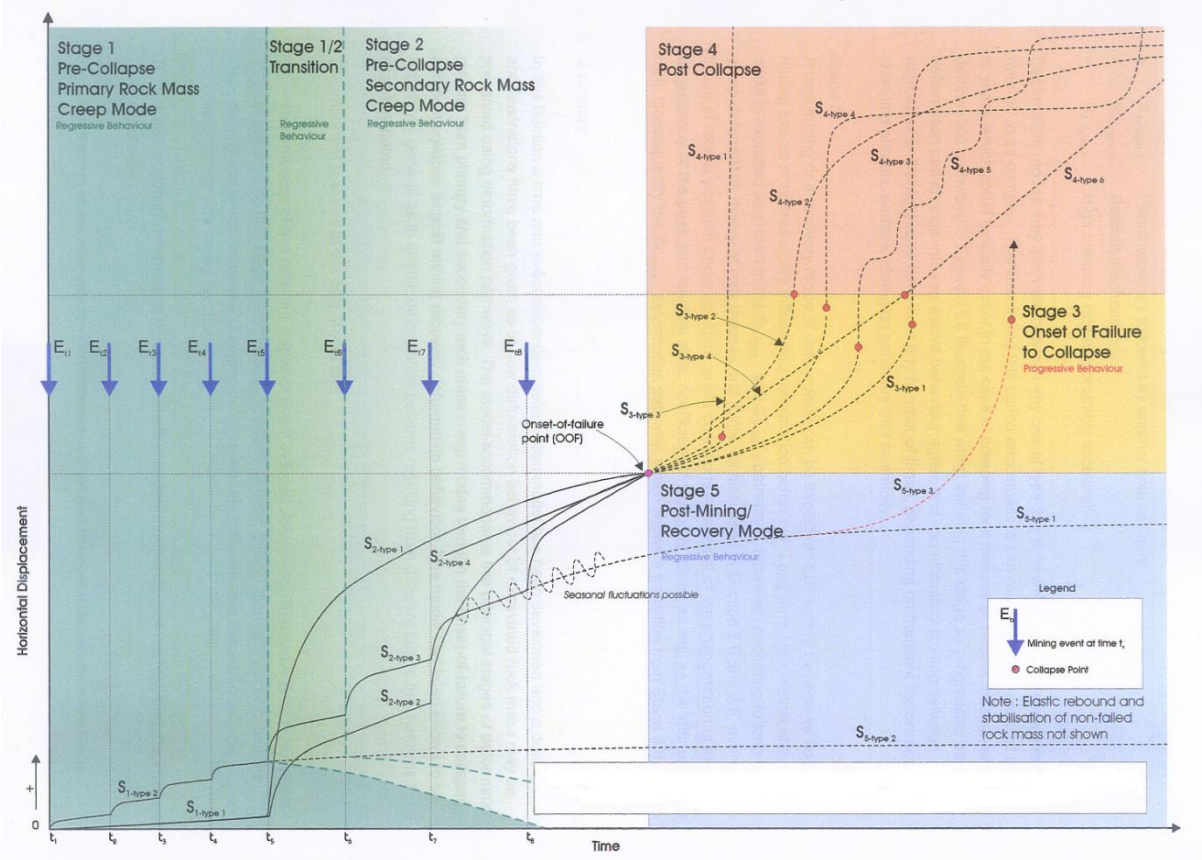


Figure 2.22. Generalised time and event dependent rock mass deformation model showing post collapse and post mining behaviour modes (Mercer, 2006).

2.9. Long Term Horizontal and Vertical (Downwards) Creep Deformation (Relaxation) Resulting from Excavation:

Call, et al. (2000) found that most creep deformation in mine slopes results from response of the rock mass to mining activities. Martin (1993) equally reported that the rate of response of rock mass subsequent to each mining event normally decreases from an initial rate of several millimetres per day to no movement over a period of time. He also showed that this decrease in response rate takes the form of a negative exponential relationship of the form:

$$R^i = Ae^{-bt} \qquad 2.2$$

Where:

R^i = rate of movement

A, b = constants depending on rock mass properties, slope geometry, which includes height and angle, mining rate, external influences and failure mechanism. Long-term creep may

occur where there is no defined failure surface, such as toppling failure, or where the change in slope geometry is very slow. Creep is fast in mine slopes and slow in mountain slopes where it may occur over hundreds of years (Martin, 1993).

2.11. Slope Movement (Velocity) Scale

Varnes (1978) classified the movement or velocity of natural slopes, as shown in table 2.1. However, the natural slope classification cannot be unilaterally applied to surface mine slopes, because of the different geology of the two.

Table 2.1: Slope Movement Scale (After Varnes, 1978)

Rate	Definition of Movement
>3m/s	Extremely rapid
>3m/min	Very rapid
>1.5m/day	Rapid
>1.5m/month	Moderate
>1.5m/year	Slow
>0.006m/year	Very slow
<.006m/year	Extremely slow

2.12. Summary

Rocks deform in various forms at different displacement magnitudes and rates under varying combination of factors. Deformation could be simple and straightforward when it occurs on pre-existing structural discontinuities, or through intact rock mass or complex when it involves a combination of failure modes, as highlighted in section 2.6 (Pitteau and Martin, 1982). The failure of mine slopes from rock deformation differs from one mine to another and sometimes from slope to slope within the same mine, thus, the issue of slope failure must be treated as mine and site specific. Pavlovic (1998) affirmed that the same rock mass in different circumstances may exhibit different reactions. Therefore, it is very important to know the possible influences of these natural and human factors on the rock mass and put them into consideration during analysis and design of mine slopes.

Monitoring the deformation behaviour of surface mine slopes has become a crucial part of mining operations. The available slope monitoring systems, together with the equipment used are discussed in chapter 3.

CHAPTER THREE

MONITORING SLOPE STABILITY

3.1 Introduction

Mining activities by open-pit or underground methods create volumetric, as well as stress and strain changes in the rock mass around a mine opening (Kayesa, 2006). Instability is generated around the mining excavation when the stress created by mining activities exceeds the rock strength (Kayesa, 2006). A review of the deformation behaviour of mine slopes caused by mining was presented in the previous chapter. The slope monitoring systems and existing technologies for achieving the objectives of a good slope monitoring programme are reviewed in chapter 3.

The most important slope stability management tool consists of a well established slope monitoring program. Kayesa (2006) defined slope stability monitoring as the recording of the stability of the rocks making up the slopes surrounding an open-pit mine. Monitoring involves periodically and automatically measuring reference points in or around an unstable area to determine the deformation.

Diligent monitoring and examination of slopes for warning signs is crucial for protecting workers and equipment. Geotechnical designs can be improved to increase factors of safety and proper bench designs can be improved to minimise rock fall hazards. However, even slopes with conservative slope designs may experience unexpected failure due to the presence of unknown geological structures, abnormal weather patterns and seismic activities (Girard, 2001). Unanticipated movement of any amount of rock may cause severe disruptions to mining operations, pose major safety concerns, results in fatalities or contribute to large financial losses for companies (Girard, 2001).

The main objectives of slope stability monitoring, as stated by Kayesa (2006) are:

- To verify mine design. Slope monitoring measurements are used as a basis for maintaining, steepening or reducing slope angles with the resultant economic and safety benefits. Slope monitoring measurements can also be used as a basis for future mine design;

- To give technical assurance to mine personnel on the stability status of the open-pit mine;
- To serve as a warning system as to which areas of the pit are unstable;
- To give measurements of rates of movement in the unstable zones; and
- To serve as a major slope stability risk management tool. Slope failure can have serious economic consequences on an open pit mine. Therefore slope monitoring is essential for making management decisions for the safety of workers and equipment, For example, not working below an unstable area, adopting special blasting precautions or evacuation.

Sjoberg (1996) stated that the three main objectives of a slope monitoring programme are to:

1) Maintain safe operational practices;
2) Provide advance notice of instability; and
3) Provide additional geotechnical information regarding slope behaviour.

3.2 Slope Monitoring Steps

Cawood and Stacey (2006) stated that the slope monitoring process involves five major steps, which starts with monitoring requirements. Monitoring requirement entails establishing the objectives, requirements, economic and safety advantages, investigating previous slope stability problems and finally preparing a detailed report to the mine management highlighting the need for monitoring. The project requirements based on pit design and risk assessment is established in the second step. The results of the second step must include the probability of failure and the variables that will most likely contribute to such failure (Cawood and Stacey, 2006). The third step involves designing the monitoring system, considering instrumentation and implementing the monitoring system (Ding, et al. 1998). The fourth step is the actual displacement measurement and recording of field data. Measuring techniques and frequencies, accuracy, precision and personnel responsibilities are very vital at this stage. The fifth step is the interpretation and reporting of monitoring data. The reporting of results and documenting of events, decisions, design changes and cost-benefit analysis complete the monitoring process (Cawood and Stacey, 2006). A typical monitoring strategy adopted at Potgietersrust (PPRust) open pit operation in South Africa is depicted in figure 3.1. The first section in figure 3.1 which shows the monitoring instrumentation corresponds to the third step in the monitoring process mentioned in Cawood and Stacey

(2006). The fourth step is similar to the identification of critically unstable areas and detailed inspections while the fifth step corresponds to the evaluation procedures.

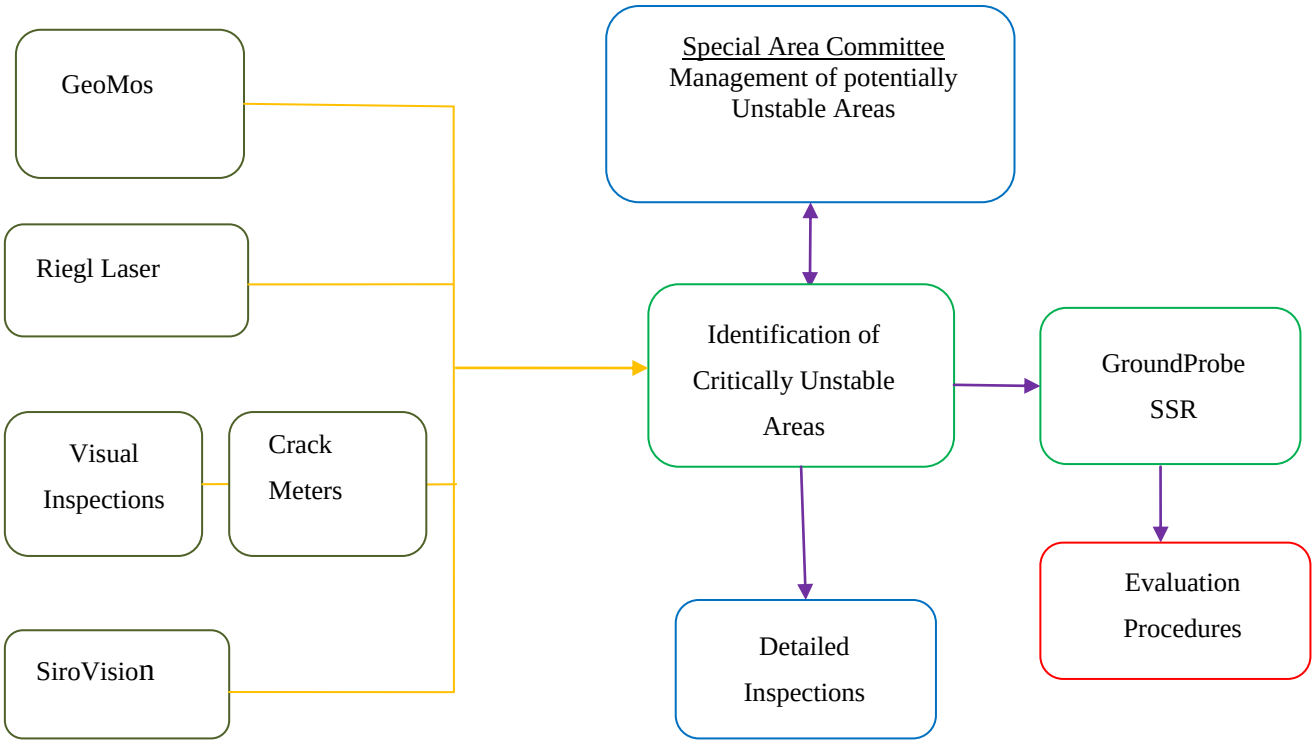


Figure 3.1: Slope monitoring strategy at PPRust open pit, Limpopo, South Africa (After Little, 2006a).

3.3 Slope Monitoring System

As illustrated in figure 3.2, a slope monitoring system can be divided into four sections namely, Visual monitoring, surface measurements, subsurface measurements and remote monitoring technologies. These divisions of a slope monitoring system will be discussed briefly in this section. A very cogent factor in an effective slope monitoring system, as pointed out by Little (2006a), is the creation of a comprehensive database system for the large volume of geotechnical information obtained from the mine. All data from exploration core logging, face mapping, rock testing, water and slope monitoring must be incorporated into the database system to ensure that no data is lost, and that the data is available for safe and productive slope design.

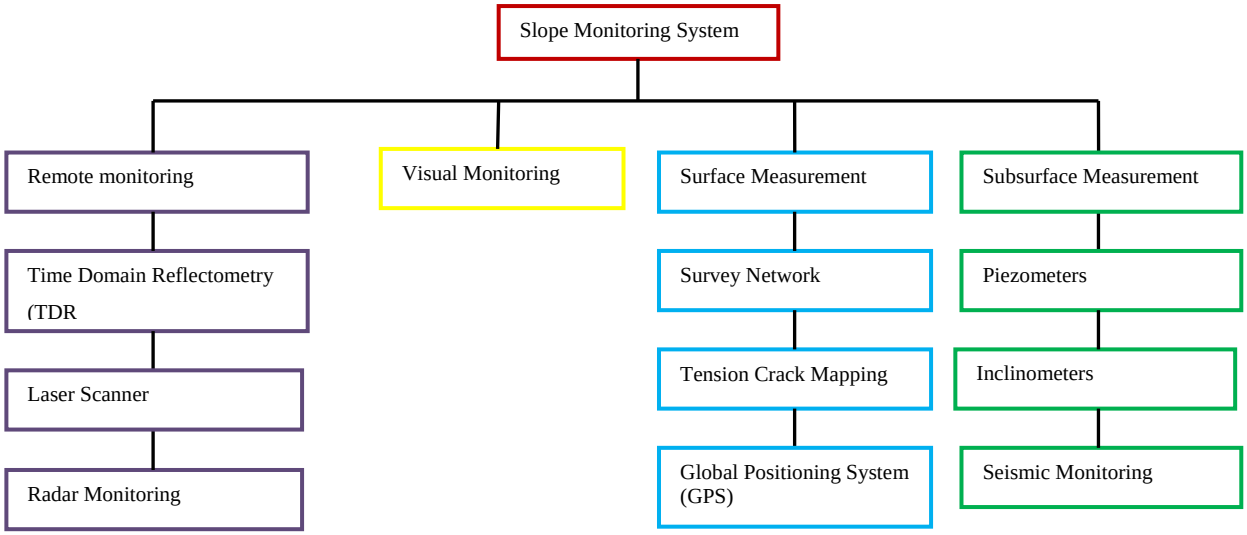


Figure 3.2: Slope monitoring system

3.4. Visual Monitoring

Visual monitoring of slope is conducted by routine inspections of the pit, access ways, high-walls, low-walls such as those in coal mines and crest that are close to potentially dangerous working areas by the geotechnical engineer. The engineer compares the last visit observations with the latest one and records any deleterious slope stability changes that may have occurred (Kayesa, 2006). The recording of any changes that occur on the open-pit slope faces by production personnel during the shift is another way of visual slope monitoring (Kayesa, 2006). Visual observations and monitoring are at the core of any monitoring programme, it is an integral part of the whole monitoring programme. Where there is accessibility, slope monitoring starts with visual inspection. Every morning before the commencement of mining operation, the geotechnical engineer or the geologist, as it applies, should walk around the mine for any visible sign of displacement. This should subsequently be reported for detailed monitoring, if necessary. Thus, every personnel involved in any operation in the mine should be indirectly involved in slope monitoring. Visual inspection, as conducted at the Potgietersrust Platinum (PPRust) Mines is grouped into four categories by Little (2006a) as:

- Daily inspections, which is performed daily by a geotechnical assistant in all working areas;
- Detailed Inspections, which is performed by a rock engineer after a Fall Of Ground (FOG), or when an unstable area is identified;

- Monthly hazard plan inspections, which is performed by a rock engineer at the end of each month for risk calculations; and
- Presplit inspections, this is performed by a geotechnical assistant on all blasted final walls.

3.5. Surface Measurement

3.5.1. Survey Network

Target prisms located on and around areas of anticipated instability on the pit slopes with one or more control points for survey stations constitute a survey network (Girard and McHugh, 2000). The stations must be located close enough to the pit crest for good visibility of all prisms, and they must also be located on completely stable ground (Girard, et al. 1998). Electronic total station that is established inside a small hut located at the station built for such purposes measures the angles and distances from the survey station to the prisms on a regular basis to establish a history of movement on the slope (Girard, et al. 1998).

Displacement data recorded by the total station is transmitted by a radio located close to the pit edge to the survey office where a computer fitted with appropriate software is located. Data enters the computer as survey coordinates of the individual prism targets. Correction for temperature and atmospheric changes is made by incorporating data collected by a combined temperature/atmospheric pressure transducer. Changes that have occurred with respect to the original position of the slope monitoring targets are calculated by the software and shown in graphical format (Kayesa, 2006). The Geodetic Monitoring System (GEOMOS) is a typical survey network for slope monitoring that runs for 24 hours a day, the system is subdivided into three parts namely data collection, date transmission, data processing and analysis (Kayesa, 2006). Nowadays, the optical mechanical theodolites are rarely used for slope monitoring, because of their low efficiency and the often significant atmospheric refraction errors in observed angles (Ding, et al. 1998). Errors caused by atmospheric factors, such as dust and haze, constitute a major problem of the survey system of slope monitoring (Ding, et al. 1998). Human error, damage to prism or displacement of the survey station as well as errors introduced by instrument or reflector set-up inaccuracies can equally affect measurement accuracy. In some locations, prism theft is another concern. (Ding, et al. 1998).

3.5.2. Tension Crack Mapping

One of the first noticeable signs of instability in a surface mine slope are the formation of cracks. "Measurement and monitoring the changes in crack width and direction of crack propagation is required to establish the extent of the unstable area" (Girard and McHugh, 2000). As suggested by Girard and McHugh (2000), observed cracks should be painted or flagged with bright colours for easy detection of new cracks during routine inspections and to notify mine personnel of the risk in such areas. Crack measuring pins located on both sides of the crack are used for measuring tension cracks. The displacement of the crack is determined by measuring the distance between the pins with a measuring tape or a vernier calliper (Hawley, et al. 2009).

Movement across tension cracks can also be monitored with a portable wire-line extensometer. Tension crack mapping is conducted with a wire anchored in unstable section of the slope with the monitor and pulley station positioned on a stable portion of the slope somewhere behind the last tension crack (Girard and McHugh, 2000). The wire runs over the top of a pulley and is tensioned by a weight suspended from the other end. When the unstable section moves away from the pulley stand, the weight moves and the displacements is recorded either manually or electronically (Girard and McHugh, 2000). Errors can be caused by long lengths of wire due to sag or to thermal expansion, so readjustments and corrections are often necessary. The length of the extensometer wire should be limited to approximately 60m (197ft) to keep errors due to line sag at a minimum (Call and Savely, 1990).

Most of the extensometers have a digital readout. Readings from the digital readout can be taken manually by site personnel or can be stored in an electronic data logger and later downloaded to a personal computer. Ding, et al (1998) suggested that electronic extensometers are very effective when linked to an alarm system. When reading exceeds a pre-set threshold, an alarm can be set off automatically to notify mine personnel of the potential danger of slope failure (Ding, et al. 1998). Under normal situation, this works very well but they can be triggered accidentally by falling rocks, birds or wild animals. However, extensometers are economical and very effective in defining the relative movements between points either on the surface or inside a pit (Ding, et al. 1998).

3.5.3 Global Positioning System (GPS)

GPS is a potential tool for surface mine slope monitoring (Ma, et al. 2007). However, the major drawback in using GPS for slope monitoring is the high cost of installing a permanent GPS receiver at each monitoring point. In order to overcome this limitation, at Xiaowan hydropower station, China, a GPS multiple-antenna switch (GMAS) that links a single GPS receiver with multiple antennas mounted at several monitoring points was developed (Chen, et al. 2005). The GPS slope monitoring system used at Xiaowan, China consists of the GMAS with antenna array and low-noise amplifier, the GPS receivers, the data link component and data processing centre (Chen, et al. 2005 and Zhang, et al. 2008). According to Chen, et al (2005), GPS slope monitoring system is highly automated, less labour intensive and offers high accuracy.

3.6 Subsurface Measurement

3.6.1 Piezometers

The effect of ground water present within the rock mass surrounding an open pit can be detrimental to the stability of the slope (Hoek and Bray, 1981) Therefore, it is expedient to constantly monitor groundwater levels as well as pore pressure to assist in the assessment of slope stability (Ding, et al. 1998). Piezometers are important for monitoring the effectiveness of mine dewatering programmes (Girard and McHugh, 2000). Measurement or calculation of water pressure is an integral part of site investigation for slope stability studies. Information on water pressures is essential for designing and maintaining safe slopes (Girard, et al. 1998).

3.6.2. Inclinometers

Inclinometers as depicted in figure 3.3 are used to monitor slopes and landslides to detect regions of movement and establish whether movement is constant, accelerating or responding to remedial measures by decelerating (Girard, et al. 1998). An inclinometer consists of a casing that is placed in the ground through the area of anticipated displacements. The end of the casing is fixed so that the lateral profile of subsurface displacement can be calculated (Girard and McHugh, 2000). The movement in the surrounding rock mass is calculated by measuring the inclination of the sensing unit at various points along the length of the installations (Girard and McHugh, 2000; Wyllie and Mah, 2004).

Kliche (1999) stated that the displacement information collected from inclinometers can be used to locate shear zones and to determine whether movement along the shear zone is steady, accelerating or decelerating. Correct placement for inclinometers for monitoring displacement of both shallow and deep-seated failure planes is shown in figure 3.4.

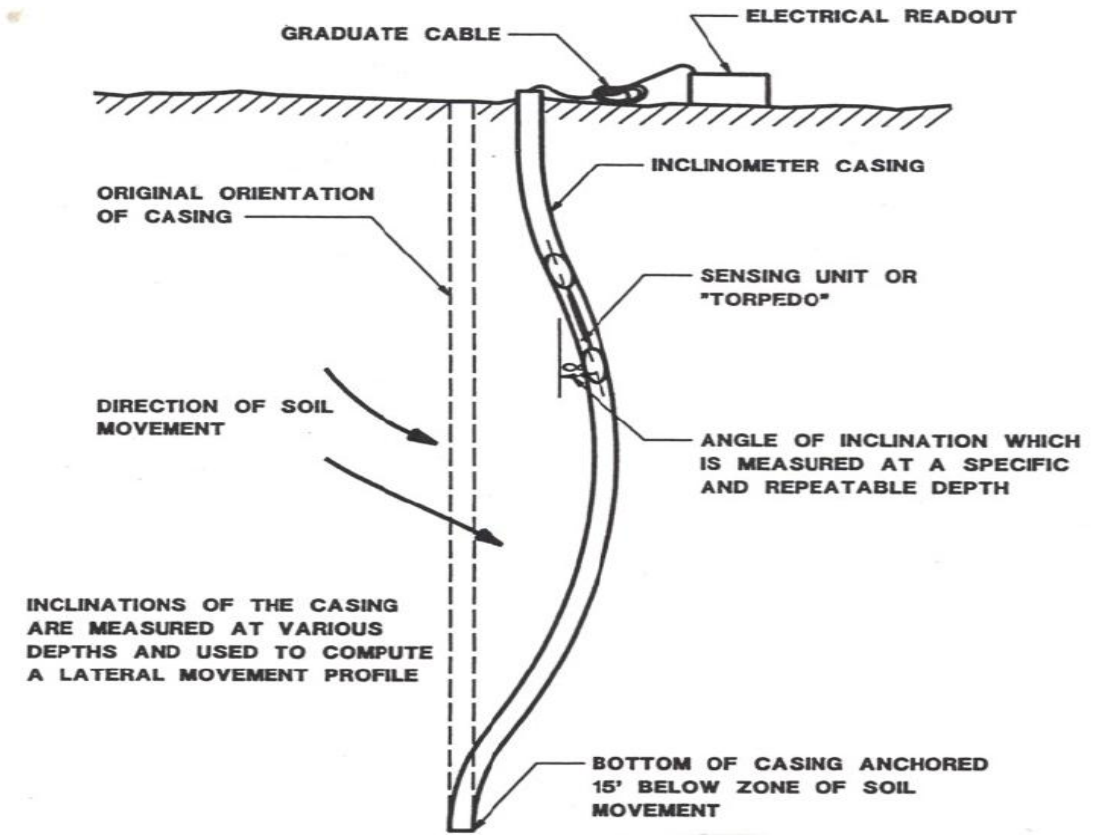


Figure 3.3: Portable borehole inclinometer system (Abramson, et al. 2002).

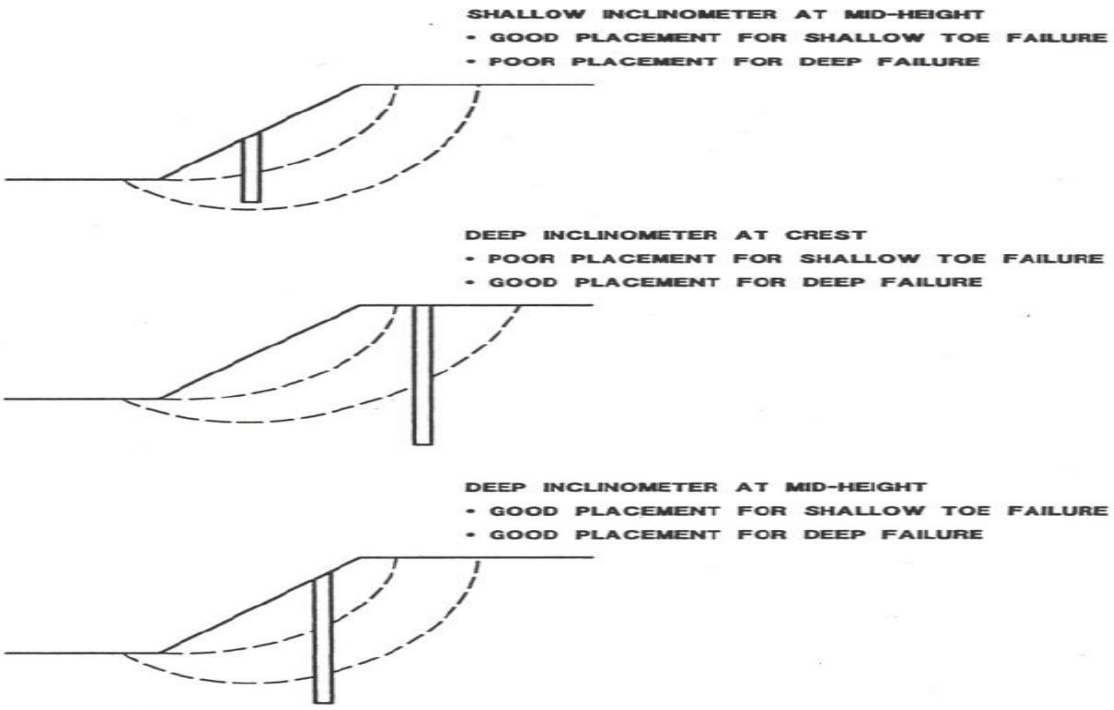


Figure 3.4: Proper inclinometer placement in a slope (Abramson, et al. 2002).

3.6.3 Seismic Monitoring

"The occurrence of seismicity in rocks is an indication of the development of new fractures due to stress" (Stacey, 2007). The benefit of seismic monitoring is in its ability to effectively monitor the occurrence of micro-fractures in rock masses prior to the formation of macroscopic fracture at the slope surface (Xu et al, 2011). Wesseloo and Dight, (2009) referred to seismic monitoring with triaxial sensors to detect the extension of existing cracks as strategic monitoring. Seismic monitoring involves the use of seismic sensors installed in drill holes in the unstable areas of the slope. The sensor detects the microseismic activities within the slope and transmits the microseismic information to a central computer via a data logger at the top of the slope (Integrated Seismic System, 2007). The ability to monitor the stability of the rock mass behind the pit walls has greatly increased the use of seismic monitoring in open-pit mines in recent years (ESG Solutions, 2010). In the work of Xu, et al (2011), investigation of excavation-induced seismicity was successfully used to define failure zones at the right bank slope of Dagangshan hydropower station. Eberhardt, et al (2004b) utilised microseismic data collected at the Randa rockslide to establish the occurrence of microseismic activity in the slope. The information obtained from seismic monitoring can be

combined with other monitoring techniques for more effective slope management (ESG Solutions, 2010; Stacey, 2007).

3.7. Remote Monitoring Technologies

3.7.1. Time Domain Reflectometry (TDR)

Time domain reflectometry is a new approach to monitoring slope movement (Kane and Beck, 1994, 1996a and 1996b). TDR was initially developed to locate breaks and faults in communication and power lines, but now it is used to locate and monitor slope failures (Kane and Beck, 1999). With a cable tester, the TDR sends an electrical pulse down a coaxial cable grouted in a borehole. When the electrical pulse encounters a break or deformation in the cable, it is reflected as a "spike" in the cable signature (Kane and Beck, 1999). The relative magnitude, rate of displacement and the location of the region of deformation can be determined immediately and accurately (Kane and Beck, 1999). The magnitude of movement is determined by the size of the spike increase through a computer connected to the tester (Kane and Beck, 1999). As discussed by Kane (1998) TDR has the following advantages over traditional inclinometers:

- Lower cost of installation: cable cost is between 2% to 38% less than inclinometer casing;
- Deeper hole depth is possible: Inclinometers in deep hole require special winches and cables due to the extreme weight of the equipment. All TDR monitoring equipment are at the surface;
- Rapid and remote monitoring is possible: TDR data can be transmitted via telecommunications with scanning and recording intervals programmed remotely to examine zones of interest (Campbell Scientific Inc. 1998);
- Immediate deformation determinations: Locations of any movement are determined immediately using TDR. Additional data reduction is generally not necessary and the cables can be used to quantify rock movement in addition to distinguishing shear and tension (Downing, et al. 1989); and
- Complex monitoring situations: TDR cables have been installed in angled boreholes and have monitored deep zones below moving upper zones. Neither installation could have been done with traditional inclinometer.

3.7.2. Laser Scanner

The monitoring of every potential failure block at every location on a mine slope with survey network is unsafe and impractical, but a new generation of scanning laser rangefinders capable of detecting movement over large areas has partially addressed this problem (McHugh, et al. 2006). The laser scanner is an active, self-contained measurement technology that generates digital models of mine slopes without reflector prisms (McHugh, et al. 2006). The scanner detects displacement by comparing successive scans of the slope face.

A modern scanner called SiteMonitor as seen in figure 3.5, was initially developed by 3D Laser Mapping Ltd, UK for monitoring slope stability on old coal mine waste tips in South Wales, UK **(**Hunter, 2007). This laser scanner can record movements in the slope surface as small as 10mm with a distance range of up to 1000m. It also records and analyses up to 8,000 measurements per second to create a detailed, accurate and continuous record of the slope profile **(**Hunter, 2007).

As stated by Hunter (2007), Anglo Platinum, the world's largest producer of platinum has adopted the SiteMonitor for slope monitoring at some of its mines. The system is specifically designed for automatic and manual long-range profiling of surfaces, operating at distances up to 2,500 meters with 50 millimeters accuracy **(**Hunter, 2007). The systems perform continuous, remote scanning for 24 hours at locations determined by the company's geotechnical team, collecting displacement information of several points daily. The point data collected by the laser scanners, which appears as point cloud is automatically analysed using Site-Monitor software (Little, 2006a). The software can detect surface movement or slope deformation by comparing readings against base measurements. The new laser scanning technology is used at Kumba Iron Ore and De Beers Kimberley diamond mine in South Africa to improve slope monitoring (Hunter, 2007). The point cloud data are also useful for volume estimations (Little, 2006a).

Unlike the survey system of slope monitoring, laser scanner monitors large slope face rapidly without the use of prism at operating range of up to 2,500m. Laser scanner is portable and can easily be moved around. Also, the risk involved in installing prisms on unstable slope face is eliminated. However, compared to the radar monitoring system, laser scanner is not commonly used for slope monitoring because of lower accuracy (Hawley, et al. 2009).



Figure 3.5: Riegel LPM-2K SiteMonitor by 3-D Laser Mapping Ltd U.K (Hunter, 2007).

3.8. Radar

3.8.1. Introduction

Radar is an acronym for "Radio Detection and Ranging" The primary purpose of radar is detection and location of the range, altitude, direction or speed of both moving and fixed targets. In 1904, Christian Hulsmeyer became the first person to use radio waves to detect the presence of distance metallic object (Burn, 1988). As stated by Burn (1988), the objective of Christian Hulsmeyer was most likely to introduce a mechanism for detecting the presence of a ship in misty or foggy conditions. Radar operates by radiating electromagnetic energy and detecting the echo returned from reflecting objects or targets. The nature of the echo signal provides information about the target (Skolnik, 1990). The range or distance to the target is determined from the time it takes the radiated energy to travel to the target and back. The angular location of the target is found with a directive antenna to sense the angle of arrival of the echo signal. Radar can derive the path or trajectory of moving targets and predict the future location (Skolnik, 1990).

Nowadays, apart from military use, radar has found application in many areas of human endeavour, such as the measurement of ocean surface waves, air traffic control, meteorological detection of precipitation, police detection of speeding traffic and lately, in mining engineering for slope stability monitoring.

3.8.2. Basic Operation of Radar

Radar as defined by Skolnik (1990) is an electromagnetic sensor for the detection and location of reflecting objects. Its operations can be summarised by Skolnik (1990) are as follows:

- The radar radiates electromagnetic energy from an antenna to propagate in space;
- Some of the radiated energy is interpreted by a reflecting object, usually called a target, located at a distance from the radar;
- The energy intercepted by the target is reradiated in many directions;
- Some of the reradiated energy is returned to and received by the radar antenna; and
- After amplification by a receiver and with the aid of proper signal processing, the target location and possibly other information about the target is acquired.

3.8.3. Types of Radar

Radar can be classified based on the major features that distinguish one type of radar from the other as follows: Pulse radar, High resolution radar, Pulse compression radar, Continuous wave radar, FM-CW radar, Surveillance radar, Moving Target Indication (MTI), Pulse Doppler radar, Imaging radar, Sidelooking Airborne Radar (SLAR), Synthetic Aperture Radar (SAR), Inverse Synthetic Sperture Radar (ISAR), Weapon control radar, Guidance radar, Weather (meteorological) observation radar, Tracking radar, which includes: Single Target Tracker (STT), Automatic Detection and Tracking (ADT), Track-While-Scan (TWS), and phased array tracker (Skolnik, 1990).

3.8.4. Synthetic Aperture Radar

Synthetic Aperture Radar (SAR) is a ground-mapping radar initially designed to be used from aircraft and satellites (Girard, et al. 1998). SAR can be used to generate terrain maps, to

produce high-quality Digital Elevation Models (DEM) and to detect surface disturbances or changes in surface moisture (Girard, et al. 1998).

SAR can operate in all weather conditions, day and night, producing high-resolution images of the earth's surface (Girard, et al. 1998). Interferometry Synthetic Aperture Radar (IFSAR or INSAR) is a technique of generating elevation maps and surface change maps by combining two or more SAR images of the same area (NASA, 2011). The introduction of spaceborne radars has allowed IFSAR to be used for studying a number of natural processes including earthquakes, volcanoes, glacier flow, landslides, ground subsidence and structural stability (Peltzer, 2010). In recent time, IFSAR is being used in the monitoring of unstable slopes in surface mines. Using INSAR images of August 1995 to August 1997 of the Frank Slide, Singhroy and Molch (2004) demonstrated that the images showed a near circular fringe corresponding to a maximum displacement value of -1.3cm, which indicates a possible rock motion before the 6000 tons rock fall of 2001.

Girard, et al (1998) found that the advantages of IFSAR over other types of monitoring systems are its effectiveness in working in all weather conditions. IFSAR can acquire imagery through fog, mist, rain, haze or cloud cover and can operate during both the day and night. Another great advantage is the ability to monitor a large area for ground displacement, which gives it an edge over other monitoring systems, such as survey networks, surface extensometers that sample movement at a few select points on the slope face (Girard, et al. 1998).

3.8.5. Slope Stability Radar (SSR)

In 2002, at the University of Queensland, Australia, a group of researchers designed a scanning radar system shown in figure 3.6, specifically for monitoring mine slopes using differential interferometry (University of Queensland 2002). The system, known as the Slope Stability Radar (SSR), uses real aperture 2° beam-width radar to scan a slope in both vertical (height) and horizontal (azimuth) directions. Scanning at a rate of 10° per second over a range of ±60° vertically and 340° horizontally, the system continuously monitors the slope face for deformations (University of Queensland 2002). The return signal phase is recorded for each point in the resulting image and phase unwrapping is used to remove the 2π ambiguity

(Reeves, et al. 1997). The SSR is a trailer-mounted unit with a 0.92m diameter scanning parabolic dish antenna, controlling/data collecting computer, remote area power supply, warning siren and lights, CCD camera, communication links, and internet compatibility. A typical scan repeat time is 15 minutes (McHugh, et al. 2006).

The SSR-X model can operate at a maximum range of 2800m from the target slope. The line of sight displacement can be measured to ±0.1 mm without the use of reflectors. The SSR can scan up to 270^0 horizontally and 100^0 vertically without being affected by vibration and local mining equipment. As stated by GroundProbe (2011a), the SSR systems have operated in extreme and varied weather conditions, from -60^0C to $+50^0$C temperatures, during 120mm/hour rain. Another important feature of the SSR is its ability to georeference deformation and photo overlays with mine coordinates and exports it to mine planning and design packages (GroundProbe, 2011a). In operation, the system scans a region of the wall and compares the phase measurement in each region with the previous scan to determine the amount of movement of the slope. It then produces an image showing spatial deformation relative to a reference image for the entire slope scanned. The displacement history of each point in the image can be plotted (Ground Probe 2003).

The SSR presents the total displacement on the slope face as colour rainbow plots, which quickly allows the user to determine the extent of the failure and the area with the maximum movement. Alternatively, the time/displacement graphs at any location can be displayed to evaluate the rates of displacement at that location (GroundProbe, 2003). Additional software is also installed to allow the data to be viewed and analysed at locations remote to the SSR site, such as offices of authorised geotechnical personnel.

The SSR systems have been deployed in many metalliferous and coal mines around the world (Noon, et al. 2011). Over 500 rock slope failure and waste dump failures have been monitored and on every occasion, precursor “warning” movements were recorded by the SSR (Harries, et al. 2006; Noon, et al. 2011). Cahill and Lee (2006) reported that the SSR has been in use since 2002 at Leinster nickel mine, Australia, for monitoring mine walls in areas with low confidence levels on the ability of prisms and visual inspection to predict failure. The Phelps Dodge Sierrita Mine is the first mine in the United State of America to use the SSR.

At the time, the SSR was the only system in the world that provided continuous sub-millimetre measurements of rock wall movements across the entire face of a wall (GroundProbe, 2003).

In 2010, GroundProbe introduced another slope monitoring equipment called the Work Area Monitoring (WAM). WAM as illustrated in figure 3.7, like the Slope Stability Radar uses a high-resolution camera and radar technology to allow a work production crew to quickly select an area to monitor. If displacement is detected on the mine slope, the machine alerts the mining personnel via wireless Personal Alerts (PALS) by displaying text messages, audio and vibrating alerts, as well as local sirens and lights (GroundProbe, 2011b). The machine, unlike the SSR, is simple to set up with automatic stabiliser legs operated by remote control and can be mounted on a truck (GroundProbe, 2011b). WAM is designed specifically to monitor dangerous work area where slope displacement is anticipated by the production crew (Noon, et al. 2011).



Figure 3.6: Slope Stability Radar (After Hawley, et al. 2009).



Figure 3.7: Work Area Monitoring (WAM) (GroundProbe, 2011b).

3.8.6. Movement and Surveying Radar (MSR)

A contemporary of the SSR called the Movement and Surveying Radar (MSR-200) was introduced into the market in January, 2006 by Reutech Radar Mining a division of Reutech Ltd. South Africa. The MSR 200 provides fully geo-referenced surveying information, thus allowing areas that are not hitherto accessible to be surveyed (Reutech, 2006a). This ability is made possible because the system incorporates a fully integrated total station, which is a surveying instrument that allows the MSR-200 to be accurately geo-referenced. The survey measurement of the MSR is capable of measuring 3-D information of the slope surface and can also be used to determine the amount of materials removed (Reutech, 2006a). Another brand model, MSR-300 as seen in figure 3.8, was introduced in June, 2008 as an improvement on the MSR-200. Like the SSR, the MSR-300 is capable of detecting sub-millimetre movement of the rock face. The MSR-300 offers continuous slope monitoring and surveying of rock surfaces up to a slant range of 2500m under all weather conditions. The MSR-300 is protected from false alarms during sudden environmental changes, such as rain, dust storms or mist formations. It equally offers significant improvement in the system's surveying capability (Reutech, 2008). The MSR system has the capacity to scan the full slope surface in real time. Data and displacement for each point and for the whole scan region can also be viewed separately (Reutech, 2006a). With radar monitoring, the displacement information of several points on the slope can be analysed to determine the precise points

where high displacement is taking place, and the magnitude of such displacement. The displacement also provides information on the regressive or progressive state of the deformation. This information can be used to determine the extent of the failure, and possibly estimate when failure will occur. Like the SSR, the MSR is gaining popularity in managing and monitoring sub-millimetre movements in mine slopes around the world.

The MSR is currently utilised in Africa, South America, United States of America, Europe, Indonesia, Papa New Guinea and Australia. Specifically, it is been used by Anglo Gold Ashanti in its Navachab open-pit mine in Namibia, Sadiola Gold mine in Mali and Sunrise Dam Gold mine in Australia (Reutech, 2006a). Six MSRs are in use at different mines operated by Anglo Coal in South Africa.

The latest product from Reutech (Pty) Ltd is the MSR-060V, shown in figure 3.9. It is truck-mounted and can quickly be deployed in critical work areas where urgent monitoring is required (Reutech, 2011). The machine offers the fully integrated slope monitoring capabilities of the MSR-300, but is limited to an operating range of 600m (Reutech, 2011).



Figure 3.8: Movement and Surveying Radar, MSR-300 (Reutech, 2008).



Figure 3. 9: Movement and Surveying Radar, MSR-060 V (Reutech, 2011).

3.8.6.1. MSR Operation

The MSR measures the slope displacement by transmitting electromagnetic energy or radio waves in the direction of the slope and then captures the reflected energy. The reflected energy records the slope displacement (Reutech, 2006b). A simplified version of the radar operation is shown in figure 3.10. In the first measurement of the slope face as illustrated in figure 3.10a, the phase angle of the return signal is zero. The second measurement, figure 3.10b shows a phase shift in the return signal. The MSR determines the phase shift between two measurements and converts it to a change in relative range or displacement in millimetre. At the radar frequency of ~10GHz, 5^0 phase shift equals 0.2mm movement. The changes in displacement are accumulated by the MSR to determine slope movement (Reutech, 2006b).

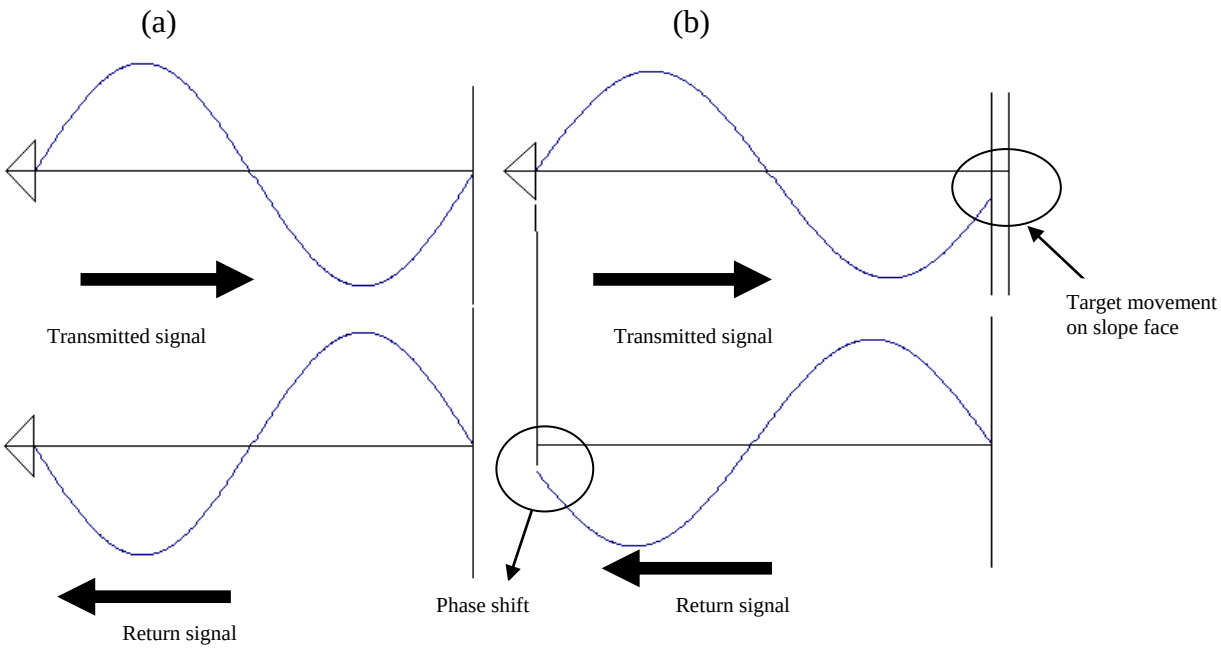


Figure 3.10: (a) First phase measurement of the MSR (b) Second phase measurement of the MSR (Reutech, 2006b).

3.8.7. IBIS-M Slope Monitoring Radar

The addition of the IBIS-M slope monitoring radar (figure 3.11) manufactured by Ingegneria Dei Sistemi (IDS) to existing slope monitoring radar shows the effectiveness and the growing popularity of the radar system in slope monitoring. The IBIS-M has the capacity to continuously measure mine wall movements with sub-millimetre accuracy. It has the highest spatial resolution of 0.5m x 4.4m resolution cell at 1km and the greatest operating distance of 4,000m compared with other slope monitoring radar currently available (Ingegneria Dei Sistemi, 2011). Other unique features of the IBIS-M are its self-powered operation with a combination of solar panels and batteries, utilizing a diesel generator only as a back-up. It can also be operated remotely through a wireless radio link (Ingegneria Dei Sistemi, 2011). Like the MSR and the SSR, the IBIS-M operates in all weather conditions and is fully geo-referenced with automatic atmospheric correction. The IBIS-M is currently used in monitoring the movement of the Turtle Mountain in Calgary, Canada (Ingegneria Dei Sistemi, 2011).



Figure 3.11: The IBIS-M Slope Monitoring Radar (Ingegneria Dei Sistemi, 2011).

3.9. Conventional Slope Monitoring versus Radar Monitoring

Bye (2009) using fault tree analysis, as illustrated in Table 3.1, gives the success rate of different slope monitoring methods. In his analysis, while the other monitoring methods without the radar have success rates of below 90%, monitoring with radar alone gives a success rate of 93%. When combined with other monitoring methods, the success rate is almost 100%. This is a pointer to the capability of the radar in mine slope monitoring. Point measurement with equipment, such as prisms and crack meters give very low and unacceptable success rates.

Table 3.1: Bye's Fault Tree Analysis (Bye, 2009).

Monitoring Type	**Success Rate**
Visual Monitoring only	32%
Prism/Crack Meters only	45%
Visual + Prism/Crack monitors	63%
Visual + Prism/Crack + Laser	86%
Radar Only	93%
Visual + Prism/Crack + Radar	97.5%
Visual + prism/crack + laser + radar	99%

3.10. Summary

Monitoring slope movement remains the most reliable method for detecting slope instability and predicting slope failure (Kennedy and Niermeyer, 1970). However, accurate measurement and interpretation for real time detection and prediction of instability depends on the type of monitoring equipment and technical knowledge of the user (Hoek et al. 2000; Mufundirwa, et al. 2010). Apart from visual inspection, conventional monitoring equipment, such as survey system theodolite and total station with reflecting prism, extensometers, inclinometers, piezometers provide information only for a single site, or at most, a small number of locations on the mine slope, therefore are limited in area of coverage (Vaziri, et al. 2010). If the monitored locations are widely separated, developing failure between the locations may go unnoticed (Vaziri, et al. 2010). In addition to these limitations, conventional monitoring tools are difficult and dangerous to install at many surface mines where steep high-walls and lack of benches limit access to the unstable areas above the working floor (McHugh, et al. 2006). Relocating monitoring equipment from one location to another is costly, time consuming, demanding and dangerous on unstable slopes. Furthermore, vegetation on the rock face reduces the accuracy of the displacement measurements while trucks and other mining vehicles send wrong signals which can cause step changes in the displacement measurements (GroundProbe, 2008).

The slope monitoring radar development resides in anomaly detection and correction module for the slope monitoring system (GroundProbe, 2008). The radar monitoring system consists of the atmospheric correction module that corrects slope displacement measurements for anomalies created by atmospheric changes, and the disturbance detection module that identifies disturbances such as truck movement that create errors in the slope displacement measurements (GroundProbe, 2008).

With the Movement and Surveying Radar, Joubert (2011) stated that while monitoring large regions, the user can set an area threshold and specify the size of the area, in points, which may fail. The MSR software will then check all possible areas of the specified size within the larger region. If the average movement of any of these smaller areas exceeds the alarm thresholds, then an alarm will be triggered and the user will be shown where the excessive movement is. This feature will prevent slope failure in small portion of the slope from going unnoticed.

The advantages of the Slope Stability Radar (SSR), the Measurement and Surveying Radar (MSR) and the IBIS-M over other methods are their ability to monitor large areas on the slope surface both day and night and in almost any weather without being affected by atmospheric dust or haze (Mchugh, et al. 2006). Among the available slope monitoring radar systems, the IBIS-M has the highest operating range of 4,000m. Table 3.2 provides a summary of the advantages and disadvantages of the slope monitoring system.

Considering the success achieved using radar for slope monitoring, the SSR, MSR and IBIS-M can be considered as the state-of-the-art technology, whose advent has completely changed slope stability management in surface mines. Radar monitoring has real possibilities of tracking development of failure and therefore possible identification of mechanisms involved, which has not existed before. The possibility of automated analysis and failure prediction will be pursued further in chapter 5 and 6 because of real time and electronic storage.

The geology of the open-cast coal mine used for the case studies, the slope stability challenges of each mine and some documented slope failure are discussed in chapter 4.

Table 3.2: Slope Monitoring System

Slope Monitoring System	**Type**	**Advantages**	**Disadvantages**	**Range**	**Slope Wall Coverage**	**Accuracy**
Visual Monitoring		Production personnel can be involved No technology is required Inexpensive	Labour intensive. Limited to safe slope areas.	Limited (20-50m)	Small area	Not applicable
Surface Measurement	Tension Crack Mapping	Economical and simple to use	Dangerous to install in unstable areas. Measures displacement of discrete points. Errors can be caused by long wire length due to sag or thermal expansion. Alarm can be triggered by falling rocks or animals	Not applicable	Discrete points	± 0.2% F.S.
	Survey Network	Automatic operation is available Valuable for identifying long term displacement trend.	Suitable only for monitoring discrete points. Prism installation is time consuming and dangerous on unstable slope. Damaged prisms are difficult to replace on steep slope with no access. Displacement data is affected by atmospheric variation in temperature and pressure. Displacement data is affected by human error.	1500m	Discrete points	± 5.0mm
	Global Positioning System (GPS)	Easy automation High accuracy Less labour intensive.	High cost of placing a permanent GPS receiver at each monitoring points Satellite signals can be obstructed by tall vegetation Usage for slope monitoring is still relatively new and expensive. Slope surface can create signal multipath error.	4,000 - 20,000m	Discrete points	±10mm
Subsurface Measurement	Piezometers	Simple to install Function well in shallow and deep holes	Careful handling is required for proper installation. Requires periodic replacement of batteries. The electronic units are susceptible to damage by lightning. Borehole drilling for installation can be expensive Requires conversion of frequency reading to pore pressure.	500m	Discrete points	0.5mm
	Inclinometers	Subsurface displacement measurement of both shallow and deep-seated failure planes. Economical and simple to use	Manual reading is time consuming and labour intensive. If not properly installed, erroneous displacement readings may be recorded.	100m	Discrete points	± 2.0mm
	Seismic Monitoring	Provides early warning of the development of deformation. Detects displacement that cannot be identified by surface measurement.	Expensive to set-up.	2,000m	Discrete points	0.001mm

Slope Monitoring System	**Type**	**Advantages**	**Disadvantages**	**Range**	**Slope Wall Coverage**	**Precision**
Remote Monitoring Technologies	Time Domain Reflectometry (TDR)	Rapid and remote monitoring is possible. Slope displacement can be determined immediately. Lower cost of installation Readings take minutes. Can be installed at great depth	Cable must be destroyed before displacement can be located. Cannot measure deformation below the water surface because of changes in electrical properties of cable from water infiltration Cannot determine the magnitude and direction of slope movement.	100m	Discrete points	$\pm$ 0.5mm
	Laser Scanner	Prisms not required for slope monitoring. Portable and can be moved around easily. Continuous and automatic operation Large area monitoring Valuable for identifying long term displacement trend	Not commonly used for slope monitoring compared to radar monitoring. Lower accuracy compared to radar monitoring. Scan processing time is too great for effectiveness. Accuracy impaired by differences in the reflectivity of the rock, the angle of the rock face, weather, vegetation Cannot provide early warning of failure.	2500m	Large area	50mm
	Radar	Continuous and automatic operation. Operates in all weather condition. Geo-referencing is possible. Sub-millimetre displacement measurement`. Large area and point monitoring.	Expensive to procure and maintain. Uncontrollable down-time.	1000m – 4000m	Large area	$\pm$ 0.2mm

CHAPTER FOUR

OPEN-CAST COAL MINE USED FOR CASE STUDIES

4.1. Introduction

Anglo Coal Operations Limited operates six open cast mines in South Africa. The mines are listed below. With Kleinkopje open-cast mine as the base, three of the six Anglo Coal open cast mines currently utilizing the MSR for high-wall and low-wall monitoring were visited. It was unnecessary to visit Mafube open-cast mine, since the mine has a new MSR radar system. Therefore, no displacement data was available on the displacement behaviour of this mine. The other two mines also not visited are Kriel and Isibonelo open-cast mines. These two mines, together with Mafube, were not visited because they fall within the Witbank coalfield which is ably represented geologically by the other mines visited within this coalfield. Also, none of the mines not visited has recorded slope failure since the inception of the MSR. However, the displacement behaviour of the monitored high-wall of Isibonelo and Kriel mines are included in this research work. The mines investigated are:

1) Kleinjopje Open-Cast Mine (Visited);
2) Landau Open-Cast Mine (Visited);
3) New Vaal Open-Cast Mine (Visited);
4) Kreil Open Cast-Mine (Not visited);
5) Isibonelo Open-Cast Mine (Not visited); and
6) Mafube Open Cast Mine (Not visited).

Only the first three mines listed above are actively utilising the MSR, although only New Vaal has recorded a few slope failures with its MSR. This can be attributed to the peculiar geology of the mine. A careful look at the stratigraphy of the mine as shown in figure 4.11 shows a high-wall consisting of 20m of soft sand overburden. This section of the high-wall is always very unstable and this explains why two MSRs are used at this mine for slope monitoring.

4.2. Organisation of the Chapter

Geological features such as soil/rock material, geological structures, discontinuities, Groundwater, ground stresses, weathering and seismic effects have profound effects on the stability of mine slopes (Abramson, et al. 2002). Identification of these geological features through site investigation and laboratory testing is crucial in designing stable mine slopes. Chapter 4 consists of geological information of the three open-cast mines visited. The chapter also include documented case studies of slope failures at the mines. The arrangement of the chapter is as follows:

- Introduction;
- Geology of the mine area;
- Mine groundwater;
- Mine slope stability problems;
- Mine slope displacement monitoring; and
- Mine case studies of slope failure.

4.3. Kleinkopje Open-Cast Mine

4.3.1. Introduction

Kleinkopje colliery is a division of Anglo Operations Limited (AOL), it is situated some 10km south of Witbank and 120km east of Johannesburg in the Witbank coalfield. This is shown by figure 4.1. The topography is undulating with elevations varying from 1,540m in the south to 1,580m in the north. Kleinkopje colliery is located within the watershed of the upper Olifants catchment, which drains into the Loskop Dam (Kleinkopje Colliery, 2009). A typical Highveld climate prevails with warm summers and cold winters. An average annual rainfall of 700mm occurs mostly between November and April (Kleinkopje Colliery, 2009). The general pit geometry of Kleinkopje is shown in table 4.1.

Table 4.1: Pit Geometry of Kleinkopje open cast mine (Kleinkopje Colliery, 2009).

Name	Pit depth	Pit slope angle
2A South	69m	89^0
2A North	69m	89^0
3A North	55m	89^0
5 West	42m	89^0

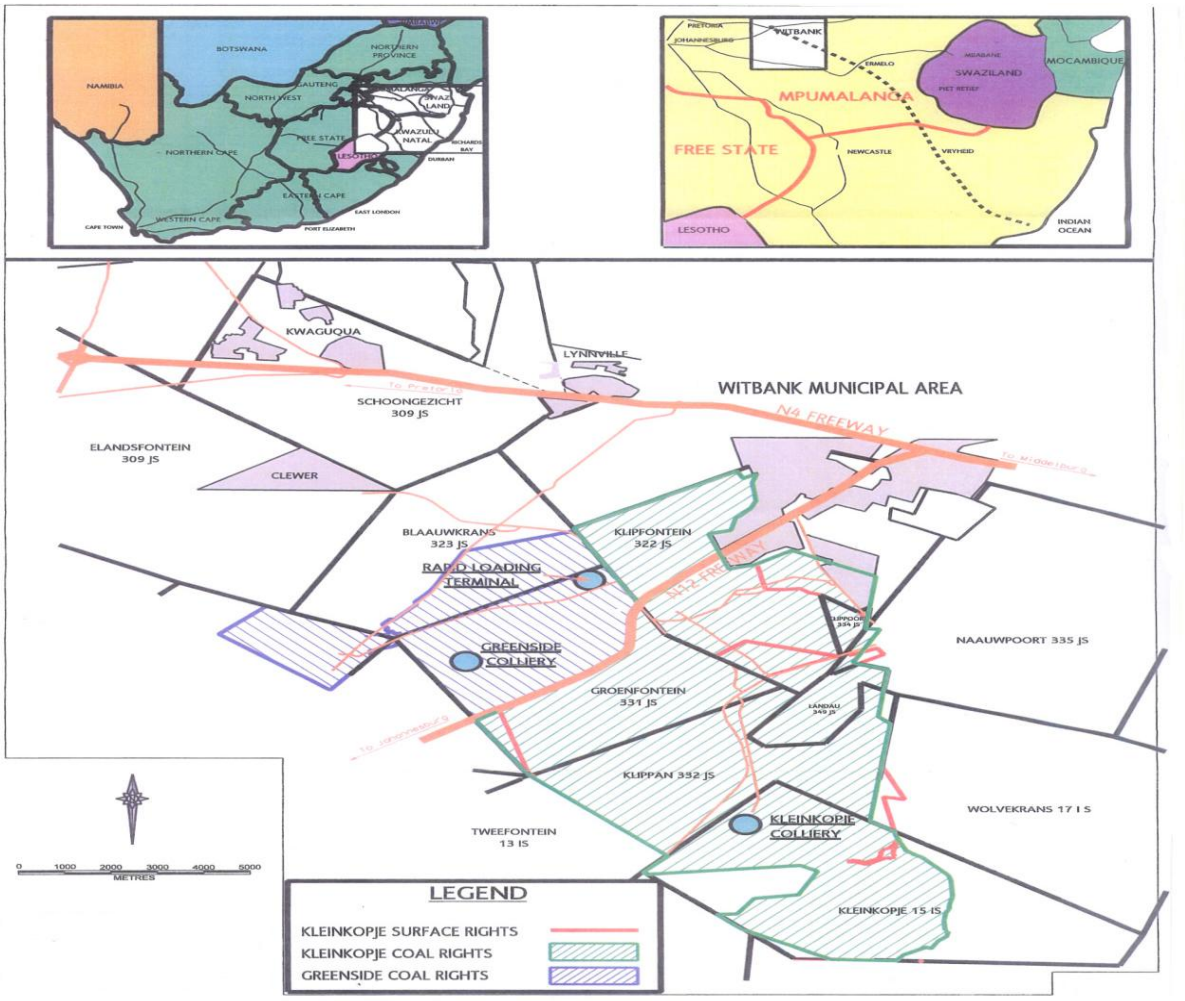


Figure 4.1: Location of Kleinkopje open-cast mine (Kleinkopje Colliery, 2009).

4.3.2. Geology of the Mine Area

The stratigraphy of the Kleinkopje coal reserve area is characteristic of the Witbank coalfield. Five main coal seams are present, namely the number 1 seam, number 2 lower seam, number 2 seam, number 4 and 5 seam (Kleinkopje Colliery, 2009). Typical borehole sections from various parts of the reserve area are shown in figure 4.2. The coal reserves are contained mostly in the number 1, 2 and 4 seams, and to a lesser extent in the number 2 lower seam (Kleinkopje Colliery, 2009).

Shale, siltstone and sandstone sediments overlie and separate the various coal seams. Underlying the bottom coal seam (number 5 seam) is a coarse grained diamictite (Kleinkopje Colliery, 2009). The overburden thickness and preservation of the coal seams is dependent on the surface topography and the pre-Karoo basement floor. In general, the depth of

weathering does not extend deeper than the first few metres of the overburden and the overburden thus comprises hard competent material (Kleinkopje Colliery, 2009). Consequently, the weathering seldom has any major impact on the slope stability of the high-wall, and the overburden and interburden lithologies vary across the reserve. An example of which is the thick massive sandstone channel of up to 15 metres in thickness occurring in the ramp 16 right area in block 5 west and when this is blasted successfully, the result is a clean, stable high-wall (Kleinkopje Colliery, 2009). Block 3A North has an area along the basement high, which has been weathered due to the shallow overburden (Kleinkopje Colliery, 2009). A typical north-south cross-section through the Kleinkopje area is shown in figure 4.3

Ogies, which separates Klienkopje Block 4 East and Block 5 West, is the only dolerite intrusion significance that has been encountered in the Kleinkopje reserve area (Kleinkopje Colliery, 2009). Minor northeast-southwest trending dykes are likely to be encountered during the mining of Block 3A North, but are not expected to impact significantly on mining. Only minor faulting has been encountered within the current mining areas of Blocks 2A North and South, and Block 5 West (Kleinkopje Colliery, 2009). In Block 3A North, a northwest-southeast trending anticline fault splits the reserve block into an eastern and western limb (Kleinkopje Colliery, 2009). The displacement across the fault varies from less than 15 metres in the northern extremity of the pit to approximately 50 metres in the south. The presence of paleo-high in the south-eastern extremity of the pit has resulted in the staggered deposition of the coal seams adjacent to this feature (Kleinkopje Colliery, 2009). A northeast-southwest trending graben was intersected in the Block 5 West mining area. The throw of the faults was up to 8 metres in the Block 5 West East mining area. A graben with throws of up to 12 metres is situated adjacent to the old workings in the western portion of Block 5 West mining area (Kleinkopje Colliery, 2009).

There are no known major aquifers within the Kleinkopje reserve area. Significant ground water inflow was encountered in Block 5 West box cut (Kleinkopje Colliery, 2009). Mining in the western portion of the Block 5 West area has affected the source of ground water that replenishes the southern Tweenfontein springs (Kleinkopje Colliery, 2009). Significant inflow of water from old underground workings was encountered during the mining of the first few cuts in Block 2A North and South (Kleinkopje Colliery, 2009). The water stored in the old Landau III underground workings will continue to have a major impact on mining of Block 2A North and South. Although, the coal seams are generally flat lying, localised “stone

roll" of up to 3 metres in height are present in the floor of the number 2 seam in the Block 2A South, 5 West and 3A North mining areas. Borehole data indicates that floor irregularities may also be present in the number 4 seam (Kleinkopje Colliery, 2009).

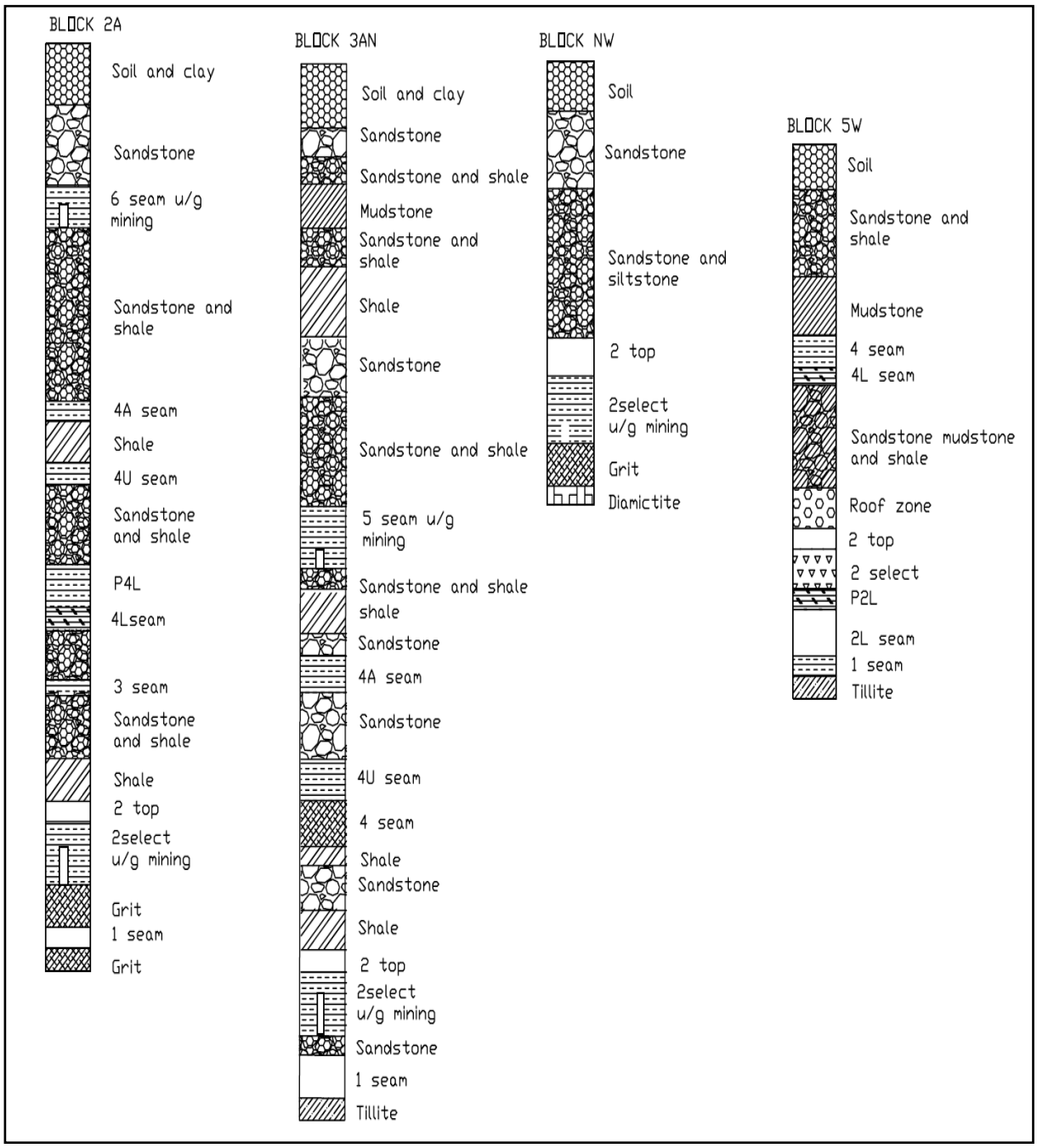


Figure 4.2: Typical borehole stratigraphy of Kleinkopje open-cast mine (Kleinkopje Colliery, 2009).

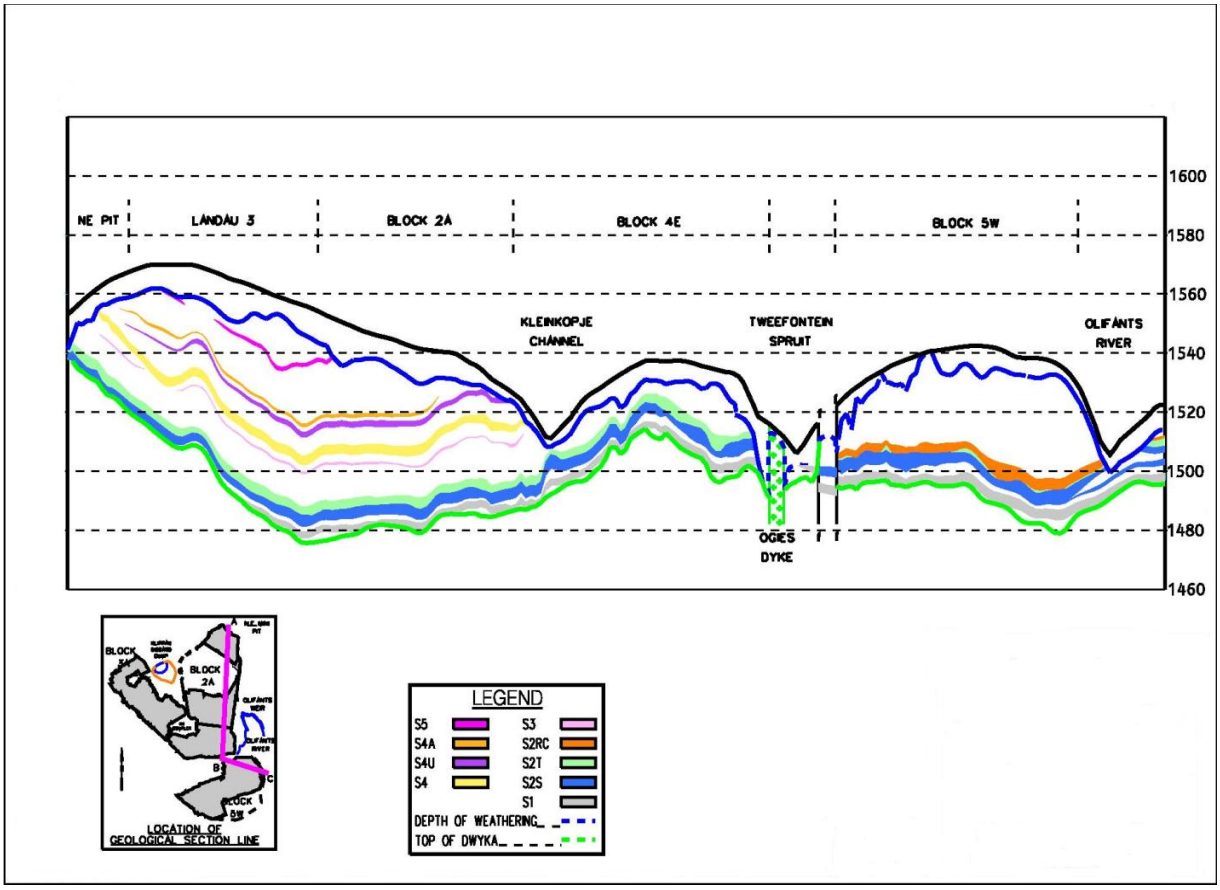


Figure 4.3: Typical geological cross section of Kleinkoje open-cast mine (Kleinkopje Colliery, 2009).

4.3.3. Mine Groundwater

The pillar of the old underground working is situated on the eastern boundary of Block 2A and separates that reserve from the adjacent Wolvekrans Colliery (Kleinkopje Colliery, 2009). Underground mining of the number 1, 2 and 4 seams at Wolvekrans have resulted in the accumulation of approximately 35,000 ML of water against the barrier pillar. Within these compartments these stored water bodies and the current 2A mining elevation difference translates into a head of water of 25m (Kleinkopje Colliery, 2009). A breach of the pillar during blasting and mining of the reserves in the Block 2A area could have potentially disastrous consequences for Kleinkopje Colliery. Consequently, a monitoring and modelling program was conducted to determine the stability of the pillar. Geophones were installed into the pillar by Snowden International to allow for the detection of any movement within the pillar (Kleinkopje Colliery, 2009).

The information obtained from these geophones did not indicate any significant movement. A drilling program was undertaken during 2005 to confirm the validity of the plans for Douglas Colliery underground workings and no discrepancies were found (Kleinkopje Colliery, 2009). A similar drilling program was conducted at the boundary to Phoenix Colliery, again without any discrepancies. eight piezometer holes have also been installed in the Wolvekrans pillar during late 2007 (Kleinkopje Colliery, 2009).

ITASCA International, using a computer program called Fast Lagrangian Analysis of Continua (FLAC) simulated the effects of blasting and mining to determine the minimum mining distance from the barrier pillar before having a detrimental effect on the integrity of the pillar (Kleinkopje Colliery, 2009). The simulation recommended optimum stopping distance of 65m for mining from the number 1 and number 2 seams and 30m for the number 4 seam from the centre of the pillar. Currently, the pit boundary is 80m from the centre of the pillar factors (Kleinkopje Colliery, 2009).

The underground workings within Kleinkopje contain approximately 31 million cubic metres of water. In order to allow mining to continue, this water is being pumped out with the Jacuzzi pump farms, and monitoring boreholes for measuring the water levels (Kleinkopje Colliery, 2009).

4.3.4. Mine Slope Stability Problems

Open-cast or strip mine, unlike open pit mine is done on fewer benches because of the nature of coal formation. Open cast mines create a high-wall and a low-wall after mining. The high-wall consists of the coal seams with the overburden and interburden. The low-wall consists of the spoil removed from the previous strip. The stability challenge in an open-cast mine is on these two walls. This is the situation at Kleinkopje open cast mine. In addition, unlike most open-cast mines, the Kleinkopje mine has a peculiar characteristic, which is the issue of spontaneous combustion. A situation caused by the exposure of previously mined out area, through underground mining to oxygen during opencast mining. The effect of this burning coal on slope stability is another stability challenge. The few stability problems encountered at the mine are discussed in the following section.

4.3.4.1. Bord and Pillar Collapse

Four reserves namely 2A North, 2A South, 3A North and 5 West exist at Kleinkopje open - cast coal mine. Three of these reserve blocks have been previously mined by bord and pillar, which is an underground mining method (Kleinkopje Colliery, 2009). Much of this mining was carried out before the introduction of legislation governing minimum pillar dimensions. Consequently, pillars were robbed and quartered without this information being accurately reflected in mining plans (Kleinkopje Colliery, 2009). The "over mining" of the pillars has adversely affected on the safety factors and has increased the risk of bords and pillars to collapse. This condition is further worsened by the fact that the number 2 top seam was often "top coaled," further reducing the safety factors (Kleinkopje Colliery, 2009).

Collapses and the resulting sinkholes as seen in appendix 1, figure 1.1, have been detected in the northwest 2A and 3A north blocks and while these collapses have not had any impact on the mining operation and have been filled with sand, further collapsing bords could negatively impact on the long-term viability of removing the pillar remnants by open-cast methods. (Kleinkopje Colliery, 2009).

4.3.4.2 Spontaneous Combustion

According to company records, spontaneous combustion was first encountered at Kleinkopje colliery within the underground workings of block 2A North in November, 1999 (Kleinkopje Colliery, 2009). It subsequently occurred along both blocks 2A North and 2A South. Hot areas have also developed with the exposure of old underground workings in pit 3A North (Kleinkopje Colliery, 2009). As mining progresses into the previously mined areas, contact of the hitherto exposed hot coal surface with oxygen results into spontaneous combustion as seen in appendix 1, figure 1.9. Spontaneous combustion has adverse effect on mining of coal but more importantly to this research work is its effects on the stability of mine slopes. Pillars from old workings exposed to spontaneous combustion are more prone to collapsing and consequently increase high-wall instability. As stated in Kleinkopje Colliery (2009), between 2003 and 2007, spontaneous combustion was a contributing factor to quite a number of minor slope failures in the mine, and this is shown in Table 4.2.

4.3.4.3. Low-Wall (Spoil) Failure

The low-wall, consisting of the overburden and interburden rock materials removed during mining is generally stable during the dry season. The main problem is the weakening of these spoils due to spontaneous combustion in some cases (Kleinkopje Colliery, 2009). However, this is controlled by cladding the low-wall with soil removed during pre-stripping. This invariably prevents some sections of the low-wall from being monitored with the MSR. Another problem encountered is occasional sloughing of the low-wall caused by reduction of shear strength from rainfall in wet seasons. This was particularly noticed in some old spoil piles, although it was far from the mine face and so did not interfere with mining operations nor pose any threat to man or machine. The base, that is, the foundation of the low-wall consists of sandstone removed immediately after pre-stripping, followed by shale and other blocks of hard interburden rocks. The composition of the low-wall makes it generally stable (Kleinkopje Colliery, 2009).

4.3.4.4. High-Wall Failure

From company records, no major high-wall failure has been experienced in any of the four pits in the mine. Minor collapses caused by the weakening of old pillars by spontaneous combustion seen in appendix 1, figure 1.10, in 2A South, 2A North and 3A North do occur. Toppling of loose overhang rocks from unexcavated frozen portion has been noticed mostly in pit 5 West, shown in appendix 1, figure 1.8. This portion remains hanging on the sandstone part of the high-wall. It has been monitored on few occasions with the MSR (Mottie, 2008). None of the monitoring data of the frozen portion showed any significant movement over the period. The over-consolidated infilling materials commonly found with sandstone in interbedded sedimentary formation like Kleinkopje gives the sandstone very high shear strength. This explains why the radar did not record any movement on the frozen portion during monitoring. Secondly, it explains why the frozen portion is not easily dislodged from the high-wall by the excavator.

However, gradual deterioration and weakening of the infilling occur over time. This results in significant loss of shear strength and subsequent toppling of the column of blocks from the frozen portion (Kleinkopje Colliery, 2009). Inaccurate pre-splitting is also deemed responsible for this. The frozen portion can be prevented by re-designing the pre-split blast or

by scaling, after it has occurred with the dragline bucket. A summary of the minor failures observed in mine between March 2003 and July 2007 is shown in table 4.2.

Table 4.2: Summary of failure at Kleinkopje mine between March 2003–July, 2007.

Location of failure	Number of failure	Percentage (%)	Type of failure	Causes of failure
High-wall	23	42.6	Toppling - Sloughing - Minor collapse - Collapse -	Loose blocks caused by steeply dipping joints overhang. Loading of soft overburden from spoiling on high-wall Spontaneous combustion weakens pillar. Bord collapse, frozen block slide
Low-wall	27	50	Sloughing -	Undercutting by dragline or rain, Water accumulation due to rainfall, Loading of soft overburden, spontaneous combustion weakening of previous workings
Bench top or slope crest	4	7.4	Ground collapse - Sink hole -	Unblasted bords exposed by collapse, Rat-hoeing from underground collapse. Progressive bord failure to surface
	54	100%		

Source: Kleinkopje Colliery, 2009

4.3.5. Mine Slope Displacement Monitoring

Monitoring the behaviour of the high-wall and low-wall at Kleinkopje is achieved by visual monitoring and radar monitoring using the MSR-200 model named MSR-004, which was procured in 2007.

4.3.6. Kleinkopje Open-Cast Mine Slope Failure Case Study

Monitoring of the low-wall in ramp 7, pit 2A south started on the 30th May 2009 after observing some tension cracks on the spoil heap (Mottie, 2008). The monitoring lasted for 15 days. The alarm threshold was set at -50mm relative range. At 8.53 am, 6th June 2009, after seven days, the alarm threshold was exceeded and the wall failed (Mottie, 2008). The trend plot of the failed low-wall is shown in figure 4.4. Prior to the onset of failure, movement oscillated between -10mm and -25mm, and this behaviour is referred to as the regressive state by Zavodni (2000). Beyond this point, displacement kept increasing progressively until failure occurred at a displacement of -50mm, and a cumulative displacement rate of -0.4mm/hr using the all data time window. Movement of the material still continued down slope at a relative range greater than -50mm and a rate of around -0.4 mm/hr (Mottie, 2008). From the company's record, this is the only failure recorded by the radar monitoring at the time of this research and the MSR record was not available for analysis.

Description of Failure

Failure was attributed to a high angle of repose of the spoil, significant swelling and weakening of interparticle bonding between the granulated overburden materials serving as a base for the rock boulders on the spoils. This resulted in the loose sandstone boulders toppling over from the uppermost part of the low-wall. A common cause of low-wall or waste rock slope failure is the reduction in shear strength due to moisture softening. This is more pronounced during rainfall, as the bond of the waste material progressively reduces with time (Mottie, 2008).

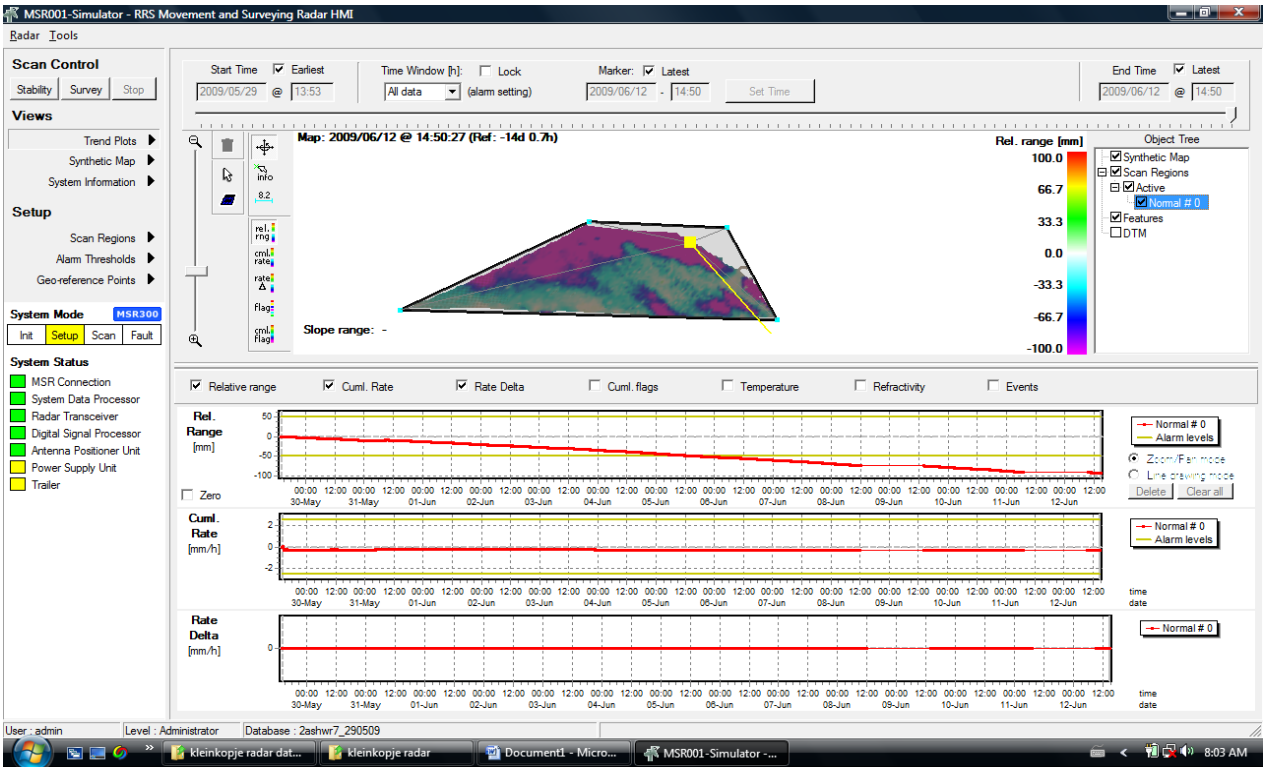


Figure 4.4: Trend plot of Kleinkopje open cast mine low-wall failure (Mottie, 2008).

4.4. Landau Open-Cast Coal Mine

4.4.1. Introduction

Landau colliery is an integral part of the South African Coal Estates complex, situated west of Witbank, about 120km east of Johannesburg, in the Witbank Coalfield, South Africa, as shown in figure 4.5. The mine is a division of Anglo Operations Limited operated by Anglo Coal, South Africa (Landau Colliery, 2009).

The surface is undulating with elevations varying from 1,580m in the south-west to 1,430m in the north (Landau Colliery, 2009). Landau colliery straddles two watershed catchment areas, namely the upper Olifants catchment area in the east and south and the Wilge catchment area in the west. Both rivers drain into the Loskop Dam (Landau Colliery, 2009).

The Townshipspruit and Schoongezichtspruit drain the Navigation area, while the Suikerboskopspruit, Kromdraaispruit and Klipspruit drain the Kromdraai area (Landau Colliery, 2009). The area is a typical Highveld climate with warm, wet summers and cold, dry winter. Average rainfall for the last ten years has been some 740mm per annum mainly between November and April (Landau Colliery, 2009)

Unlike the Kleinkopje which has all its coal reserve located at Kleinkopje opencast mine, the coaling reserve and resource areas at Landau Colliery have been redefined and divided into 3 open-cast areas, where mining operation is currently on-going:

1) Kromdraai Opencast;
2) Schoongezicht Opencast; and
3) Umlalazi (Navigation) Opencast.

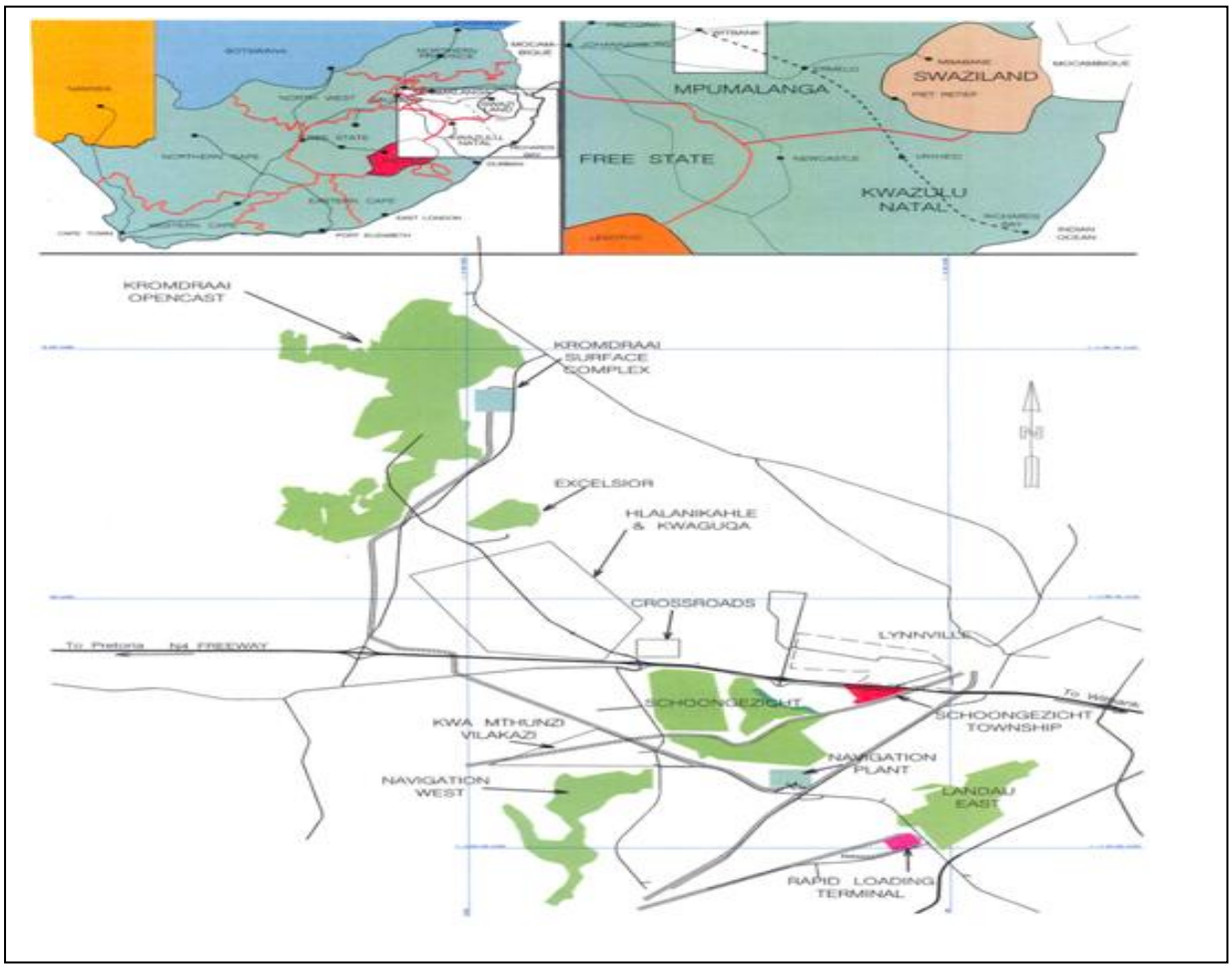


Figure 4.5: Locality plan of Landau open cast mine (Landau Colliery, 2009).

4.4.2. Geology of the Mine Area

4.4.2.1. Introduction

The coal measures form part of the Vryheid formation of the Ecca Group as seen in figure 4.6. Of the five identified seams within the Witbank coalfield, only the number 1 and 2 seams are preserved in the Kromdraai open-cast reserve area (Landau Colliery, 2009). The remaining seams, number 3, 4 and 5 seams have been removed by weathering processes, except, in the south, where the number 3 and 4 seam are preserved (Landau Colliery, 2009). The number 1 and 2 seams are separated by gritty sandstone parting, referred to as the P1 parting. This unit varies in thickness from 0m to 3.0m, but is typically 0.5m thick (Landau Colliery, 2009). A representative geological cross-section and stratigraphy of Landau open-cast mine is shown in figure 4.7 and 4.8 respectively.

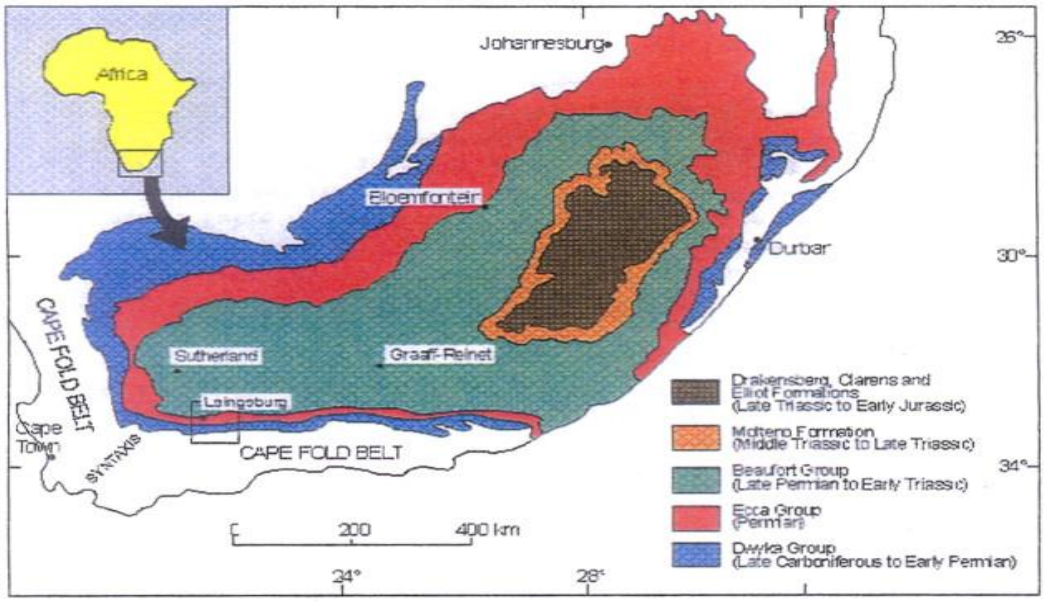


Figure 4.6: The Karoo basin in Southern Africa (Landau Colliery, 2009).

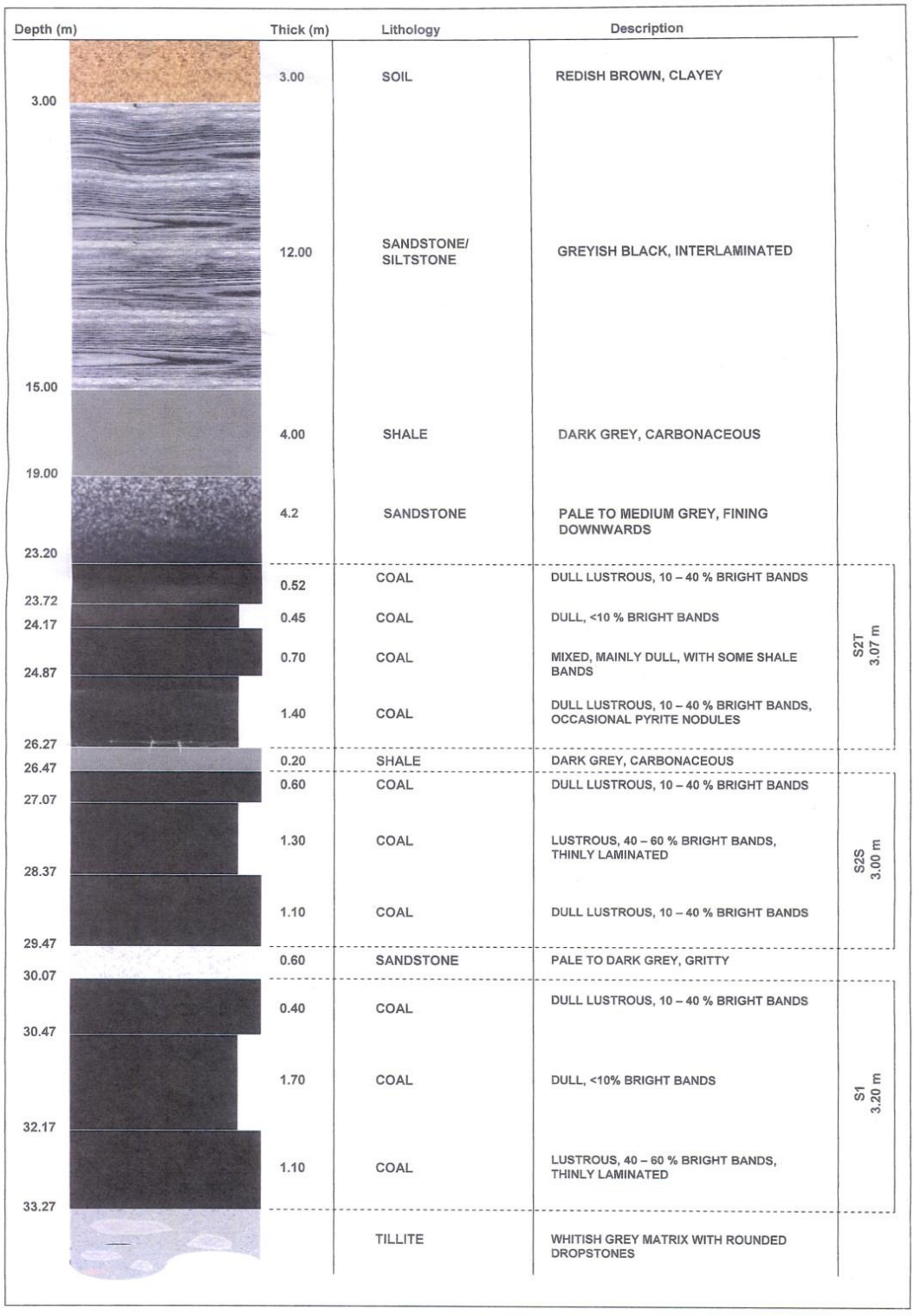


Figure 4.7: Typical borehole stratigraphy of Landau open cast mine (Landau Colliery, 2009).

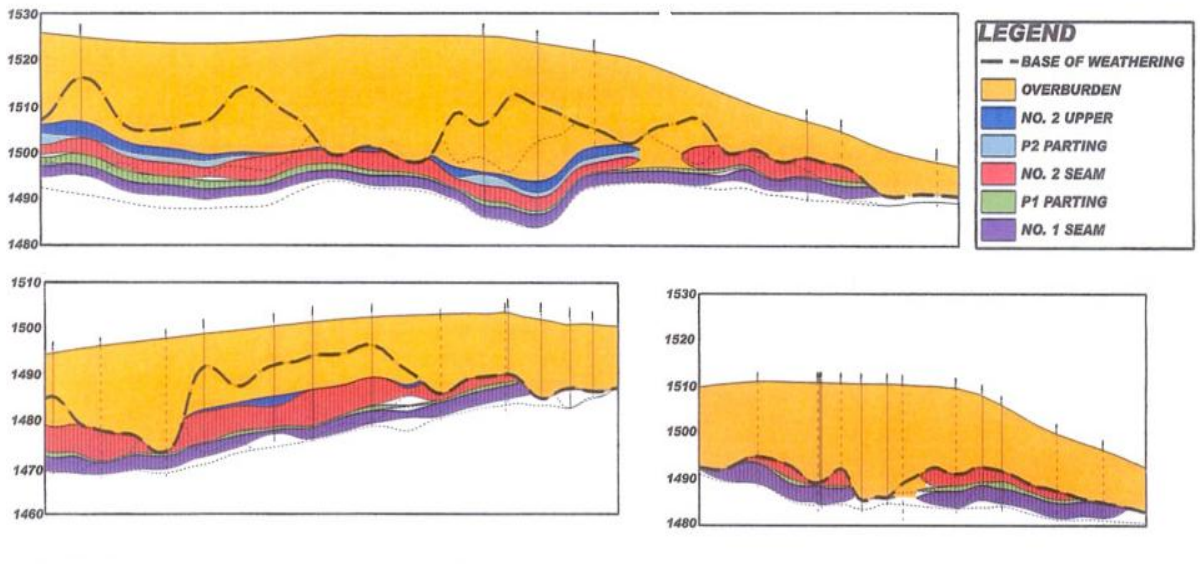


Figure 4.8: Typical geological cross section of Landau open cast mine (Landau Colliery, 2009).

4.4.2.2. Kromdraai Open-cast Mine

The Kromdraai open-cast coalfield is situated on a north-south trending ridge (Landau Colliery, 2009). The overburden thickness and preservation of the coal seam is dependent on the surface geomorphology as well as on the palaeotopography of the pre-Karoo basement floor. Interbedded shale, sandstones and siltstones comprise the overburden sequence at Kromdraai (Landau Colliery, 2009).

Washouts, where the coal seam has been eroded by river current action, have been intersected in the North Reserve Block, with the resultant channel filled with clastic sediments, such as sandstones and siltstones. The edge of the washouts at Kromdraai open-cast is diffused by differential compaction (Landau Colliery, 2009). The typical example is the no-coal zone, called “doughnut.” trending roughly north-south in the North Reserve Block. Floor rolls have been encountered at Kromdraai open-cast. The general trend of the floor rolls is northeast/southwest (Landau Colliery, 2009).

Faults intersected in number 1 seam workings were extrapolated into virgin areas at Kromdraai open-cast. These faults are fairly common and they are usually accompanied by less than 3m displacement (Landau Colliery, 2009). Sinkholes occur in the shallower areas of

the old underground workings, where small-scale faulting and tension fractures are common (Landau Colliery, 2009).

4.4.2.3. Mine Groundwater

There are no known major aquifers within the Kromdraai open-cast reserve area. However, significant ground water inflows were encountered in the original Kromdraai mini pit, mostly along the north-south trending graben (Landau Colliery, 2009). Large volumes of water have accumulated in the low-lying areas of the old underground workings as a result of seepage through a fairly permeable overburden. The old underground workings at central Block contain an estimated 2.7 million m^3 of water (Landau Colliery, 2009).

The mine has an effective dewatering programme in place to remove the stored water in the old underground compartments. There is also a ground water monitoring system established to monitor the elevations of the various water storage compartments in order to evaluate the dewatering requirements for the mine (Landau Colliery, 2009).

4.4.2.4. Schoongezicht/ Umlalazi (Navigation) Open-cast

The stratigraphy of Schoongezicht and Umlalazi reserve area is typical of the Witbank coalfields. The coal seams are contained in the Vryheid formation of the Ecca Group. The five main coal seams present are numbered in ascending stratigraphic order, namely the number 1, 2, 4 and 5 seams (Landau Colliery, 2009).

Shale, siltstone and sandstone separate the coal seams. Overburden thickness and preservation of the coal seams are dependent on the surface geomorphology and the pre-Karoo basement floor (Landau Colliery, 2009). The main coal reserves at Schoongezicht and Umlalazi (Navigation) are contained within the number 1, 2 and 4 seams as well as in the number 5 seam in the deeper Umlalazi area. Open-cast mining of the number 4 seam has been completed at the Schoongezicht number 4 seam mini-pit (Landau Colliery, 2009).

The number 2 and 1 seam are mined in the Schoongezicht number 2 seam mini-pit to the east of the number 4 seam mini-pit (Landau Colliery, 2009). Three minor dolerite dykes were

encountered in the number 2 seam mini-pit, but did not significantly hinder mining operations (Landau Colliery, 2009).

4.4.2.5. Mine Groundwater

The number 5 seam is largely pre-mined with extractions of around 75%. The large amount of water contained within these old underground workings will have a significant impact on the mining operations (Landau Colliery, 2009). Numerous water bodies have been identified and water monitoring boreholes have been drilled. Like other Anglo Coal mines, a good dewatering programme is constant at the mine to facilitate safe and efficient operation (Landau Colliery, 2009).

4.4.2.6. Mine Slope Stability Problems at Landau Open-Cast Mine

Erosions have removed the coal from the number 3 seam upwards, because of the proximity of Landau colliery to the northern sub-outcrop of the Witbank coal field. Subsequent atmospheric exposure and groundwater penetration have weathered the remaining overburden and coal seams to various degrees (Landau Colliery, 2009). Zones of deep weathering present more risk in terms of high-wall stability and sinkhole formation than fresh zones and thus, all areas have been classified in terms of Base Horizon of Weathering (BHWE) and Base of Horizon of Hard Weathering (BHHW) (Landau Colliery, 2009). The slope stability problems experienced at Landau open-cast mine are similar to the ones at Kleinkopje open-cast mine. They are classified as follows:

4.4.2.7. High-wall Failure

Major high-wall failure, or mass instability, is very rare at the mine except when caused by a panel failure after mining (Landau Colliery, 2009). Incomplete pre-split blasting and joints parallel to the high-wall face are the main factors responsible for the occasional failure at the high-wall face. This face instability due to joints parallel to the high-wall is avoided wherever possible by laying out the strips perpendicular to the jointing (Landau Colliery, 2009). Minor and localised falls of rock blocks or wedges from the high-wall face is occasionally experienced. Consequently, the high-wall can be assumed to be relatively stable (Landau Colliery, 2009).

4.4.2.8. Low-wall (spoil) Failure

The low-wall, consisting of the overburden and interburden removed in the process of coal extraction, is generally stable, especially during the dry, cold winter and wet, summer season (Landau Colliery, 2009). However, there is little potential for circular failure, or sloughing during the wet, summer season, particularly if it is undercut. Low-wall stability is not an issue in the mine. The probability of failure is very low and where there are chances of failure, enough space is created for containment.

4.4.2.9. Spontaneous Combustion

Although, the Landau open-cast mine does experience spontaneous combustion, the magnitude is nothing compared to that of Kleinkopje open-cast mine. This is because their buffer blasting operation is probably working well. Other reasons could also be responsible, but the investigation of those factors is outside the scope of this research work.

4.4.2.10. Bord and Pillar Collapse

The majority of the coal mining horizon at Kromdraai and Excelsior mini-pits comprises of previously mined 1 seam coal, P1 parting and virgin 2 seam. With approximately 70% of the 1 seam extracted, the risks of sinkhole formation and high-wall stability is real (Landau Colliery, 2009).

The higher the degree of weathering the overburden has experienced the less stable or competent the high-wall is expected to be, and the higher the risk of sinkhole formation becomes (Landau Colliery, 2009). If the BHWE extends into the coal seams, the area is classified as high risk in terms of sinkhole formation and high-wall stability. Conversely, where the BHWE does not intersect the coal seam, the area is classified as low risk. Medium risk areas are classified as zones where the BHHW intersects the coal seams (Landau Colliery, 2009). In these areas, all the overburden is weathered to a smaller degree and thus classified as medium risk (Landau Colliery, 2009).

4.4.2.11. Mine Slope Displacement Monitoring at Landau

The displacement on high-wall and low-wall at Landau open-cast mines are monitored with visual monitoring and radar monitoring using the MSR-200 model, named MSR-007. The MSR is moved from time to time to unstable areas with potentials for failure on the high-wall and low-wall.

4.4.2.12. Landau Open Cast Mine Case Study

A serious high-wall failure was experienced on the 30th July 2008 at the Schoongezicht open-cast mine as seen in figure 4.9. The failure occurred as the coal was been mined. The overburden above the coal seam consists of a thin layer of soil and very brittle sandstone that had been highly affected by weathering and weakened by continuous infiltration of water through the thin soil layer. Two set of joints are presumed to be responsible for this failure; a bedding plane perpendicular to the high-wall, which is conspicuous from the high-wall face, and a second non conspicuous vertical joint parallel the high-wall, which provides the release surface. The parallel joints were hidden because pre-stripping of the top soil was not done before drilling. It is the belief that the mine was trying to save cost in this regard.

These two joints both provide a release surface for composite failure of complete pack of sandstone blocks. Composite rock mass failure is a failure involving intact rock material, as well as fracture and shear on existing defects (Simmons and Simpson, 2006). The high-wall was not being monitored by the MSR radar during the failure, and therefore, displacement and displacement rates could not be documented. The suddenness of failure indicates the importance of monitoring and the slope monitoring radar remains the only monitoring technique that could detect such failures.

At the time of this research, the above failure remains the only failure documented at the mine. Only one other slope failure could be retrieved from the MSR, with none from the company's record. However, some of the displacements behaviour of the stable high-wall and low-wall monitored by the MSR at the mine are included in the interpretation of the deformation behaviour of open cast mine slopes. Although, it is impractical to have all the high-walls at the mine monitored by the MSR, it is important to identify unstable areas with high failure potentials. This will enable careful planning to avoid or contain failure, if and

when it does occur. The failure reported at Landau was unexpected and could have been fatal because the slope was deemed safe.



Figure 4.9: Failed high-wall at Landau open-cast mine (Landau Colliery, 2009).

4.5. New Vaal Open-Cast Coal Mine

4.5.1. Introduction

New Vaal Colliery, a division of Anglo Coal Operations Limited, is located in the magisterial district of Sasolburg at approximately 18 kilometres north-east of the Sasolburg Central Business District, and forms part of the Vaal Dam Regional Rural Transitional Council (New Vaal Colliery, 2009a). The open cast mine is located immediately south of the Vereeniging Central Business District and approximately 12km to the east of Vanderbijlpark. The extent of the mine is indicated by the red circle in Figure 4.10 (New Vaal Colliery, 2009a).



Figure 4.10: Map showing location of the New Vaal open-cast mine (New Vaal Colliery, 2009a).

The mine is bound by the Vaal River meander to the east and north. To the west, the mine is bound by the secondary road R82 to Heilbron, and the railway line from Vereeniging to Sasolburg (New Vaal Colliery, 2009a). To the south, the mine is bound by a carriageway of the freeway P10/2 (PWV22). 33kV Eskom power lines are situated in the southern boundary of the mine lease area. Immediately to the south of the mine lease area, lies Lethabo Power station, which the mine supplies with coal for power generation (New Vaal Colliery, 2009a).

4.5.2. Geology of the mine area

The typical geological setting at New Vaal Colliery, as described from the youngest to the oldest, comprise a sequence of Aeolian and alluvial sediments (New Vaal Colliery, 2009a). These sediments are made of mixed layers of clayey, silty sands that average 16m in thickness. Figure 4.11 shows this unconsolidated unit, which is referred to as the soft overburden (New Vaal Colliery, 2009a). Underlying the soft overburden is the hard

overburden that averages about 8m, but can attain a maximum thickness of 37m in the southern-most part of the mine area. Hard overburden mainly comprises mudstones, siltstones, fine-grained sandstones, which may not contain the leader seam coal. Leader seam averages 0.5m in thickness and is therefore uneconomical to mine (New Vaal Colliery, 2009a).

Top seam coal directly underlies the hard overburden but where the latter is not present, top seam occurs directly underneath the soft overburden. In terms of calorific value, the top seam coal is the poorest, with 13.9MJ/Kg Calorific Value (CV) on average, of all the mineable coal seams (New Vaal Colliery, 2009a). Although top seam has a thickness of 7.0m in most parts of the mining area, it can reach a maximum of 13m on the south (New Vaal Colliery, 2009a).

A coarsening upward sequence grading from a carbonaceous mudstone on the interburden floor, through shale and siltstone to fine-grained sand stone forms the interburden succession. The average thickness of the interburden unit is 11.6m. This sequence separates the top seam coal from the middle seam coal (New Vaal Colliery, 2009a).

Middle seam ranges in thickness from 6.9m to a maximum of 13m in the southern-most part of the mine area. It is of a better quality with CV of 17.1 MJ/Kg, than the top seam, but of poor qualities when compared to bottom seam. In most part of the mine area, middle seam is split into two layers by a mudstone band of about 0.4m, but can reach 1.00m in some other locations (New Vaal Colliery, 2009a).

The middle seam is separated from the bottom seam by parting and parting seam which comprise of carbonaceous silty mudstone sometimes with thin layers of coal overlying the gritty sandstone bed (New Vaal Colliery, 2009a). The average parting thickness is 1.5m in most areas but can reach 7.5m at other locations (New Vaal Colliery, 2009a). The bottom seam is of better quality than all the others, with an average calorific value of 19.1 MJ/Kg and ash content of 29.7%. The seam is mostly 4.0m thick but can range from less than 1m to 13.5m (New Vaal Colliery, 2009a). Bottom seam thinning is normally encountered and attributed to the paleo-karst topography of the pre-Karoo Tranvaal Supergroup dolomites. These dome-like shaped features are termed pinnacles (New Vaal Colliery, 2009a).

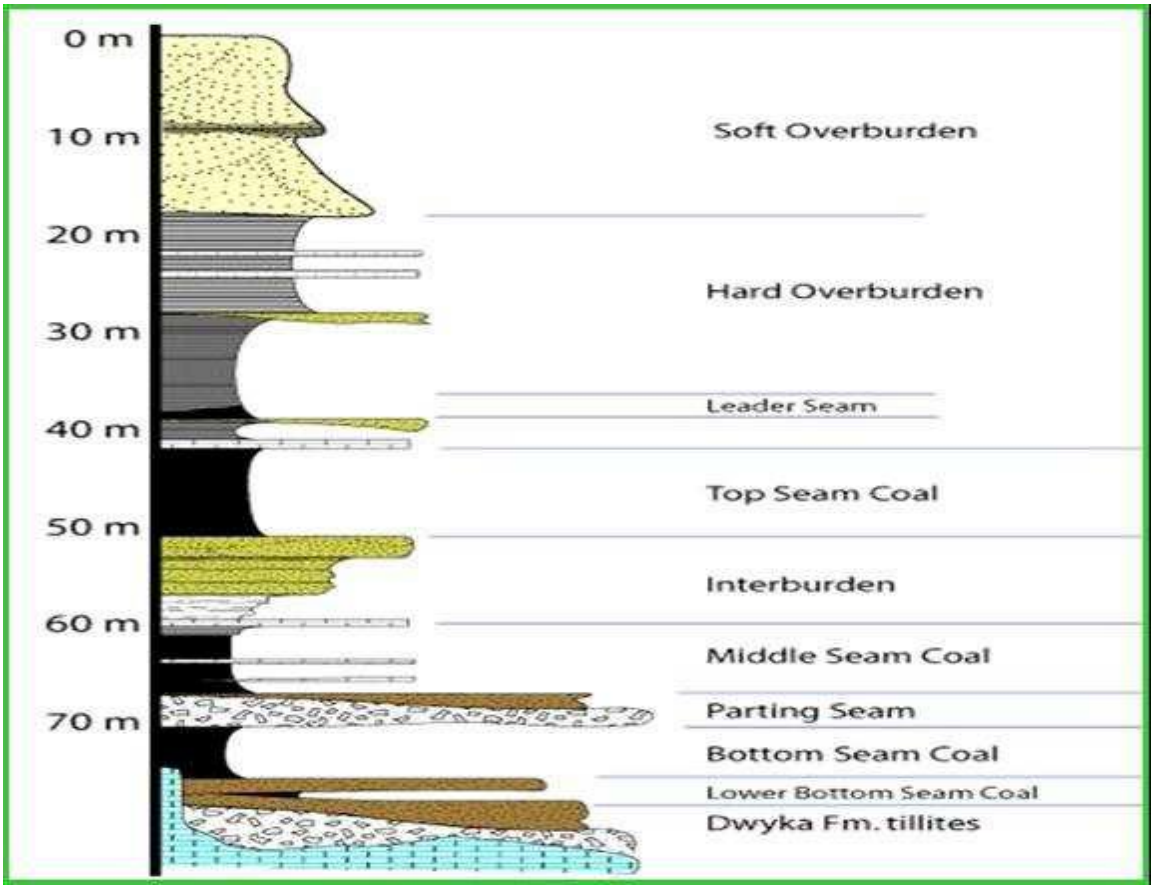


Figure 4.11: Typical stratigraphy column for New Vaal open cast mine (New Vaal Colliery, 2009a).

4.5.3. Geological structures

The dykes in the northern part of the area are east-west striking. This was revealed from the intersections in underground workings, borehole intersections and by ground magnetometry traverses (New Vaal Colliery, 2009a). The dykes compartmentalise the dolomitic groundwater system into a northern Vereeniging area, and a southern Maccauvlei area. The fault positions were established from underground working layouts, elevation differences and underground geological mapping (New Vaal Colliery, 2009a).

There are numerous faults in the area with some having major displacements occurring (New Vaal Colliery, 2009a). The southern boundary of the colliery is defined by the Northern Viljoensdrift fault zone. This is locally called the Southern Boundary Fault. The fault zone is one of a pair that created a graben with an approximately 90m downthrow known as the Valley area (New Vaal Colliery, 2009a). An east-west striking fault, called the C3 fault

associated with the Southern Boundary Fault zone and has been traced about 2.5km into the reserve area by both drilling and exposure during mining (New Vaal Colliery, 2009a). The region of disturbance about the fault can be up to 20m in width. The influence and amount of throw on this fault recedes to the west and is currently manifested as a floor roll with minimal displacement. A number of faults with throws of less than 2m occur throughout the pit. Most of these strike north-east, south-west or east-west (New Vaal Colliery, 2009a).

A number of palaeo-sinkhole features occur in the western half of the lease area. These features are mostly characterised by a circular to ellipsoidal shape, and are bound by steep dips and faults (New Vaal Colliery, 2009a). The strata within the feature are downthrown by 10m to 40m. The coal seams within the palaeo-sinkholes are generally thicker than in the adjacent areas, with the bottom seam coal showing the largest increase of up to two or three times the normal thickness (New Vaal Colliery, 2009a). Numerous palaeo-highs occur in the form of ridges and pinnacles. These features area associated with the pinching out of the bottom seam in those areas (New Vaal Colliery, 2009a).

4.5.4. Mine Groundwater

The basic features of the aquifers at New Vaal Colliery are outlined below:

Soft Overburden: This is a free aquifer consisting of recent alluvial sand and clay deposits, which are recharged directly by rainfall. The storage capacity is medium to low, with delayed drainage occurring as a result of the clay content in the sands (New Vaal Colliery, 2009a). Where a basal pebble bed is well developed, it acts as a conduit for water. The system is rapidly recharged by rainfall, especially where vegetation has been removed. Recharge to the toe of sand may occur within 24 to 48 hours where little clay exists, (New Vaal Colliery, 2009a).

The Karoo Supergroup: This acts as a semi-confined aquifer comprising Vryheid Formation shales, sandstones and coal seams in addition to Dwyka Group tillite. It is a low-capacity water holder and as most horizons are impermeable, the movement of water is generally via fissures in the coal seams (New Vaal Colliery, 2009a). The basal Dwyka tillite forms an impermeable barrier to the underlying dolomite aquifer and has a permeability of 0.0001m per day. However when fractured the permeability can increase to 0.1m per day.

Since little water is contained in these rocks, this groundwater has little effect on mining (New Vaal Colliery, 2009a).

The Transvaal Dolomite: As stated in New Vaal Colliery, (2009a), the dolomitic groundwater system is a confined aquifer composed of two units:

1) **The Transition Zone:** consists of chert pebbles in a calcareous / dolomitic matrix with numerous solution channels, and occasionally interbedded Dwyka material.
2) **Dolomite:** consists of dark, blue-grey to black dolomite, essentially massive with a secondary permeability along faults, fractures and joints.

A secondary permeability of 0m to 20m per day has been revealed through testing (New Vaal Colliery, 2009a). The two units are regarded as a single groundwater system hydraulically separated from the overlying aquifers by the impermeable Dwyka tillite (New Vaal Colliery, 2009). As the water is confined, it has a piezometric pressure head, which acts against this barrier (New Vaal Colliery, 2009a). Within the lease area, the undisturbed dolomitic groundwater level or pressure head is in the range of 1418m to 1420m above mean sea level. The natural recharge of the dolomites is by rainfall infiltration in outcrops occurring north of Vereeniging, specifically along the Klip River (New Vaal Colliery, 2009a). Dolomitic water flows from the north-west to the south-east. Dolomite underlying the colliery is hydraulically continuous with that beneath Vereeniging, although this connection is modified by the presence of dolerite dykes (New Vaal Colliery, 2009a)

4.5.5. Mine Slope Stability Problems at New Vaal

The different categories of slope stability problems experienced at New Vaal Colliery are highlighted below.

4.5.5.1. Soft Overburden and Spoils (Low-wall) Failure

The soft overburden is a combination of alluvial and Aeolian sand deposit with clay lenses that occur on the high-wall (New Vaal Colliery, 2009a). Spoils are waste material of varying compositions and size distribution, usually with overburden sand at the base. The spoils are placed on the low-wall. Both the soft overburden and spoil material are associated with

circular failures as seen in appendix 2, figure 2.2. This type of failure occurs when the spoil materials have low cohesion and low friction angle values (New Vaal Colliery, 2009a). The scale of the failure may be exacerbated by the presence of palaeo-highs and lows, water accumulations and pore water pressure build within the soil itself, demonstrated in appendix 2, figure 2.3. Such a failure is common in spoils and/or sand that contains weathered material and can be initiated by undercutting and spontaneous combustion (New Vaal Colliery, 2009a).

4.5.5.2. High-wall Failure

The hard overburden on the high-wall is not particularly hard and has a natural tendency to weaken upon exposure to the atmosphere. Unstable high-wall conditions may occur due to deep weathering, especially where bedding planes dip into the void (New Vaal Colliery, 2009a). According to New Vaal Colliery (2009a), if jointing or faulting is present, the hard overburden is particularly prone to wedge failure. Wedge failure occurs when the boundaries of the wedge are slip planes, and the line of intersection daylights in the high-wall face (New Vaal Colliery, 2009a).

In some areas, the top seam coal lies directly below the soft overburden. In these areas, the upper portion of the top seam coal has been partially eroded and weathered (New Vaal Colliery, 2009a). Instability may also arise from the presence of palaeo-highs and lows due to steep dipping angles normally associated with faults along the edges of such structures (New Vaal Colliery, 2009a).

4.5.5.3. Bord and Pillar Collapse

The middle and bottom seam has previously been extensively mined by bord and pillar methods. Therefore, toppling and floor failure may occur where the parting seam will collapse into the bords (New Vaal Colliery, 2009a). The doline structures create more mining problems in this seam than in the other coal seams, as in most cases the bottom seam will tend to follow the steep gradients that are created by the pre-Karoo topography, or dolines. Blasting may induce this type of failure, as it provides a source of energy to instigate failure. Floor failure may also occur where there are underground workings as reported in New Vaal Colliery (2009a). This failure involves material sagging from pressure exerted by overlying

material, into the void below. Buffer blasting is done primarily to minimize spontaneous combustion by collapse bords and pillars. Buffer blasting is a control blasting technique which involves loading of blast-holes with small quantity of explosives in order to limit rock breakage to specified areas. However buffer blasting also affects slope stability. Buffer blasting destroys the geological discontinuities and features which could cause failure (New Vaal Colliery, 2009a).

4.5.5.4. Spontaneous Combustion

Spontaneous combustion is peculiar to any open-cast mine where underground mining has previously taken place. However, the magnitude varies with each mine, depending on the level of underground mining and effectiveness of the mining method (New Vaal Colliery, 2009a). Mild spontaneous combustion possibly due to effective buffer blasting was observed at New Vaal Colliery.

4.5.6. Mine Slope Displacement Monitoring

Like the other Anglo Coal open-cast mines, high-wall and low-wall monitoring at New Vaal Colliery is achieved by visual monitoring and radar monitoring using the MSR-200 and MSR-300 model, named the MSR-002 and MSR-003 respectively. New Vaal is the only Anglo Coal open-cast mine in South Africa with two monitoring radars. This underscores the magnitude of the slope stability problems at the mine.

4.5.7. New Vaal Open Cast Mine Case Studies

4.5.7.1. Case Study 1

On July 31st, 2009 in Ramp 6-7, spoil sloughing into the cut was observed by the geotechnical personnel when the dragline was exposing the middle seam (New Vaal Colliery, 2009b). Consequently, the radar was deployed to monitor the spoils. The slope gradually started displacing on the 7th August, 2009. The relative range of between -20mm and -30mm was reached between the 8th -11th August and between the 12th -19th August, the relative range or displacement of movement increased to greater than -50mm. The slope failure occurred on the 19th August at a movement of -100mm and a cumulative rate of displacement of -

0.4mm/hr, as coaling of the Bottom seam was progressing. Mining personnel were subsequently withdrawn from the area for safety reasons and to provide room for sand dozing of the failed area. Mining resumed the following day when the radar information indicated that the slope had stabilised (New Vaal Colliery, 2009b). The synthetic map and trend plot of the failed area is shown together in figure 4.12.

Description of Failure

The failure was largely due to the presence of a palaeo-low and water accumulation at the toe of spoils, as illustrated in figure 4.13. The weakening of the spoil base and the reduction of the effective stress of spoil material resulted in the upward propagation of tension cracks within the spoil heap. These factors possibly caused the spoil to slough (New Vaal Colliery, 2009b).

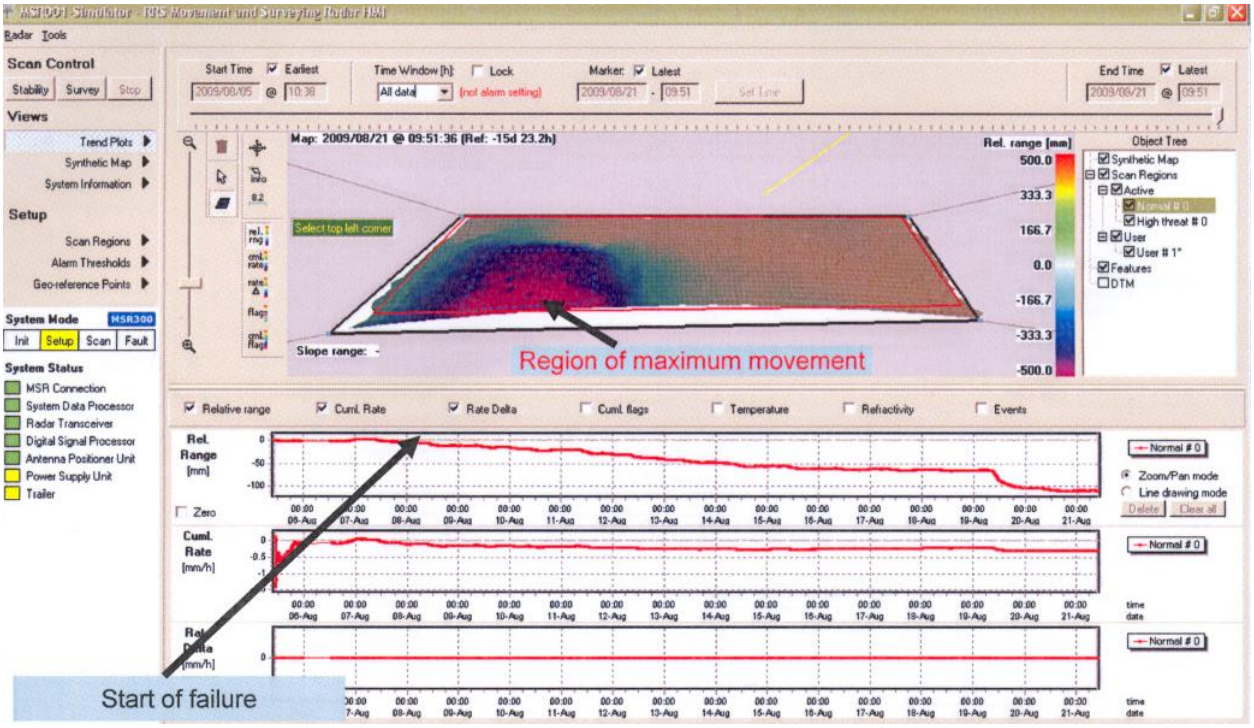


Figure 4.12: MSR trend plots and synthetic map of the scanned low-wall (New Vaal Colliery, 2009b).

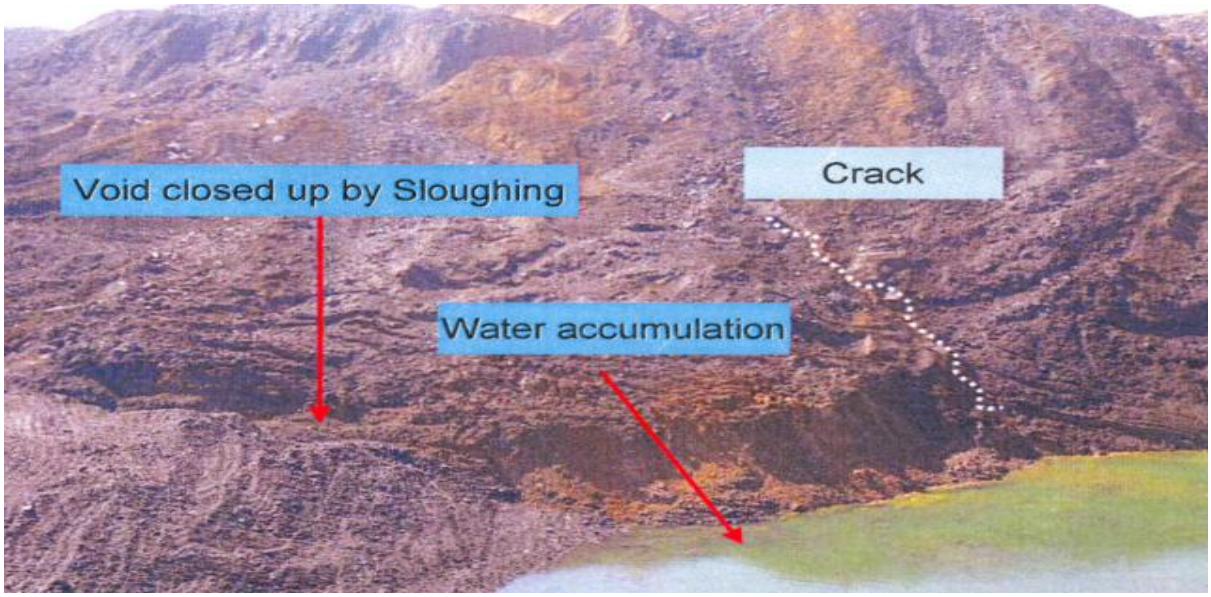


Figure 4.13: Unstable low-wall before failure (New Vaal Colliery, 2009b).

4.5.7.3. Case Study 2

Tension cracks were observed on the soft overburden on the 6th November, 2007 in ramp 12. After an assessment of the risk by the mine geotechnical personnel, it was apparent that a slope failure was imminent (Zindela, 2008). The MSR was then positioned to scan the unstable high-wall. It was observed that prior to sudden collapse as seen in figure 4.14 and 4.15, it took approximately five hours for a displacement of -50mm to occur, whereas during the sudden failure it took only two hours for the same magnitude of movement to occur (Zindela, 2008). The increase in movement was accompanied by an increase in cumulative rate of displacement from -10mm/hr to -25mm/hr during slope failure (Zindela, 2008).

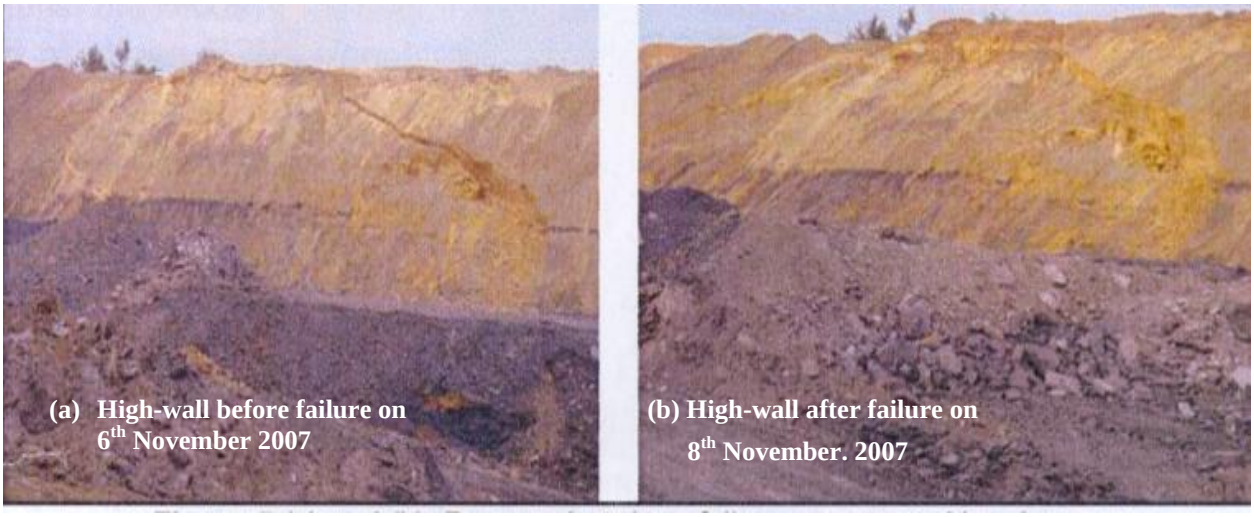


Figure 4.14: High-wall before and after failure (Zindela, 2008).

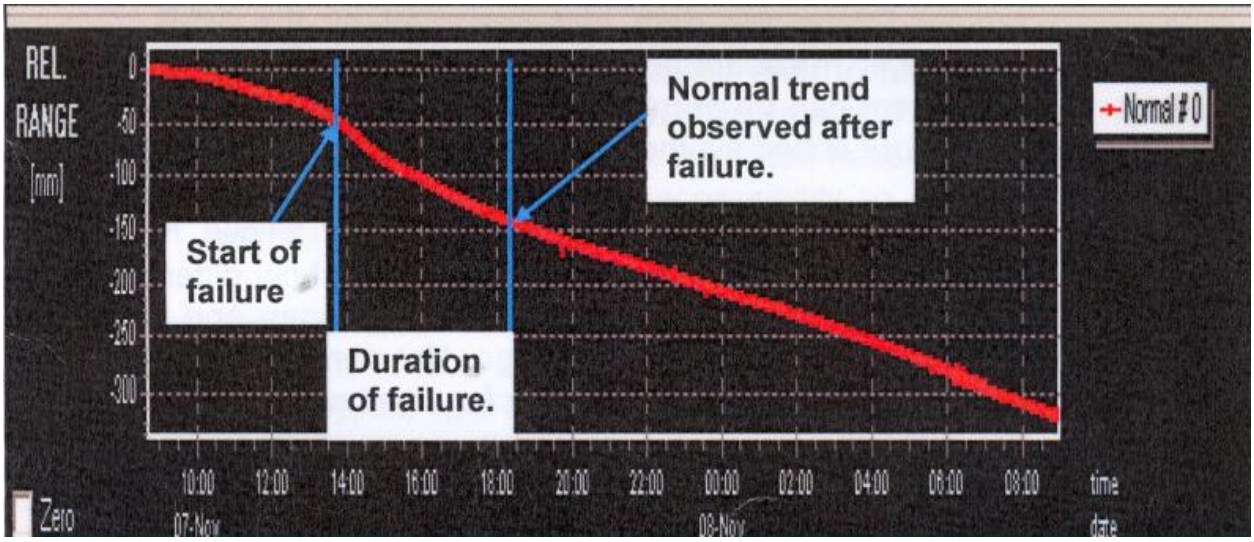


Figure 4.15: MSR trend plot of the high-wall displacement (Zindela, 2008).

Description of Failure

This type of failure can be described as progressive displacement behaviour. Initial movement was gradual and regressive but it became rapid and progressive very close to failure. After failure, the slope returned to its pre-failure state as the cumulative rate of displacement has decayed (Zindela, 2008).

4.5.7.5. Case Study 3

On the 6th of July 2008, sloughing of the low-wall was triggered by blasting of the top seam in Ramp 8 and 9. The factors that were most likely responsible for the slope failure are surcharge loading, water and dipping floor strata (Zindela, 2008). After establishing the level of instability from visual observation, the MSR was positioned on the high-wall to scan and monitor the unstable low-wall (spoil). The displacement trend obtained from the MSR is shown in figure 4.16.

The synthetic map shown in figure 4.16 indicated that the relative movement in the unstable region is higher than the other scan region. Although the slope movement was gradual initially, a sudden movement of -100mm occurred at about 21.00pm on the 9th of July 2008 (Zindela, 2008). During this sudden slope movement, the cumulative rate of displacement also increased from 0mm/hr to -10mm/hr, which caused transition from a steady to a progressive displacement. After 6:00 on the 10th, the slope started stabilising (Zindela, 2008).

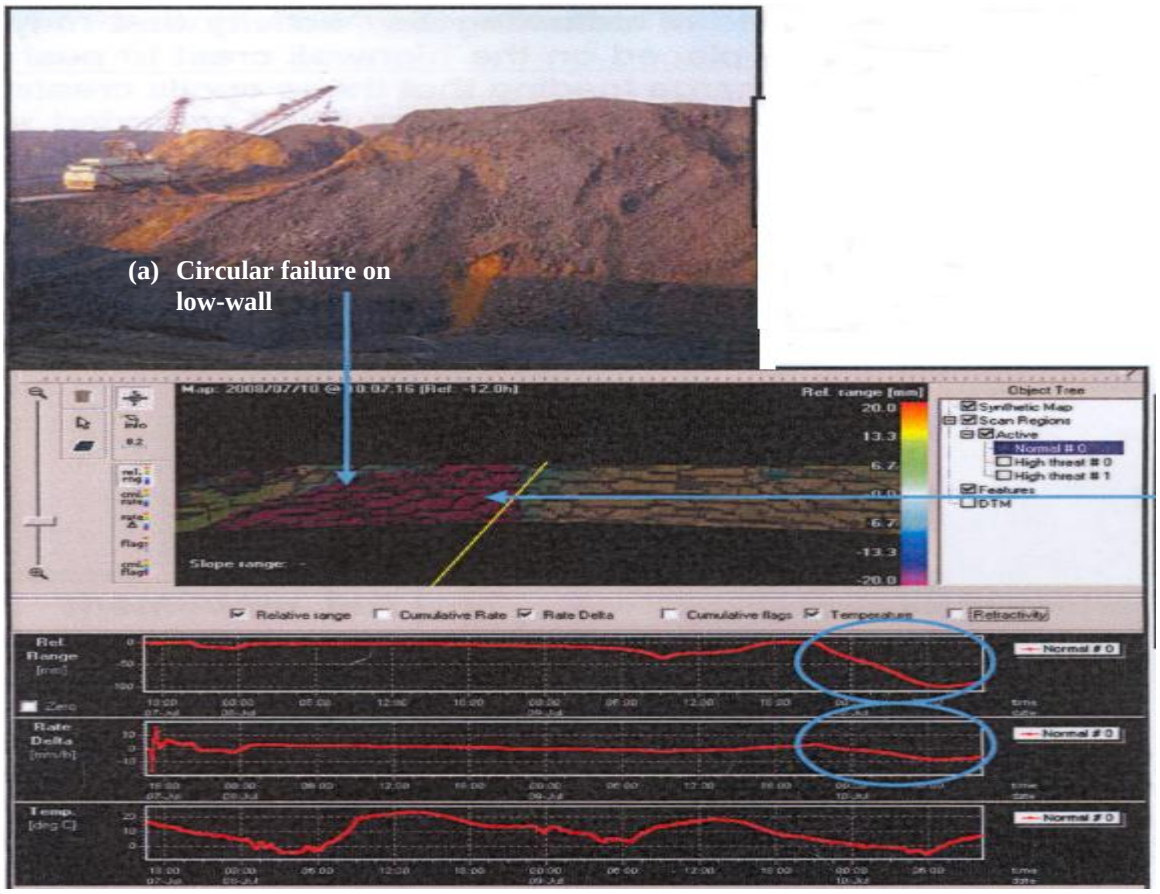


Figure 4.16: MSR synthetic map and trend plots of low-wall displacement (Zindela, 2008).

4.6. Summary

Three of the six Anglo Coal open-cast mines were visited in the course of this research work as highlighted in section 4.1 of the chapter. It was not considered necessary to visit Isibonelo, Kriel and Mafube open-cast coal mines because they are both within the Witbank coalfield, which has the same geology and has been adequately represented by the other two Ango Coal mines visited in the region. In addition, the three unvisited mines have relatively new MSR systems in place and hence, there was no radar database on slope displacement for analysis.

The open cast coal mines within the Witbank coalfield have very similar slope stability problems and this is due to the general geology of the coalfield. Overhang of rock material on the high-wall due to incomplete pre-split blasting and weakening of high-wall by spontaneous combustion, are peculiar to all the mines. The low-walls are generally stable except when weakened by spontaneous combustion and undercutting. With the exception of Landau open cast mine, which has radar monitoring record of one slope failure, there was no radar monitoring record of slope failure at the other mines. However, the monitoring records of stable slopes were available for analysis.

The low-wall and high-wall slope stability challenges at New Vaal open cast mine are due to the presence of unconsolidated soil overburden. The soil overburden which constitutes the largest percentage of the spoil material is a major factor responsible for the low strength of the low-wall.

In chapter 5, the deformation behaviour and the underlying mechanisms of both stable and unstable slopes are discussed. The chapter also contains a discussion on slope failure mechanisms observed from the displacement records.

CHAPTER FIVE

DEFORMATION BEHAVIOUR OF MINE SLOPES CASE STUDIES

In the previous chapter, detailed descriptions of the geology of the open-cast coal mines used for case studies were presented. Case examples of slope failure at the mines, some of which were monitored with the Movement and Surveying Radar (MSR) were also presented. The importance of slope monitoring was highlighted in the case example presented in section 4.4.2.12, where a sudden high-wall failure occurred. Before the failure, the high-wall was presumed stable and was therefore not monitored.

The slope failure from the visited open-cast mines, in addition to a few slope failures from some other open-cast mines, are analysed in this chapter to understand the deformation behaviour of both stable and unstable slopes of open-cast mines. The chapter is divided into four sections. The first section contains a brief description of the operations of the MSR, and interpretations of some MSR and deformation behaviour terminologies. The second section contains the description of the general deformation behaviour of the stable slopes. The third section contains the descriptions of the deformation behaviour of the unstable slopes, based on displacement data obtained from the MSR and from field observations of the monitored areas, where available. The fourth and final section discusses the observed mechanisms of failure from the radar displacement monitoring records.

5.1. MSR and Deformation Behaviour Terminology

To facilitate better understanding of the description of the deformation behaviour of mine slope case studies, the following brief discussion of terminologies used is deemed necessary.

MSR Terminology

Time Window: The MSR offers seven different time windows which are 1hour, 2hour, 4hour, 6hour, 12hour, 24hour, and the "all data" time window. The user has the option of choosing any of the time windows for viewing slope displacement. For example, the user can view the movement that has occurred in the last 1hour, 2hour, 4hour, 6hour, 12hour and 24hour, instead of seeing the total accumulated movement (Reutech, 2006b).

Displacement (Relative Range, mm): This is the slope movement between the first scan and the last scan if no time window is selected. If a time window is selected, it is the movement between the first scan and the last scan of the time window period (Reutech, 2006b). Displacement can be either positive or negative.

Positive Displacement: Positive displacement is a slope movement away from the MSR which means the slope is stabilising or stable.

Negative Displacement: Negative displacement is a slope movement towards the MSR, which means the slope is deforming or unstable.

Relative Range Colour Bar: The colour on the relative range bar represents the magnitude of movement on the map representing the slope movement.

Cumulative Rate of Displacement (mm/hr): This is determined by dividing the total accumulated movement by the total time or the total accumulated movements within a specific time window divided by the time of the time window (Reutech, 2006b). The cumulative rate of displacement is the MSR form of velocity, which could either be on the negative or positive axis. Like the displacement, a negative cumulative rate of displacement means that the slope is deforming while a positive cumulative rate means the slope is stabilising.

Point: Locations on the monitored slope are represented by points on the radar computer with each monitoring point identified by its coordinates. In radar monitoring, displacement information of sections and points on the slope are calculated.

Radar Scan Time: This is the time taken to complete a full scan of a selected area on the mine slope. Typical scan time for radar monitoring is 1 to 10 minutes, depending on the size of the scanned area (Harries and Holmstrom, 2007).

Deformation Behaviour Terminology:

Stable Slope: All slopes experience deformation as a result of elastic rebound, and relaxation of the rock mass due to changes in stresses caused by excavation (Zavodni, 2000). When the magnitude of deformation is not strong enough to cause failure, the slope is regarded as a stable slope.

Unstable Slope: Following each cycle of excavation, slopes which experience high magnitude of deformation above the rock strength are unstable slopes.

Onset of Failure: This is the point which describes the transition from regressive deformation stage to progressive deformation stage (Broadbent and Zavodni, 1982)

Deformation Pathway: A deformation pathway indicates the continuous deformation time relationship of a specific monitoring point on a slope (Mercer, 2006).

Rebound Pathway: A rebound pathway indicates the continuous rebound time relationship of a specific monitoring point on a slope.

5.2. Deformation Behaviour of Stable Slopes

The behaviour of a stable slope is characterised by the cyclical increase and decrease in the cumulative rate of displacement referred to by Broadbent and Zavodni (1982) as regressive deformation behaviour. This cyclic behaviour is presumed to be the effects resulting from activities such as mining and/or propagation of deformation within the rock mass itself. If the slope remains undisturbed, that is, no triggering factors, such as blasting and groundwater are introduced, two possible things are likely to occur. One, the slope will stabilise with time, and two, the slope may transition from the regressive stage and begin an accelerating trend to failure. This could occur with time, even in the absence of any triggering factor, and this behaviour is referred to as time dependent deformation. From the observation of the MSR data of monitored slopes, stable slope deformation behaviour has been classified into two types:

- Type I: Slopes with negative-positive regressive cumulative rate of displacement. These slopes exhibit cyclical regressive behaviour between the negative and positive axis. Such slopes are relatively stable as compared to type II slopes and will require a

very strong trigger to collapse. Figure 5.1 is a type I behaviour observed at Landau open-cast coal mine. The slope behaviour is regressive between negative and positive cumulative rate of displacement.

- Type II: Slopes with entirely negative regressive cumulative rate of displacement behaviour. These are slopes that are exhibiting deformation, although the magnitudes of deformation may not be strong enough to progress into failure. The tendency of the slope to progress to failure depends on a number of factors, chief among them being events such as blasting, water infiltration, slope undercutting and strength deterioration of the rock mass with time. Type II behaviour demands careful monitoring as this slope may begin a progressive acceleration to failure within a short period. It is considered to be, "a slope failure in waiting." This type of behaviour is represented in figure 5.2, wherein the slope cumulative rate of displacement is negative and regressive.

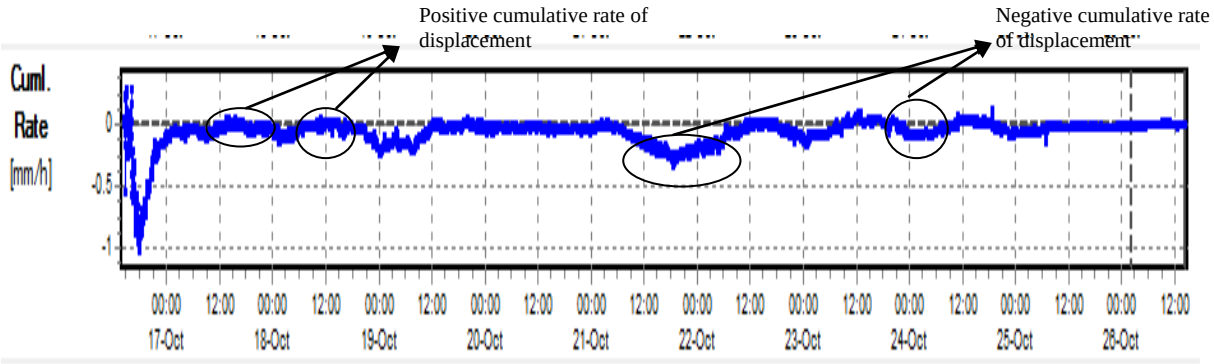


Figure 5. 1: Negative-positive regressive behaviour of stable slope at Landau open cast mine (Type I).

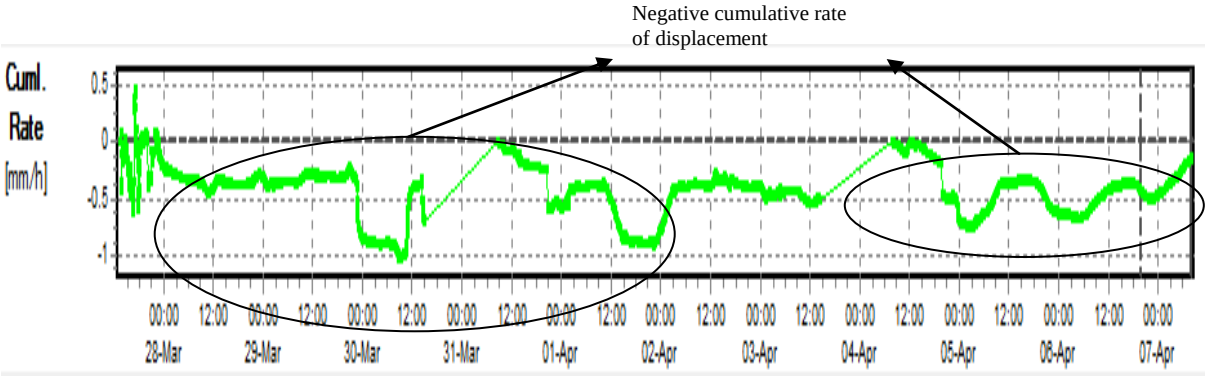


Figure 5. 2: Negative regressive behaviour of stable slope at Landau open-cast mine (Type I).

5.3. Deformation Behaviour of Unstable Slopes

This section contains detailed descriptions of the various stages in the deformation behaviour of unstable slopes. Six case examples of unstable slopes from different open-cast mines are analysed. The analyses are based on the displacement records from radar monitoring, and from field observations, where applicable. The approaches adopted in understanding the deformation behaviour of the unstable slopes before and after failure are as follows:

- The scanned region of the slope obtained from the MSR is sub-divided into a number of sections depending on the size of the monitored area. The sizes of the sections are not uniform since the monitored areas as well as the unstable sections of the slope vary in size. The purpose of dividing the monitored area into sections is to identify the unstable section where failure actually took place. A detailed analysis of the deformation behaviour is done using the 12-hour time window data extracted from the MSR. The 12 hour time window was arbitrarily chosen, since the displacement pattern is the same irrespective of time windows;
- Once the failure section had been identified, five to eleven representative points depending on the size of the unstable section are selected from the area exhibiting the highest displacement. The displacement and the cumulative rate of displacement for each point are exported into an Excel spread sheet for analysis; and
- Thereafter, the deformation process is divided into stages based on the cumulative rates of displacement of the failure region.

5.3.1. Case Example 1 (High-wall Failure)

The slope failure in this case example occurred on the high-wall of an open-pit copper mine. Information on the geological setting and location of the mine was not made available for the research and information on the field observations are also not available. Hence, the description of failure is based solely on the displacement data from the MSR. Monitoring took place from the 4th to the 7th August, 2008, giving a total of three days of monitoring data.

5.3.1.1. Locating the Area of Failure

The monitored area of the slope is divided into 9 sections as shown in figure 5.3. Figure 5.4 and 5.5 show the displacements and cumulative rates of displacement for sections one to nine. The analysis of the data indicates that all the sections except section 7 are stable, with small displacements and at negligible cumulative rates of displacement. The stable sections exhibited type I behaviour of stable slopes. The plot of the data for each section showed that failure only occurred in section 7. The magnitude of displacement and cumulative rate of displacement for the sections and points are different since they are dependent on size.

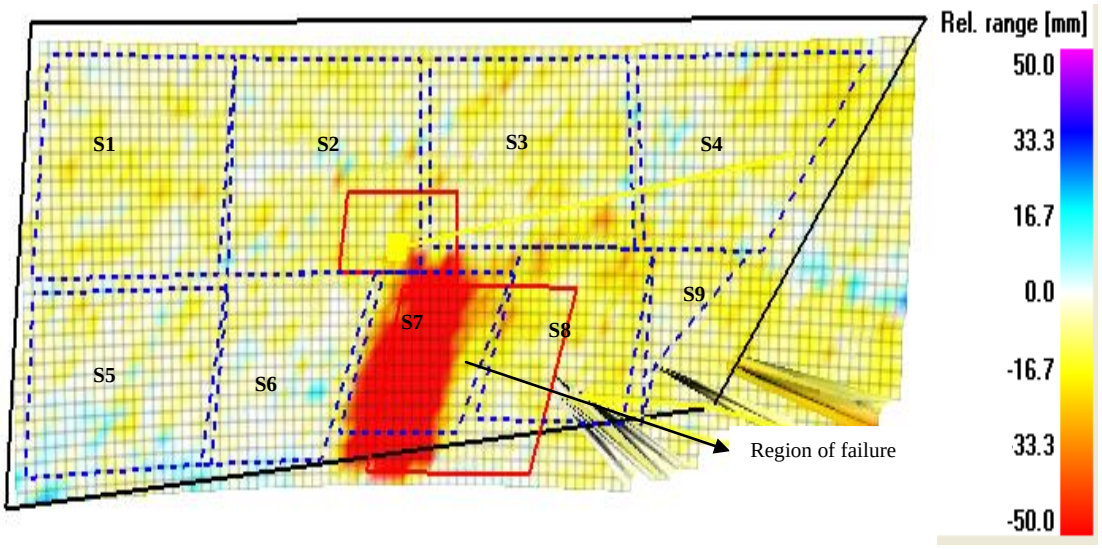


Figure 5.3: The scanned region of case example 1 slope

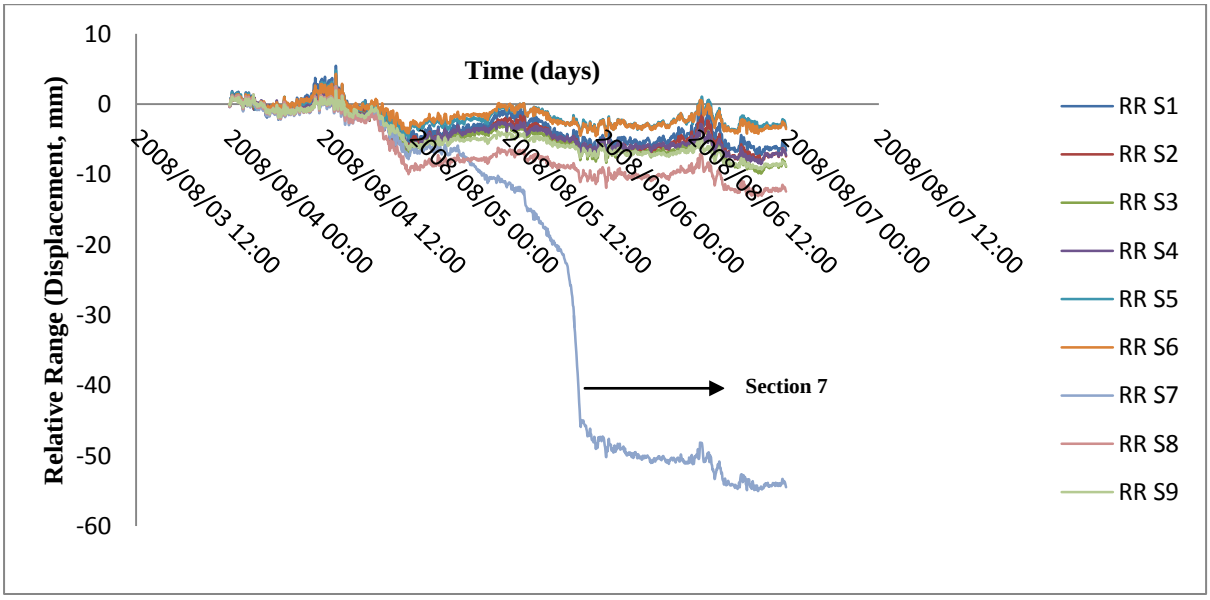


Figure 5.4: Relative range (Displacement, mm) of sections 1-9 of case example 1 slope.

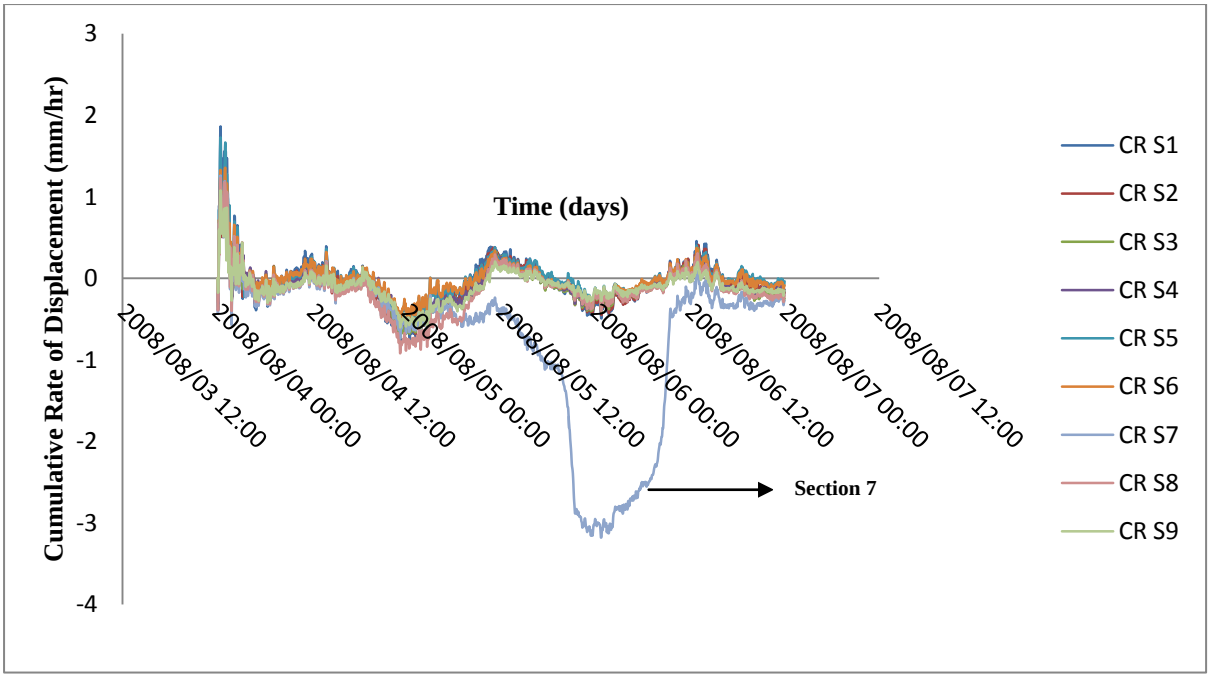


Figure 5.5: Cumulative rate of displacement (mm/hr) of sections 1- 9 of case example 1 slope.

5.3.1.2. Description of Case Example 1 Slope Failure

Figure 5.7 shows the area of failure in section 7. Data from ten different points were exported from the MSR into a Microsoft Office Excel spread sheet for a detailed analysis of the failure. Figure 5.7 and 5.8 show the plots of displacement and cumulative rates of displacement for the ten points from the failure section.

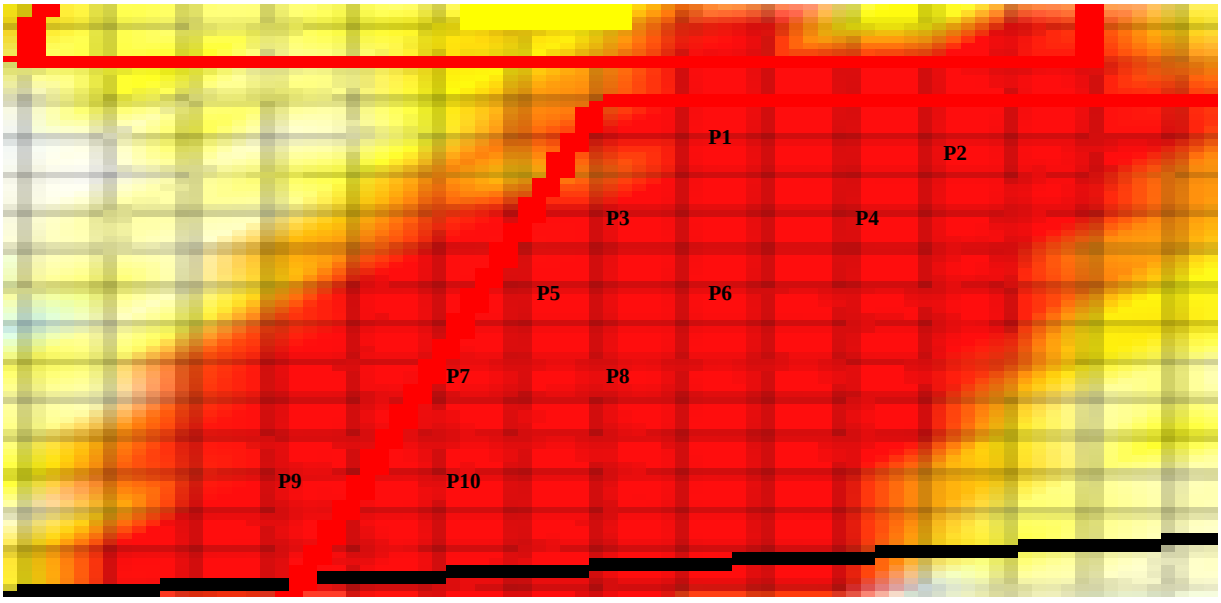


Figure 5.6: Failure section showing the locations of ten selected points in case example 1 slope.

Six identifiable stages of displacement were observed in the slope failure data obtained from the MSR.

Stage 1

Zavodni (2000) described this stage in the deformation of a mine slope as the stage of short-term decelerating displacement cycles. He further stated that in a number of cases, most slope failure starts as regressive and gradually transits to the progressive stage or becomes stable if events causing the regressive nature are removed. During this stage in the deformation of the observed slope, the displacement was from -0.41mm to -1.18mm, and the cumulative rate of displacement was between -0.41mm/hr and +0.0002 mm/hr using the average value for the failure section. This is the steady deformation stage and is characterised by the decelerating cycle of the displacement, and the cumulative rate of displacement of the slope. The displacement behaviour oscillated between negative and positive displacement, which indicates an elastic rebound in the rock mass as it resists deformation. This behaviour is similar to the vertical deformation behaviour of non-failed slopes described by Mercer (2006).

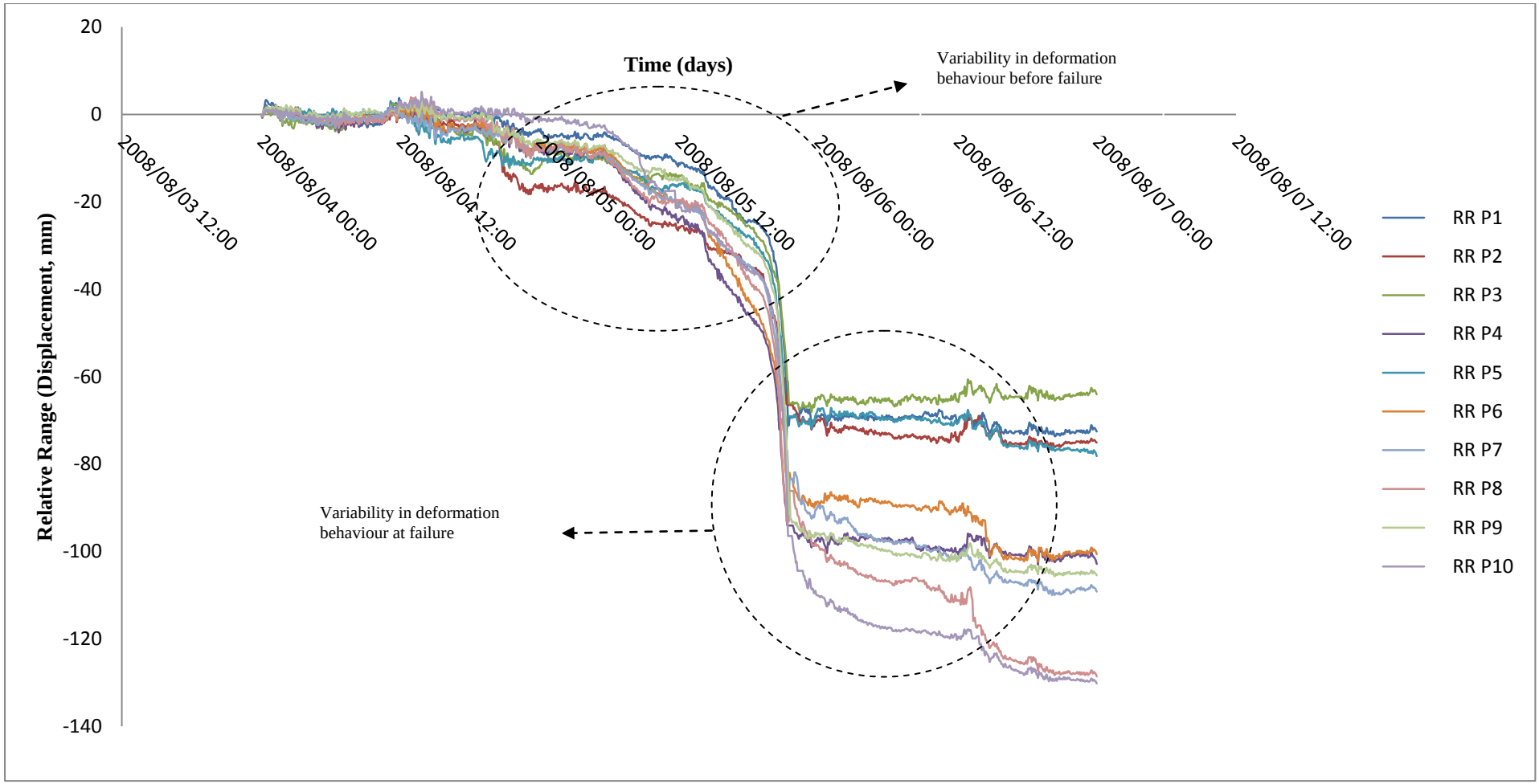


Figure 5.7: Relative range (Displacement, mm) of 10 points in the failure section of case example 1 slope.

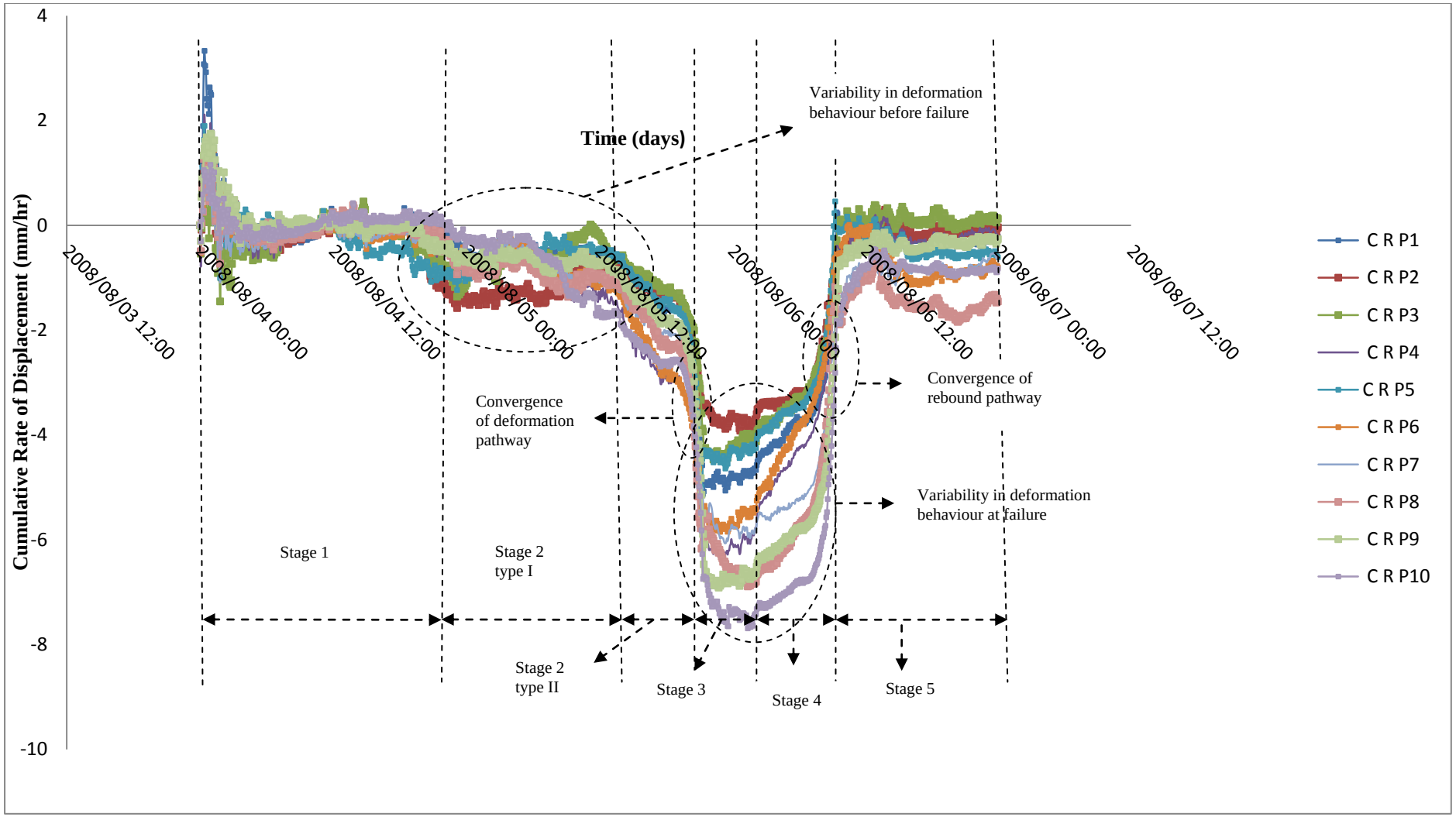


Figure 5.8: Cumulative rates of displacement, (mm/hr) of 10 points in section 7 of case example 1 slope.

Stage 2 Type I

This represents the acceleration stage referred to by Broadbent and Zavodni (1982) as the progressive stage. Sjoberg (1996) described progressive failure as the successive development of a failure surface in a slope through stress redistribution and loss of shear strength of the slope material. It is the first accelerating stage usually resulting in slope failure. This stage was reached between 17:02 and 19:07 on the 4th of August, 2008. Close observation of the failure data using the data from the ten points in the failed region showed that failure was likely to have been initiated around points 8 and 9 at the toe of the scanned area. This conclusion was arrived at because of the sudden increase in cumulative rates of displacement experienced around these points. Point 8 increased in cumulative rate of displacement by about 680% (-0.0238mm/hr to -0.1383mm/hr), while point 9 increased by nearly 1900% (-0.0056 mm/hr to -0.1106 mm/hr). The high cumulative rate of displacement relative to other points is suspected to have resulted in strength reduction around these points. This weakness is interpreted to have propagated to point 6, which experienced a sudden increase of 188% in cumulative rate of displacement (-0.00775 mm/hr to -0.2239mm/hr).

The transition from stage 1 to stage 2 is reflected in a complete change of displacement behaviour. Stage 2 reflects the inability of the rock mass to continue resisting deformation. The rock mass is deemed to have yielded or succumbed to deformation. The yielding became manifest in the variability in displacement behaviour of the different points as depicted in figure 5.7 and 5.8. Variations in the displacement behaviour indicate that complex deformation mechanisms are taking place in the rock mass during the development of the slope failure (Stacey, 2007). This behaviour eventually leads to the second acceleration stage in the progressive deformation of the slope.

Stage 2 Type II

This is the second acceleration stage, also referred to as the onset of failure. It is a stage of imminent failure where the slope progresses at high acceleration to failure when internal deformation is deemed to have taken place (Stacey, 2007). Stage 2 type II sometimes occurs concurrently with stage 2 type I (Hamiel, et al. 2004). The slope reached this stage on the 5th of August, 2008 around 14:44. Most of the points were moving at a cumulative rate of displacement above -1mm/hr. Exceptions were points 1, 3 and 5, which had cumulative rates of displacement of -0.99 mm/hr, -0.79 mm/hr and -0.85 mm/hr respectively. Once this stage is reached, failure is initiated and the time span to failure from that point is always short.

Stage 3

The slope failed on the 5th of August at a cumulative rate of displacement of -3mm/hr for the entire failure section. At failure, all the ten points within the failure region were at a cumulative rate above -3mm/hr individually. Point 4 showed the highest cumulative rate of -6mm/hr at failure. Although the displacement rates at failure were high and different, there was a convergence of the displacement pattern shortly before failure. The convergence of the displacement pattern is considered by Mercer (2006) as a merger of deformation pathway of all points (points) into a single pathway. The interpretation of the merger of pathways is that all the points failed simultaneously at high displacement rates. According to Mercer (2006), the convergence of the deformation pathways occurs when the unstable rock mass failed to disintegrate. Before stage 4 was reached, a peak cumulative rate of between -5mm/hr and -7mm/hr was experienced around points 7, 8, 9 and 10.

Stage 4

This stage precedes ultimate stability after failure, as the slope begin to regain stability by experiencing an elastic rebound from a peak cumulative rate of -4mm/hr to -0.2mm/hr for the failed section. As shown in figure 5.8, there was a big variation in the displacement behaviour of the different points at stage 4. Points 1, 2, 3 and 5 experienced rebound before the other points, followed by points 4, 6 and 7, while points 8, 9, 10 rebounded last. Again, there was convergence of the displacement behaviour pattern towards the end of stage 4. The rebound merged into a single rebound pathway.

Stage 5

The slope became stable at this stage with a negligible cumulative rate of displacement of -0.1mm/hr. The values of the cumulative rates showed that the slope has regained stability and a complete decay in cumulative rates has occurred.

Summary of Mechanisms

In case example 1, the deformation behaviour was variable before the onset of failure as a result of different responses to deformation at different points on the slope. It is most likely that the deformations at different locations resulted in the final failure on a sliding surface. This is shown by the convergence of deformation pathways shortly before failure. However, at failure, the variability in deformation resumed before the rebound stage.

5.3.2. Case Example 2 (Ramp 0 Low-Wall Failure)

Slope monitoring of the low-wall at ramp 0 at the New Vaal coal mine was carried out over a 25-day period from 13th March to 7th April 2008. The low-wall is made of a mixture of large quantity of clayey, silty sands and fragmented siltstones removed from the soft and hard overburden overlying the coal seam. The clay content in the low-wall delays drainage when recharged by rainfall (New Vaal Colliery, 2009a). Both the geological information and the MSR data are incorporated into the description of the failure.

5.3.2.1. Locating the Area of Failure

The monitored region of the slope is divided into seven different sections, as reflected in figure 5.9, to ascertain the unstable areas where failure took place. Figures 5.9 to 5.11 show that failure occurred in all the sections, because they all experienced high displacement magnitudes. All the sections experienced displacements in excess of -400mm, and a cumulative rate of displacement above -2mm/hr.

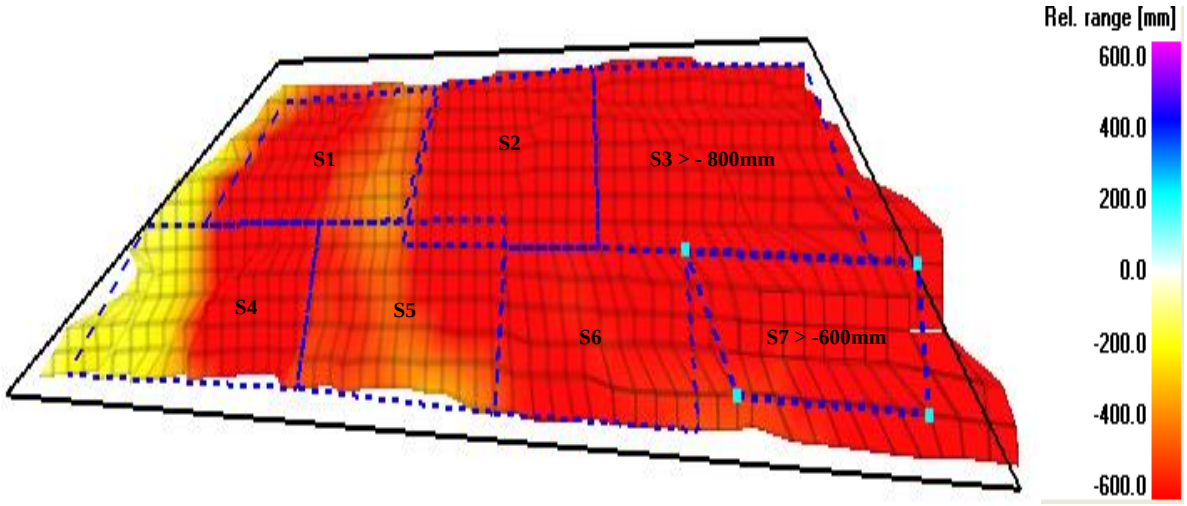


Figure 5.9: The scanned region of ramp 0 slope.

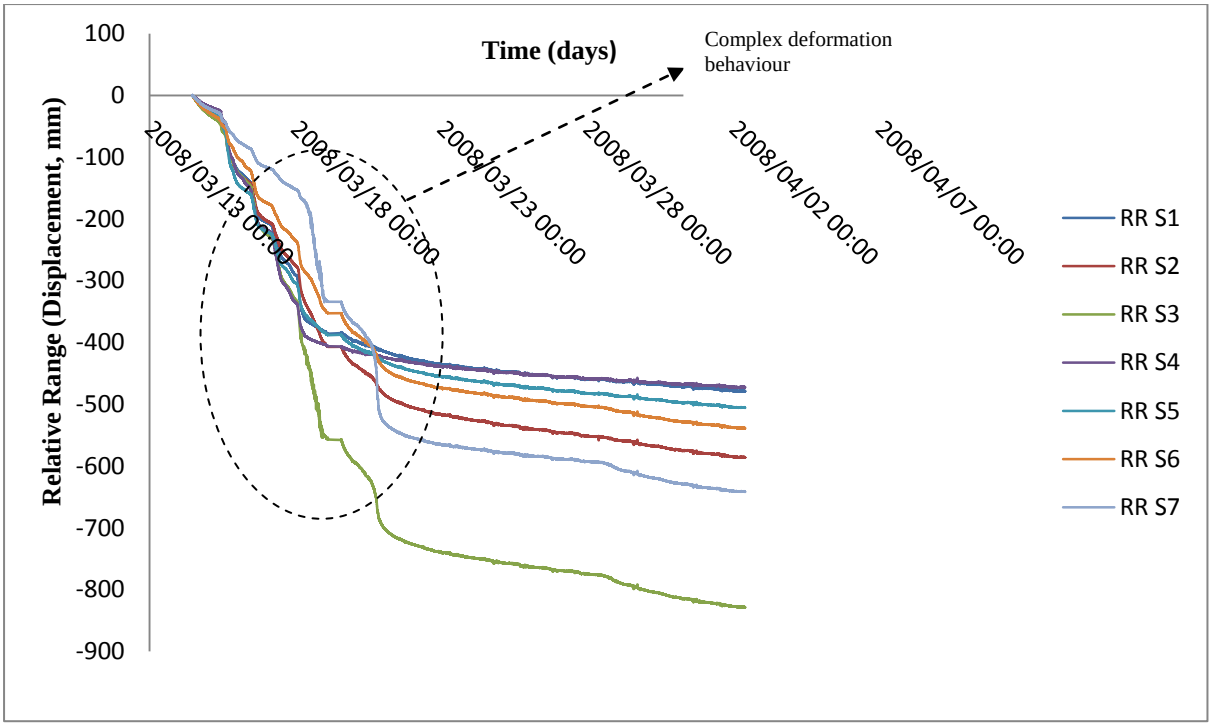


Figure 5.10: Relative range (Displacement, mm) of sections 1-7 of ramp 0 slope.

5.3.2.2. Description of Ramp 0 Slope Failure

Ramp 0 failure occurred on the entire monitored section. Since all the sections failed, the whole section becomes the failure section. Hence, the description of the deformation behaviour is based on the analysis of the displacement data for each section. The displacement data of seven points, representing the seven failure sections, are extracted for the description of the deformation behaviour. The analysis of the data obtained from the MSR indicates that the slope experienced the following five stages of failure:

Stage 1

The slope experienced cyclical displacement behaviour between the negative and positive axis from 0.3mm to -0.9mm and cumulative rates of displacement between 0.3mm/hr and -1.2mm/hr. The deformation behaviour is a type I regressive behaviour of stable slopes as described in section 5.2. The regressive behaviour lasted for two days, between 13th and 15th March 2008. Within two days of the commencement of monitoring with the MSR, the transition to stage 2 was indicated.

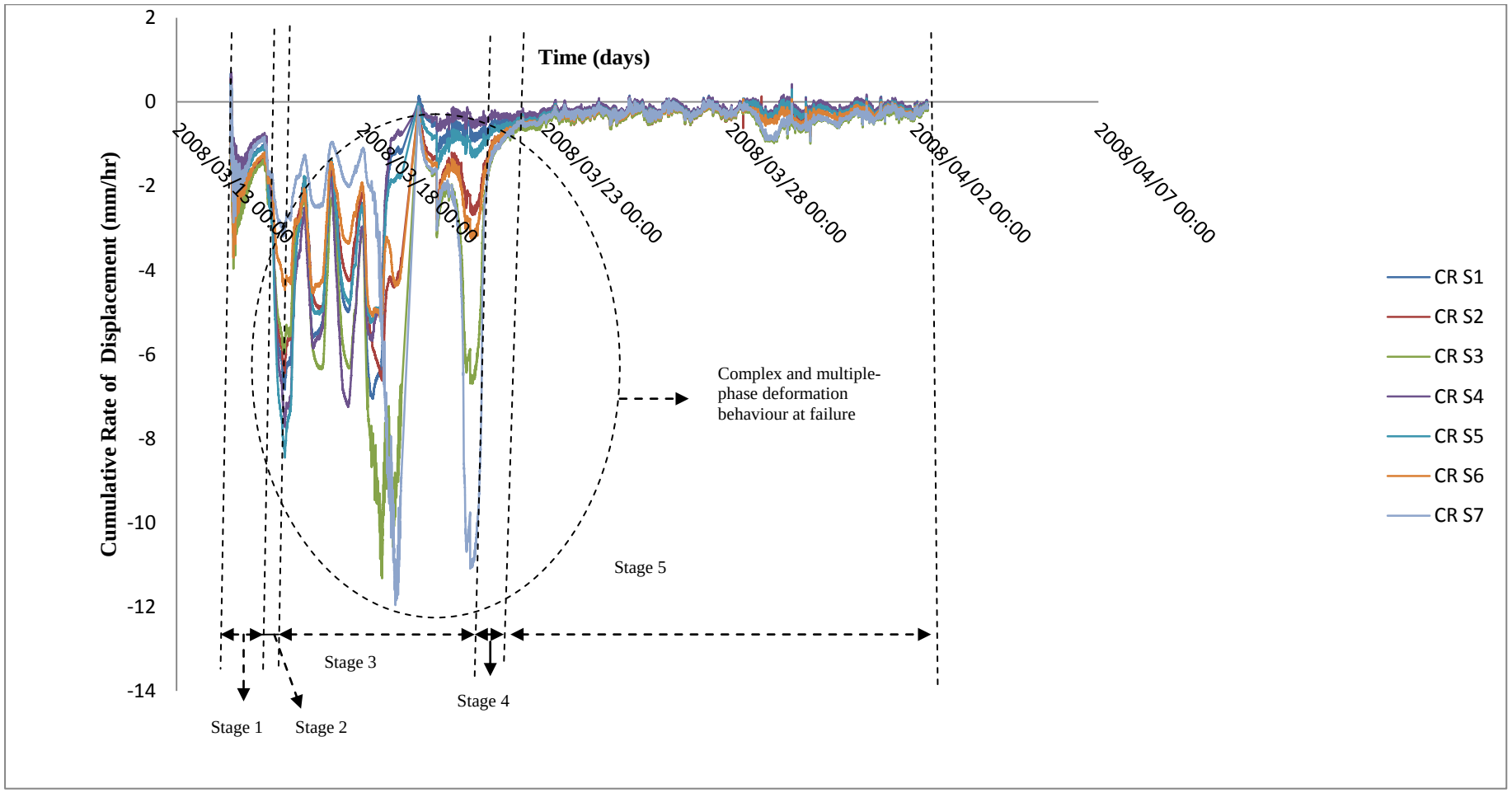


Figure 5.11: Cumulative rate of displacement (mm/hr) of sections 1-7 of ramp 0 slope.

Stage 2

In addition to being the progressive stage of failure, this stage is also the onset of failure. There was no distinct onset-of-failure transition point as both progressive displacement and onset of failure occurred concurrently (Hamiel, et al. 2004). From the onset of progressive deformation up until failure, similar displacement behaviour occurred at different points on the slope, as shown in figure 5.11. The low strength of the low-wall, resulting largely from its friable soil composition possibly resulted in the creation of a slip surface for failure to occur. Field observation at the mine showed groundwater as the common failure trigger, and water pressure must have played a role in the reduction of shear strength and subsequent creation of the slip surface. As the magnitude of displacement increased, the similar deformation behaviour gave way to a non-uniform behaviour and stage 3 was reached.

Another notable observation in this case example is that at a small displacement of between -1.4mm and -3.5mm, a high cumulative rate of displacement of about -2.4mm/hr was observed. This observation illustrates that displacement rate rather than displacement magnitude, is the true measure of slope deformation (Zavodni, 2000).

Stage 3

This is the failure stage as can be seen in figure 5.11. The slope experienced multiple-phase failures, with the first phase occurring at a cumulative rate of -2.36mm/hr and a displacement of just -3.7mm. The second, third and fourth phases occurred at cumulative rates of displacement of -2.0mm/hr to -6mm/hr with the fifth and sixth phase at a cumulative rates of displacement of -2.0mm/hr to -10mm/hr. This multiple phase of mechanism corresponds with the deep-seated circular failures at the Gold Quarry Mine, Nevada, described by Yang, et al. (2011). The back-analyses conducted on the Gold Quarry slope failure confirmed deep-seated circular failures through weak rock mass in the Carlin Formation, which was sensitive to groundwater pressure (Yang, et al. 2011). The similar displacement pattern observed in stage 2 is interpreted to have been associated with a "major" slip surface. However, this uniformity of behaviour was replaced by complex and irregular deformation behaviour after the first failure phase. Analysis of the data showed that the fifth and sixth phase occurred only in sections 2, 3, 6 and 7. While these sections showed fifth and sixth phases of failure, sections 1, 4 and 5 had already self-stabilised and returned to type I regressive behaviour of stable slopes. Only the first failure phase was common to all the sections. Probably, a major slip surface within the slope allowed all the material to experience the first phase as a unit. It

is possible that the first failure caused shearing to occur on several slip surfaces within the rock mass resulting in irregular behaviour.

Sections 3 and 7 were the most active, with displacements in excess of -800mm and -600mm respectively. The highest cumulative rates of displacement of -11mm/hr and -9mm/hr were also observed in sections 3 and 7 respectively.

Stage 4

As can be seen in figure 5.11, only sections 2, 3, 6 and 7, which showed the fifth and sixth phases of failure, experienced this post-failure stage. These areas of the slope started a late rebound to stability after the fifth and sixth phases. The sections eventually stabilised together with the other parts of the slope by returning from a peak cumulative rate of displacement of about -12mm/hr to a rate of -0.05mm/hr. There was also a merger of rebound pathways.

Stage 5

Eventually, the entire slope returned to type I regressive behaviour of stable slopes, implying that the slope was still experiencing some negative displacement behaviour. Further failure did not occur in this event and monitoring was discontinued when rates of displacement decayed completely at low cumulative value of -0.1mm/hr.

Summary of Failure Mechanisms

Ramp 0 low-wall failure is a multiple-phase failure, which occurred in six phases. The displacement behaviour can be regarded as complex, possibly with chaotic deformation on several slip surfaces. A major slip surface must have resulted in the subsequent multiple-phase failure.

5.3.3. Case Example 3 (Ramp 5 High-wall Failure)

This is an high-wall failure which occurred in ramp 5 of Landau open-cast coal mine. The high-wall is a typical Witbank coalfield high-wall consisting of 5 coal seams numbered in ascending stratigraphy order, namely the numbers 1, 2, 3, 4 and 5 seams (Landau Colliery, 2009). Overburden thickness and preservation of coal seams are dependent on the surface geomorphology and the pre-Karoo basement floor (Landau Colliery, 2009). Slope monitoring lasted nine days, from 17th - 26th October 2007, giving a total of ten days of monitoring data.

5.3.3.1. Locating the Area of failure

Figure 5.12 shows the division of the scanned area into 10 sections. Analysis of the displacement and cumulative rates of displacement for the sections, as seen in figure 5.13 and 5.14, indicated that failure took place in sections 4 and 9. Displacement at the two sections were greater than -60mm, with cumulative rates of displacement greater than -2mm/hr. The displacement experienced at the other sections were generally less than -25mm, with cumulative rates of displacement less than -1.5mm/hr.

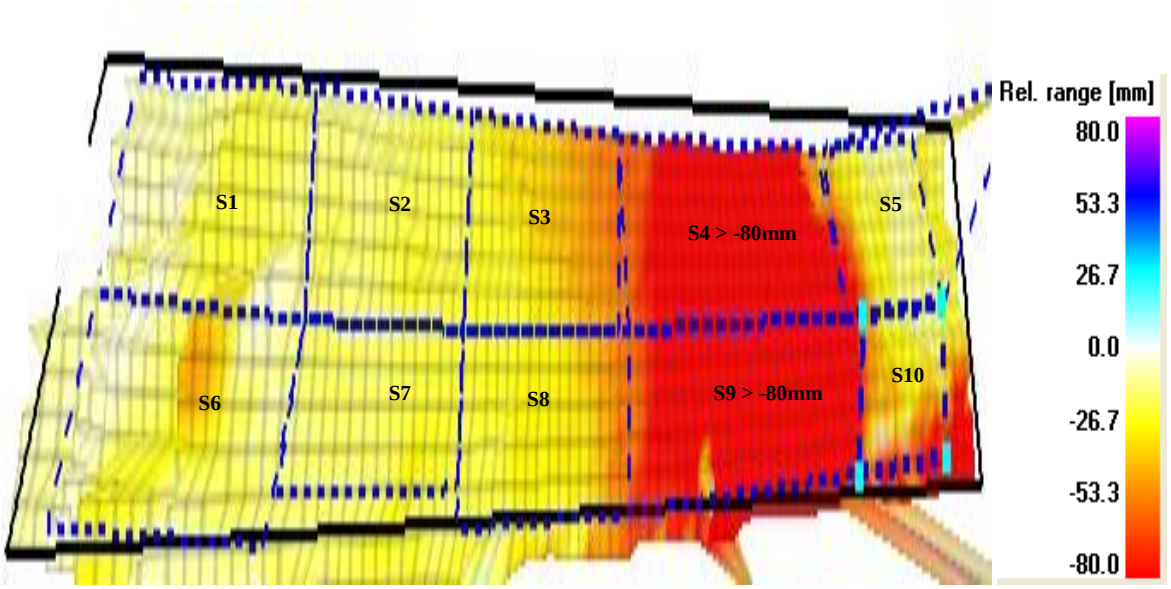


Figure 5.12: The scanned region of ramp 5 slope.

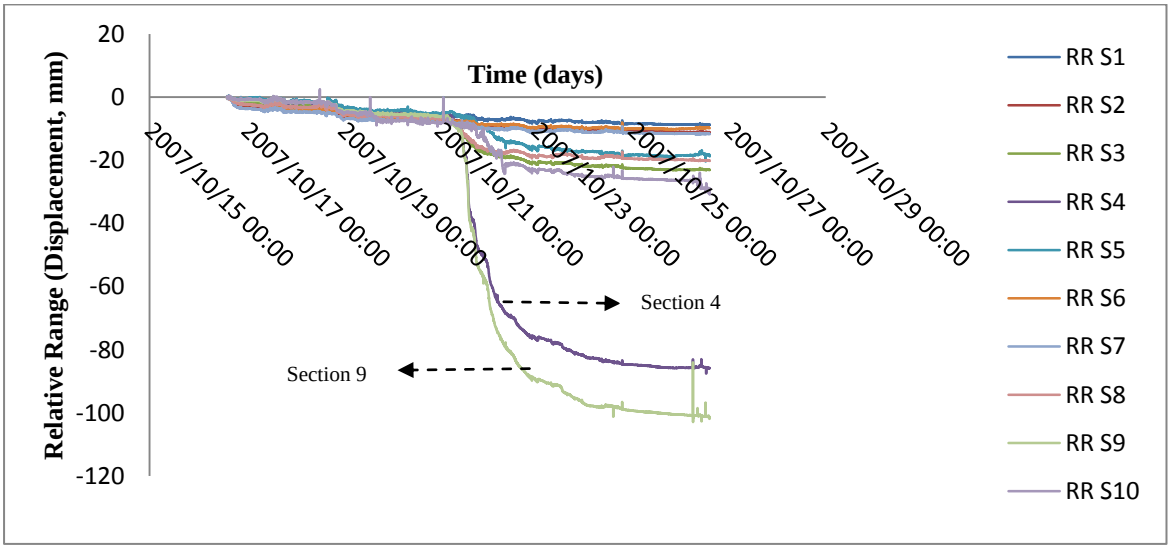


Figure 5.13: Relative range (Displacement, mm) of sections 1-10 of ramp 5 slope.

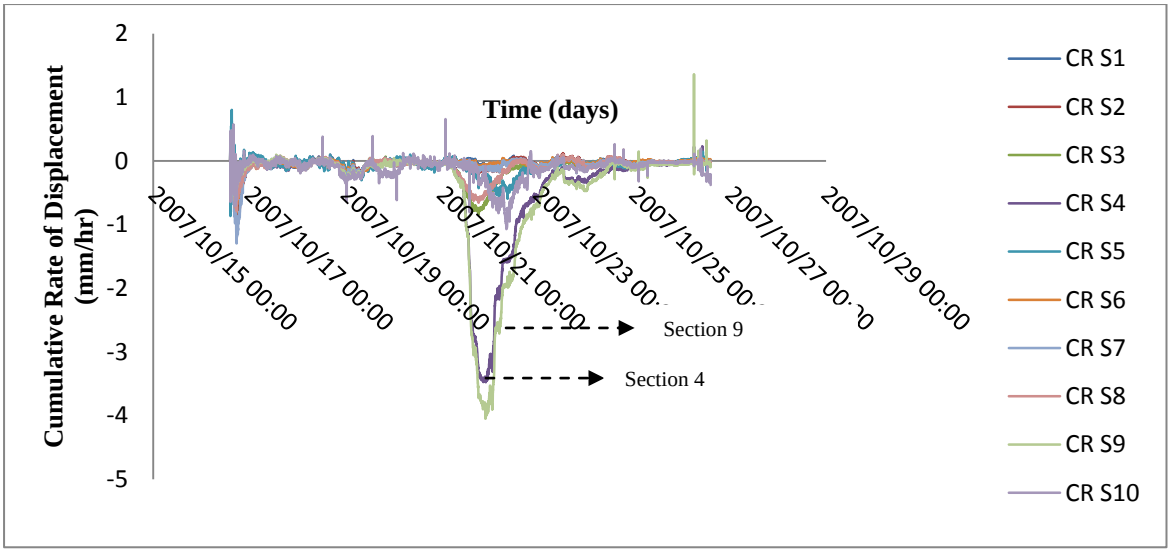


Figure 5.14: Cumulative rate of displacement (mm/hr) of sections 1-10 of ramp 5 slope.

5.3.3.2. Description of Ramp 5 Failure

Figures 5.15 to 5.17 show the analyses of displacement data of eleven points in the failure section, namely sections 4 and 9.

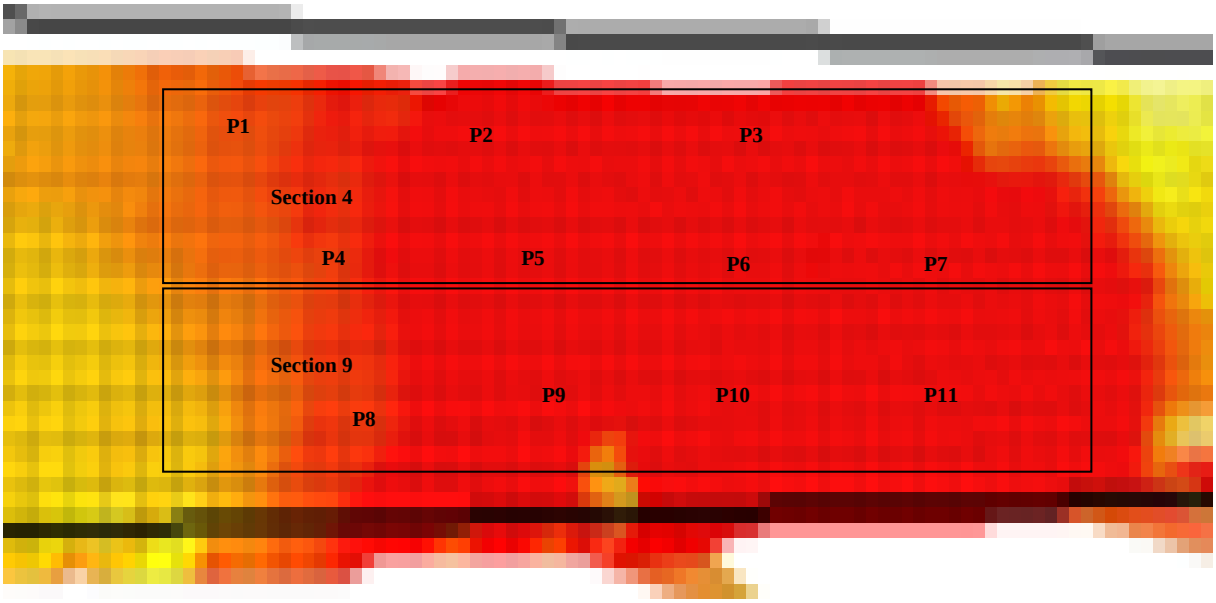


Figure 5.15: Failure section of ramp 5 showing the locations of eleven selected points.

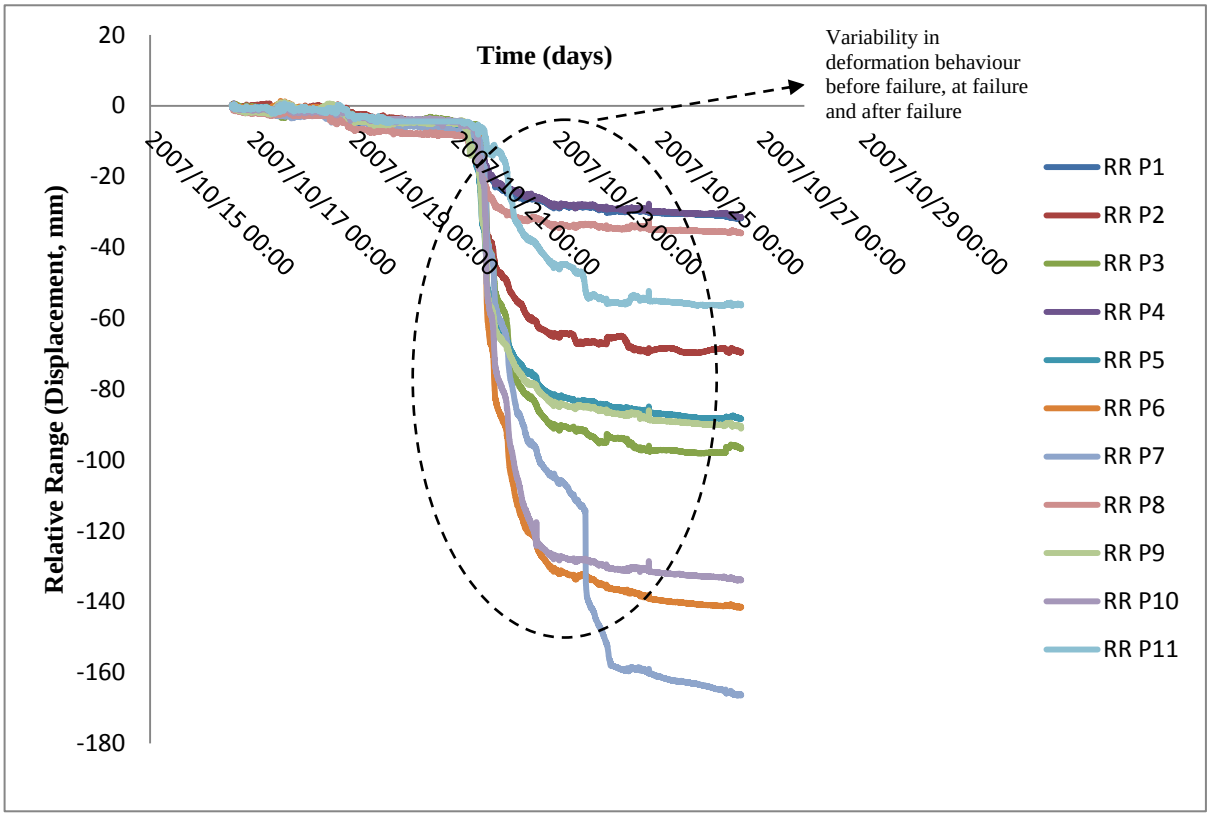


Figure 5.16: Relative range (Displacement, mm) of eleven points in ramp 5 failure region.

A total of five stages of displacement were observed in the development of ramp 5 slope failure. These stages and the underlying mechanisms are discussed in detail in the following section.

Stage 1

This is the regressive displacement stage which in some occassions may be prolonged for a long time, sometimes for years, a condition referred to as creep. Creep in rock mass is regarded as the gradual movement of the rock material on the slope without the formation of a failure surface (Radbruch-Hall, 1978). In other cases, regressive displacement lasts only for days or hours. From the commencement of monitoring, ramp 5 slope failure was at this stage of slow cumulative rate of displacement for a period of five days before progressing to stage 2. The slope experienced an elastic rebound between negative and positive cumulative rates of displacement between 0.1mm/hr and -0.04mm/hr. These values represent the cyclical displacement behaviour of the failure region at stage 1. The surrounding stable regions of the slope have lesser values of cumulative rates of displacement.

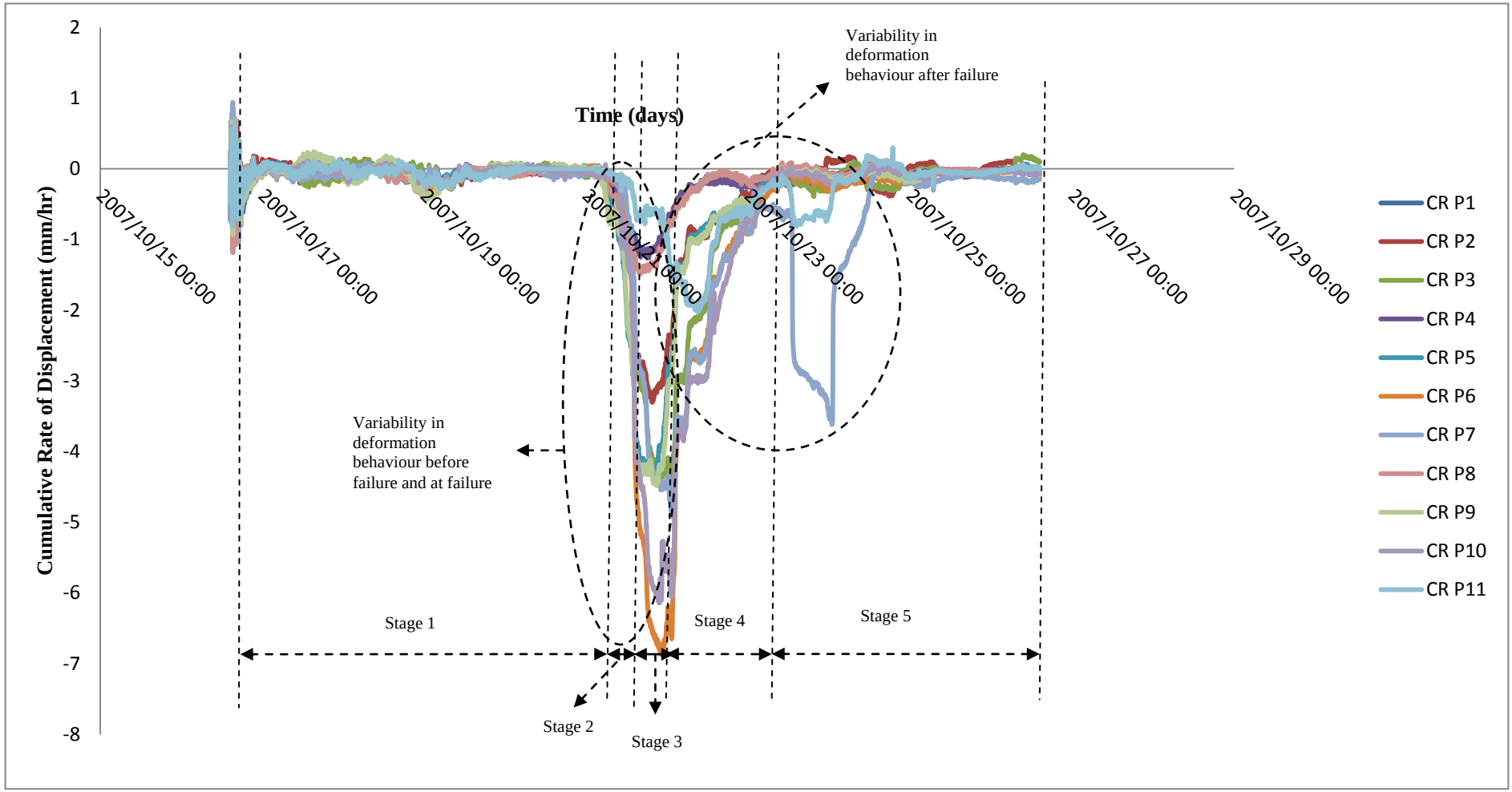


Figure 5.17: Cumulative rate of displacement (mm/hr) of eleven points in ramp 5 failure region.

Stage 2

The entire failed section of the slope attained a peak cumulative rate of displacement of -0.7mm/hr at stage 2. There was no distinction between progressive displacement and the onset of failure, as both behaviours occurred concurrently. Analysis of the data from eleven selected points from the failure section indicates that points 6 and 7 were the most active. The cumulative rate of displacement at point 6 increased from -0.0226mm/hr to -0.0454mm/hr, while point 7 increased from -0.0371mm/hr to -0.171mm/hr, representing a 100% and a 361% increase respectively. This is interpreted as the most active points on the slope and must have influenced the failure of the other points. As shown in figure 5.16 and 5.17, different deformation behaviour occurred simultaneously at different points on the slope. This corresponds with the observation made by Stacey (2007) during some slope model tests. In the study, Stacey (2007) stated that deformation may take place at different locations throughout the rock mass prior to failure. While deformation was taking place around points 6, 7 and 10, others points were rebounding concurrently. The displacement behaviour can be described as progressive and complex.

Stage 3

The slope failed around 15:00pm on the 21st of October 2007, before experiencing a rebound. The failure must have been initiated by the strength deterioation around points 6 and 7. The non-uniform behaviour noticed in stage 2 became advanced in stage 3 with no convergence of deformation pathways at failure. Both points 4 and 8 rebounded earlier than the other points on the slope. The lack of convergence of deformation pathways in stage 2 and 3 demonstated that the slope did not fail as a rigid body.

Stage 4

After attaining a cumulative rate of displacement of -3.9mm/hr, the slope began the process of rebound to a regressive state. The cumulative rate of displacement progressively decreased to -0.2mm/hr from a peak of -6.5mm/hr. It was also observed that the rebound pathways were not uniform, and each point rebounded at its own rate. Only points 4 and 8 rebounded on the same pathway, and this again supports the idea of complex deformation in the slope.

Stage 5

After undergoing rebound, the slope completely returned to type I regressive displacement behaviour with the exception of point 7. The complexity observed in stage 2 is interpreted to

have triggerred another failure around point 7. The second collapse occurred simultaneously with regressive displacement taking place at other points on the slope. The second collapse was probably due to the inabilities of the rock mass to withstand the localised deformation left by the first failure. Mercer (2006) referred to this event as "para-sympathetic failure" which occurs when a collapse of a section of the rock mass triggers collapse in adjacent sections of the surrounding rock mass. Evetually, the slope became stable as all the points returned to their pre-failure state wherein displacement was cyclical between negative and positive cumulative rates of displacement. When monitoring was discontinued, there was a complete decay in the cumulative rates of displacement at all points.

Summary of Failure Mechanisms

The displacement behaviour of Ramp 5 high-wall failure can be described as complex and highly variable both at failure and after failure. There was no convergence of both deformation and rebound pathways. It appears that the rock mass did not fail as a rigid body, but possibly by damage progression through shearing in the rock mass.

5.3.4. Case Example 4 (Ramp 11 High-wall Failure)

The high-wall of New Vaal coal mine consists of unconsolidated soft overburden of clayey, silty which is highly susceptible to failure. In ramp 11 of the mine, a small slope failure occurred in the weak soil layer of the mine high-wall. The slope was monitored for a total of five days, between the 29th January and 5th February 2008.

5.3.4.1. Locating the Area of Failure

In order to locate the critical area of failure, the monitored area of the slope is divided into eight sections as shown in figure 5.18. The analysis of the displacement records, as shown in figures 5.19 and 5.20, indicated that failure occurred in sections 2, 3, 4, and 8, with small and negligible deformation in sections 1, 5, 6 and 7.

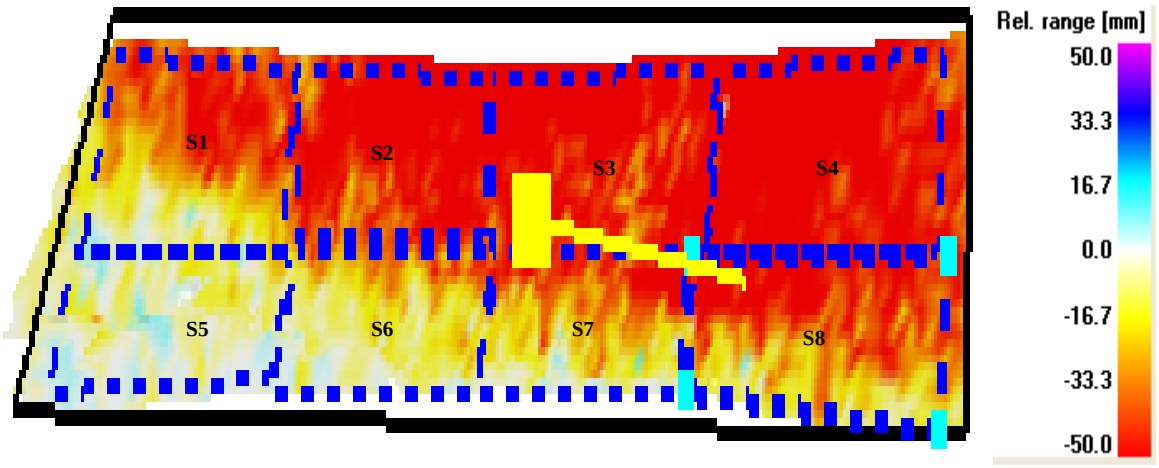


Figure 5.18: The scanned region of ramp 11 slope.

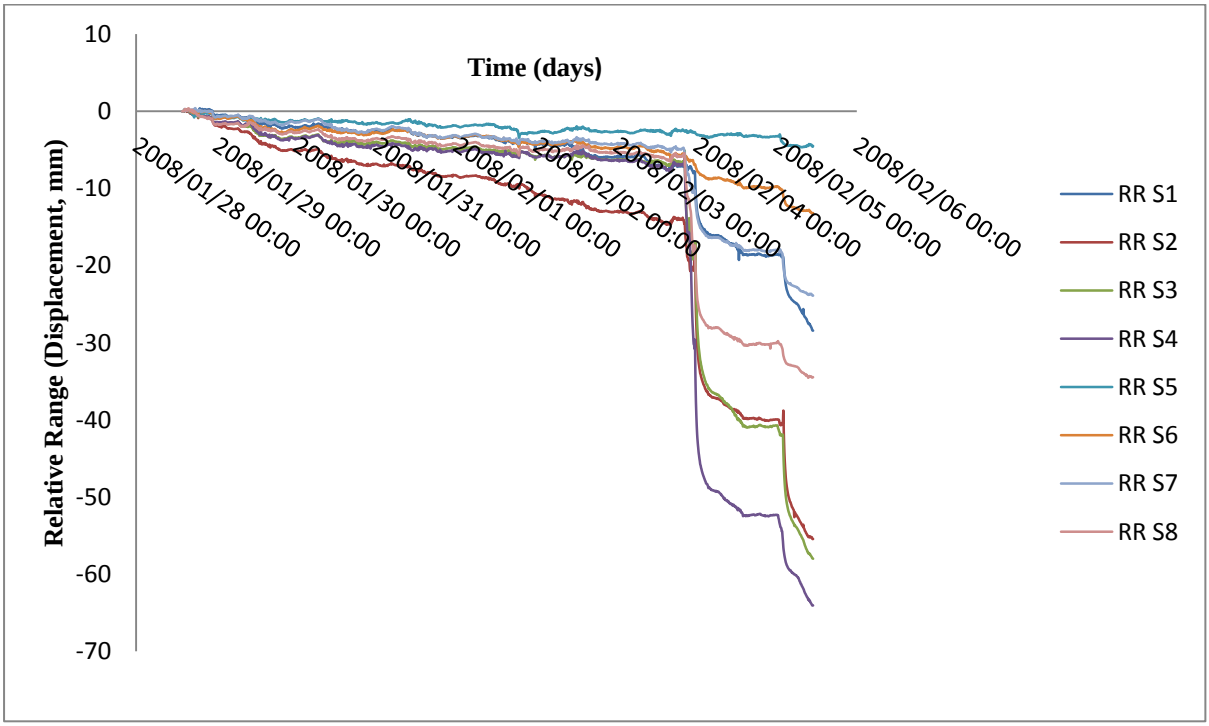


Figure 5.19: Relative range (Displacement, mm) of sections 1-8 of ramp 11 slope.

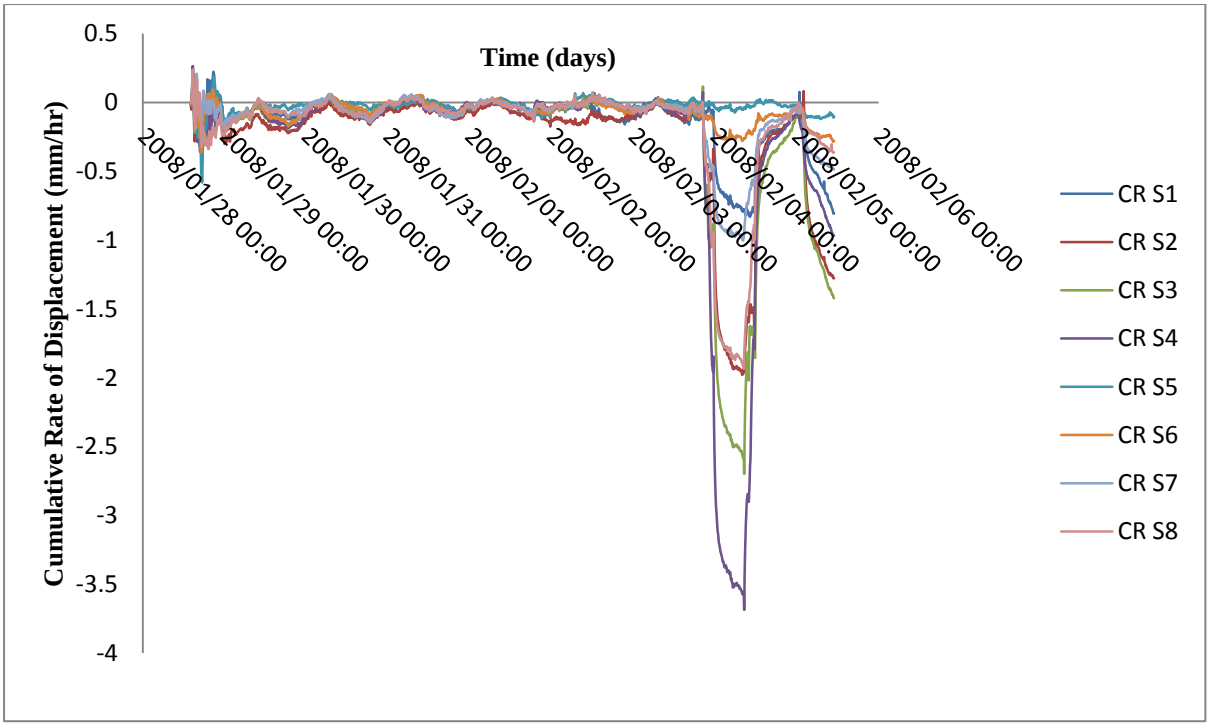


Figure 5.20: Cumulative rate of displacement (mm/hr) of sections 1-8 of ramp 11 slope.

5.3.4.2. Description of Ramp 11 Failure

The description of ramp 11 failure is based on the displacement behaviour of 10 selected points, as can be seen in figure 5.21, from the identified failure sections. Plots of the displacement and cumulative rates of displacement of the points are shown in figure 5.22 and 5.23 respectively.

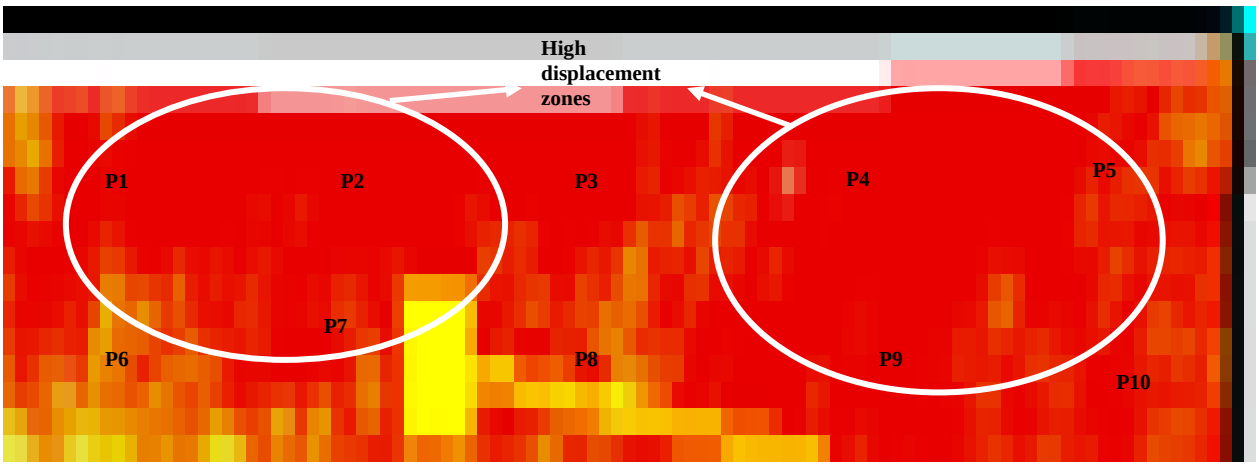


Figure 5.21: Failure section of ramp 11 slope failure showing the locations of ten selected points.

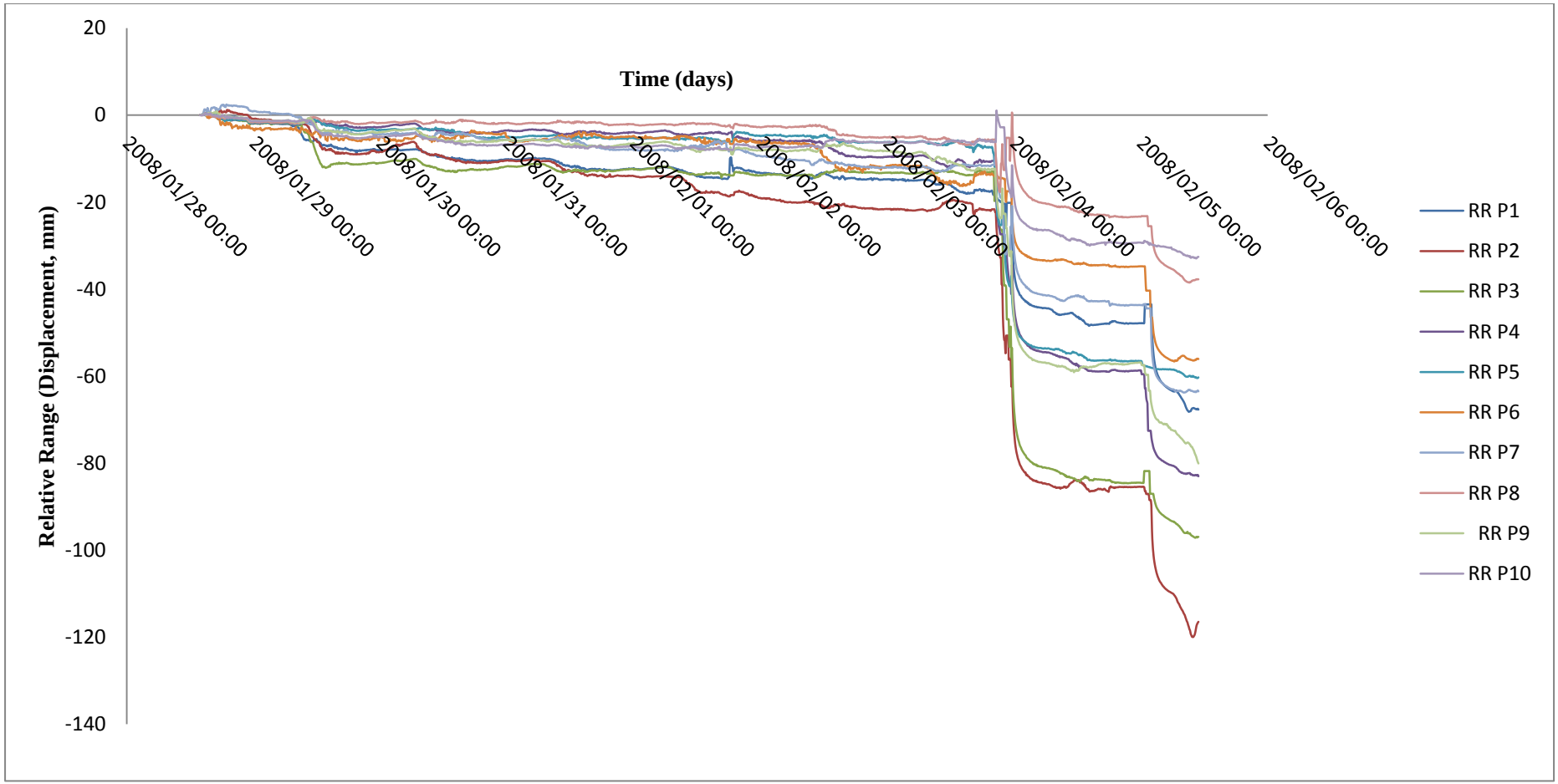


Figure 5.22: Relative range (Displacement, mm) of 10 points in ramp 11 failure sections.

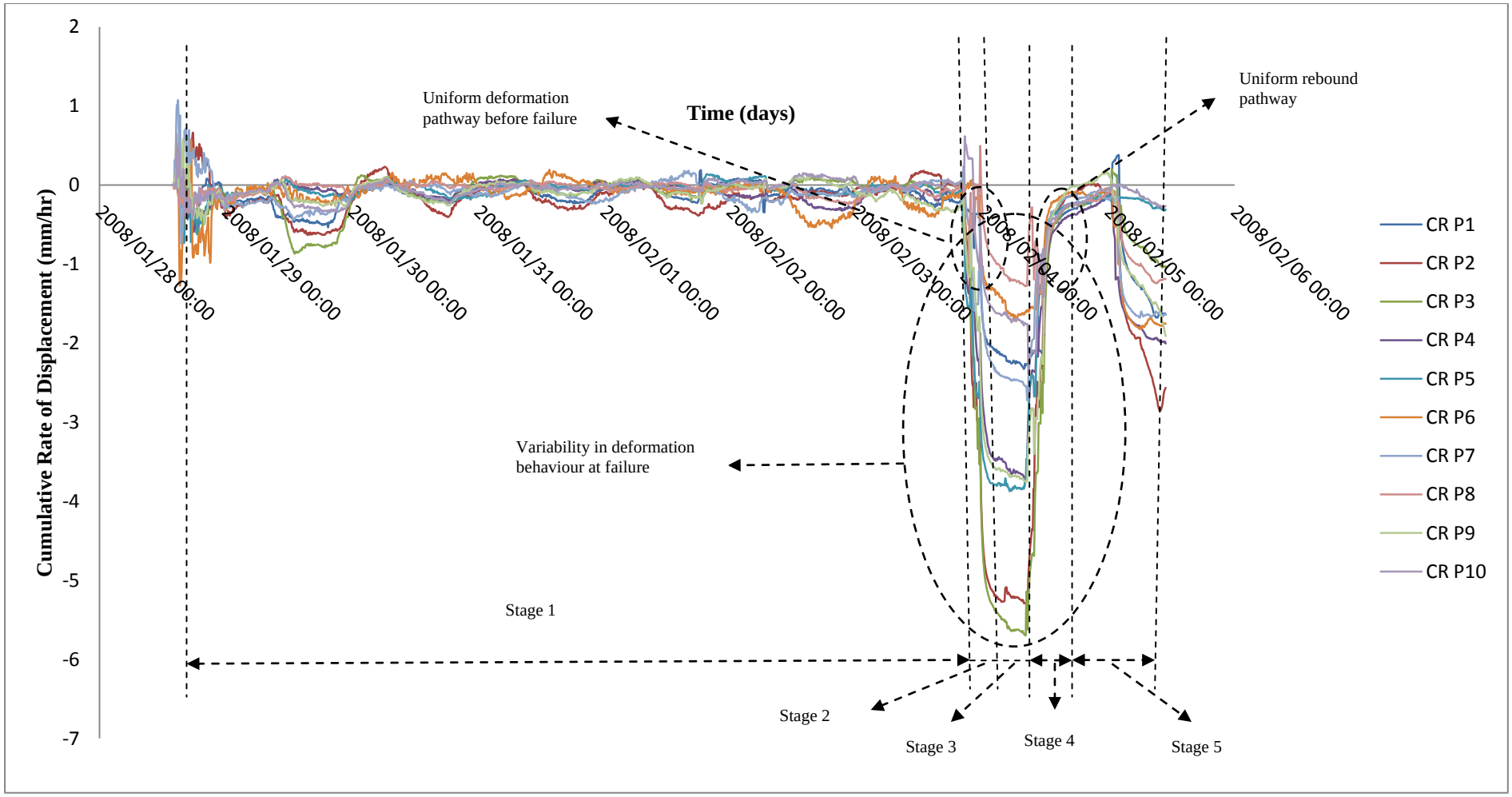


Figure 5.23: Cumulative rate of displacement (mm/hr) of 10 points in ramp 11 failure sections.

Utilising the cumulative rates of displacement, the slope failure developed over five stages from pre-failure stage to post-failure stage. A description of the deformation behaviour and observed mechanisms are discussed in the following sections.

Stage 1

The regressive displacement behaviour observed at this stage is of type I behaviour of stable slopes. It is a recurring displacement behaviour between positive and negative cumulative rates of displacement. The failure sections of the slope experienced small cumulative rate of displacement between 0.2 mm/hr and -0.1mm/hr, and similar movement was also observed in the stable sections of the slope. Shortly before the slope became progressive, some points on the slope, specifically point 1 and 9 which are located in the high displacement zone moved from type I to type II regressive displacement behaviour of stable slopes. This occurred while other points experienced type I regressive behaviour. This variation in displacement behaviour was short-lived and transition to stage 2 occurred at all points on the slope without much variation in deformation behaviour. The regressive behaviour became progressive with cumulative rates of displacement being absolutely negative.

Stage 2

The slope became progressive when the average cumulative rate of displacement for the failure sections attained -0.5 mm/hr. In this case example, there was no clear onset of failure in the displacement behaviour of the slope. Also, there were similarities in the displacement behaviour among all the points at the progressive stage prior to failure. Convergence of deformation pathway occurred before failure. Analysis of the data from the ten points showed that point 7 increased in cumulative rate by 822% (-0.0167mm/hr to -0.1541mm/hr). The sudden increase in cumulative rate, must have caused an increase of 41% (-0.3459mm/hr to -0.4879mm/hr), 41% (-0.4147mm/hr to -0.5843mm/hr) and 40% (-0.4943mm/hr to -0.6943mm/hr) in neighbouring points 2, 3 and 8 respectively. It was equally observed that point 5 had an increase of 79% (-0.74mm/hr to -1.3346mm/hr), which possibly influenced the 20% (-0.8094mm/hr to -0.9791mm/hr) increase in cumulative rate of displacement noticed in point 4. Only point 6 and 10, which falls outside the high displacement zone, showed decrease in cumulative rates.

Stage 3

Failure occurred on the 4th of February, 2008 around 00:36am. The duration of stage 2 to stage 3, which is the onset of failure to actual failure stage occurred within five hours. Using the average value for the failure region, failure occurred at a cumulative rate of displacement of about -2.1mm/hr. This increased as the slope failed until a cumulative rate of displacement of about -2.6mm/hr was reached. At failure, only points 2 and 3 attained the highest cumulative rates of displacement above -5.00mm/hr. The deformation behaviour was highly variable at failure. As illustrated in figure 5.23, the points moved in five different groups at different cumulative rates of displacement. The transition from uniform displacement behaviour before failure to non-uniform behaviour at failure indicated the different reactions to deformation at both stages. As shown in figures 5.21 to 5.23, the magnitude of displacement varies at different points on the slope.

Stage 4

Stage 4 represents the first post-failure stage wherein the slope rebounds to its original state. From a peak cumulative rate of displacement of -2.6mm/hr at failure, the slope rebounded to a rate of -0.19mm/hr, using average value for the failure section. Every slope experiences a rebound after failure before final stability. As the cumulative rate of displacement decreased, all the points in the failure section rebounded on a uniform pathway shortly before complete stabilisation.

Stage 5

After the rebound in stage 4, the slope became temporarily stable. Before monitoring was discontinued, a second progressive displacement behaviour was observed on the slope. The cumulative rate of displacement increased again around point 2 from -0.19mm/hr to -1.15mm/hr. Further analysis could not be done since monitoring was stopped.

Summary of Failure Mechanisms

Ramp 11 failure experienced a convergence of deformation pathways before failure as all the points moved on the same deformation pathway, which possibly indicates that failure occurred on a common sliding surface. However, at failure, the deformation behaviour became variable as the points failed in groups.

5.3.5. Case Example 5 (Ramp 12 High-wall Failure)

Ramp 12 high-wall of New Vaal coal mine was monitored for seven days between the 7th and 14th march, 2008 with the MSR. The slope failed around 16.00 on the sixth day of monitoring, and monitoring was discontinued on the seventh day when the slope showed signs of stabilisation. The geology of the mine is the same as the geology of case example 4.

5.3.5.1. Locating the Area of Failure

As illustrated in figure 5.24, the scanned region of the slope is divided into ten sections. The displacement data of each section is analysed to determine the extent of the failure. Figures 5.25 and 5.26 showed that failure occurred in the entire scanned region. Cumulative rates of displacement above -2mm/hr and relative range above -40mm were observed in sections 3, 4, 5, 6, 7, 8 and 9 while cumulative rates of displacement of -1.5mm/hr with relative range under -40mm were observed in sections 1 and 2.

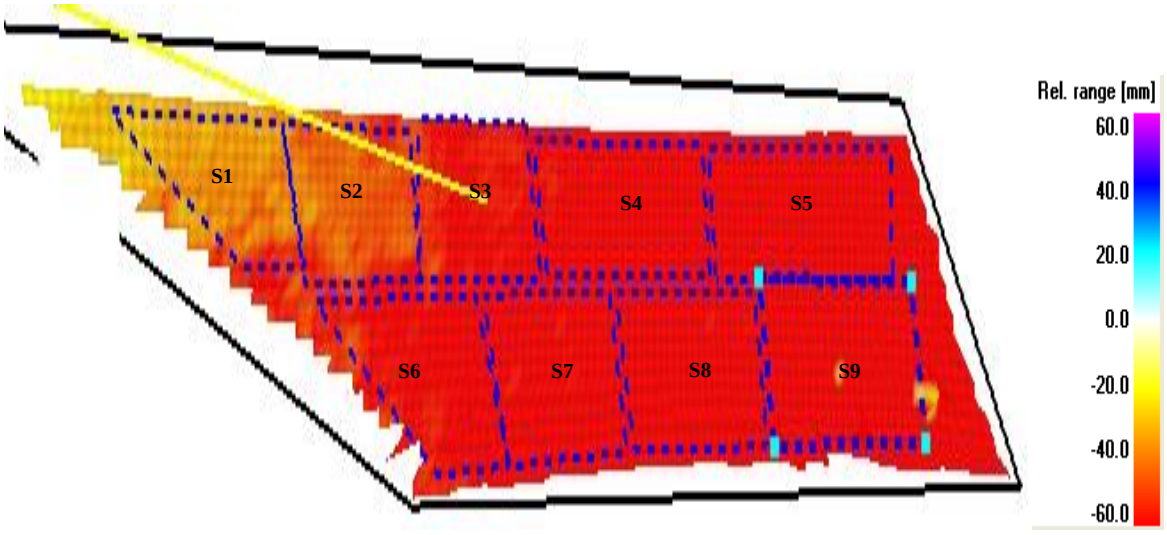


Figure 5.24: The scanned region of ramp 12 slope.

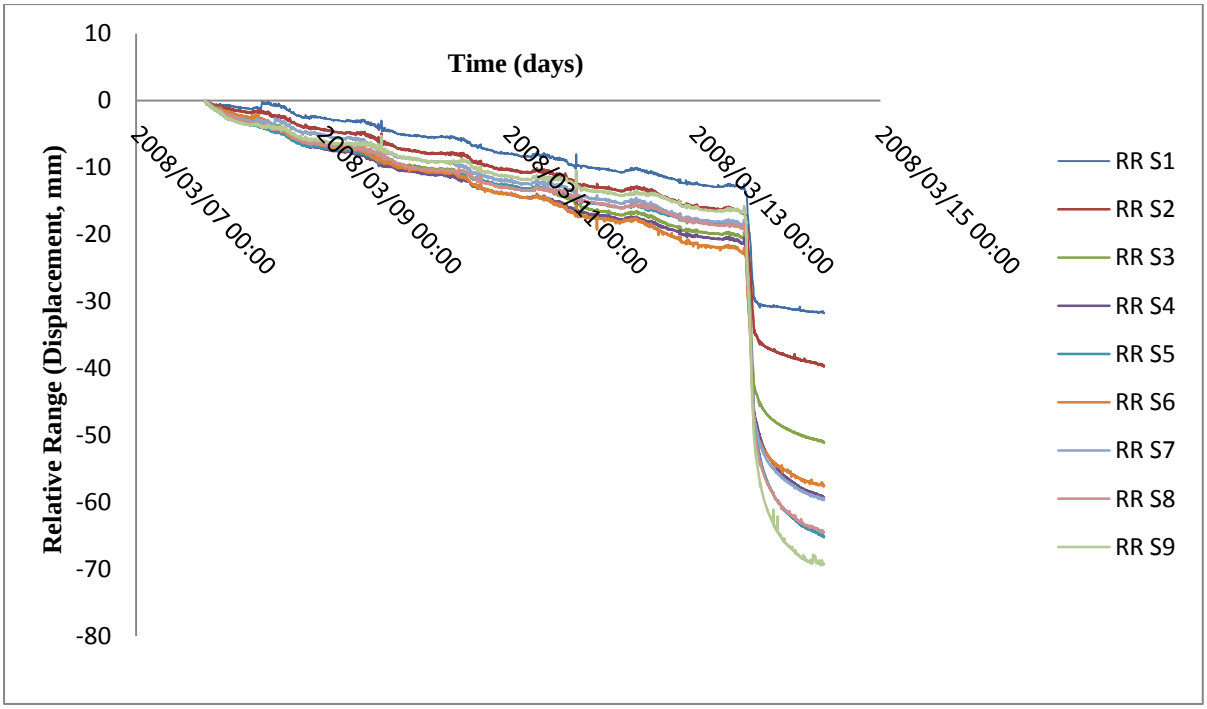


Figure 5.25: Relative range (Dispalcement, mm) of sections 1-9 of ramp 12 slope.

5.3.5.2. Description of Ramp 12 Slope Failure

As shown in figures 5.25 and 5.26, the failure covered the entire monitored region. Therefore, the description of the deformation behaviour is based on the displacement information of nine points, representing the nine failure sections. Five stages of deformation behaviour are identified in the development of ramp 12 slope failure, and these constitute both the deformation behaviour before failure and after failure.

Stage 1 Type I

After the slope was visually monitored, the radar was deployed for monitoring. When monitoring started, the displacement records from the radar showed that the slope displacement was in a regressive state. The highest cumulative rate of displacement, -0.5mm/hr was observed in section 9, while the lowest cumulative rate of dispalcement, 0.08mm/hr was noticed in section 1. Generally, the displacement behaviour of the failure region was regressive and of type I behaviour of a stable slope. Type I regressive displacement behaviour occurs when the the slope moves between negative and positive cumulative rates of displacement in response to deformation. It is a regressive displacement behaviour of stable slopes, which represents a natural "relaxation" of the rock mass (Zavodni, 2000; Wessels and Naismith, 2005).

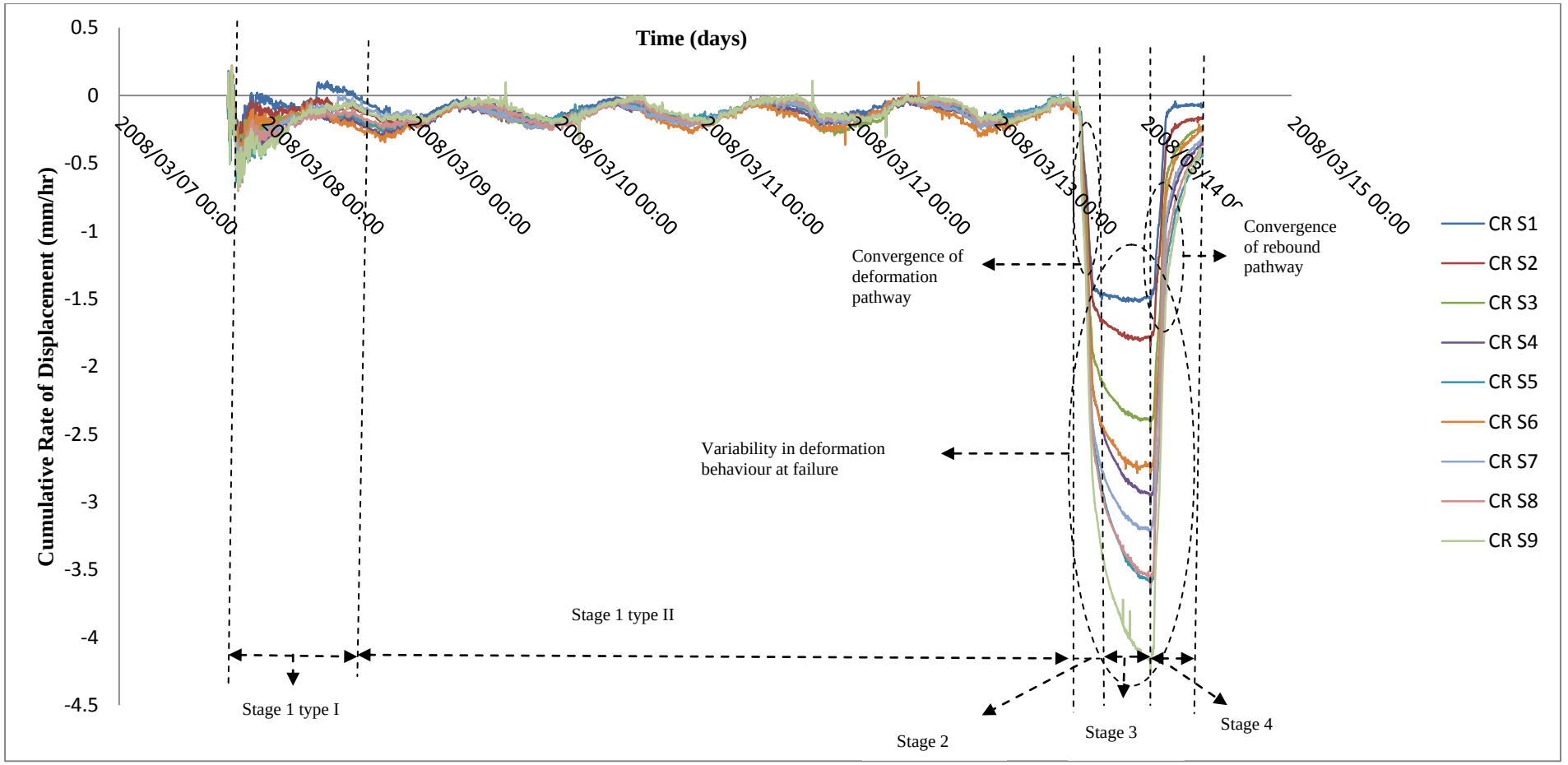


Figure 5.26: Cumulative rate of displacement (mm/hr) of sections 1-9 of ramp 12 slope.

Stage 1, Type II

Stage 1 type II deformation behaviour occurs when the regressive behaviour of the slope is entirely negative. Although the slope was still regressive, the behaviour was different from stage 1 type I wherin the slope cumulative rates of displacement was both positive and negative. This behaviour lasted for five days and constitute the longest duration in the stages of failure development. All the sections of the monitored slope showed type II deformation behaviour of stable slopes. The slope was regressive at cumulative rate of displacement between -0.05mm/hr and -0.12mm/hr. Transition from from type I to type II deformation behaviour indicated a gradual developemnt of failure, which showed that deformation was building up within the slope.

Stage 2

All the sections of the slope became progressive, and the displacement changed from decelerating behaviour to accelerating behaviour. This occurred when the cumulative rate of displacement attained -0.5mm/hr on 13/03/2008 at about 13:18. Deformation in a sense was not restricted to a particular section. The entire scanned region was at a cumulative rate of displacement between -0.5mm/hr and -1.9mm/hr. Another noticeable thing with this failure is that it was difficult to explain where failure started. All the failed sections showed very low increase in cumulative rate of displacement of between 5% and 15%. Specifically, sections 3, 6, 8 and 9 increased by 11% (-0.4357mm/hr to -0.4806mm/hr), 10% (-0.4357mm/hr to -0.4806mm/hr), 9% (-0.5842mm/hr to -0.6388mm/hr) and 6% (-0.6816mm/hr to -0.7262mm/hr) respectively. No section displayed a magnitude strong enough to be regarded as the most active point on the slope. A possible reason for this behaviour is that the sand overburden of the high-wall at the mine allowed a relatively uniform deformation within the failed section. The relatively uniform deformation is likely to have generated a slip surface for failure.

In addition, the progressive stage is also the onset of failure stage. There was no distinct onset of failure stage, as both stages occurred concurrently. As illustrated in figure 5.26, the deformation pathway of all the sections merged into a single pathway shortly before failure.

Stage 3

The slope failed at a cumulative rate of displacement of about -1.5mm/hr to -1.9mm/hr. An analysis of the monitoring data showed that sections 1 and 2 rebounded from their peak

cumulative rates of displacement earlier than the other sections. At failure, cumulative rates of displacement greater than -3mm/hr were attained before complete rebound. Cumulative rates of displacement greater than -3.00mm/hr were noticed in sections 7, 8 and 9 before they converged with the other sections on a single rebound pathway. Displacement was also greater than -55mm in all the sections. The only significant variability in deformation was noticed at the failure stage. Each section deformed individually without moving in clusters with others, but eventually rebounded as group on the same rebound pathway.

Stage 4

Stage 4 represents the behaviour of the slope immediately after failure, and it is the rebound stage. The rebound pathways of all the sections merge into a single pathway. From cumulative rates of displacement greater than -3.00mm/hr, the slope rebounded to a cumulative rate of about -0.30mm/hr. At this rate, monitoring was stopped, thereby preventing the MSR from recording the final stage of stabilisation. From the onset to the end of monitoring the displacement pattern for every section of the slope was very similar, and this supports the idea of uniform deformation on the slope behaviour.

Summary of Failure Mechanisms

Ramp 12 high-wall failure most likely occurred on a sliding surface as indicated by the convergence of the deformation pathways. However, as the slope failed, it is possible that the general slip surface generated other slip surfaces as each point moved independently. Also, the displacement behaviour was similar at all points both before and after failure, which supports the idea of uniform deformation in the slope.

5.4.6. Case Example 6 (High-wall Failure)

The name and location of the mine where this slope failure occurred was not made available, but what is known is that it occurred in an open-pit mine. For this reason, the geology and hydrogeology of the mine is not included in this study. The slope was monitored for four days, between the 30th January and 3rd February, 2009 (Reutech, 2009).

5.4.6.1. Locating the Area of Failure

The area of the slope monitored with the MSR is shown in figure 5.27. The area monitored with the radar is divided into 11 sections to determine the critical area of instability. Analysis of the displacement data extracted from the MSR as shown in figures 5.28 and 5.29 indicated that only section 10 experienced failure. With the exception of section 10, all the remaining sections of the slope were very stable and showed no significant displacement. The stable sections of the slope exhibited only type I regressive displacement behaviour of stable slopes. This type of displacement behaviour is refferred to as natural "relaxation" of the slope (Zavodni, 2000; Wessels and Naismith, 2005).

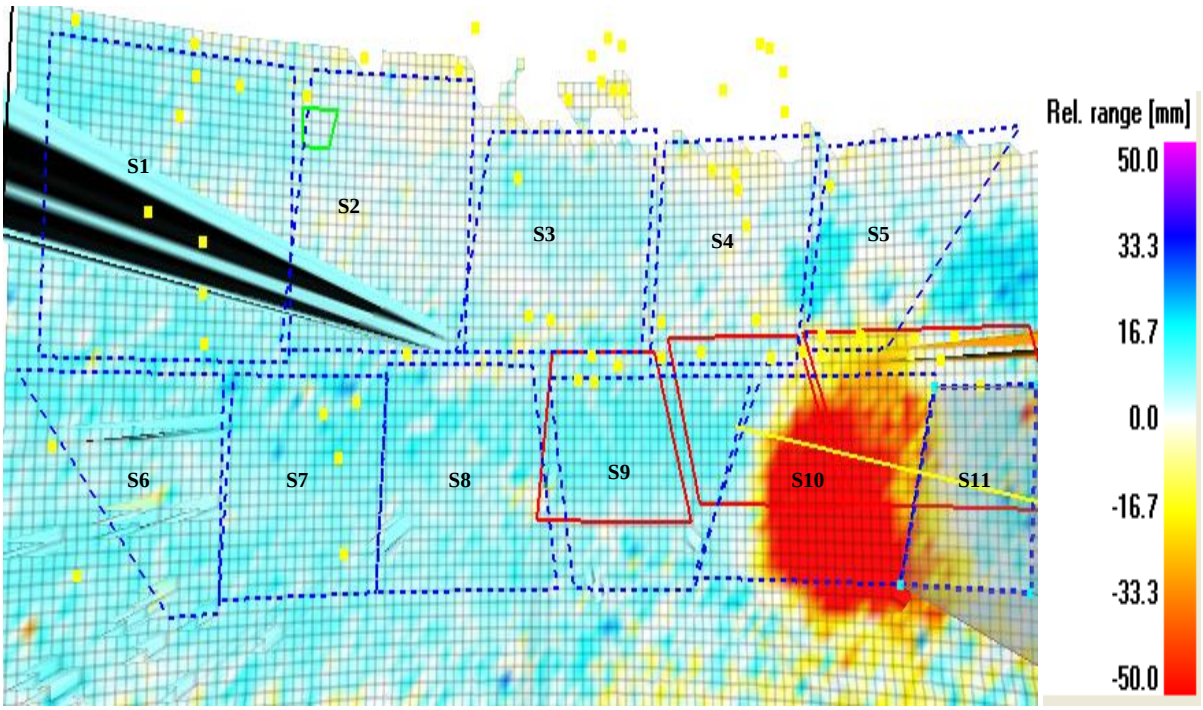


Figure 5.27: The scanned region of case example 6 slope.

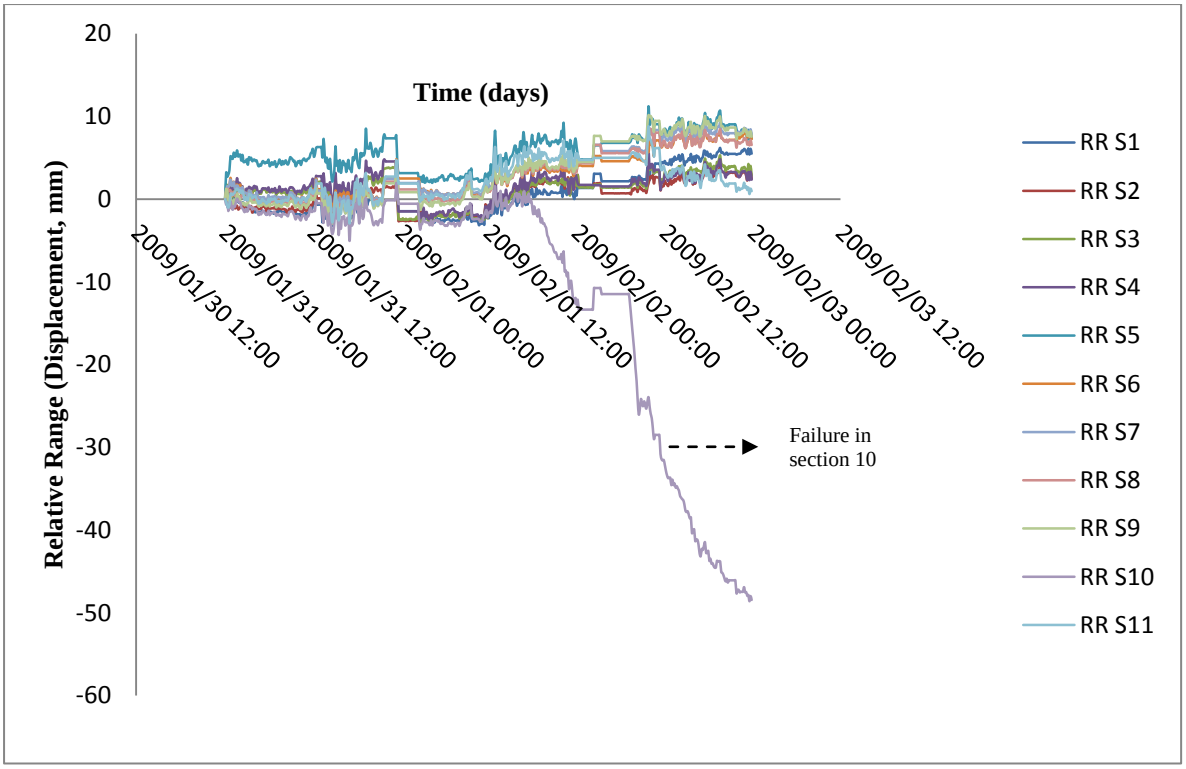


Figure 5.28: Relative range (Displacement, mm) of sections 1-11 of case example 6.

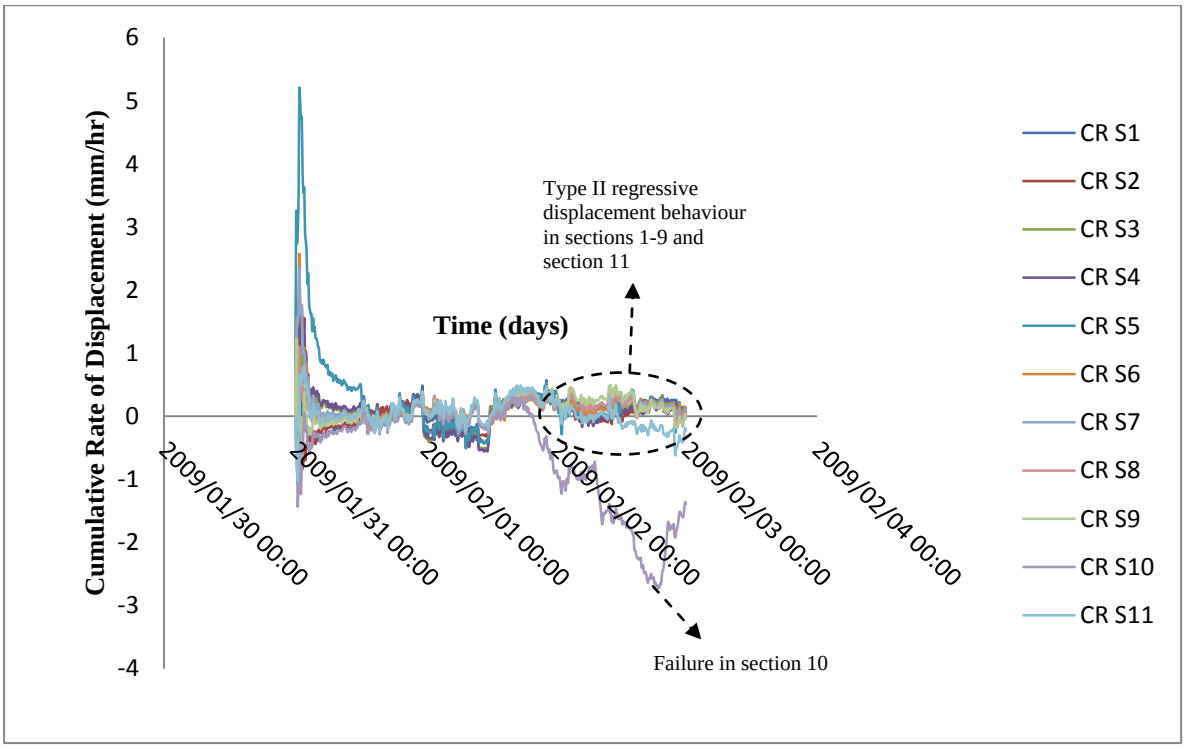


Figure 5.29: Cumulative rate of displacement (mm/hr) of sections 1-11 of case example 6.

5.4.6.2. Description of Case Example 6 Slope Failure

The description of failure 6 is based on the behaviour of ten selected points from section 10, which is the failure section as seen in figure 5.30. Each point is analysed based on the displacement and cumulative rates of displacement, as shown in figure 5.31 and 5.32. The deformation behaviour observed in the development of the failure is classified into five stages.

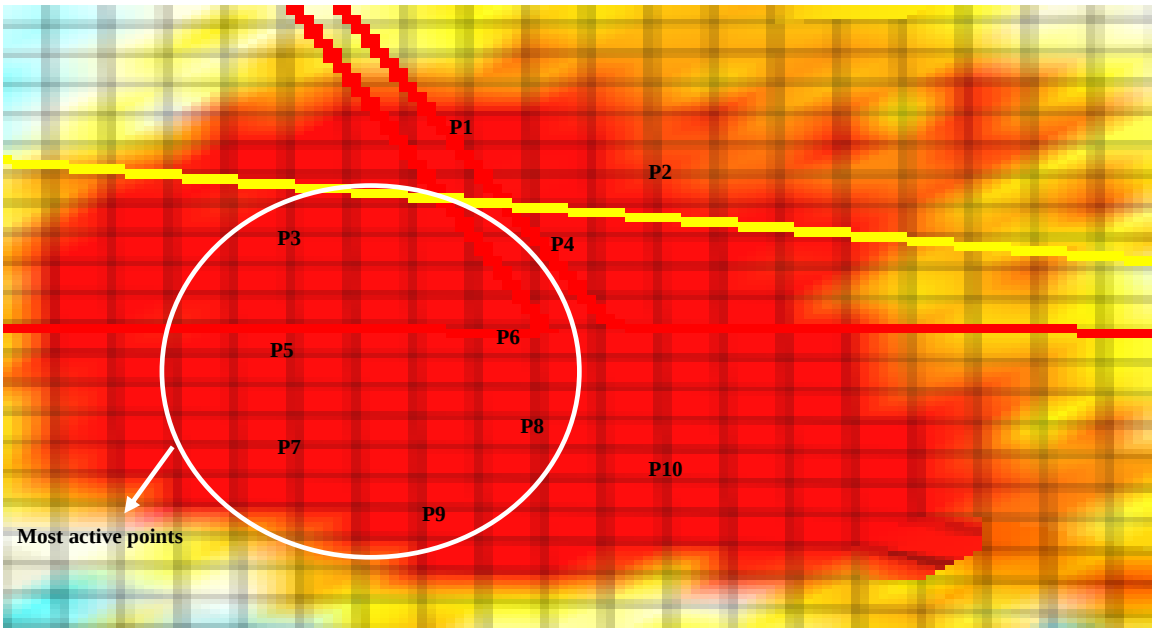


Figure 5.30: Failure section of case example 6 showing the locations of ten selected points.

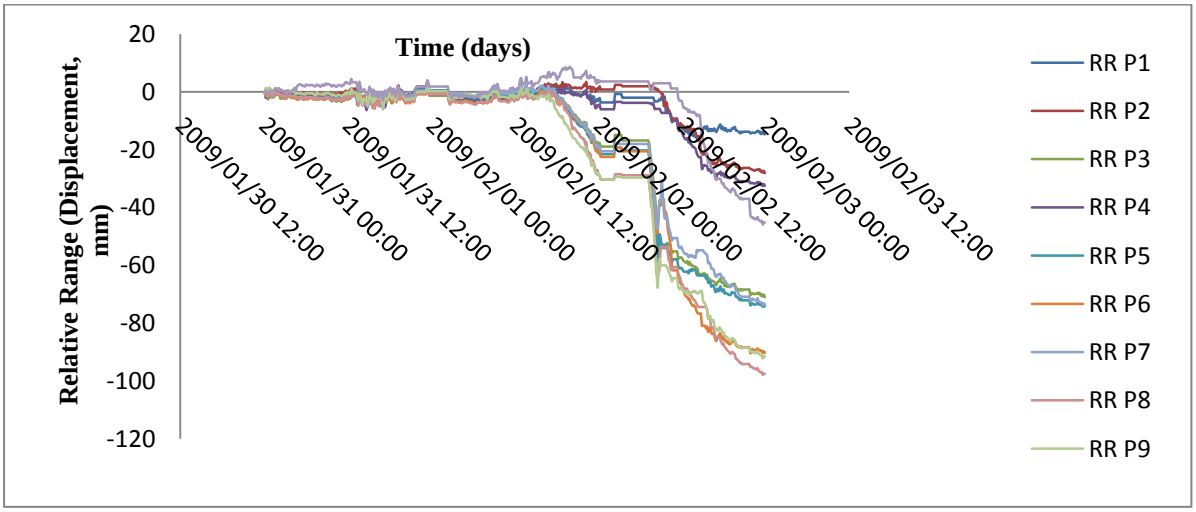


Figure 5.31: Relative range (Displacement, mm) of 10 points in the failure section of case example 6.

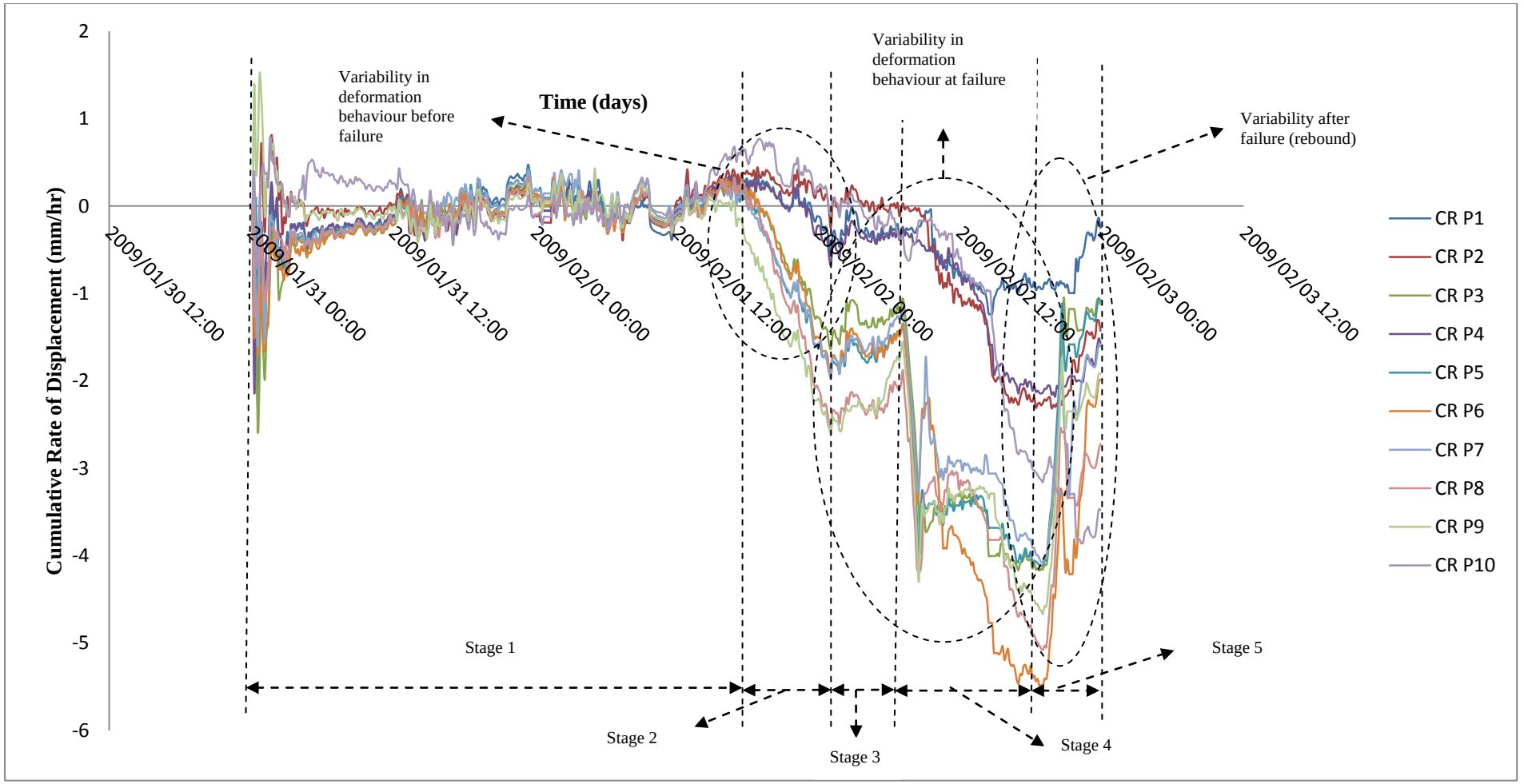


Figure 5.32: Cumulative rate of displacement (mm/hr) of 10 points in the failure section of case example 6.

Stage 1

Stage 1 constitutes the regressive displacement behaviour stage in which the slope experienced type I displacement behaviour of the stable slopes. Although the initial values of cumulative rate of displacement of -0.87mm/hr was high, the displacement behaviour was generally regressive with cumulative rate of displacement receding in some occasions to 0.06mm/hr. This lasted fo a period of two days, between 31st January and 1st February, 2009. All the ten points experienced a natural "relaxation", an indication of relative stability.

Stage 2

The slope became progressive at a cumulative rate of displacement of -0.40mm/hr on the third day of monitoring, specifically on the 1st of February, and attained a cumulative rate of displacement of -1.22mm/hr. Both progressive displacement and onset of failure occurred simultaneously. The progressive displacement of the ten points on the slope became variable as the points moved in clusters. The ten points moved in two clusters, where the most active cluster consisted of points 3, 5, 6, 7, 8 and 9, while the less active clusters consisted of points 1, 2, 4 and 10. From figure 5.30, the most active points located in the epicentre of the failure section represent the weakest points on the slope where deformation was more pronounced. The occurrence of the clusters indicated complex displacement behaviour within the slope as shearing became pronounced.

Stage 3

The analysis of the displacement data for the ten points indicates that the slope experienced failure at stage 3. Points 3, 5, 6, 7, 8 and 9 of the most active points failed when the cumulative rate of displacement was -2mm/hr. This failure again confirms a relatively high deformation around these points. While the active points failed, the less active points were at the progressive displacement state.

Stage 4

After experiencing failure in stage 3, the active points showed temporary signs of relaxation at high, but stable, cumulative rates of displacement. The cumulative rate of displacement for the entire failure section decreased from a peak rate of -1.22mm/hr to -0.92mm/hr. However, the relaxation was short-lived as the slope started to accelerate, again resulting in another collapse. The variability in displacement behaviour, which started at stage 2, continued till the second collapse. From a relaxed state of -0.92mm/hr, the slope rapidly progressed to

failure, attaining a cumulative rate of displacement of -3.20mm/hr for the failure section. All the points were involved in the second collapse at cumulative rates of displacement greater than -1.5mm/hr, points 3, 5, 6, 7, 8 and 9, which failed the first time all showed cumulative rates of displacement greater than -4.0mm/hr during the second collapse. The implication of this is that deformation, which was actually concentrated around these closely located points, was transfered to the other points. The first failure, which occurred at the centre of the failure section possibly removed the buttress from the other points on the slope causing the second collapse involving all the points.

Further analysis of the ten points in the failure section during the first and second progressive acceleration showed that all the points experienced less than 50% increase in cumulative rate of displacement. The deformation pathway at failure did not merge into a single pathway. The lack of merger of deformation pathway is an indication that the failed rock mass most likely did not fail as a rigid body (Mercer, 2006).

Stage 5

From a peak cumulative rate of displacement of -4mm/hr, and displacement greater than -56mm, the slope decelarated to a cumulative rate of displacement of -1.68mm/hr when monitoring was put on hold. Stage 5 is the rebound stage, wherein the slope decelerates to stability. However, in this case example, there was no merger of rebound pathways into a single pathway.

Summary of Failure Mechanisms

The mechanisms of the slope failure in case example 6 can be described as complex, possibly with shearing through the rock mass. The movement of the points in two clusters indicates varying magnitudes of deformation at different locations in the slope. It is possible the slope did not fail on a single slide surface, neither as rigid body as indicated by the non convergence of deformation pathways.

5.5. Discussion on Slope Failure Mechanisms Based on Displacement Records

Slope failure mechanisms, based on the displacement records observed in the case studies, are discussed in the following two sections, namely the concept of surface displacement trends, and deformation propagation. Displacement trend is a graphical illustration of the

continuous deformation time relationship of a specific monitoring point on a slope. Deformation propagation involves the progressive transfer of deformation from the most active point to other points on the slope.

5.5.1. Surface Displacement Trend

The surface displacement trends, based on slope displacement rates, are a representation of the deformation taking place within slope prior to failure, at failure and after failure (El Bedoui, et al. 2009). From the displacement trends of the case studies of the failed slopes in both open-pit and open-cast mines, five distinct stages of failure can be identified, of which three are pre-failure stages (Broadbent and Zavodni, 1982; Sijing, 1981; Varnes, 1982; Mercer, 2006) and two are post-failure stages (Mercer, 2006). The complete stabilisation stage is similar to the post mining/recovery behaviour stage identified by Mercer (2006). The five stages of displacement trends and their underlying mechanisms are as follows:

- Stage 1 - Regressive displacement stage;
- Stage 2 - Progressive displacement stage;
- Stage 3 - Onset of failure to failure stage;
- Stage 4 - Post-failure stage; and
- Stage 5 - Complete stabilization stage.

Each stage is dealt with in detail below.

Stage 1- Regressive Displacement Stage: This constitutes the first stage in the life of a failing or potentially failing slope wherein the displacement is minimal and cyclical. The behaviour is such that the slope experiences relaxation between negative and positive cumulative rates of displacement. In all the case examples, prior to failure, during this early stage of displacement, deformation was characterised by highly non uniform displacement patterns. The non uniform and cyclical displacement indicates an elastic rebound in the rock mass as it resists deformation. The slope could either:

1) become stable when the deformation is not high enough, but dissipates or decays;

2) become unstable and progressive when there is accumulation of deformation, which ultimately exceeds the rock mass strength. The two classifications of regressive deformation

behaviour are type I and type II. Type I regressive behaviour is a situation where the slope experiences negative-positive cumulative rates of displacement while type II regressive displacement behaviour occurs when the slope experiences entirely negative regressive cumulative rates of displacement.

Stage 2 - Progressive Displacement Stage: Once the rock mass strength can no longer sustain the accumulated deformation, progressive and irreversible displacements set in. Progressive displacement is a pointer to the development and propagation of a shear surface (Bjerrum, 1967; Eberhardt, et al. 2004a), which is the reason progressive displacement always leads to slope failure. Within the unstable region of the slope, the transition of various points to progressive displacement does not always occur concurrently. For example, in case example 3, figures 5.16 and 5.17, all the points moved independently, while in case example 6, figures 5.31 and 5.32, movement was different for two separate clusters of points. The displacement pattern is a function of the response of the rock to varying magnitudes of deformation.

Stage 3 - Onset of Failure to Failure Stage: On some occasions, the progressive stage is also the onset of failure stage, when both stages occur concurrently. This supports the observation made by Hamiel, et al (2004) that a direct transition from decaying regressive displacement to onset of failure, with no clear progressive displacement, does occur. On other occasions, there is a clear distinction between the progressive displacement stage and the onset of failure stage, as observed in case example 1. In case example 1, stage 2 type I was the progressive displacement stage, while stage 2 type II represented the onset of failure stage. The moment the onset of failure stage is attained, a close to linear trend of the cumulative rates of displacement was observed, and this was more noticeable if the displacement of a single point within the failed region was plotted (Hamiel, et al. 2004). It appears that onset of failure is the resultant effect of progression of failure close to the most active points, resulting in rapid development of the failure. The most active points are defined as the points with the highest cumulative rates of displacement at the onset of failure to failure stage. This mechanism agrees with the study by Petley, et al (2005) that initiation of crack growth at a point in the Vaiont landslide resulted in the development of shear plane and the subsequent linear progressive displacement to failure. The transition from onset of failure

to failure is rapid, and occurred in no more than a few hours in the observed slopes. The onset of failure is also referred to as the tertiary creep stage (Crosta and Agliardi, 2003).

Stage 4 - Post-Failure Stage: Two classes of post failure behaviour, namely class 1 and class 2, were observed in all the case examples. Class 1 behaviour is the post-failure behaviour of the failed block of rock. This occurs when the failed rock is not completely detached from the rock mass. In such situations, the failed rock is still within the scan view of the MSR. In class 2 post-failure behaviour, the failed rock is completely detached from the rock mass and it is no longer within the scan view of the MSR. In such situations, a fresh rock face is being scanned by the MSR. The post-failure behaviour is the behaviour of the fresh rock face. In both classes, that is, class 1 and 2, the post-failure behaviour may be simple or complex. It is simple when a single class of behaviour occurs and complex when the slope moves from one class of behaviour to another. From the analysis of the case studies, three types of class 1 post-failure behaviours, and one type of class 2 post-failure behaviours were observed.

- **Post-failure Class 1 Type I:** It is a simple behaviour with the slope rebounding immediately after failure and completely stabilising. This post-failure behaviour is depicted in figure 5.33, where decay in cumulative rate of displacement has occurred at different locations simultaneously. All the points merge into a single rebound pathway.
- **Post-failure Class 1 Type II:** This occurs when both rebound and deformation occur simultaneously at different locations within the slope. In post-failure class I type II, as shown in figure 5.34, the points within the unstable region are classified into two groups. The points in the first group are those in areas of high displacement, which experienced further deformation after the first general failure experienced by all the points. The points in the second group are in areas of low displacement, where decay in cumulative rate of displacement has occurred, thus resulting in the points experiencing a rebound earlier than others.
- **Post-failure Class 1 Type III:** This occurs when the slope experiences another minor collapse after the first failure without any part of the slope rebounding. Sometimes the slope shows signs of a mini-rebound before the second collapse. An example of this type of behaviour is presented in figure 5.35.

- **Post-failure Class 2 Type I:** This behaviour is shown in figure 5.34. A mini-failure occurred at a point after all the other points had rebounded and stabilised. The rebound in the failed section of the slope showed that the cumulative rates of displacement have decayed in a large section of the slope.

Stage 5 - Complete Stabilisation Stage: Before the slope completely stabilises, a complete decay of the cumulative rates of displacement has taken place. Overall, the slope deformation is completely regressive, without any further indication of failure.

5.5.2. Deformation Propagation

The onset of failure is interpreted as the transition point from gradual accumulation of deformation to accelerated deformation in the slope. It is interpreted as the point of loss of strength of the rock mass. When this transition point is reached, deformation is transferred to other locations from the most active points on the slope. Call, et al (2000) confirmed from monitoring data that slope displacement initially develops in lower strength and highly fractured rocks. As pointed out by Call, et al (2000) and Fell, et al (2000), shortly after the peak stress stage the stress condition progressively attains the critical stress stage where shear stress is transferred to neighbouring points. In the failed sections of the case examples, it appears that deformation is propagated from a point on the slope. The point where deformation is propagated was noticed to experience a sudden increase in cumulative rate of displacement of above 50% when compared to the other points at the onset of failure. This is interpreted as a representation of the point of greatest weakness, where deformation is propagated to other locations. The strength of the rock mass in the neighbouring points determines their response to the transferred deformation.

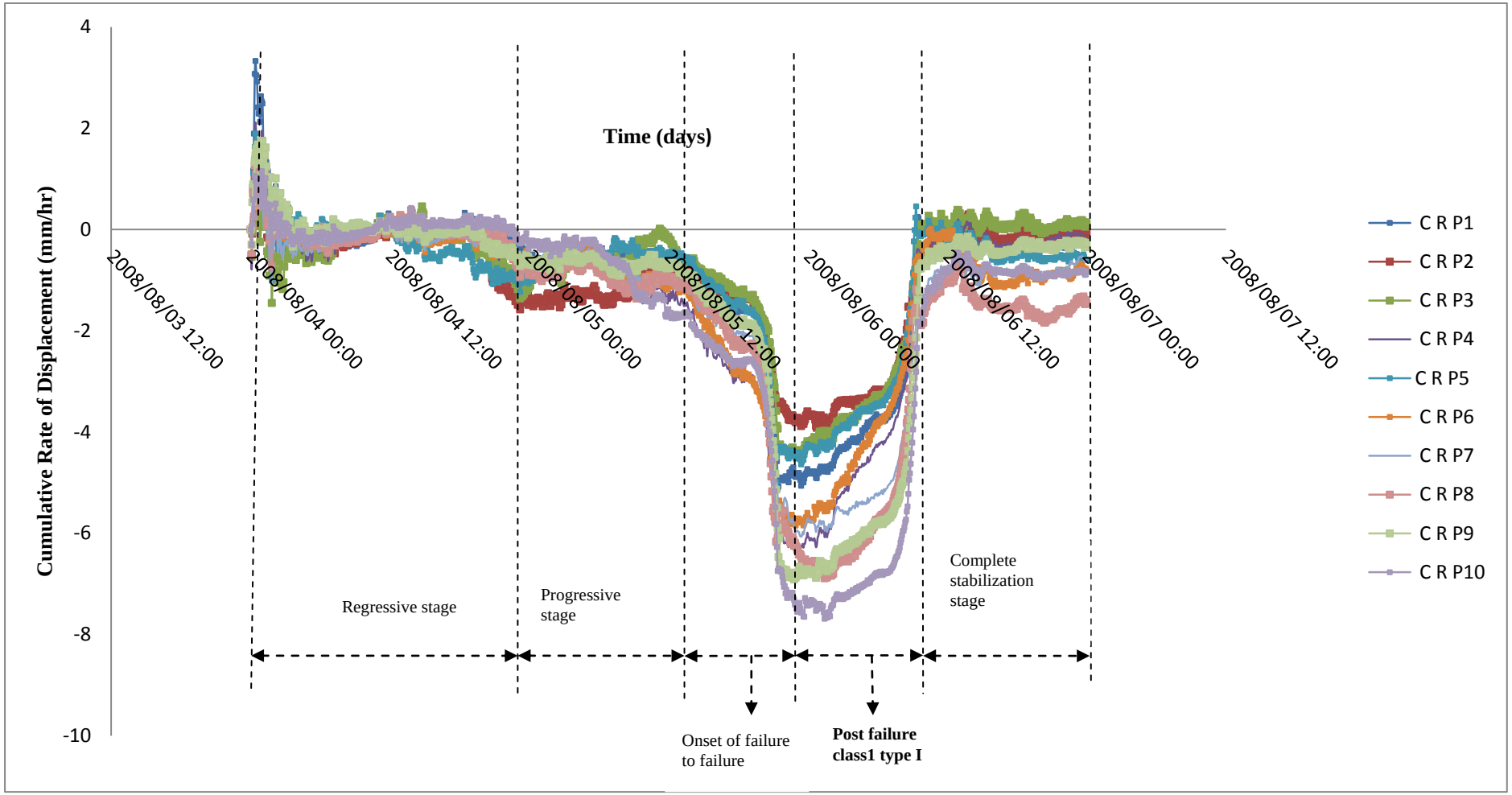


Figure 5.33: Post-failure class 1 type I displacement behaviour.

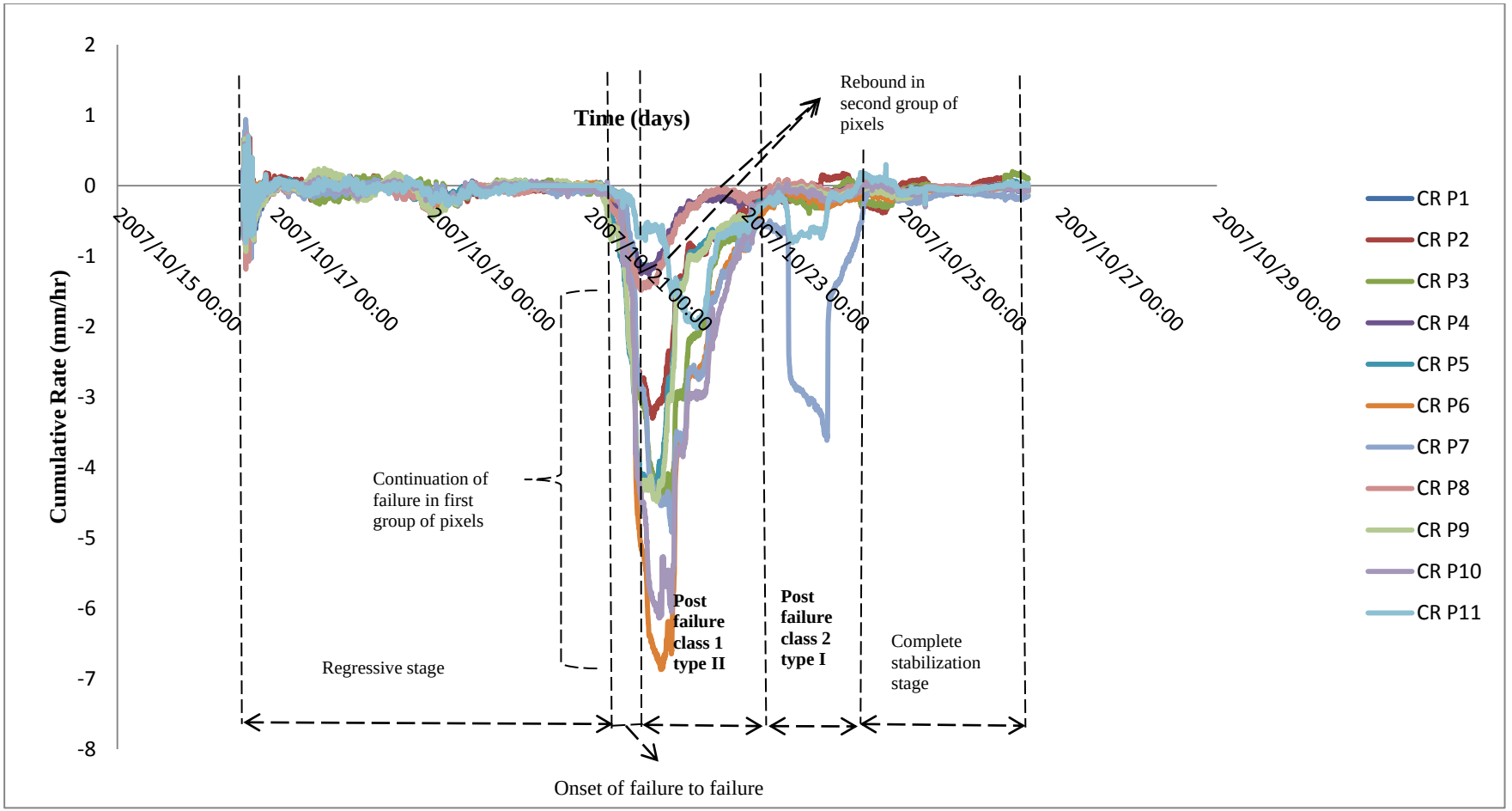


Figure 5.34: Post-failure class 1 type II and class 2 type I displacement behaviour.

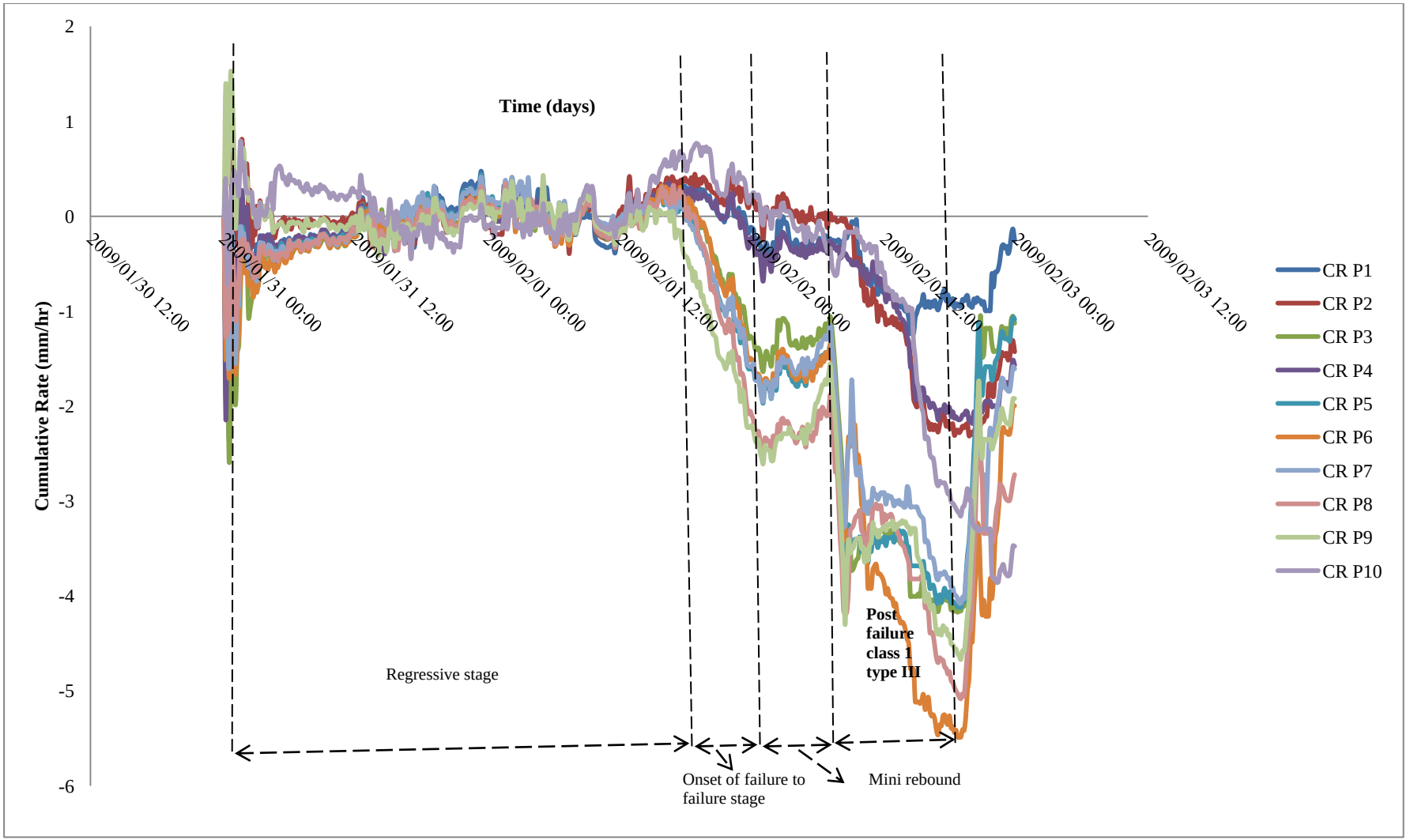


Figure 5.35: Post-failure class 1 type III dispalcement behaviour.

5.6. Validity of Commonly Recognised Slope Failure Mechanisms

For many years, slope stability analysis and slope design have been based on the existence and study of the four primary failure mechanisms namely, circular failure, wedge failure, plane failure and toppling failure (Stacey, 2007; Wyllie and Mah, 2004). However, recent studies by Severin, et al (2011), Dight (2006), Lucas (2006), Simmons and Simpson (2006), Stacey (2006), Wessels and Naismith (2005) and Sjoberg (2000) showed that other complex failure mechanisms occur in slopes, which are not consistent with the established failure mechanisms. Eberhardt, et al (2004a) suggested that massive natural rock slope failures involve a complex interaction between existing discontinuities and brittle fracture propagation through the intact rock. Severin, et al (2011) generated vector maps from displacement magnitudes of the Highland Valley copper mine high-wall obtained from two IBIS-M monitoring radars. The analysis of the vector maps indicated the existence of a distinctly different failure mechanism from the toppling mechanisms previously interpreted (Severin, et al. 2011). The study demonstrated the capability of using radar monitoring in providing further insight into the failure mechanisms in mine slopes. Radar monitoring provides real-time displacement information of several points on the slope. The major slope failure at Nchanga open-pit mine is a good illustration of this capability of radar monitoring (Wessels and Naismith, 2005). Before the deployment of the radar, the Nchanga open-pit mine was monitored with a combination of visual monitoring and survey network. Wessels and Naismith (2005) designated the unstable areas of the slope identified with the survey network and visual monitoring system as, "Area of Concern." Subsequently, specific rules governing mining operations in the unstable area were implemented (Wessels and Naismith, 2005). With the increasing deterioration of the unstable slope, the survey network was deemed inadequate and the SSR was deployed to enhance monitoring and allow 24 hours of mining operation (Wessels and Naismith, 2005). According to Wessels and Naismith (2005), within a few hours of monitoring, the radar indicated the occurrence of deformation in other areas not detected by survey and visual monitoring. This observation highlighted the safety and economic benefits of radar monitoring by providing 24hours monitoring in real-time.

The analysis of the displacement data from the MSR indicated that deformations occur concurrently at different locations on the slope at varying magnitudes. Either at varying magnitudes or at relatively uniform magnitudes, failure is preceded by the gradual accumulation of deformation in the slope. The gradual accumulation of deformation occurs at

the regressive stage, and it is possibly responsible for the cyclical nature of the displacement graph. This behaviour could continue for a long time without reaching the progressive stage, if disturbing events are eliminated (Zavodni, 2000). However, if the disturbing events are not removed, as deformation accumulates, a point is reached beyond which the rock mass can no longer withstand deformation and the rock transitions from gradual to accelerated deformation. This transition point is interpreted as the loss of strength of the rock, which also represents the onset of failure (Sijing, 1981, Crosta and Agliardi, 2003). When this occurs, a complete change from regressive displacement to progressive displacement is seen on the displacement graph. If there is coalescence of deformation prior to failure, the variability in deformation disappears and the slope fails on a uniform deformation pathway. It is likely that when there is a convergence of deformation pathways, a sliding or release surface for failure has developed (Mercer, 2006). This observation was made in case example 1, 2 and 5. In case example 1 (figure 5.8), variable deformation was observed before the onset of failure, but as deformation accumulates and the rock strength was lost, convergence of deformation on the same pathways occurred shortly before failure. At failure, collapse occurred concurrently at all locations and at different magnitudes of displacement and cumulative rates of displacement. In case example 5, figure 5.26, relatively similar deformation occurred at different locations before the convergence of deformation on the same pathways.

Alternatively, non-convergence of deformation pathway does not reflect the formation of a sliding surface for failure. The interpretation is that failure most likely occurred through the rock mass. This was observed in case example 3 and 6. In case example 3, figure 5.17, deformation behaviour was identical at various points on the slope prior to the onset of failure. As the rock mass lost its strength and progressive acceleration commenced, the deformation behaviour became variable without converging on the same pathway. Thereafter, each point failed independently, which suggested that progressive damage progression, may have occurred through the rock mass (Eberhardt, et al. 2004a). Figure 5.32 of case example 6 provides a very good illustration of non-convergence of deformation pathways and damage progression with variability before and after failure. The variability in deformation behaviour was evident at the regressive stage and it became pronounced at the progressive stage and continued at failure. On other occasions, variability may start at the progressive stage, and continue throughout the failure and rebound stage, as shown in figure 5.17 of case example 3. In case example 1, figure 5.8, the variability started at the progressive displacement stage,

receded briefly as the deformation pathway converged very close to failure and started again at failure. In case example 2, figure 5.11, variability in deformation behaviour occurred at failure, consequently causing multiple-phase failure and continued until the rebound stage. The slope failure in case example 2 can be regarded as a combination of failure on a sliding surface and multiple-phase failure. Meanwhile, the slope failure in case example 3 and 6 can be regarded as failure through progressive damage progression in the rock mass. The variability in deformation behaviour at different points on the mine slopes is a function of the magnitude of deformation taking place. It is also evidence of complex mechanisms, which are contrary to common failure mechanisms, and are most likely caused by the rock mass resistance to deformation.

Back-analysis of slope failure is used to provide information on the strength and deformation parameters of the supposed sliding surface for design and analysis purposes (Stacey, 2007). However, the research has established that multiple deformations occur concurrently at different location on the slope, therefore the back-analysed parameters obtained from the supposed sliding surface may not be representative of the overall behaviour of the slope at all points. For example, in case example 1, varying magnitudes of deformation occurred concurrently at different points on the slope before the development of a sliding surface shortly before failure. If the sliding surface is back-analysed, the strength and deformation parameters obtained may not adequately represent the slope behaviour at all locations. In addition, if the strength and deformation parameters are used for slope design in similar geological conditions, the results may not be completely valid. The slope failures in case examples 3 and 6 do not correspond with any commonly recognised slope failure mechanisms. Therefore, predicting such slope behaviour on the basis of the known mechanisms is not likely to be a correct prediction. In slopes wherein circular failure on a sliding surface is normally expected, such as the slope in case example 2, multiple-phase failure occurred on more than one sliding surface. The progression of internal deformation within the slope most likely resulted in development of the primary sliding surface which in turn initiated other secondary sliding surfaces. This deformation behaviour is illustrated in figure 2.18. When this occurs, damage zones are created between the multiple surfaces within the slope subsequently allowing movement to take place (Martin and Kaiser, 1984; Mencl, 1966 and Eberhardt, et al. 2004a).

The analysis provided in this research has shown the potential of displacement trends from point monitoring in understanding the deformation behaviour of open-cast mine slopes. At present, slope monitoring radar remains the only monitoring equipment capable of monitoring every point on a large slope in real time. This capability of radar should be used to determine the points with high displacements, and to delineate such points as high deformation zones for further observation and analysis.

5.7. Summary

Slope monitoring radar is still relatively new and as a result, well documented displacement records of slope failure are not readily available. Mining companies that have detailed records of slope failures are reluctant to release the information for research purposes and this explains why only six slope failure case studies were analysed. The analysis of the case studies, and the MSR displacement data in general, showed that the stable slopes exhibit two types of deformation behaviours which are classified as type I and type II. Type II slopes are relatively stable, but could become unstable in the presence of some local triggering factors, such as blasting vibrations, undercutting and mine water. Type I slopes, although more stable than type II slopes could equally become unstable with strong triggers.

The five stages of slope displacement, observed in the displacement behaviour of the unstable slopes are consistent with the work of Broadbent and Zavodni (1982) and Mercer (2006). A summary of the displacement behaviour of the case examples is shown in table 5.1. The analysis of several points within the failed region of the unstable slopes revealed that reactions to deformation vary with locations on the slope. The analysis also showed different clusters of movement, with some points more active than others. The most active points where deformation is propagated to other locations represent the point of greatest weakness on the mine slope. The different response to deformation, particularly between the onset of failure to the post-failure stage explains the different categories of behaviour shown at these stages.

In addition to circular, planar, wedge and toppling failure mechanisms, many unknown and complex failure mechanisms exist in surface mine slopes. The failure mechanisms observed from displacement data in chapter 5 indicated that it is not always necessary to have a sliding

surface for failure to develop. In addition, analysis of the failure mechanisms demonstrated the significance of point monitoring in understanding the behaviour of slopes. Based on the observed mechanisms, it can be concluded that surface monitoring is essential, since any points on the slope could be the failure initiation point. The slope monitoring radar provides this capability and since rates of displacement can be calculated after each scan, this was considered to have potential for use in prediction of time to failure. The development of a Slope Failure Prediction Model (SFPM) for failure time prediction will be described in the next chapter.

Table 5. 1: Summary of Case Examples Displacement behaviour

Case Example	Mine Name	Type of Slope	Number of Monitoring Days	No of Failed Section	Failure Stages	Post Failure Class	Duration of Onset of Failure to Failure (hours)	Rate of Displacement at Onset of Failure (mm/hr	Rate of Displacement at Failure (mm/hr)	Displacement at Failure (mm)
1	Unknown (copper mine)	High-wall	3	1	5 stages (stage 1, stage 2 type I, Stage 2 type II, Stage 4 and Stage 5)	Class 1 type I	6 .5	-1.4	-5	-80
2	New Vaal Coal Mine (Ramp 0)	Low-wall	25	7	5 stages (stage 1, stage 2, stage 3, stage 4 and stage 5)	Class 1 type III	13.5	-1.4	-4	-200
3	Landau Coal Mine (Ramp 5)	High-wall	9	2	5 stages (stage 1, stage 2, stage 3, stage 4 and stage 5)	Class I type I and Class 2 type I	5	-1	-3	-36
4	New Vaal Coal Mine (Ramp 11)	High-wall	5	4	5 stages (stage 1, stage 2, stage 3, stage 4 and stage 5)	Class 1 type III	2.5	-0.5	-2	-40
5	New Vaal Coal Mine (Ramp 12)	High-wall	7	9	4 stages (stage 1 type I, stage 1 type II, stage 2 , stage 3 and stage 4)	Not defined – no post-failure data	3	-0.5	-2	-46
6	Unknown	High-wall	4	1	5 stages (stage 1, stage 2, stage 3. Stage 4 and stage 5)	Class 1 type III	8	-1.2	-2	-30

CHAPTER SIX

DEVELOPMENT OF AN EMPIRICAL THRESHOLD MODEL AND A SLOPE FAILURE PREDICTION MODEL

Chapter 5 discussed the deformation behaviour of both stable and unstable open-cast mine slopes. The failure mechanisms underlying the deformation behaviour of unstable slopes were interpreted from the MSR data. The analysis revealed that slope failure is preceded by gradual accumulation of varying magnitudes of deformation at different locations on the slope. Therefore, to understand the deformation process and estimate the time to failure, the points where the highest displacement is taking place and the magnitudes of the displacement must be identified.

With this understanding, a model for estimating the time to failure of open-cast mine slopes named the Slope Failure Prediction Model (SFPM) is developed in this chapter. Another empirical model for estimating the threshold value for the cumulative rates of displacement and determining the displacement state of the slope is also developed.

6.1. Predicting Time of failure of a Mine Slope

Mine slope failure can occur with devastating consequences on production, mine personnel and the mining company. However, with the availability and proper utilisation of modern monitoring equipment, such as the radar, the consequences of slope failure can be avoided. For this to be avoided, a method that can confidently predict the time to failure of mine slopes is necessary. A classic example of the importance of such slope failure prediction is the accurate prediction of the 18th February, 1969 slope failure at the Chuquicamata mine in Santiago. Slope monitoring was conducted with quadrilateral tension crack stakes, tape and transit lines, crack extensometers or platinas and seismograph between January 1968 and February 1969 (Kennedy and Niermeyer, 1970). On 13th of January, 1969, when the slope deformation became fully progressive, it was necessary to predict the time to failure in order to minimise stoppage of mine operations. The fastest moving point, Point 5 on F-2 bench, gave the earliest date of failure as 18th February, 1969. As stated by Kennedy and Niermeyer (1970), the mine was closed temporarily at 15.00pm on 16th February, 1969. At 18:58pm on

18th February, 1969, the slope failure occurred (Kennedy and Niermeyer, 1970). Full production resumed on 19th February, 1969, as displacement measurement showed that the slope had stabilised (Kennedy and Niermeyer, 1970). The time to failure prediction from the fastest moving point resulted in the loss of production time of only 65 hours, with no damage to either equipment or injury to mine personnel.

In the last four decades, several attempts have been made by researchers to develop acceptable methods of predicting the time to failure of open-cast mine slopes. However, no single method has been found to be universally acceptable for mine slope failure prediction. The difference in the models used for predicting the time to failure of mine slopes depends on the adopted function, with the mostly used functions being the linear function, exponential function and power law function (Crosta and Agliardi, 2003). Variables, such as the strain or displacement or rates of displacement describing the slope behaviour before failure are used in the models (Crosta and Agliardi, 2003). An example of such a model developed by Saito and Uezawa (1961) using equation 6.1, claimed that the logarithm of the time to failure(t_f) is proportional to the logarithm of the rate of displacement(Ω^i).

$$Log\,(t_f) = c - m\log(\Omega^i) \qquad 6.1$$

Where:

c and m are empirical constants;

t_f = time of failure (day); and

Ω^i = rate of displacement (cm/day).

In order to predict the time to failure of a slope, Zavodni and Broadbent (1980) analysed a typical time versus displacement graph of slope movement, as shown in figure 6.1, and developed a semi-log time-velocity in feet per day preceding the slope failure at the Liberty Pit, Nevada.

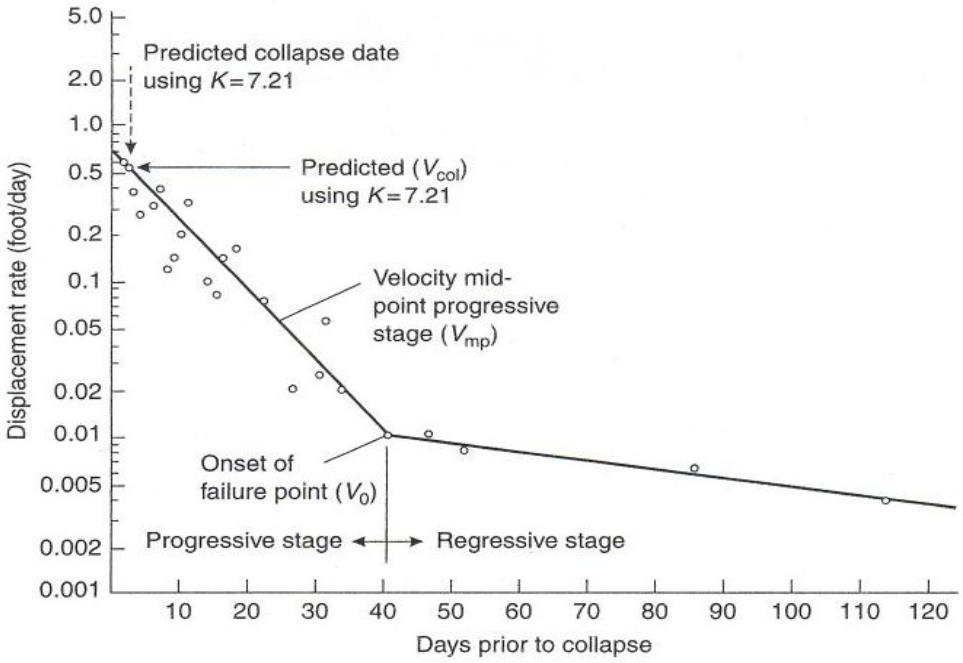


Figure 6.1: Displacement rate curve and failure collapse prediction (After Zavodni and Broadbent, 1980).

V_0 and V_{mp} are the velocity at onset and the mid-point of the progressive displacement stage respectively. A constant, K, is given as:

$$K = \frac{V_{mp}}{V_0} \quad 6.2$$

The general equation for a semi-log straight-line graph is given as:

$$V = Ce^{St} \quad 6.3$$

Where:

V = velocity (ft/d);

C = intercept of the line on the time axis;

e = base of natural logarithm;

S = slope of the line; and

t = time (days).

Assuming t = 0 at the collapse onset point, velocity as in equation 6.3, at any time becomes:

$$V = V_0 e^{St} \quad 6.4$$

The velocity at collapse (V_{col}) is obtained from equation 6.2 and 6.4 as:

$$V_{col} = K^2 V_0 \quad 6.5$$

Zavodni and Broadbent (1980) estimated the time to failure with equation 6.5 and the time-velocity plot in figure 6.1. From the figure, K = 7, V_o = 0.4 mm/hr, hence V_{col} is 20 mm/hr. Extrapolation of the velocity-time line shows that at 20 mm/hr, collapse will occur in 61 days which was close to the actual day of collapse. After testing this equation, Zavodni and Broadbent (1980) suggested a reduction in the average value of constant K from 7.21 to 6.70. They also stated that as acceleration increases, extrapolation from linear regression becomes less accurate (Zavodni, 2000). This necessitates Call (1982) to suggest that additional regressions must be done after each new displacement data point is plotted for better velocity prediction of failure. Ryan and Call (1992), after studying 11 failures found a mean velocity of 0.5 mm/hr for the progressive displacement stage, and suggested that a minimum of 48 hours exist before slope collapse when velocity reaches 2.1 mm/hr. Martin (1993) stated that a displacement rate in excess of 1cm/d is an indication of progressive failure. Cruden and Masoumzadeh (1987) stated that threshold velocities of 1.2 mm/hr and 6 mm/hr marked the initiation of the second and third accelerating stages in slope displacement behaviour prior to failure. Various combinations of factors, such as the geomechanical characteristics of the slope, slope geometry and groundwater influence slope displacement behaviour. Therefore, a universal threshold velocity is impractical.

Fukuzono (1985) developed the inverse-velocity method of time to failure prediction as shown in figure 6.2. The method is based on linearity of the slope deformation before failure. The displacement data used for the study was obtained from simulated rain-induced landslides in soil under laboratory conditions (Fukuzono, 1985). The conditions simulated were deemed to be typical of accelerating displacement under gravity loading (Rose and Hungr, 2007). The time to failure is estimated by projecting a trend line through values of inverse velocity versus time to intersect the zero value on the x-axis (Rose and Hungr, 2007). Fukuzono (1985) fitted concave, convex and linear plots, defined by equation 6.6, to the

obtained laboratory data and concluded that a linear trend fit through inverse-velocity data usually provided a reliable estimate of failure time, shortly before failure (Rose and Hungr, 2007).

$$V^{-1} = [A(\alpha - 1)]^{\frac{1}{\alpha-1}}(t_f - t)^{\frac{1}{\alpha-1}} \quad 6.6$$

Where t is time, t_f is the time to failure, A and $\boldsymbol{\alpha}$ are constants derived from relationship $\Omega^i = A\Omega^{i\alpha}$, which describes the accelerating creep of materials by relating rates of displacement, Ω^i to changes in rate of displacement, Ω^{ii} (Voight, 1988).

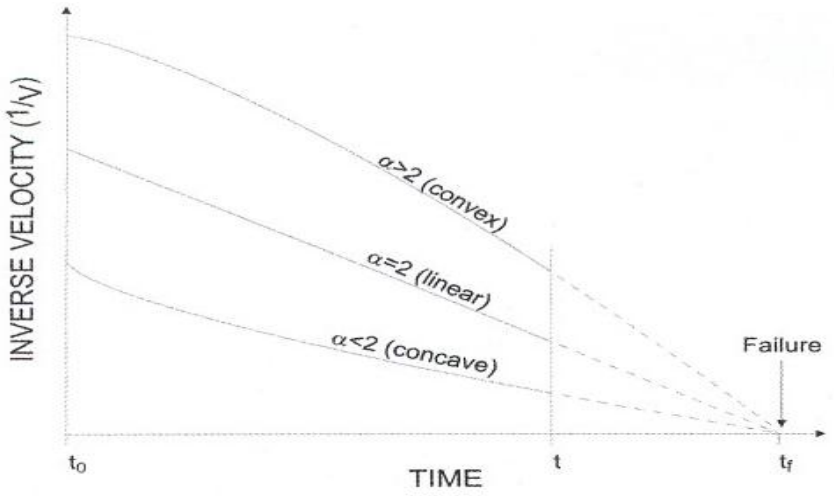


Figure 6.2: Inverse velocity versus time relationships preceding slope failure (After Fukuzono, 1985).

Voight (1988) established a failure relation, $\Omega^{ii} = A\Omega^{i\alpha}$, which relates acceleration (Ω^{ii}) to velocity(Ω^i), where A and α are rate coefficients under time invariant external conditions of load and temperature. From the Voight's relationship, Cornelius and Scott (1993) derived equation 6.7 for calculating time of failure(t_f):

$$t_f = \frac{{\Omega^i}_f^{(1-\alpha)} - {\Omega^i}_0^{(1-\alpha)}}{A(1-\alpha)} + t_0 \quad 6.7$$

Where:

t_f = Time to failure (day);

Ω^i_f = Velocity (displacement rate, cm/day) at the time of failure;

t_0 = Initial time (days); and

Ω^i_0 = Initial velocity, (displacement rate, cm/day).

The model was used to calculate the time to failure of the 1963 Mount Toc rockslide in Italy using the displacement data between 6th August and 4th October, 1963. The calculated time to failure was 8th October, while the actual failure occurred on 9th October (Cornelius and Scott 1993).

In the work of Mercer (2006), curve fitting was done using a polynomial fit of the logarithm of the measured displacements. First and second order differentiation of the equation of the fitted curve were performed to obtain the equations of the displacement rate and acceleration. With a selected limiting deformation rate of 1m/day, the differential equation of the displacement rate was solved at pre-selected time increments and the result continuously checked to confirm if the value equals or exceeds the limiting deformation rate. Whenever there is convergence of the result of the differentiation to the limiting deformation rate, the corresponding time is the time to failure (Mercer, 2006). Mufundirwa et al. (2010) developed a method of computing failure time based on the slope gradient of displacement data. Their research was based on the formula representing strain divergence in terminal phase of creep failure in rocks proposed by Fukui and Okubo (1997). The method produced between 57% and 75% safe predictions when validated with displacement data from the Asamushi landslide, Vaiont landslide and a slope failure in a limestone open-pit mine in Japan (Mufundirwa, et al. 2010). Despite the supposed effectiveness of these failure prediction methods by their developers, they remain academic exercises until they are validated by a third party in real mine situations. However, the inverse velocity method remains the only failure prediction method thus validated. Rose and Hungr (2007) successfully used the inverse velocity method to predict failure time at Betze-Post open-pit mine in Nevada. According to Rose and Hungr (2007), the advantages of the Fukuzono's inverse velocity method over other methods are its ability to:

- significantly improve the interpretation of monitoring data; and
- estimate the time to failure by simply extrapolating the inverse-velocity time graph towards the time of failure.

These advantages of the inverse velocity method will be explored in developing a model that can reliably estimate the time to failure of mine slopes.

6.2. Determination of a Threshold Value for the Cumulative Rate of Displacement

The cumulative rate of displacement threshold value represents the onset of failure, that is, the point of imminent slope failure. The threshold value gives advance warning of slope failure, which determines when mine personnel and equipment must evacuate the unstable area of the slope. The empirical model for the determination of the threshold value for the cumulative rate of displacement is shown in figure 6.4. The model, which represents the displacement behaviour of the mine slopes, is useful for quick estimation of the cumulative rate of displacement threshold in mm/hr. The onset of failure refers to a point of sudden increase in displacement, that is, transition from slow regressive deformation to rapid or accelerating progressive deformation rates before complete failure (Zavodni, 2000). From the back-analysis of slope failure at Nchanga open-pit mine, Wessels and Naismith (2005) recommended an evacuation threshold of 10mm/hr at two hours before failure for Nchanga mine personnel. Little (2006b) recorded eight brittle failures at Sandsloot mine with the SSR that occurred in less than two hours, giving little time for evacuation. In case example 1, section 5.3.1, cumulative rate of displacement of -1.4mm/hr represents the onset of failure at six hours before failure. In case example 3, section 5.3.3, onset of failure started three hours before failure at cumulative rate of displacement of -1mm/hr. In case example 4 of New Vaal coal mine, section 5.3.4, onset of failure started two hours before failure at cumulative rate of displacement of -0.5mm/hr while in case example 5, also at the New Vaal coal mine, onset of failure commenced three hours before failure at a cumulative rate of displacement of -0.5mm/hr. In case example 6, section 5.3.6, onset of failure started nine hours before failure at a cumulative rate of displacement of -1.2mm/hr. This observation shows that an evacuation threshold is mine and slope specific. Therefore, it must be based on experience and peculiarity of each mine.

During slope monitoring with the MSR, the displacement information of points, as well as selected large areas on the slope can be evaluated. However, the empirical model is based on point monitoring only. This is because of the following reasons:

1) The need to identify the active points on the slope;

2) The variations in displacement behaviour at different points; and

3) The uniform size of all points per database, as opposed to the non-uniform size of the large area.

Point area monitoring and large area (ABCD) monitoring are illustrated in figure 6.3. With the MSR, users can specify the size of the small area, which may fail within a large monitored area and set cumulative rate of displacement threshold based on the selected size (Joubert, 2011).

The cumulative rate of displacement threshold model, as shown in figure 6.4, is based on three slope failures at the New Vaal coal mine. The cumulative rate of displacement values at progressive displacement and at failure were obtained by calculating the average cumulative rate of displacement values at the onset of progressive displacement and at failure respectively.

The cumulative rate of displacement threshold value should lie within the progressive behaviour stage, as depicted in figure 6.4. The evacuation thresholds represented by the red line were calculated at an hour before failure. The selection of evacuation threshold an hour before failure was arbitrary. However, threshold selection should be based on factors, such as experience, the access and size of the pit and size of failure. The cumulative rate of displacement threshold, illustrated in figure 6.4, is divided into the regressive displacement region, the progressive displacement region and the failure region.

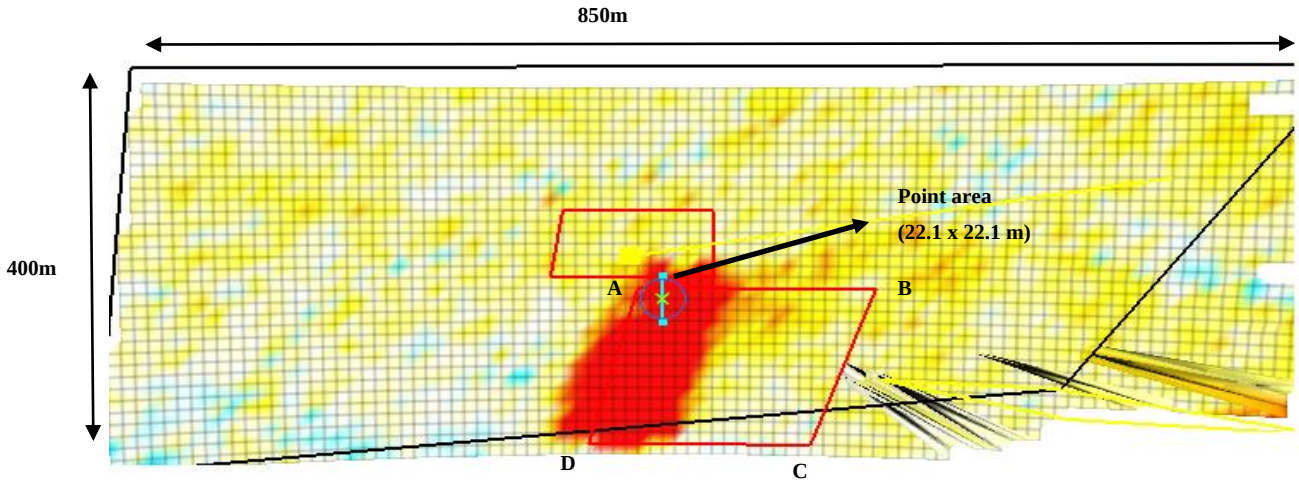


Figure 6.3: Point area monitoring with the MSR (Area ABCD, AB = 133m, BC = 75m).

The cumulative rate of displacement threshold varies with time window adopted for monitoring by the user of the MSR. The cumulative rate of displacement is calculated by dividing the relative range by the number of scans in the time window. A short time window has a small number of scans while a long time window results in a large number of scans. The longer the time window, the smaller the cumulative rate of displacement, and this is depicted in figure 6.4. In the course of this research, it was observed that mine personnel have little understanding of the significance of the time windows. As a result, usage of the time window was inconsistent and arbitrary.

The following steps explain how to use the model for selecting the threshold value for the cumulative rate of displacement. From figure 6.4, assuming that the six hour time window is selected by the user of the MSR for slope monitoring, to determine the cumulative rate of displacement threshold values for personnel evacuation:

I. Go to the time window axis;
II. Select the six hour time window; and
III. Draw a vertical line downwards to intersect the threshold line (red graph), the corresponding value of cumulative rate of displacement on the Y-axis is the threshold value. Approximately, the value is -1.9mm/hr, as shown in figure 6.4.

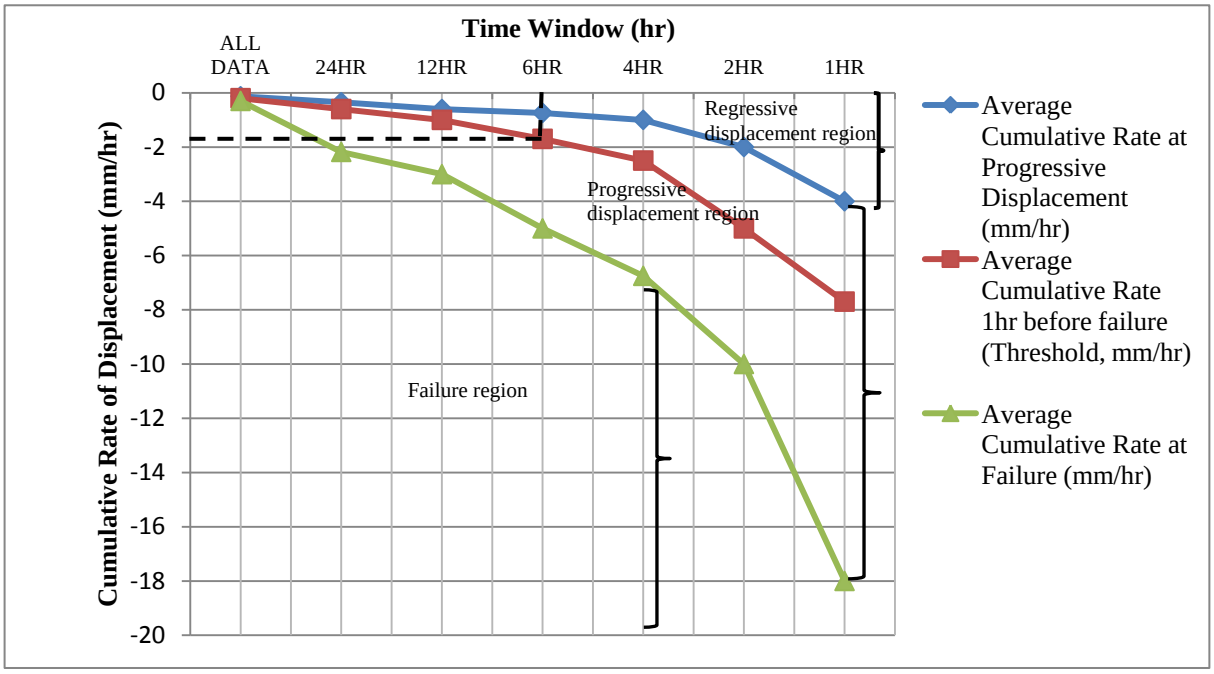


Figure 6.4: Cumulative rate of displacement (mm/hr) threshold determination based on point monitoring for the New Vaal coal mine.

Whenever the cumulative rate of displacement values fall within the progressive region, detailed attention must be given to slope monitoring. The progressive displacement region signifies the development of failure and it is within this region that the time to failure prediction can be made.

6.3. Development of Slope Failure Prediction Model (SFPM)

6.3.1. Introduction

The following steps are adopted in developing a computer model termed Slope Failure Prediction Model (SFPM) based on the inverse rates of displacement of open-cast mine slopes.

6.3.2. STEP 1: Inverse Rate of Displacement (RD) Calculation

When the progressive displacement stage is reached, the displacement data and time are extracted from the MSR, and the time interval between each scan is determined.

Using the cumulative time (min) and the corresponding displacement values (mm), the rate of displacement, (mm/min) is calculated using equation 6.8 over a given time interval. The method results in the filtering of the displacement data, with the degree of filtering increasing with the increase in the length of the time interval. The effect of data filtering is explained in section 6.3.3. As observed by Rose and Hungr (2007), no general rule regarding filtering can be given, since it depends on the measurement time interval as well as the type and quality of measurements. Therefore, optimal filtering is determined by trial and error to remove variation, without concealing displacement trends.

$$\frac{du}{dt} = \frac{u_i - u_{i-n}}{t_i - t_{i-n}} \ (i = n+1, n+2, \ldots . m) \qquad 6.8$$

Where:

$\frac{du}{dt} = Rate\ of\ displacement, RD\ \ (mm/min)$;

t_i = recent time;
u_i = recent displacement; and
n = *n*th observation.

Convert the obtained rate of displacement to inverse. Note that the rates of displacement will be negative since displacements are measured as negative in the MSR. Therefore, multiply by negative to obtain a positive inverse rate of displacement values using equation 6.9. Conventionally, mine slope displacement is measured as positive, and hence, this particular step will not be necessary with other monitoring instruments.

$$\frac{1}{RD}(-1)(min/mm) = positive\ inverse\ rate\ of displacement \qquad 6.9$$

6.3.3. Effects of Data Filtering on Rate of Displacement Calculation

Data filtering is a means of cleaning data to remove outliers and misplaced data points in a large database. The effects of data filtering on rates of displacement of a set of displacement

data is shown in figures 6.5 to 6.11. The displacement data of four points are selected from case example 5.3.1. The time interval between the data is four minutes, corresponding to four minutes for every single data interval when calculating the rate of displacement.

At a data interval of 1, 2, 5 and 10, corresponding to time intervals of 4, 8, 20 and 40 minutes respectively, as depicted in figure 6.5 to 6.8, using equation 6.8 and 6.9, the trend plots of inverse rates of displacement remain full of serious deviations with negative inverse rates of displacement and no clear trends. Note that slope failure prediction cannot be made when the trend is unclear and the inverse rate of displacement is negative. The degree of filtering is increased as the data interval is increased, specifically at 15, 20 and 25, as in figure 6.9 to 6.11 corresponding to time intervals of 60, 80 and 100 minutes respectively. These observations prompt the inclusion of the option of data interval number of 15, 20 and 25 in the Slope Failure Prediction Model (SFPM). However, the best trend was observed at 20 and 25 data intervals. It is advised that users be consistent in the use of data intervals. Further illustration of the significance of data filtering on the inverse rate of displacement of a single point (point1) at 2, 5, 10 and 15, 20 25 data interval is shown in figure 6.12 and 6.13 respectively.

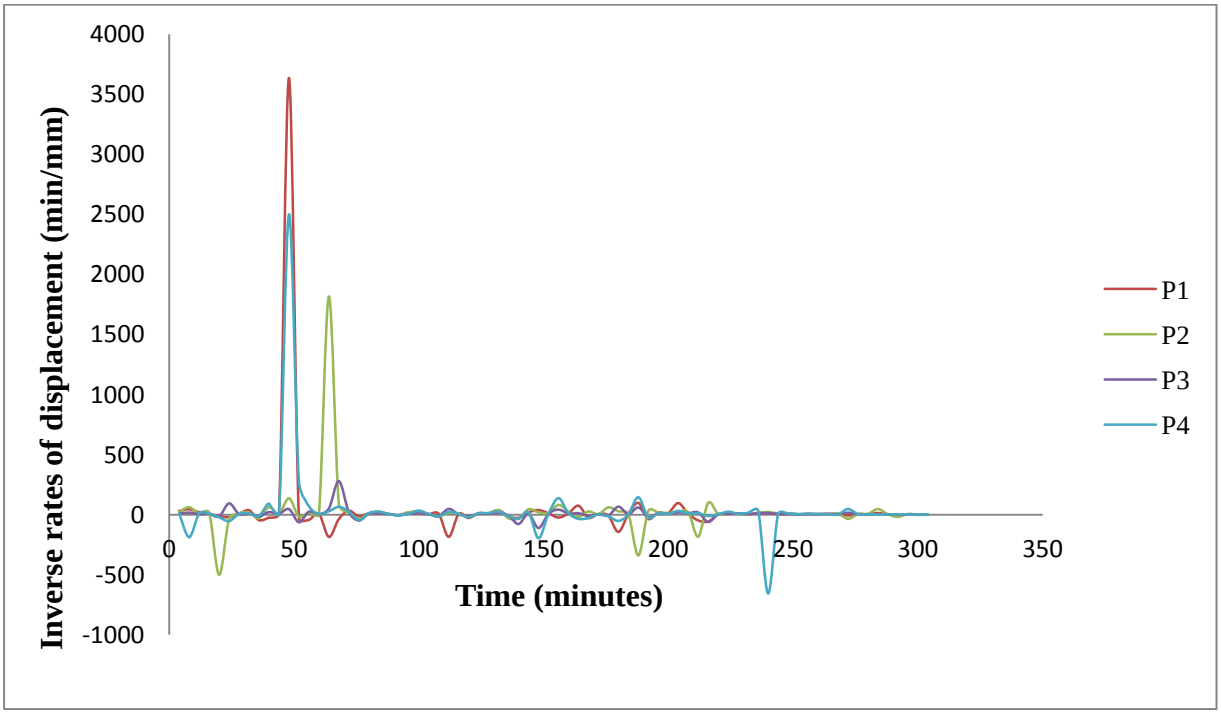


Figure 6.5: Inverse rates of displacement at 1 data interval (4 minutes).

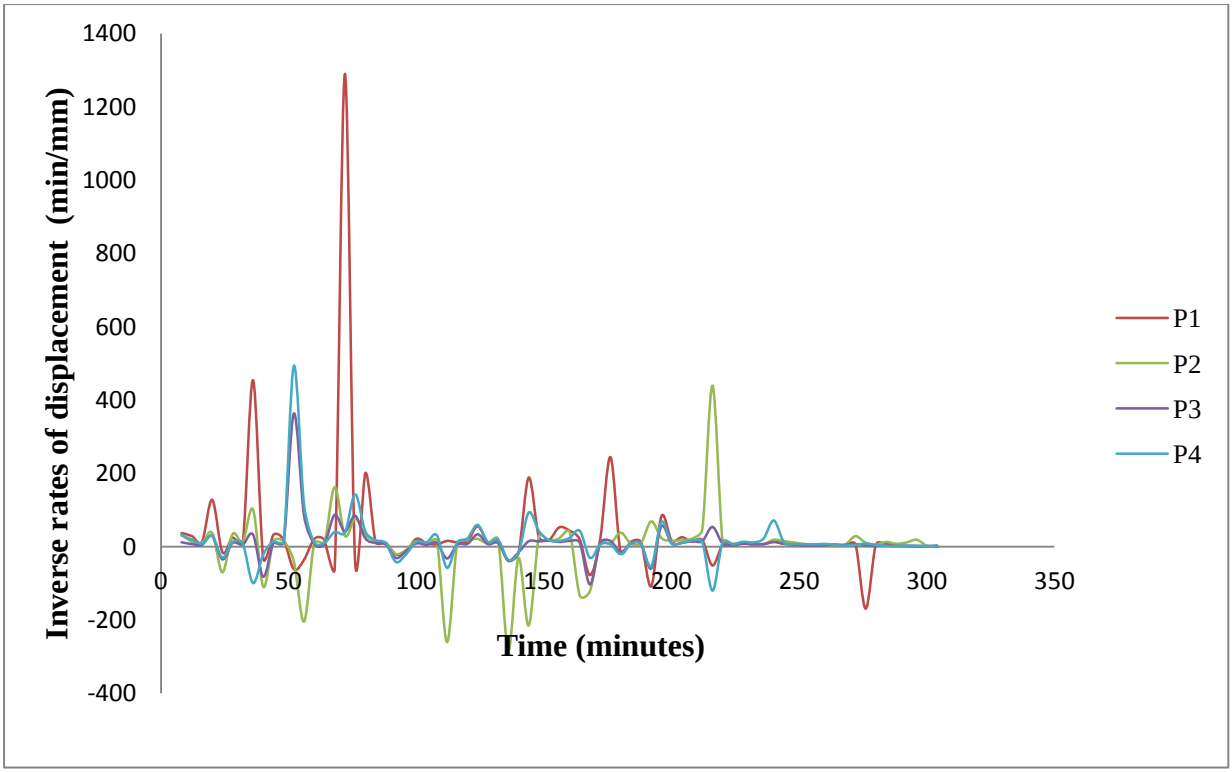


Figure 6.6: Inverse rates of displacement at 2 data interval (8 minutes).

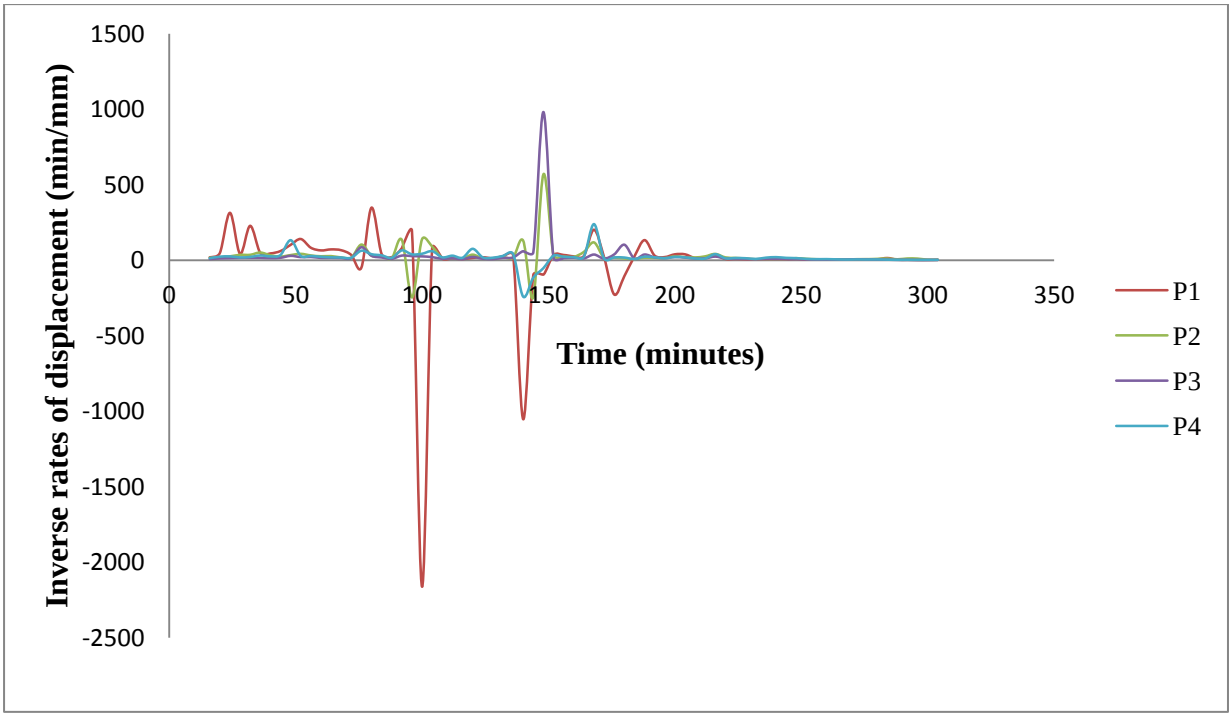


Figure 6.7: Inverse rates of displacement at 5 data interval (20 minutes).

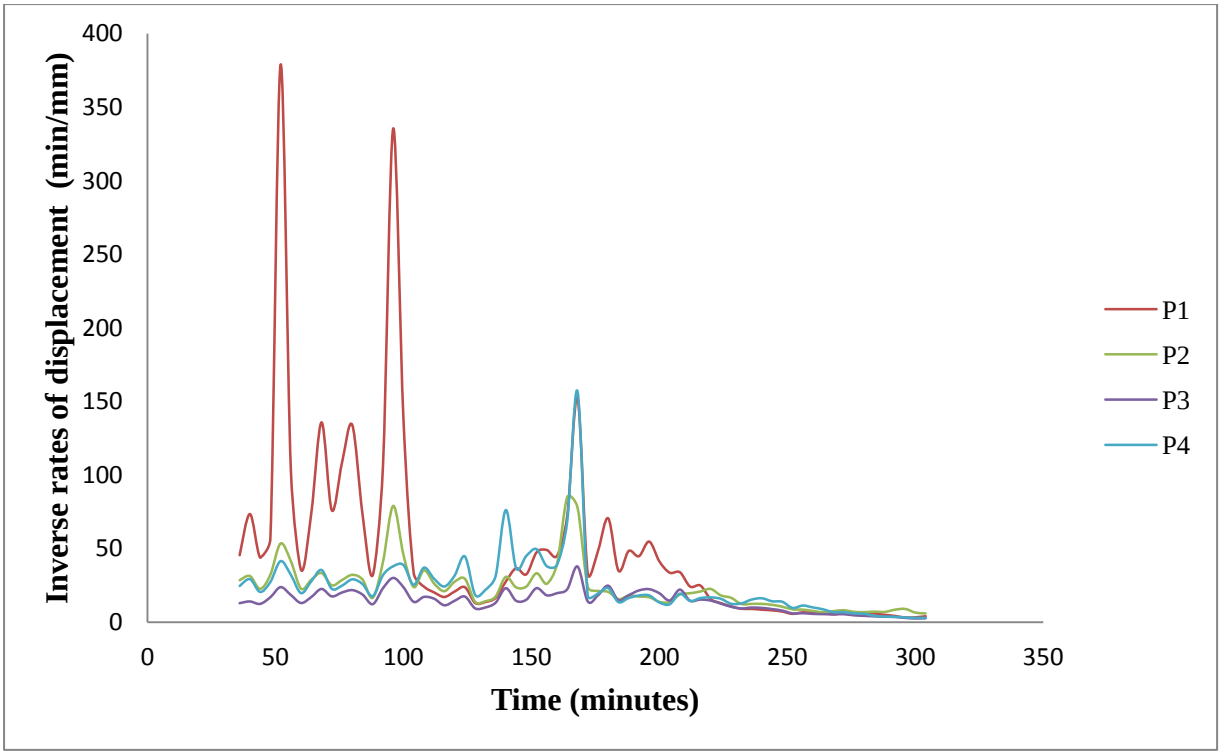


Figure 6.8: Inverse rates of displacement at 10 data interval (40 minutes).

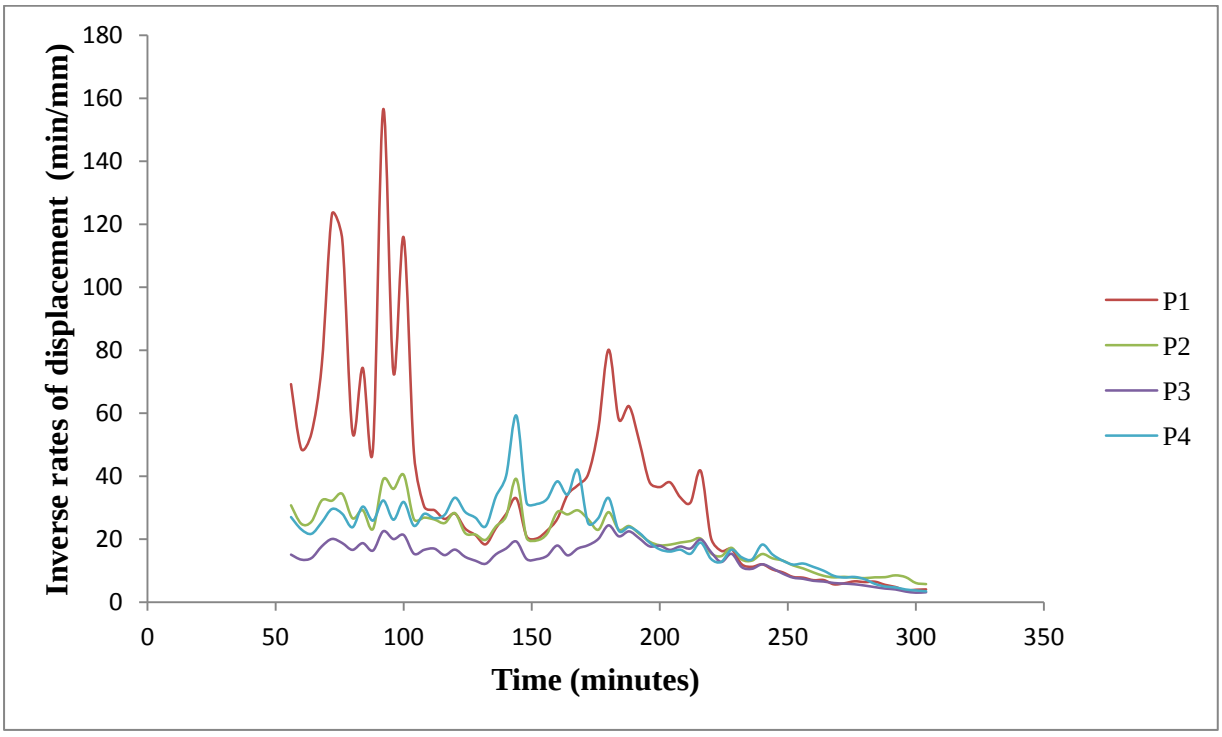


Figure 6.9: Inverse rates of displacement at 15 data interval (60 minutes).

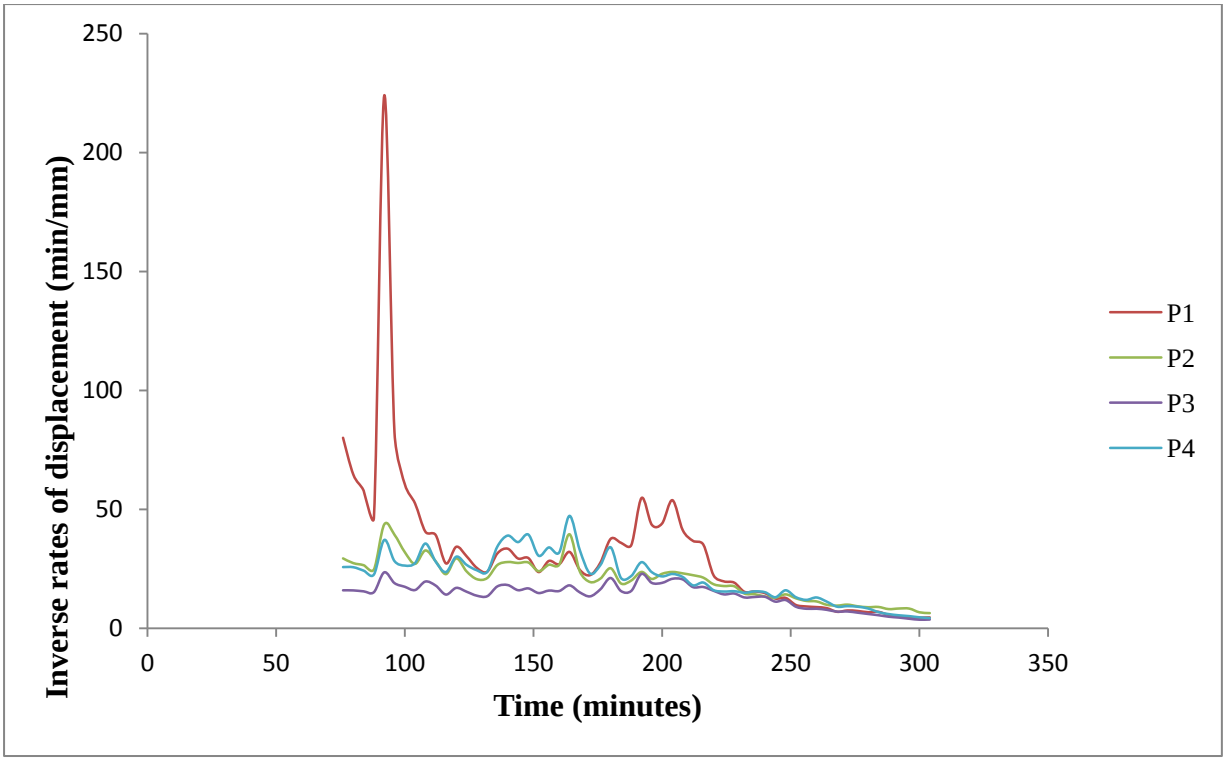


Figure 6.10: Inverse rates of displacement at 20 data interval (80 minutes).

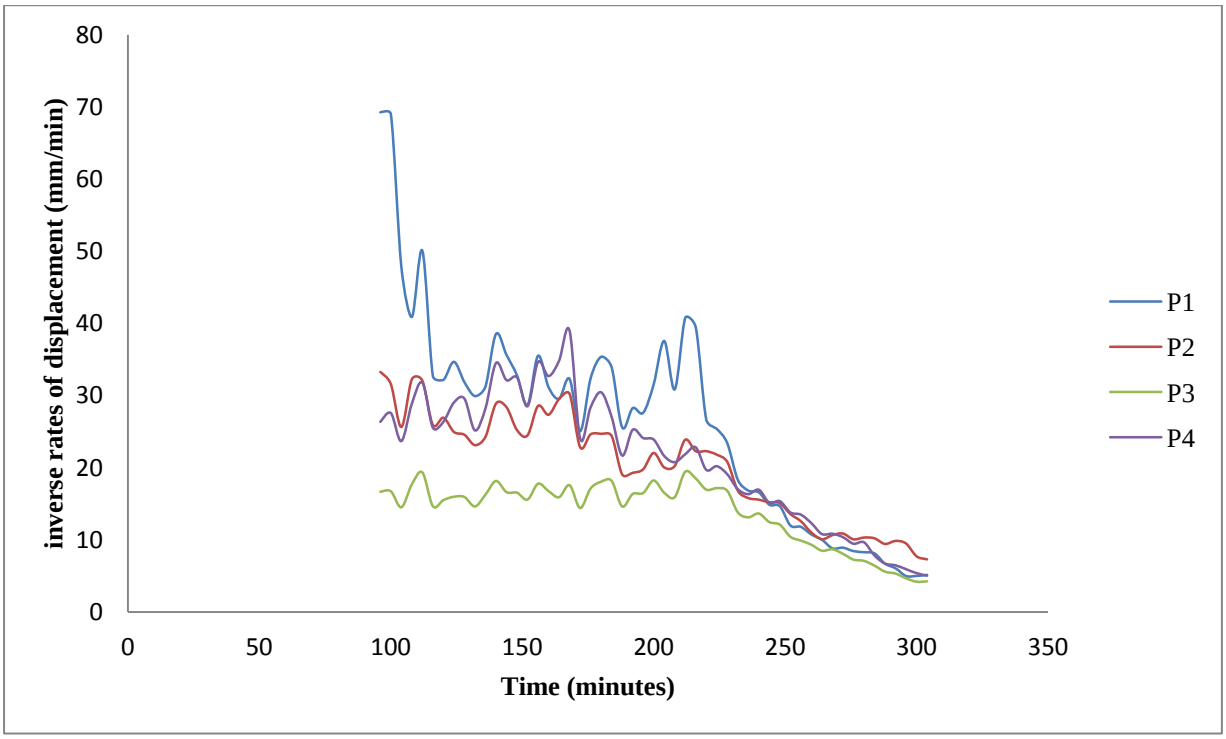


Figure 6.11: Inverse rates of displacement at 25 data interval (100 minutes).

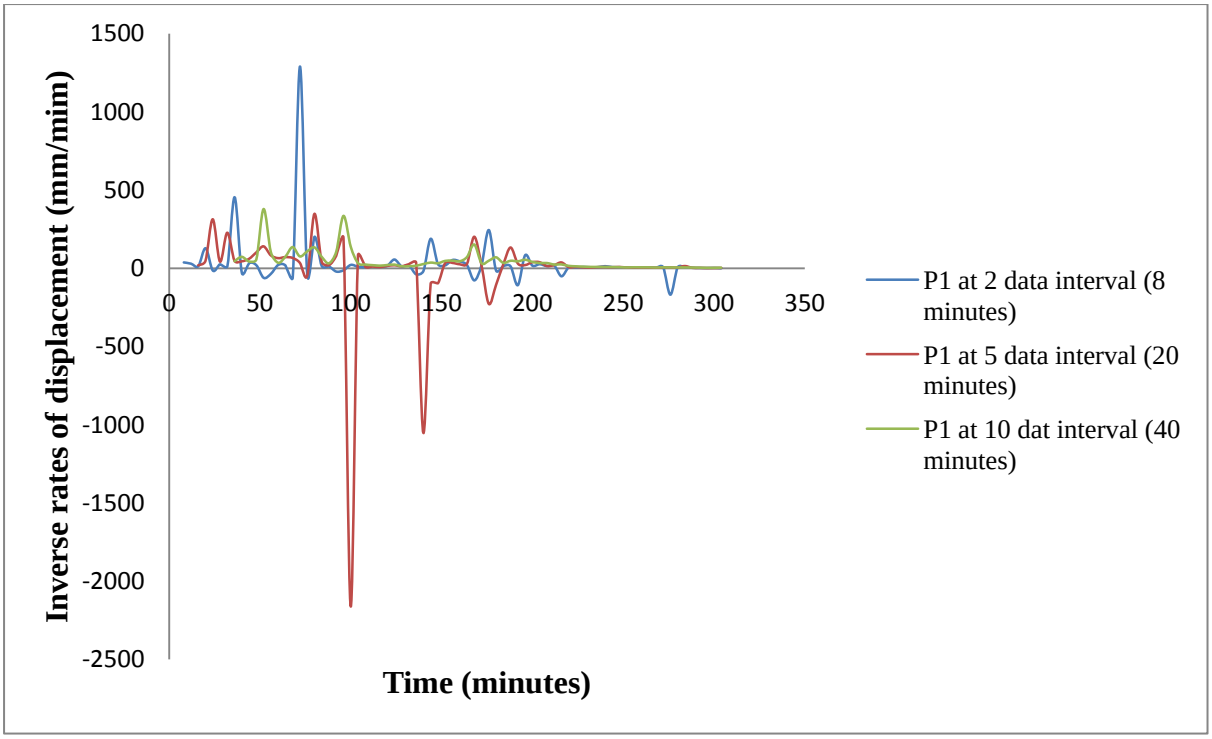


Figure 6. 12: Inverse rates of displacement at 2, 5 and 10 data interval (8, 20 and 40 minutes).

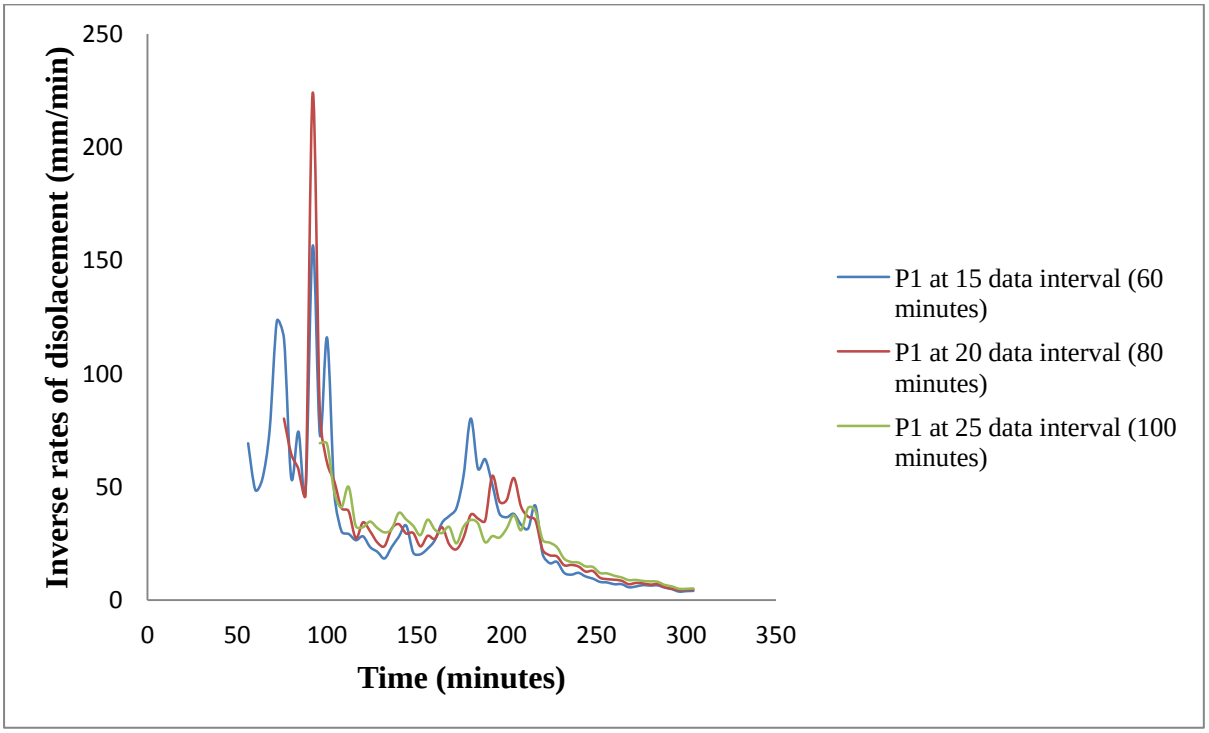


Figure 6.13: Inverse rates of displacement at 15, 20 and 25 data interval (60, 80 and 100 minutes).

6.3.4. STEP 2: Simple Linear Regression

Linear regression analysis is a statistical technique of determining the relationship that exists between two variables. The inverse rate of displacement method of predicting failure time is based on the degree of linearity between time variable (minutes) and the inverse rate of displacement variable (min/mm).

The term, "simple linear regression" is used because there is just one independent variable, X, which is time in minutes, in the model. X is also called the regressor or predictor variable. Y is the dependent variable, also known as the response (Montgomery, et al. 2012). To fit a linear trend to predict the time to failure from the values of time versus inverse rate of displacement, the linear equation to fit the trend is obtained using equation 6.10:

$$y = a + bx \qquad 6.10$$

The mean value of y is assumed to follow a linear relation $a + bx$ that is

$E(y) = a + bx$

The slope and the intercept of the line, E(y) = a + bx are called regression coefficients. The slope is the change in the mean value of y for a unit change in x.

6.3.5. STEP3: Regression Line

To fit a regression line, which is step 3 of the SFPM process, b and a are determined using equation 6.11 and 6.12 respectively:

$$b = \frac{n\sum_{i=1}^{n} x_i y_i - \left(\sum_{i=1}^{n} x_i (\sum_{i=1}^{n} y_i)\right)}{n(\sum_{i=1}^{n} {x_i}^2) - (\sum_{i=1}^{n} y_i)^2} \qquad 6.11$$

$$a = \frac{\sum_{i=1}^{n} y_i - b(\sum_{i=1}^{n} x_i)}{n} \qquad 6.12$$

With b and a known, the fitted regression line can then be written as equation 6.13

$$\hat{y} = a + bx \qquad 6.13$$

The fitted value, y_i, for a given value of the predictor variable, x_i , may be different from the corresponding observed value, y_i. The difference between the two values is called the residual, e_i , given in equation 6.14 as:

$$e_i = y_i - \hat{y}_i \quad 6.14$$

6.3.6. STEP 4: Coefficient of Regression

The coefficient of regression provides a measure of how well future outcomes such as time to failure, are likely to be predicted by this model (Montgomery, et al. 2012). An R^2 of 1.0 means that the regression line perfectly fits the data. It is calculated using equation 6.15 and this corresponds with step 4 of the SFPM process.

$$R^2 = 1 - \frac{SS_{err}}{SS_{tot}} \quad 6.15$$

Where:

$$SS_{tot} = \sum_{i=1}^{n}(y_i - \bar{y})^2 \quad 6.16$$

$$SS_{err} = \sum_{i=1}^{n}(y_i - \hat{y}_i)^2 \quad 6.17$$

$\bar{y}$ is the mean value of all recorded values, that is, inverse rate of displacement (min/mm) and $\bar{x}$ is the mean value of all values of the predictor variable, which is time (min). $\bar{y}$ and $\bar{x}$ are calculated using equation 6.18 and 6.19 respectively:

$$\bar{y} = \left(\frac{1}{n}\right) \sum_{i=1}^{n} y_i \quad 6.18$$

$$\bar{x} = \left(\frac{1}{n}\right) \sum_{i=1}^{n} x_1 \quad 6.19$$

The SFPM automatically carries out steps 1 to 4 for a given set of displacement data to determine the time to failure. The estimated time to failure is the point of intersection of the linear regression line, and the time axis (x-axis), when the

prediction criteria are satisfied. That is, when the inverse rate of displacement is positive and $0.7 \leq R^2 \leq 1.0$. If the criteria are not satisfied, the process is repeated after every two new scans by the radar.

6.4. Prediction of the Time of Failure from the Most Active Points

The following steps, together with the flow chart, as shown in figure 6.14, explains how the SFPM predicts the time to failure from the most active points:

- While the MSR is scanning, the displacement pattern is monitored for the development of a progressive displacement. At the formation of a clear progressive pattern, the displacement data of five or more points, depending on the size of the unstable area, are exported into the SFPM. Automatic activation of the SFPM could be achieved if an interface is created between the MSR and the SFPM. However, in the current research, this is done manually.
- From the points, between 1 and 5 most active points or sensitive moving points, are automatically selected based on the point(s) with the lowest inverse velocity. To select the most active points on the slope, the SFPM iterates from a maximum of 5 points to a minimum of 1 point. The number of most active points selected depends on the size of the unstable area.
- Once the most active points have been identified, the programme automatically predicts the time to failure from the identified most active points. In order to make accurate predictions, the software scans through the available data by stepping it forward after every two new scans to make predictions.
- When the criteria stated in step 4 for selecting the most linear section of the data and making prediction are met, the time to failure prediction is made. If the criteria are not met, the user is notified and the SFPM continues to review the predictions after every two new scans until the criteria are met. The premise of the inverse velocity method is the development of a linear relationship between the inverse velocity and time during deformation shortly before failure (Fukuzono, 1985).

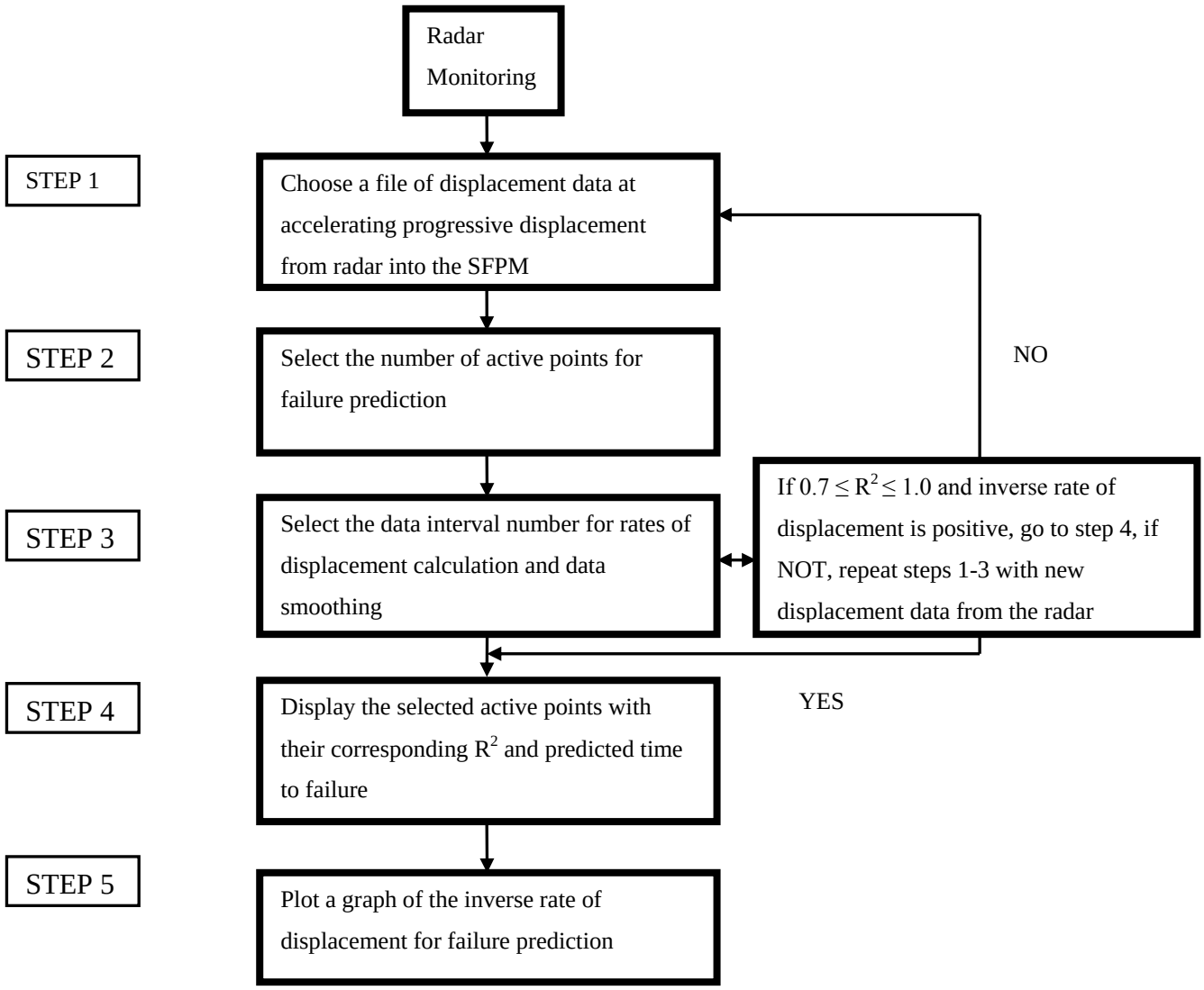


Figure 6.14: SFPM flow chart.

6.5. SFPM Home Page

The SFPM home page consists of the input and output, or results sections. Figures 6.15 shows the appearance of the home page without input data, while figure 6.16 shows the home page with displayed results.

Input Section

Choose File: The MSR displacement file is chosen from the radar in an Excel spread sheet format and input into the SFPM.

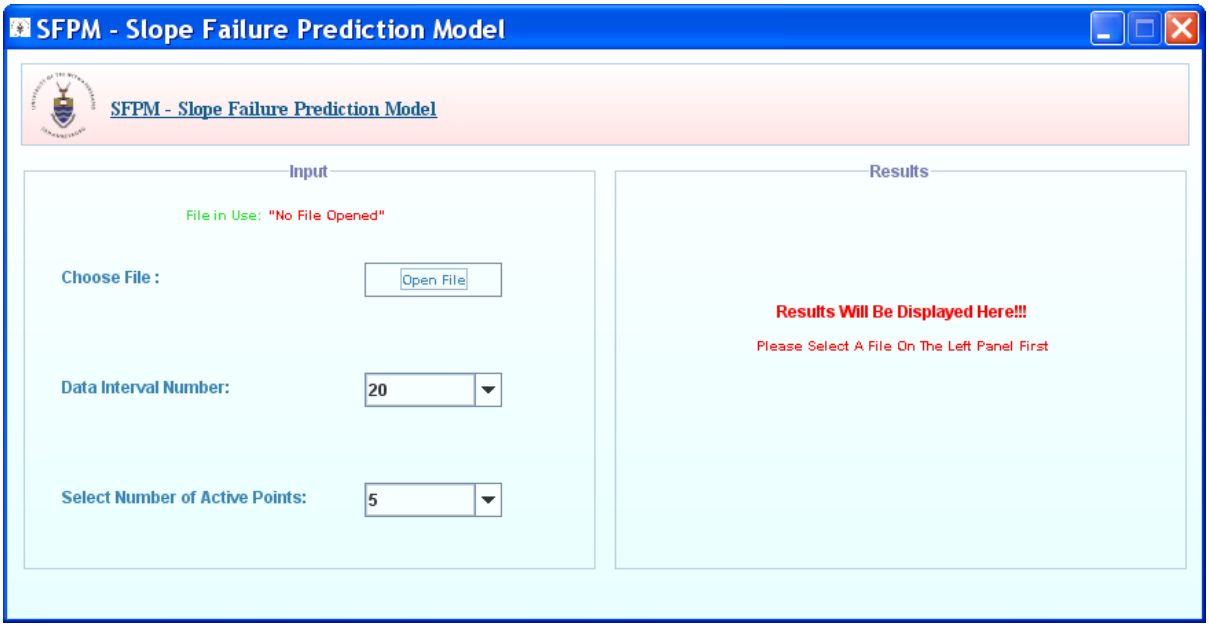


Figure 6.15: SFPM home page without results.

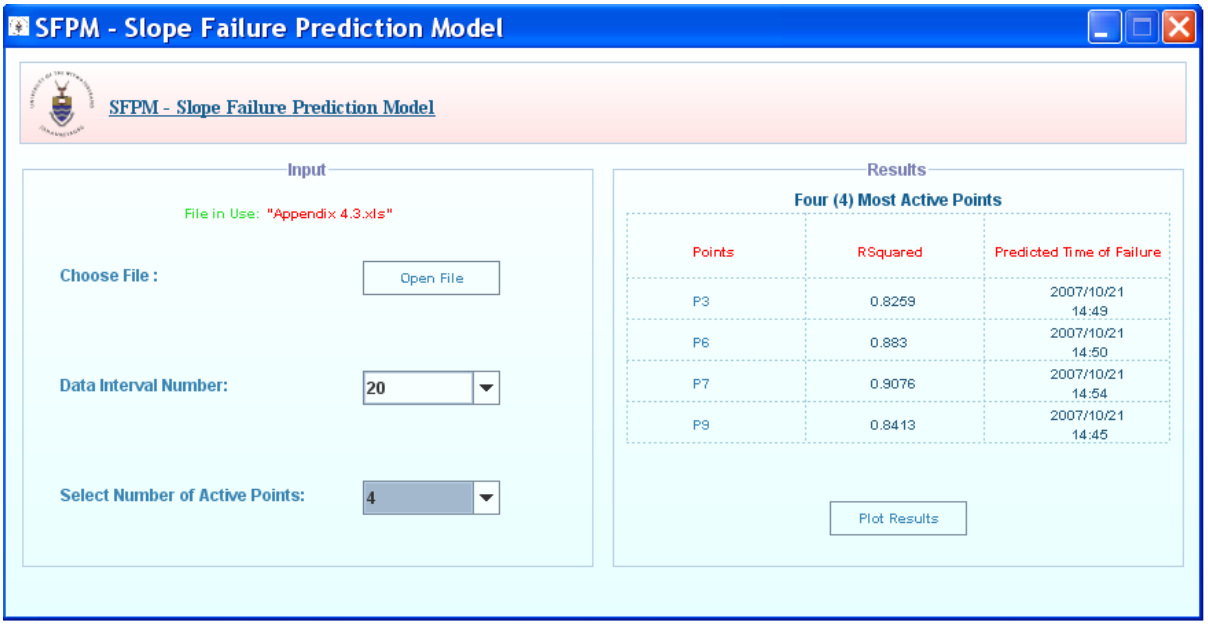


Figure 6.16: SFPM home page with results.

Data Interval Number: A data interval number from among 15, 20 and 25 is selected for rates of displacement calculations and data smoothing. Consistent use of data interval is advised.

Select Number of Active Points: The SFPM automatically selects between 1 and 5 most active points. Depending on the number of active points selected, this icon helps the user in selecting and comparing the predictions from the most active points.

Output Section

Results: The results of the selected active points with the corresponding regression coefficient, R^2, and the predicted time to failure are displayed.

Plot Results: An example of the graphical illustration of the active points obtained using the, "plot results," icon is displayed in figure 6.17.

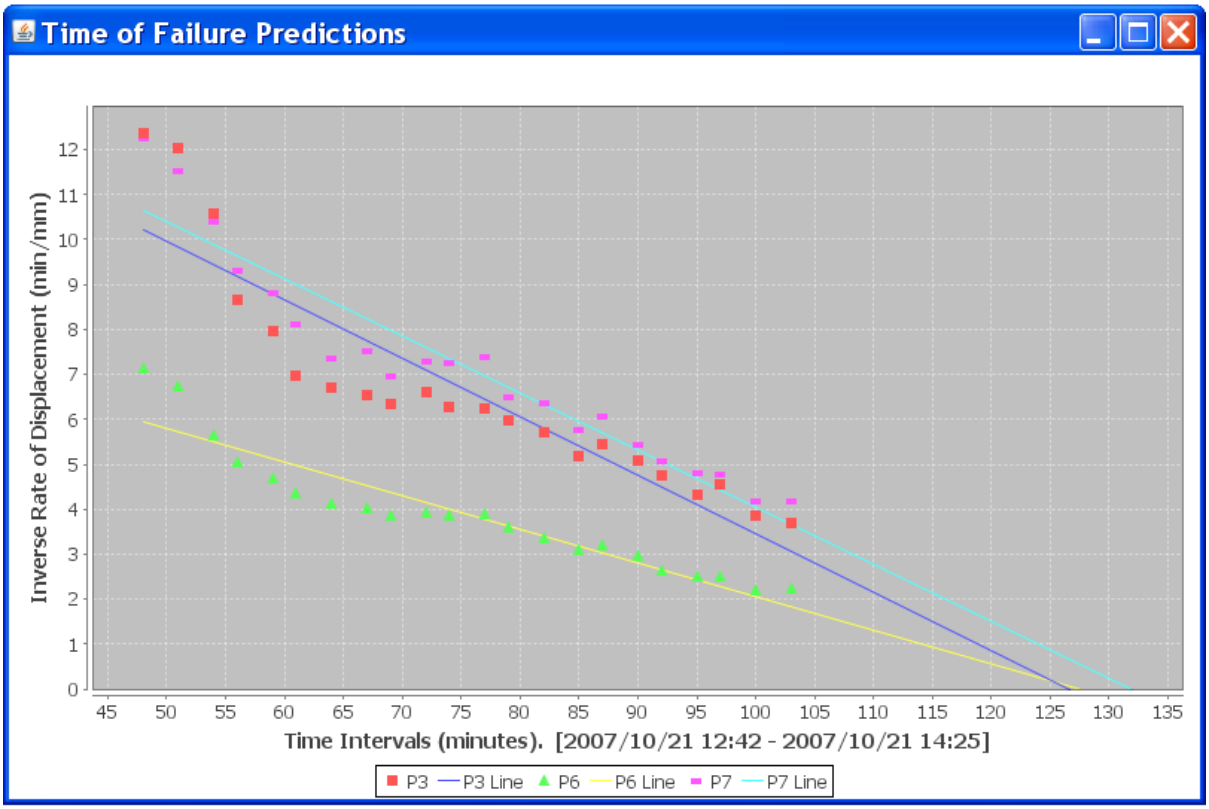


Figure 6.17: Graphical illustration of predictions from the active points.

6.6. Validation of the Slope Failure Prediction Model (SFPM)

In order to validate the effectiveness of the SFPM in predicting impending slope failure, four selected examples of surface mine slope failures recorded with the MSR are used. Predicted

time to failure can either be a safe prediction or an unsafe prediction. As illustrated in equation 6.20, when the estimated or predicted time to failure is less than the actual time of failure, the prediction is regarded as safe, but when the estimated or predicted time to failure is greater than the actual time of failure, the prediction is unsafe. Safe predictions give advance warning of the time to failure which is the time difference in minutes between the actual time of failure and the time of failure prediction. Advance warning is calculated with equation 6.22.

Safe prediction $= TF_P < TF_a$ 6.20

Unsafe prediction = $TF_p > TF_a$ 6.21

Advance warning = $TF_a - TFP$ 6.22

Where:

TF_a = Actual time of failure;

TF_p = Predicted time to failure; and

TFP = Time of Failure Prediction;

6.6.1. Validation Test 1 (Copper Mine)

The slope failure used for the first validation test occurred in a copper mine. The name and geology of the mine were not available. However, a detailed description of the failure can be found in section 5.3.1.

From the displacement record of the slope, the onset of progressive displacement commenced on 5th September, 2008 around 02:00 and failure occurred on the same day at 21:11. The entire duration of failure, from the onset of progressive displacement until failure, is a total of 1090 minutes which is approximately 18 hours. The relative range or displacement, of the ten points in the failure section is shown in figure 5.8.

First Prediction

At the formation of a clear progressive trend, when the average displacement of points in the unstable area was around -10mm, the SFPM was activated with the displacement data of ten

points within the unstable region. This constitutes the displacement data from 02:02 to 19:59, as seen in appendix 3.1. All the ten points failed to meet the criteria for good predictions, and the prediction was subsequently revised, as depicted in figure 6.18.

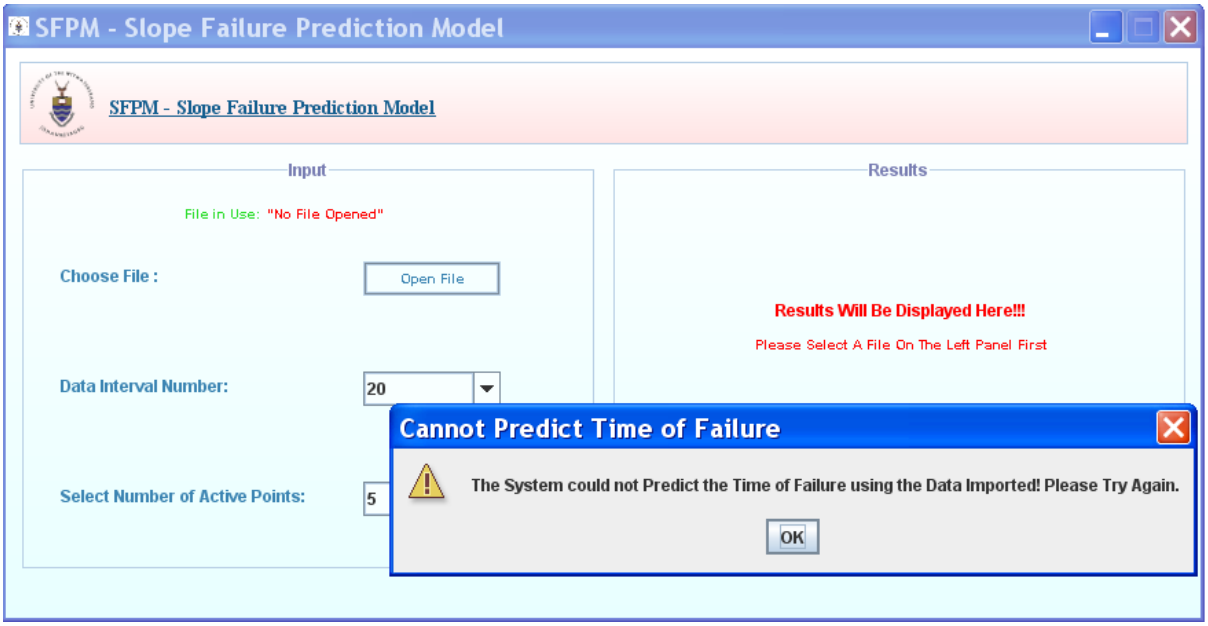


Figure 6.18: Failed first prediction of validation test 1.

Second Prediction

After two new radar scans, the displacement data increased from 19:59 to 20:07 as shown in appendix 3.1. From a total of ten points, the five most active points being points 1, 3, 4, 6 and 9 were selected by the SFPM for predictions. The predicted results are as displayed in figure 6.19, with the graphical illustration shown in figure 6.20.

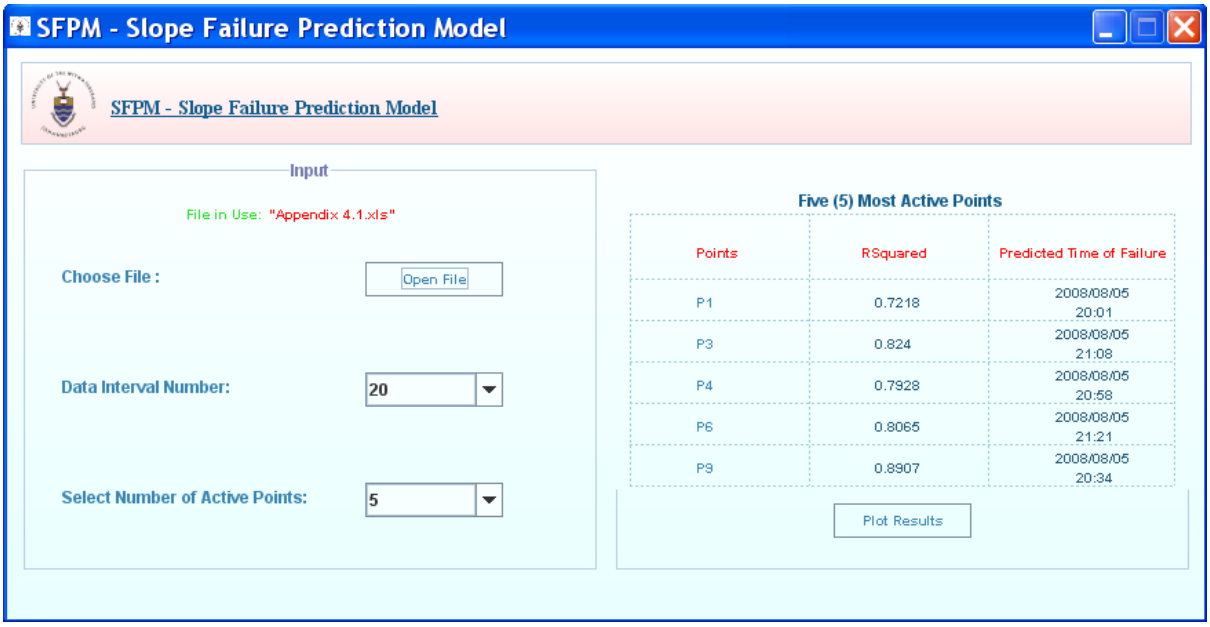


Figure 6.19: Second prediction of validation test 1.

The summary of the predictions obtained from the five most active points of validation test 1 is presented in figure 6.19 and table 6.1. Point 1 predicted a failure time of 20:01, which is 70 minutes before the actual failure time of 21:11pm. However, the prediction was incorrect, because the predicted time to failure (TF_P) was earlier than 20:07, when the failure prediction was made. Point 3, 4 and 9 predicted that failure would occur at 21:08, 20:58 and 20:34 respectively. Point 3 fell short of accurate prediction by 3 minutes, point 4 by 13 minutes and point 9 by 37 minutes. Although all predictions from points 3, 4 and 9 were safe predictions, the best prediction of 21:08, which is only 3 minute short of an accurate prediction, was from point 3. The prediction from point 6 was unsafe by 10 minutes. As shown in figure 6.21, the three most active points, that is, the points with the lowest inverse velocity are given as points 1, 3 and 4. In a real mining situation, time to failure prediction can reliably be estimated by comparing the two closest results from the three most active points. A comparison of the predictions from the three most active points in this case example indicated the two closest predictions of 21:08 and 20:58 from points 3 and 4 respectively. With the exception of points 1 and 6, all predictions made at 20:07 were safe predictions with advance warning of the time to failure.

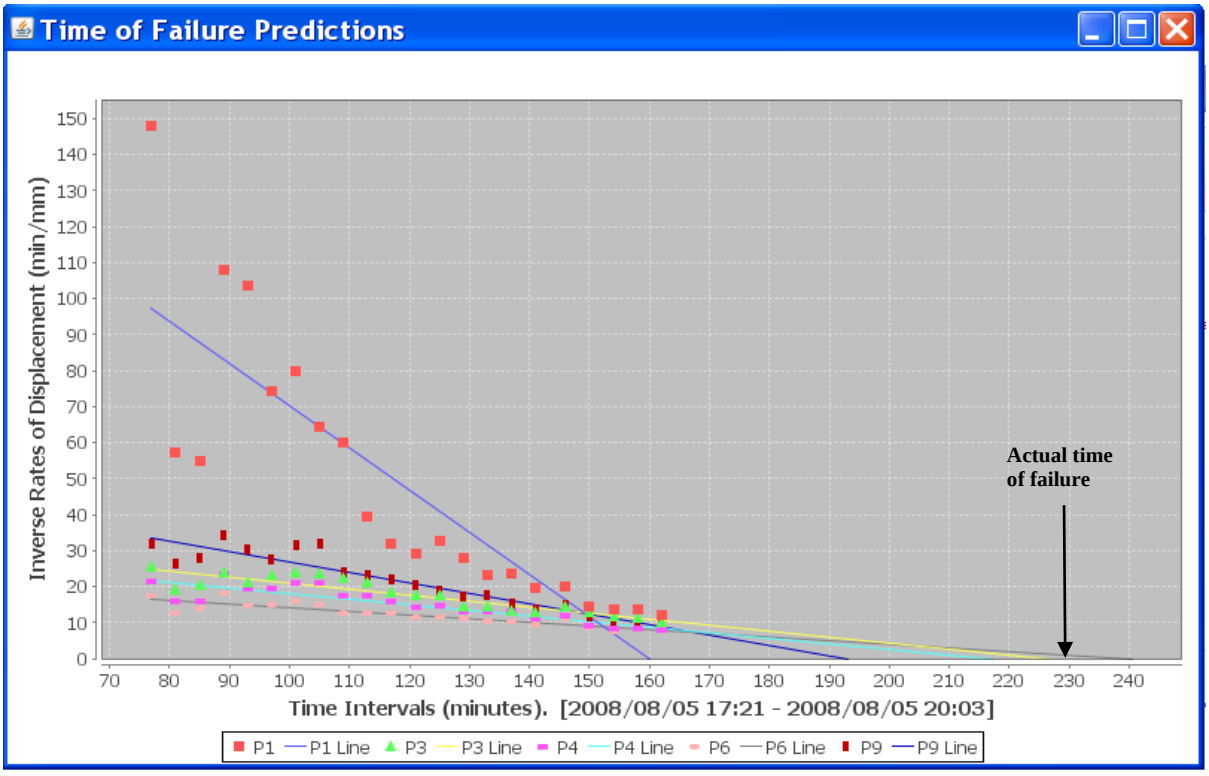


Figure 6.20: Graphical illustration of the five most active points of validation test 1.

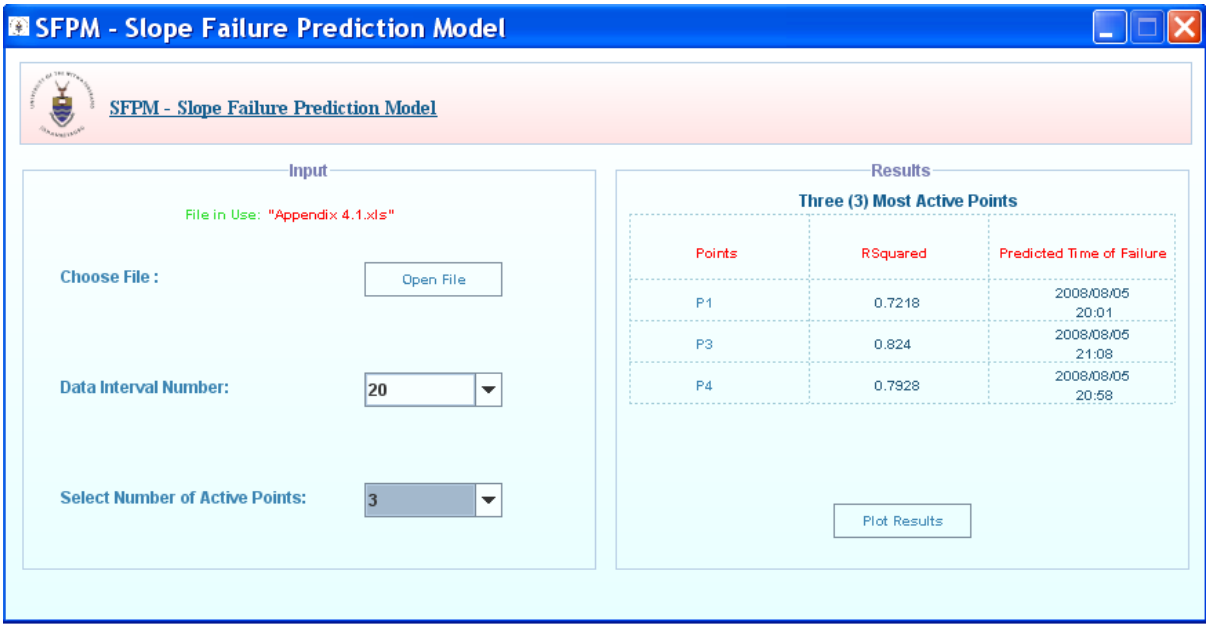


Figure 6.21: Predictions with three most active points of validation test 1.

Table 6.1: Summary of prediction results of validation test 1 conducted at 20:07 on 5th August, 2008.

Most Active Points	R^2	Predicted Time of failure (TF_p)	Actual Time of failure (TF_a)	Safe Prediction ($TF_p < TF_a$) (minutes)	Unsafe Prediction ($TF_P > TF_a$) (minutes)	Advance warning (TF_a – TFP) (minutes)
P1	0.7218	2008/08/05 20:01	2008/08/05 21:11	Yes	No	64
P3	0.824	2008/08/05 21:08	2008/08/05 21:11	Yes	No	64
P4	0.7928	2008/08/05 20:58	2008/08/05 21:11	Yes	No	64
P6	0.8065	2008/08/05 21:21	2008/08/05 21:11	No	Yes	Not applicable
P9	0.8907	2008/08/05 20:34	2008/08/05 21:11	Yes	No	64

TFP – Time of Failure Prediction (20:07)

6.6.2. Validation Test 2 (Ramp 12 High-wall Failure, New Vaal Open-Cast Coal Mine)

The slope failure data used for validation test 2 occurred on the high-wall of New Vaal open-cast coal mine, South Africa. The slope started experiencing progressive displacement on 13th March, 2008 at 13:18 when the average displacement of the points in the critical area of instability was –22mm. Information obtained from the geotechnical staff showed that failure occurred around 16:20 on 13th March, 2008. Figure 6.22 illustrates the relative range or displacement, of the ten points selected from the nine unstable sections shown in figure 5.24.

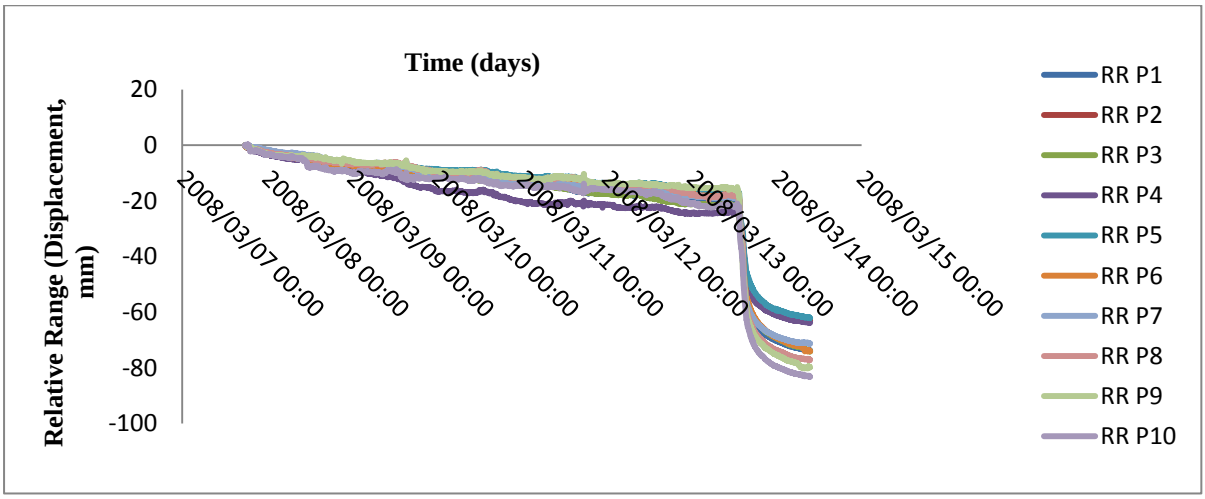


Figure 6.22: Relative range (Displacement, mm) of 10 points used for validation test 2.

First Prediction

The first prediction was conducted with the displacement data between 13:26 and14:59, as shown in appendix 3.2. At this time, the progressive displacement trend was well pronounced. Ten points were selected from the unstable region, but none of them met the criteria for predictions and hence the prediction was revised.

Second Prediction

After two new scans, from 13:26 to 15:04, the criteria for predictions were still not satisfied. Subsequently, the prediction was reviewed for a third time.

Third Prediction

At the third prediction, this was based on the data from 13:26 to15:09, as depicted in appendix 3.2, the prediction criteria were met. The results of the predictions are shown in figure 6.23 and table 6.2, with the graphical illustration displayed in figure 6.24. According to the SFPM, the five most active points are points 1, 6, 7, 8 and 10. The predicted time to failure from points 1, 6, 8 and 10 are 15:38pm, 16:16, 15:43 and 16:00 respectively, while point 7 predicted a failure time of 16:24. Point 1 failed to predict an accurate time to failure by 42 minutes, point 8 by 37 minutes, while point 7 over-predicted failure by four minutes. The most accurate predictions are from point 6 and 10. Both points fell short of accurate predictions by 4 minutes and 20 minutes respectively. A fourth prediction was conducted using the displacement data between 13:26 and 15:19 and the result was the same as that of the third prediction. This indicates the needlessness of a continuous prediction once the prediction criteria are satisfied. The three most active points are points 1, 6 and 7 as shown in figure 6.25.

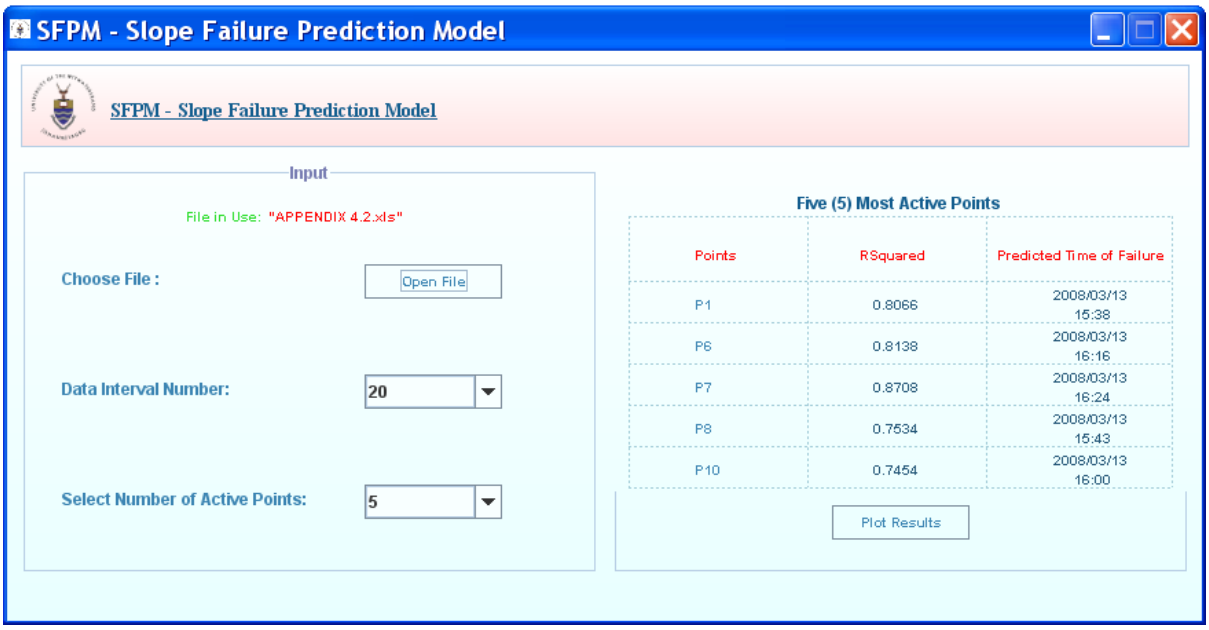


Figure 6.23: Third predictions of validation test 2.

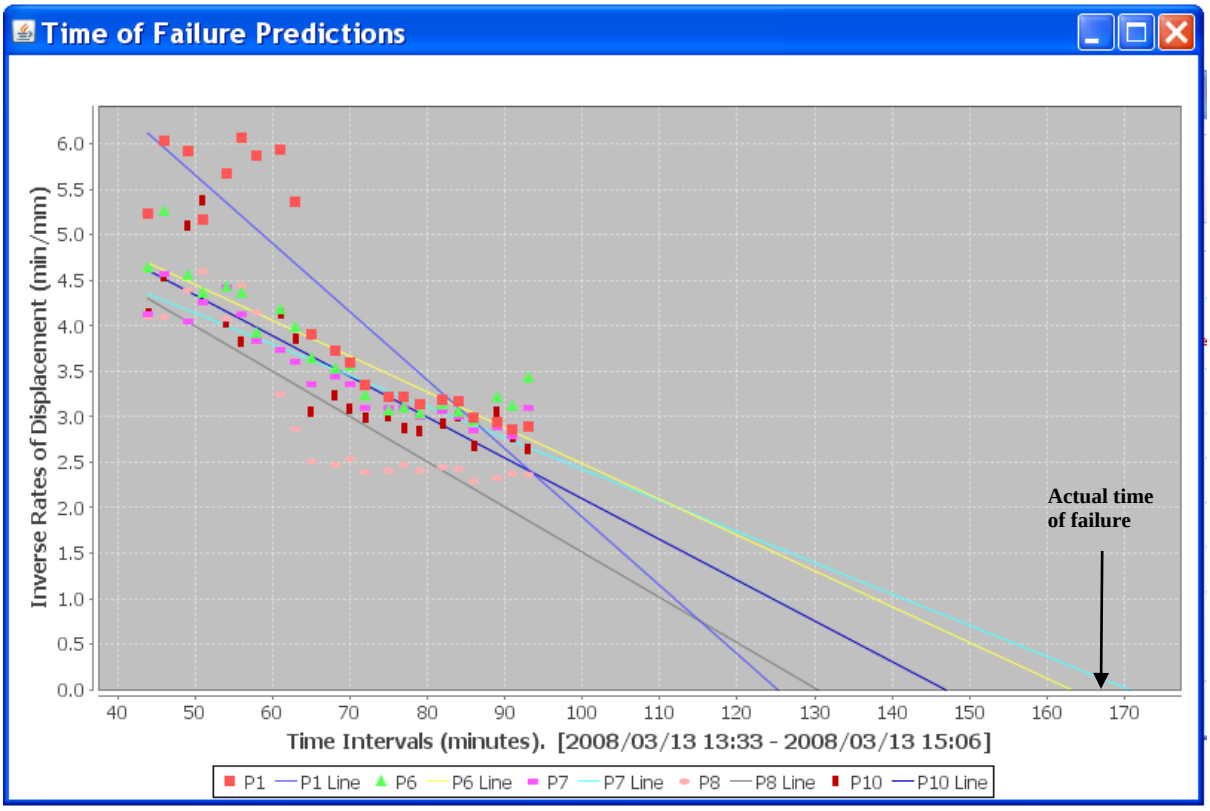


Figure 6.24: Graphical illustration of the five most active points of validation test 2.

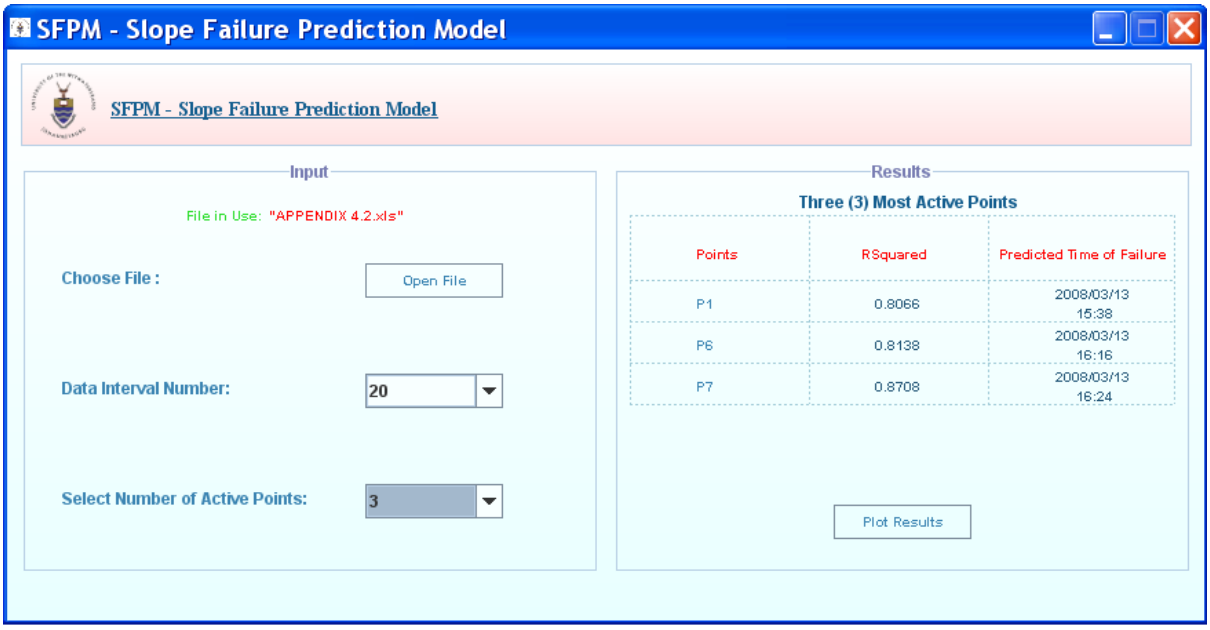


Figure 6.25: Predictions with three most active points of validation test 2.

Table 6.2: Summary of prediction results of validation test 2 conducted at 15:09 on 13th March, 2008.

Most Active Points	**R^2**	**Predicted Time to Failure (TF_p)**	**Actual Time of Failure (TF_a)**	**Safe Prediction ($TF_p < TF_a$) (minutes)**	**Unsafe Prediction ($TF_P > TF_a$) (minutes)**	**Advance warning (TF_a – TFP) (minutes)**
P1	0.8066	2008/03/13 15:38	2008/03/13 16:20	Yes	No	71
P6	0.8138	2008/03/13 16:16	2008/03/13 16:20	Yes	No	71
P7	0.8708	2008/03/13 16:24	2008/03/13 16:20	No	Yes	Not applicable
P8	0.7534	2008/03/13 15:43	2008/03/13 16:20	Yes	No	71
P10	0.7454	2008/03/13 16:00	2008/03/13 16:20	Yes	No	71

TFP – Time of Failure Prediction (15:09)

6.6.3. Validation Test 3 (Ramp 5 High-wall Failure, Landau Open-Cast Coal Mine)

The slope failure used in the third validation test occurred on 21st October at 15:00, 2007 in ramp 5 high-wall of Landau open-cast coal mine. The relative range or displacement of eleven selected points within the failure section is illustrated in figure 5.16.

First Prediction

With the progressive trend fully established, the first prediction was carried out with the displacement data between 11:53 and 13:59, as seen in appendix 3.3. The average displacement then was -52mm. The criteria for prediction were not satisfied by any of the 11 points selected from the critical region, and for that reason a second prediction was necessary.

Second Prediction

After two new radar scans, at 14:04, the prediction was reviewed and the displacement data still did not attain the criteria for good prediction.

Third, Fourth and Fifth Predictions

The prediction was repeated for a third, fourth and fifth time, with more displacement data at 14:09, 14:14, and 14:19 respectively. The predictions were unsuccessful, as the data failed to meet the prediction criteria, implying that a close to linear displacement prior to failure was not fully formed.

Sixth Prediction

At the sixth prediction at 14:25, the requirement for a good quality prediction was achieved and a prediction was made with five of the eleven points. From the SFPM, a linear displacement occurred with the data interval between 12:42 and 14:25 which is illustrated in figure 6.27. The results of the predictions made with the five most active points, namely points 3, 6, 7, 9 and 10, are presented in figure 6.26 and table 6.3.

Since the actual failure occurred around 15:00, analysis of the results indicated very good predictions from all the five most active points. Point 3, 6 and 7 predicted a failure time of 14:49, 14:50 and 14:54 respectively, while points 9 and 10 predicted the time to failure of 14:45 and 14:39 respectively. The three most active points, namely points 3, 6 and 7, as shown in figure 6.28, failed to correctly predict the time to failure by 11 minutes, 10 minutes and 6 minutes correspondingly. Point 9 failed to predict a correct failure time by 15 minutes, while point 10 failed by 21 minutes. Although no point predicted an accurate time of failure, the predictions were nevertheless safe.

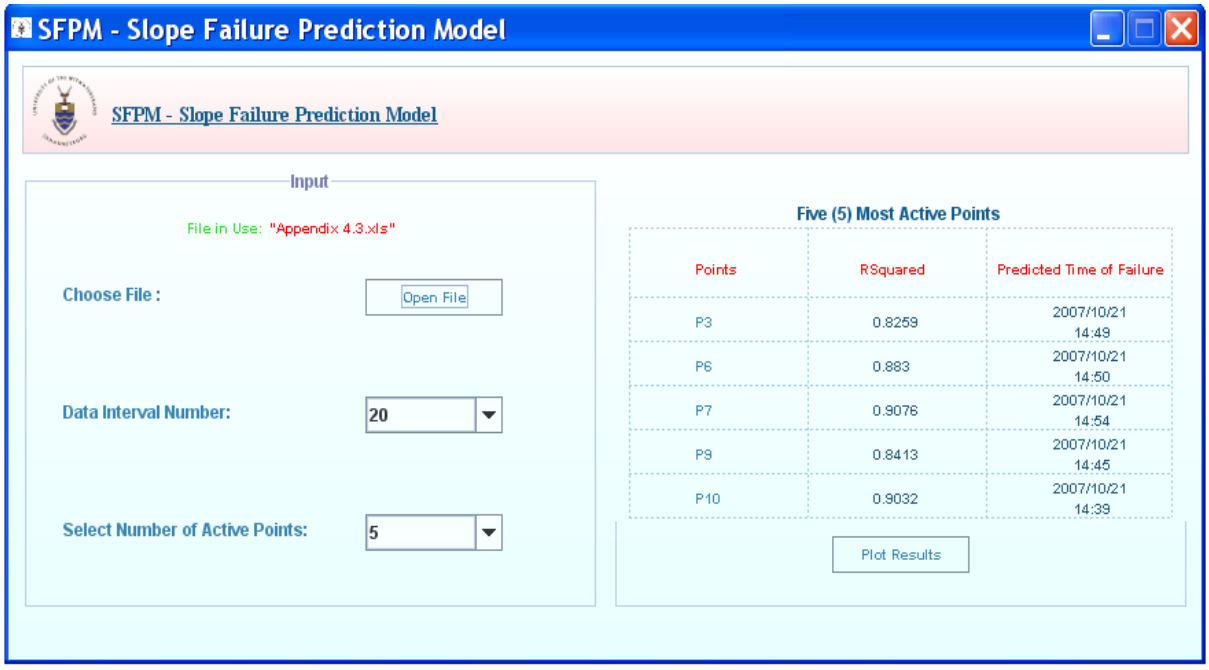


Figure 6.26: Sixth prediction of validation test 3.

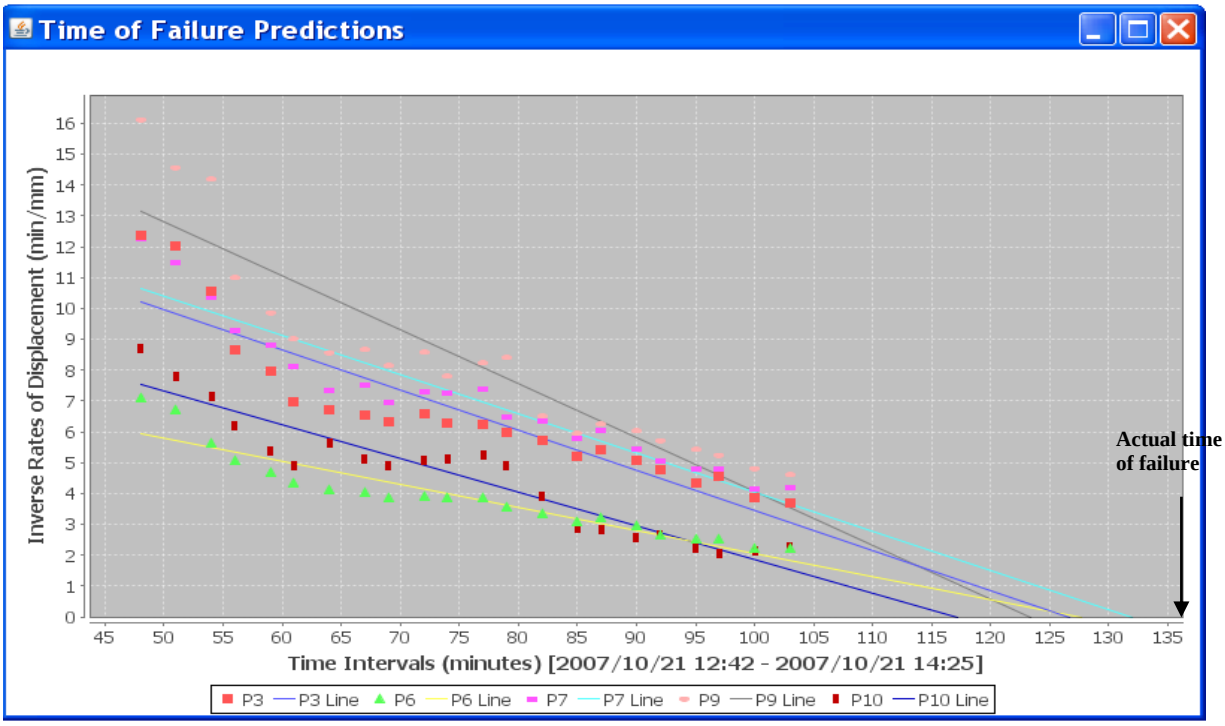


Figure 6.27: Graphical illustration of the five most active points of validation test 3.

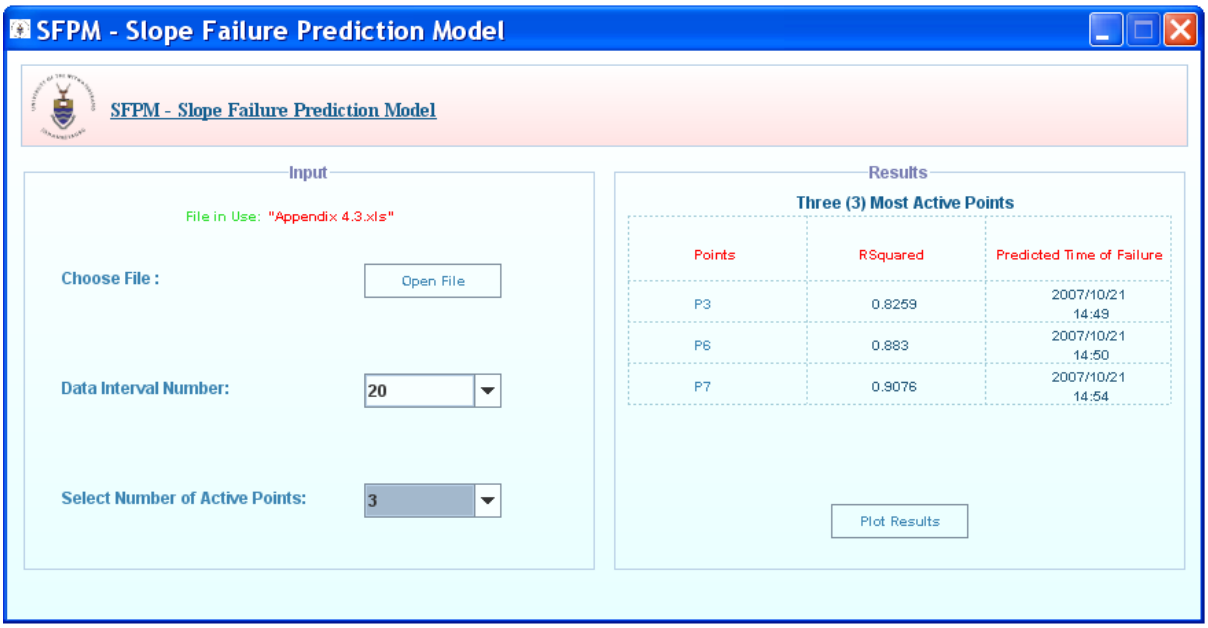


Figure 6.28: Predictions with the three most active points of validation test 3.

Table 6.3: Summary of prediction results of validation test 3 conducted at 14:25 on 21st October, 2007.

Most Active Points	R^2	Predicted Time to failure (TF_p)	Actual Time of failure (TF_a)	Safe Prediction ($TF_p < TF_a$) (minutes)	Unsafe Prediction ($TF_p > TF_a$) (minutes)	Advance warning (TF_a – TFP) (minutes)
P3	0.8259	2007/10/21 14:49	2007/10/21 15:00	Yes	No	35
P6	0.883	2007/10/21 14:50	2007/10/21 15:00	Yes	No	35
P7	0.9076	2007/10/21 14:54	2007/10/21 15:00	Yes	No	35
P9	0.8413	2007/10/21 14:45	2007/10/21 15:00	Yes	No	35
P10	0.9032	2007/10/21 14:39	2007/10/21 15:00	Yes	No	35

TFP – Time of Failure Prediction (14:25)

6.6.4. Validation Test 4 (Mine Name Unknown)

The identity of the mine where the displacement data used for validation test 4 was obtained is unknown, as well as the actual time to failure. From the information gathered, slope failure occurred around 11:07 on 13th February, 2011. Radar monitoring started on the 11th February, 2011 at 12:52 and ended on 14th February, 2011at 09:23. Only six points were selected for

prediction because of the small size of the unstable section. The graphical illustration of the relative range or displacement, of the selected points is given in figure 6.29.

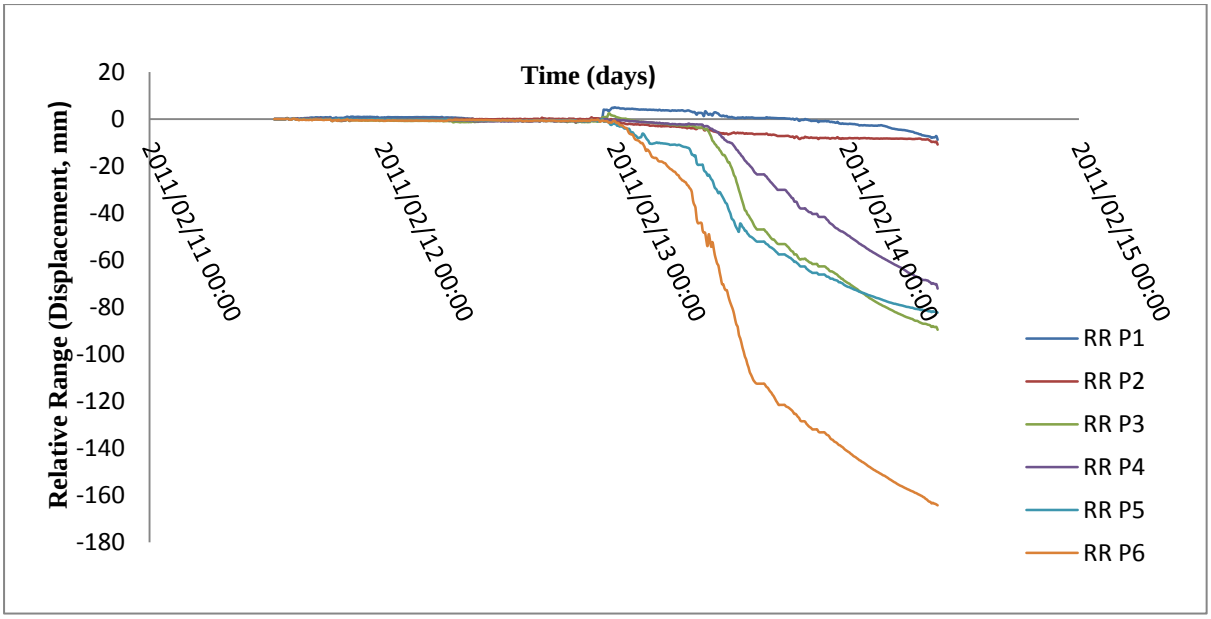


Figure 6.29: Relative range (Displacement, mm) of 6 points used for validation test 4.

First Prediction

Progressive displacement started at an average point displacement of -5mm at 01:32 on 13th February, 2011 and was fully developed at an average point displacement of -30mm on the same day. At 06:53, the SFPM could not make predictions from any of the six selected points.

Second, Third and Fourth Predictions

The prediction was repeated for a third, fourth and fifth time at 07:08, 07:23 and 07:38 respectively, with additional displacement data, as seen in appendix 3.4. Nevertheless, no prediction was made possible.

Fifth, Sixth and Seventh Predictions

The predictions were repeated again at 07:53am, 08:08am, and 08:23am with no results.

Eighth prediction

At 08:38 on 13th February, 2011 as given in appendix 3.4, the eighth prediction yielded results from a maximum of two most active points, namely point 5 and 6. This implies that the predictions were made from the SFPM after the fourth iteration. The predictions from the two points are shown in figure 6.30 and 6.31, with the summary in table 6.4. Point 5 predicted a time to failure (TF_p) at 08:21. However, the prediction was wrong, as it was earlier than the time at which failure prediction was made (TFP). Point 6 produced a reasonably accurate prediction of 10:19 which was 48 minutes before the actual time of failure (TF_a) of 11:07. The time to failure prediction from only two points indicated that the failure zone was small.

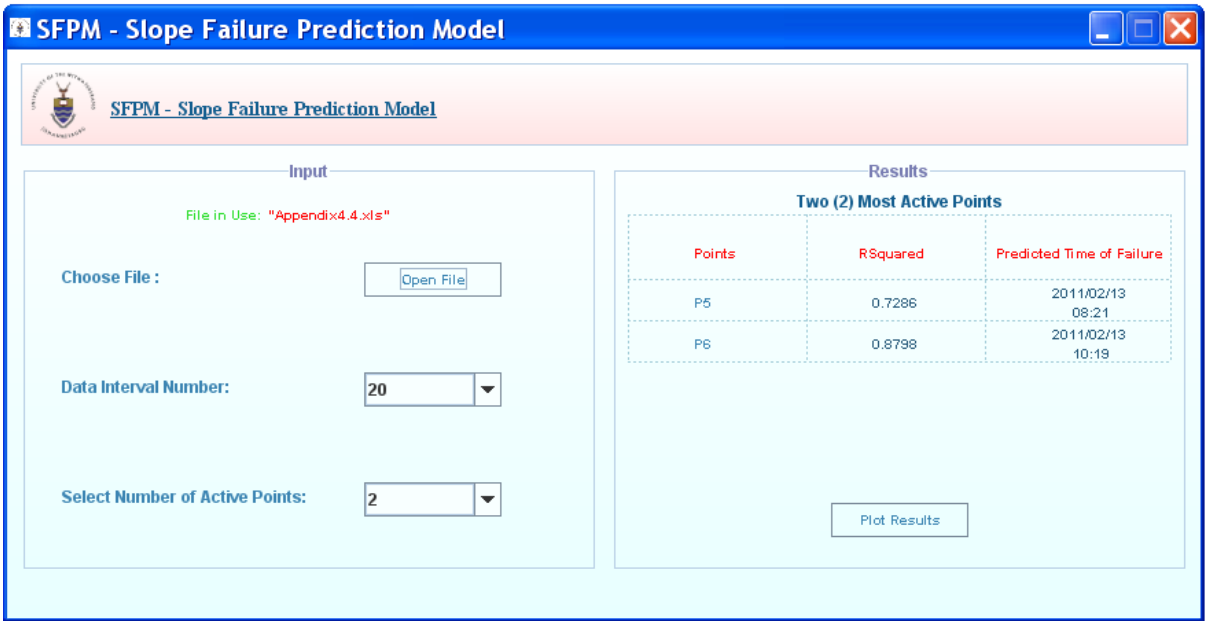


Figure 6.30: Eighth prediction of validation test 4.

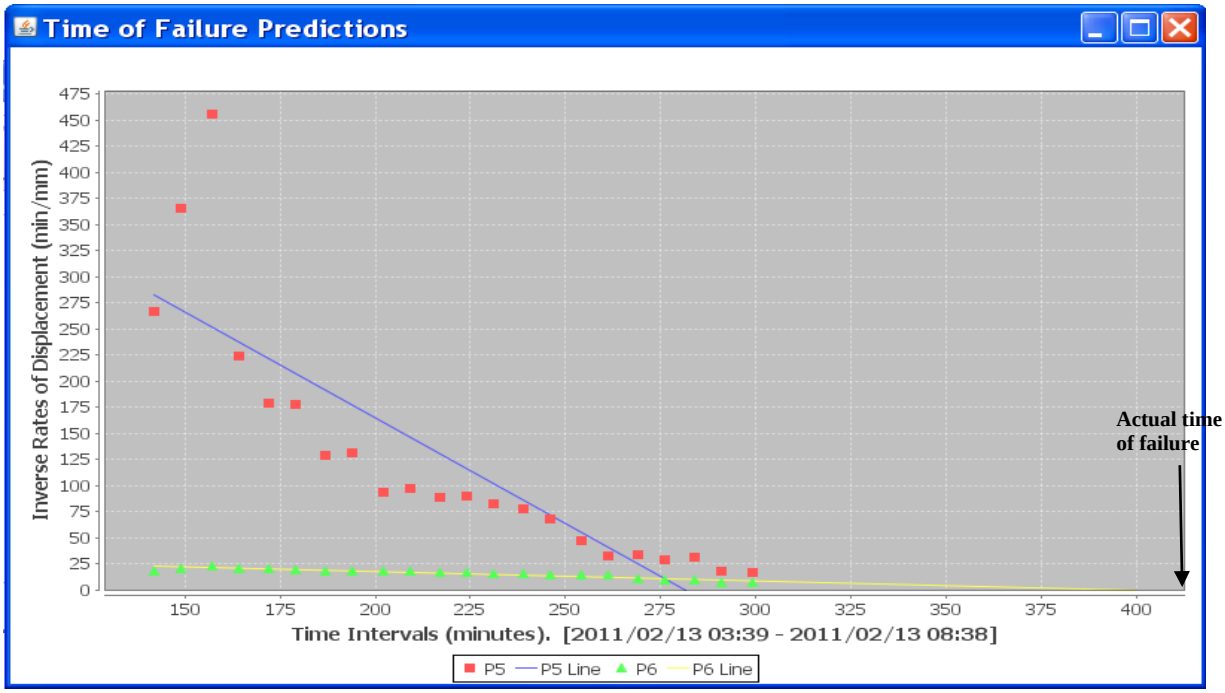


Figure 6.31: Graphical illustration of the two most active points of validation test 4.

Table 6.4: Summary of prediction results of validation test 4 conducted at 08:38 on 13th February, 2011.

Most Active Points	**R^2**	**Predicted Time to failure (TF_p)**	**Actual Time of failure (TF_a)**	**Safe Prediction ($TF_p < TF_a$) (minutes)**	**Unsafe Prediction ($TF_P > TF_a$) (minutes)**	**Advance warning (TF_a – TFP) (minutes)**
P5	0.7286	2011/02/13 08:21	2007/10/13 11:07	Yes	No	149
P6	0.8798	2011/02/13 10:19	2007/10/13 11:07	Yes	No	149

TFP – Time of Failure Prediction (08:38)

6.7. Summary

Predicting the time to failure of mine slopes has been a research subject for decades and with all the efforts it has not been possible to agree on an acceptable method of predicting the time to failure. Similarly, determination of a universal rate of displacement threshold of mine slopes has not been possible. This underscores the variations existing in the mechanisms and factors governing slope failure. The selected prediction threshold depends not only on the geology of the rock but also on the geotechnical personnel and the slope monitoring equipment in use. Having established that failure mechanisms may vary within the same, it

therefore means that rates of displacement threshold can vary within the same mine. The rate of displacement threshold of slopes must be determined by the geotechnical personnel from experience, analysis and design. Once the threshold is reached, Ryan and Call (1992) suggested that mining should be discontinued until an acceptable relaxation limit is achieved. They also recommended that by controlling the mining rate, the rates of displacement of surface mine slopes will be controlled.

Among the numerous attempts made at developing an acceptable method of predicting the failure time of mine slopes, the Fukuzono's inverse velocity method offers the best chance of producing a close estimate of failure time (Rose and Hungr, 2007). This is because of the observation that close to linear behaviour occurs shortly before slope failure (Fukuzono, 1985; Hamiel et al. 2004).

The SFPM interface is user-friendly, and the result is available to the user with just five clicks. The unique characteristics of the SFPM are its ability to:

1. Automatically detect the most active points or sensitive moving points among several points on the scanned mine slope;
2. Capture within a large range of displacement data, the most linear section for failure time prediction; and
3. Keep reviewing its prediction until the displacement pattern is linear enough for confident prediction.

The SFPM was validated using four MSR data from unstable open cast mine slopes and the results showed the effectiveness of the programme in estimating a very reasonable time to failure. Like any other method adopted in estimating the failure time of mine slopes, the SFPM must be used in conjunction with detailed and regular visual observation of the slope. The experience of the geotechnical personnel must also not be neglected in using the model.

For the SFPM to automatically predict the time to failure once the onset of failure is reached, an interface must be created between the monitoring radar and the SFPM. At present, this is not possible because of copyright issues. Once this obstacle is removed and the interface is

created, the SFPM can be completely automated. When the onset of failure displacement is attained, prediction of the time to failure is made if prediction criteria are met. If otherwise, the programme automatically updates its prediction as new data is made available from the radar. However, since the SFPM operates automatically, it is not compulsory to pre-select the onset of failure values for commencement of prediction. The development of the SFPM makes automatic prediction of time to failure possible in real time, thereby increasing the safety and economic benefits of slope monitoring. Although the model has been developed for open-pit mines, it is equally applicable for time to failure prediction in landslides and rockfalls. The ability of the SFPM to identify the most active points from among several points, and make predictions from the active points, is a significant feature of the model. This feature will greatly enhance the performance of radar for real time monitoring.

In addition to the SFPM, another simple empirical model was developed for selecting cumulative rate of displacement threshold based on point monitoring. The model showed that the cumulative rates of displacement threshold for the all-data and 24 hour time window appears so insignificant as seen in figure 6.4, that it may allow failure to go unnoticed. The data from these two “time windows” are based on large window scan resulting in small cumulative values.

The regressive and progressive displacement regions in figure 6.4 represent the safe areas. The failure region is the unsafe section and it is expected that no personnel would be anywhere near the unstable slope when the cumulative rate of displacement lies within this region. An evacuation threshold scheduled an hour before the attainment of the failure zone was used in the model. However, evacuation threshold depends on the mine, on access and other factors and is therefore mine specific.

CHAPTER SEVEN

CONCLUSIONS AND RECOMMENDATIONS

7.1. Conclusions

The main objectives of this research work were to interpret the failure mechanisms and deformation behaviour of open-cast mine slopes and to develop a method that can reasonably estimate the time to failure of open-cast mine slopes using radar monitoring displacement data. In order to achieve these objectives, the Movement and Surveying Radar (MSR) displacement data for both stable and unstable open-cast mine slopes were collected from Anglo Coal open-cast coal mines in South Africa. In addition, the MSR displacement data from other open-cast mines were also collected from Reutech (Pty) Ltd, Stellenbosch, South Africa. The following conclusions are drawn from the research:

Radar Monitoring versus Conventional Slope Monitoring

As highlighted in chapter 3, the advantages of radar monitoring system over conventional slope monitoring system are numerous. However, as observed in this research, the most significant advantage of the radar monitoring system over conventional slope monitoring is its unprecedented capacity to:

- Monitor the full slope face and provide displacement information of every location in real time, therefore preventing any developing failure from going unobserved; and
- Track development of failure by gathering information on the magnitudes of displacement, rates of displacement and the locations of the displacement.

Conventional slope monitoring systems, on the other hand, are limited in area of coverage and provide displacement information only for a single point or at most, a few locations on the slope. Displacement information between the points is not recorded. Therefore, a developing failure between the points is not observed. Despite the benefits of the radar monitoring system, it is still underutilised. To derive maximum value from radar monitoring, a very good understanding of its safety and economic benefits to the mine personnel and the mining organisation is crucial.

Slope Failures at Anglo Coal Open Cast Coal Mines

Low-wall and high-wall instability constitutes the major area of challenge at the New Vaal coal mine. Large volume of soil overburden removed for coal extraction is the base on which other waste rock is placed. The weakening of the low-wall base and subsequent reduction of the strength of spoil material, particularly when groundwater is present, causes the low-wall to slough. High-wall failures on the soft sand overburden can also be attributed to surcharge from rain and gravity loading. At the Kleinkopje open cast mine, spontaneous combustion and removal of lateral support, or undercutting of the low-wall remains the major cause of low-wall failure. High-wall weakened by spontaneous combustion and rock fall from over-hang resulting from inaccurate blasting are the other high-wall problems. Over steepening, which was based on the assumption of a strong and stable high-wall, resulted in the only documented failure at the Schoongezicht open cast mine.

Slope Deformation and Failure Mechanisms

The process of failure development of an unstable mine slope occurs in five different stages which is classified into three pre-failure stages and two post-failure stages. The pre-failure stages consist of the regressive displacement behaviour stage, the progressive displacement behaviour stage and the onset of failure to failure stage. The post-failure stages consist of the rebound stage and the stabilisation stage. Stable slopes exhibit two types of deformation behaviour which are type I and type II deformation behaviour. Type I deformation behaviour requires a strong trigger to progress to failure while type II deformation behaviour requires a minor trigger to progress to failure. Both types of deformation behaviour will remain regressive, if the events disturbing the stability of the slope are removed. The displacement data of unstable slopes indicated the occurrence of complex and variable deformation behaviour, especially at progressive deformation stage up until the post-failure rebound stage. The occurrence of complex deformation behaviour is not restricted to the progressive stage but may commence at the regressive stage. The complex and variable deformation behaviour at different locations on the slope indicates the diverse reactions in the rock mass to deformation, specifically, the formation of multiple sliding surfaces and damage zones through shearing. It was also found that slope failure is preceded by gradual accumulation of deformation at the regressive displacement stage.

Slope Failure Prediction Model (SFPM)

The research established that variations in displacement occur at different locations on the slope. With this understanding, a prediction model that can estimate the time to failure using only the most active points on the slope was developed. The Slope Failure Prediction Model (SFPM) for predicting the time to failure of slope was developed based on the inverse velocity method developed by Fukuzono (1985). The SFPM was validated with four case examples from different mines and proved to be effective in predicting the time to failure with ample time for personnel evacuation. The model can be incorporated into any monitoring system, such as radar and survey network for automatic prediction of time to failure. The unique characteristics of the SFPM are the ability:

- To automatically detect the most active points, or sensitive moving points, among several points on the scanned mine slope;
- To make predictions using only the active points;
- To capture, within a large range of displacement data, the linear section for failure time prediction; and
- To keep reviewing its prediction until the displacement pattern is linear enough for prediction.

The development of the SFPM has made automatic prediction of time to failure possible in real time. This new capability has the potential to contribute very significantly to increasing the safety and economic benefits of slope monitoring.

Cumulative Rates of Displacement Threshold Determination Model

The cumulative rate of displacement threshold value represents the onset of failure. When the threshold value is reached, slope failure is imminent, and mine personnel and equipment must vacate the unstable area of the slope. The model for estimating the threshold value for the cumulative rate of displacement is simple and easy to use, and can be adapted for any open-cast mine where the MSR is used for slope monitoring. By simple visual inspection of the model, the evacuation threshold can be determined. At a specific cumulative rate of displacement, the displacement state of the slope can also be evaluated.

Commonly Recognised Slope Failure Mechanisms

The stability analysis of open-cast mine slopes is based on geotechnical data obtained from face mapping, oriented drill cores, structural geology, rock strength testing, and down-hole geophysics. The data thus obtained only provide information on common failure mechanisms, such as wedge failure, toppling failure and planar failure, which are structurally controlled. Structurally controlled mechanisms occur on existing structures or defects within the rock mass (Simmons and Simpson, 2006). However, Stacey, (2007), Dight (2006), Simmons and Simpson (2006) and Lucas (2006) have documented sudden and unexpected slope failures that are not structurally controlled and in areas considered safe from a stability point of view.

Based on the radar monitoring data, the research confirmed the occurrence of complex failure mechanisms, which are inconsistent with the established mechanisms. The research showed that slope failure does not always require a sliding surface to occur. Slope failure may occur through progressive damage development in the rock mass without being structurally controlled. The implication of this observation is that such slope failure will go undetected. Radar monitoring, with the capacity to monitor large sections of the slope, and provide displacement information at every point for both the unstable and stable sections in real time, will provide the solution. This capacity of radar monitoring must be utilised to identify the unstable regions of the mine slopes, which were not detected nor expected from geological and geotechnical analysis.

Concluding Remarks

Deformation behaviour of open-cast mine slopes is not always as straightforward as commonly thought. Slope deformation begins with gradual accumulation of deformation within the slope. This research has contributed to understanding slope deformation behaviour and failure mechanisms at the pre-failure, failure and post-failure stages based on displacement data from radar monitoring. The research is possibly the first attempt at interpreting deformation behaviour and failure mechanisms using radar monitoring data. The time to failure prediction model developed is reliable, user friendly and should greatly enhance the capacity of radar monitoring systems. The research has achieved the stated objectives and has answered all the research questions.

7.2. Recommendations for Further Research

The slope monitoring radar has the capacity to collect large amount of displacement data, but this data is underutilised and sometimes not properly documented by the mining companies. Concerted efforts should be made by the mine geotechnical personnel to build a robust database of slope failures at different mines. This information in the database will include, among other things, the name of the mine, the specific location of the failure, the weather conditions at failure and the mining activities at the time of failure. From this database, more validation of the cumulative rate of displacement threshold model and the Slope Failure Prediction Model should be carried out. In addition, to improve the slope monitoring quality of the MSR, further development of the SFPM for longer warning time may be necessary.

During the progressive displacement stage wherein the behaviour of the displacement pattern becomes almost linear, the time to failure of the mine slope, X, can be estimated. This can be achieved with the linear equation of the slope displacement, if the cumulative rate of displacement, Y, at failure, which is either estimated or assumed from experience, is known. However, this remains a good area for further research.

This research has demonstrated the possibility of understanding slope deformation and failure mechanisms from surface displacement data. However, combining the surface displacement data from radar monitoring with sub-surface deformation data from sub-surface monitoring, will provide additional knowledge of failure mechanisms.

References

Abramson, L. W., Lee, T.S., Sharma, S. and Boyce, G. M. (2002) Slope Stability and Stabilization Methods, 2nd ed. John Wiley & Sons, New York, 712pp.

Adhikary, D. P. and Dyskin, A. V. (2007) Modelling of Progressive and Instantaneous Failures of Foliated Rock Slope, *Journal of Rock Mechanics and Rock Engineering*, Vol. 40, no 4, pp 349-362.

Alejano, L. R, Gomez-Marquez, I. and Martinez-Alegria, R. (2010) Analysis of a Complex Toppling-Circular Slope Failure, *Journal of Engineering Geology*, Vol. 114, pp103-104

Atkinson, L. C. (2000) The Role and Mitigation of Groundwater in Slope Stability in Slope Stability in Surface Mining, W.A. Hustrulid, M.K. McCarter & D.J.A. Van Zyl (eds) Society for Mining, Metallurgy and Exploration (SME), Littleton, Colorado, pp 89-96.

Bjerrum, L. (1967) Progressive Failure in Slopes of Overconsolidated Plastic Clay and Clay Shales, *Journal of Soil Mechanics Foundation*, Vol. 93 (SM 5), pp 1-49

Brady, B. H. G. and Brown, E.T. (2006) Rock Mechanics for Underground Mining, 3rd ed. Springer, Dordrecht, 628pp.

Broadbent C.D. and Zavodni, Z.M. (1982) Influence of Rock Structures on Stability, in Stability in Surface Mining, Society of Mining Engineers, Denver, Co. Vol. 3, Ch. 2.

Burn, K.W. ed., (1988) Radar Development to 1945" Peter Peregrinus Ltd. London, 528pp.

Bye, A. (2009) GroundProbe Unique Measurement Systems, Ground Probe newsletter, available at: http://www.infomine.com/publications/docs/InternationalMining/IMOct2009b. (Accessed 8 July, 2009)

Cahill, J. and Lee, M. (2006) Ground Control at Leinster Nickel Operations, *International Symposium on Stability of Rock Slopes in Open Pit Mining and Civil Engineering, The South African Institute of Mining and Metallurgy*, Symposium Series 44, pp 321-334.

Calder, P. N. and Blackwell, G. (1980) Investigation of a Complex Rock Slope Displacement at Brenda Mines, *CIM Bulletin*, pp 73-82.

Call, R. D. (1982) Monitoring of Pit Slope Behaviour, in Stability in Surface Mining, Society of Mining Engineers, Denver, Co. Vol. 3, Ch 9

Call, R. D. and Savely J. P. (1990) Open Pit Rock Mechanics, in Surface Mining, 2nd ed. Society for Mining, Metallurgy and Exploration (SME), Littleton, Co. pp 860-882.

Call, R. D., Cicchini, P. F., Ryan, T. M. and Barkley, R.C. (2000) Managing and Analysing Overall Pit Slopes, in Slope Stability in Surface Mining, W. A. Hustrulid, M. K. McCarter & D. J. A. Van Zyl (eds), Society for Mining, Metallurgy and Exploration (SME), Littleton, Co. pp 39-46.

Campbell Scientific Inc. (1998) Time Domain Reflectometry for Measurement of Rock Deformation, Product Brochure, pp 1-6

Cawood, F. T. and Stacey, T. R. (2006) Survey and Geotechnical Slope Monitoring Considerations, *Journal of the South African Institute of Mining and Metallurgy*, Vol. 106, No. 7, pp 495-501.

Chen, Y., He, X., Ding, X. and Sang, W. (2005) Steep Slope Monitoring, Available at: www.gpsworld.com/survey, (Accessed 13 August 2012)

Coates, D. F. (1977) Design in Pit Slope Manual Report, *Canadian Centre for Mineral and Energy Technology (CANMET)*, Ottawa, Canada, 77pp.

Coates, D. F. (1981) Rock Mechanics Principles, *Canadian Centre for Mineral and Energy Technology (CANMET)*, Ottawa, Canada. 410pp.

Coggan, J. S., Stead. D., and Eyre, J. (1998) Evaluation of Techniques for Quarry Slope Stability Assessment, *Trans Institute of Mining and Metallurgy,* Section B, Applied Earth Science, 107, pp 139-147.

Cornelius, R. R. and Scott, P. A. (1993) A Materials Failure Relation of Accelerating Creep as Empirical Description of Damage Accumulation, *Journal Rock Mechanics and Rock Engineering,* Vol. 26, no 3, pp 233-252.

Crosta, G. B. and Agliardi, F. (2003) Failure Forecast for Large Rock Slides by Surface Displacement Measurements, *Canadian Geotechnical Journal,* Vol. 40, pp 176-191.

Cruden, D. M. and Masoumzadeh, S. (1987) Accelerating Creep of the Slopes of a Coal Mine, *Journal of Rock Mechanics and Rock Engineering,* Vol. 20, pp 123-135.

Deere, D. U. and Patton, F.D, (1971) Slope Stability in Residual Soils, *Fourth Pan-American Conference on Soil Mechanics and Foundation Engineering, American Society of Civil Engineers,* Vol. 1, pp 87-170.

Dight, P. M. (2006) Pit Wall Failures on "Unknown" Structures, *Journal of the South African Institute of Mining and Metallurgy,* Vol. 106, pp 451-458.

Ding, X., Montgomery, S. B. and Tsakiri, M. (1998) Integrated Monitoring Systems for Open Pit Wall Deformation, Australian Centre for Geomechanics, *MERIWA Project* Report No 186, 148pp.

Downing, C. H., Su, M. B. and O'Connor, K. M. (1989) Measurement of Rock Mass Deformation with Grouted Coaxial Antenna Cable, Rock Mechanics and Rock Engineering, Vol. 22, pp 12-22.

Eberhardt, E., Stead, D. and Coggan, J. S. (2004a) Numerical Analysis of Initiation and Progressive Failure in Natural Rock Slopes – the 1991 Randa Rockslide, *International Journal of Rock Mechanics & Mining Sciences,* Vol. 41, pp 69-87.

Eberhardt, E., Spillmann, T., Maurer, H., Willinberg, H., Loew, S and Stead, D. (2004b) The Randa Rockslide Laboratory: Establishing Brittle and Ductile Instability Mechanisms Using Numerical Modelling and Microseismicity, *9th International Symposium of Landslides, Rio de Janeiro,* pp 481-487.

El Bedoui, S., Guglielmi, Y., Lebourg, T. and Pérez, J. (2009) Deep-Seated Failure Propagation in a Fractured Rock Slope over 10,000 years: The La Clapière Slope, the South-Eastern French Alps" *Geomorphology*, Vol. 105, pp 232-238

ESG Solutions (2010) Open Pit Mine Monitoring, Available at: www.esgsolutions.com (Accessed 30 September, 2011).

Fell, R., Hungr, O., Leroueil, S. and Riemer, W. (2000) Geotechnical Engineering of the Stability of Natural Slopes, and Cuts and Fills in Soil, *Keynote Lecture at the Geotechnical Engineering Conference,* Melbourne, Australia, 100 pp.

Fukui, K. And Okubo, S. (1997) Life Expectancy and Tertiary Creep for Rock, Proceedings of the Fall Meeting of the Mining and Materials Processing Institute of Japan, pp 9-94.

Fukuzono, T. A. (1985) A New Method for Predicting the Failure Time of a Slope, *Proceedings of the Fourth International Conference and Field workshop on Landslides,* Tokyo, Japan Landslide Society, pp 145-150.

Gayer, R. A., Hathaway, T. and Davis, J. (1995) Structural Geological Factors in Open Pit Coal Mine Design, with Special Reference to Thrusting: Case Study from the Ffyndaff Sites in the South Wales Coalfield" *Geological Society London, special publications,* Vol. 82, pp 233-249.

Girard, J. M. (2001) Assessing and Monitoring Open Pit Mine High-walls, *Proceedings of the 32nd Annual Institute of Mining Health, Safety and Research,* Roanoke, VA, pp 159-171.

Girard, J. M. and McHugh, E. L. (2000) Detecting Problem with Mine Slope Stability, National institute for occupational safety and health, *NIOSHTIC-2*, No – 10006193, pp 1-2

Girard, J. M., Mayerle R. T. and McHugh, E. L (1998) Advances in Remote Sensing Techniques for Monitoring Rock Falls and Slope Failures" *Proceedings of the 17th International Conference on Ground Control in Mining, NIOSHTIC-2*, No 20000186, pp 326-331.

Glawe, U. (1991) Analysis of Failure Mechanisms for a Large Scale Slope Movement, *Master of science Thesis*, Royal School of Mines, Imperial College of Science and Technology. London 71pp.

Goldberg, W .C. and Frizzell, E. M. (1989) Pit Slope Monitoring and Back Analysis of the Berkeley Pit, *Journal of Mining Engineering*, pp 1191-1195.

Goodman, R. E. and Bray, J. W. (1976) Toppling of Rock Slopes in Rock Engineering for Foundations and Slopes, *ASCE Specialty Conference*, Boulder, Colorado, August 15-18, Vol. 2, pp 201-234

GroundProbe (2003) The Use of Slope Stability Radar (SSR) for Managing Slope Instability Hazards, Product Brochure, Available at: http://www.groundprobe.com (Accessed 5 October, 2008)

GroundProbe (2011a) Slope Stability Radar (SSR), Product Brochure, Available at: http://www.groundprobe.com /docs (Accessed 30 September, 2011)

GroundProbe (2011b) Work Area Monitoring (WAM), GroundProbe Newsletter, Available at: http://wam.groundprobe.com/whatiswam.html, (Accessed 11 May 2011)

GroundProbe (2008) Interferferometric Signal Processing, Available at:http://patents.com/us-7768442.html, (Accessed 10 September 2010)

Hamiel, Y., Liu, Y., Lyakhovsky, V., Ben-Zion, Y. and Lockner, D. (2004) A Viscoelastic Damage Model with Applications to Stable and Unstable Fracturing, *Geophysical Journal*, Vol. 159, pp 1155-1165.

Harries, N and Holmstrom, M. (2007) The Use of Slope Stability Radar in Monitoring Slopes and Managing Slope Instability Hazards, Available at: www.tmr.qld.gov.au, (Accessed 14 August, 2012).

Harries, N., Noon, D. and Rowley, K. (2006) Case Studies of Slope Stability Radar in Open Cut Mines, *International Symposium on Stability of Rock Slopes in Open Pit Mining and Civil Engineering, The South African Institute of Mining and Metallurgy*, Symposium Series 44, pp 335-342

Harrison, J. P. and Hudson, J. A. (2000) Engineering Rock Mechanics, Part 2, illustrative worked examples, Pergamon Press, Oxford, 506pp.

Hawley, M., Marisett, S., Beale, G. and Stacey, P. (2009) Performance assessment and monitoring, in guidelines for Open Pit Slope Design, Read, J. and Stacey, P. (eds), CSIRO Publishing, Collingwood, pp 327-379.

Hoek, E., Read, J., Karzulovic, A., and Chen, Z. Y. (2000) Rock Slopes in Civil and Mining Engineering, *Proceedings of the International Conference on Geotechnical and Geological Engineering*, Melbourne, 17pp.

Hoek, E. and Bray, J. W. (1981) Rock Slope Engineering, Revised 3rd ed, Institute of Mining & Metallurgy, 308pp.

Hoek, E., Rippere, K. H. and Stacey, P. F. (2000) Large-Scale Slope Designs – A Review of the State of the Art, in Slope Stability in Surface Mining, W.A. Hustrulid, M.K. McCarter & D.J.A. Van Zyl, (eds), Society for Mining, Metallurgy and Exploration (SME), Littleton, Co. pp 3-10.

Hunter, G. (2007) Mapping with 3D Lasers, Available at: www.eepublishers.co.za, (Accessed 11 January, 2010)

Jaeger, J. C. and Cook, N.G.W. (1979) Fundamentals of Rock Mechanics, 3rd ed. Chapman and Hall, London, 593pp

Ingegneria Dei Sistemi (2011) IDS – Radar for Mining Applications, Available at: www.mining-technology.com/contractors/exploration/idsingegneria (Accessed 05 October, 2011)

Integrated Seismic Systems. (2007) Micro-seismic Monitoring of Slopes" Available at **www.issi.co.za/Y27/apps27/openpit.htm** (Accessed 30 September, 2011)

Joubert, A. (5 April 2011) Slope Monitoring with the Movement and Surveying Radar (MSR), *Unpublished Letter to K. S. Osasan*

Kane, W. F. and Beck, T. J. (1999) Advances in Slope Instrumentation: TDR and Remote Data Acquisition Systems, *Proceedings at the 5th International Symposium on Field Measurements in Geomechanics,* Singapore, pp 101-105

Kane W. F. (1998) Time Domain Reflectometry, KANE GeoTech, Inc. Available at: ourworld.compuserve.com/homepages/wkane/tdr.htm (Accessed 3 March 2009)

Kane, W. F and Beck, T. J. (1998) Instrumentation Practice for Slope Monitoring, *Journal of Engineering Geology Practice in Northern California*, Available at: www.iti.northwestern.edu/tdr, (Accessed 15 August 2012)

Kane, W. F. and Beck, T. J. (1994) Development of a Time Domain Reflectometry System to Monitor Landslide Activity, *Proceedings of the 45th Highway Geology Symposium*, Portland, Oregon, pp 163-173.

Kane, W. F. and Beck, T. J. (1996a) Rapid Slope Monitoring in Civil Engineering, American Society of Civil Engineers, New York, 666, pp 55-58.

Kane, W.F. and Beck, T. J. (1996b) An Alternative Monitoring System for Unstable Slope, *Geotechnical News*, 143, pp 24-26

Kasmer, O., Ulusay, R. and Gokceoglu, C. (2006) Stability of Spoil Piles at Two Coal Mines in Turkey, Geotechnical Characterization and Design Considerations, *Journal of Environmental and Engineering Geosciences*, Vol. 12, no 4, pp 337-352.

Kayesa, G. (2006) Prediction of Slope Failure at Letlhakane Mine with the Geomos Slope Monitoring System, *International Symposium on Stability of Rock Slopes in Open Pit Mining and Civil Engineering Situations.* S44, pp 606-607.

Kelso, I. J. (2011) High-wall Slope Stabilisation by the Soft wall Method, *Proceedings, Slope Stability 2011, International Symposium on Rock Slope Stability in Open Pit Mining and Civil Engineering,* Vancouver, Canada, pp N/A

Kemeny, J. (2003) The Time-dependent Reduction of Sliding Cohesion Due to Rock Bridges along Discontinuities: A Fracture Mechanisms Approach, *Journal of Rock Mechanics and Rock Engineering*, Vol. 36, pp 27-38.

Kennedy, B. A. and Niermeyer, K. E. (1970) Slope Monitoring Systems used in the Prediction of a Major Slope Failure at the Chuquicamata Mine, Chile, In Planning Open Pit Mines, P. W. J. Van Rensburg (ed), The South Africa Institute of Mining and Metallurgy, Bakema, pp 215-225.

Kleinkopje Colliery (2009) Business plan and Four Year Forecast C2010 – C2013, Section 6.1 – 6.4, Section 7.1 – 7.5.

Kliche, C. (1999) Rock Slope Stability, Society for Mining, Metallurgy and Exploration, Inc, Colorado, 253pp.

Lajtai, E.Z. and Bielus, L.P. (1986) Stress corrosion cracking of Lac du Bonnet granite in Tension and Compression, *Journal of Rock Mechanics & Rock Engineering*, Vol.19, pp 71-87.

Lajtai, E.Z. and Schmidtke, R.H. (1986) Delayed Failure in Rock Loaded in Uniaxial Compression, *Journal of Rock Mechanics & Rock Engineering,* Vol. 19, pp 11-25.

Landau Colliery (2009) Business Plan and Five Year Forecast C2010 – C2013, Section 5.1 – 6.1.

Little, M.J. (2006a) Slope Monitoring Strategy at PPRust Open Pit Operations, *International Symposium on Stability of Rock Slopes in Open Pit Mining and Civil Engineering, The South African Institute of Mining and Metallurgy*, Symposium Series 44, pp 211-230.

Little, M.J. (2006b) The Benefit to Open Pit Rock Slope Design of Geotechnical Databases, *International Symposium on Stability of Rock Slopes in Open Pit Mining and Civil Engineering, The South African Institute of Mining and Metallurgy,* Symposium Series 44, pp 97-116.

Lorig, L., Stacey, P. and Read, J. (2009) Slope Design Methods, in Guidelines for Open Pit Slope Design, J. Read and P. Stacey (eds), CSIRO Publishing, pp 237-364.

Lucas, D. (2006) Stress Failure of a Shallow Open Cut Mine, *Australian Centre for Geomechanics, Newsletter,* Vol. 27, pp 4-6.

Ma, E., Chen, Y., and Ding, X. (2007) Monitoring of Slope Stability by Using Global Positioning System (GPS), Available at: http://plan.geomatics.ucalgary.ca, (Accessed 14 August, 2012)

Mandzic, E. H. (1992) Mine Water Risk in Open Pit Slope Stability, *International Journal of Mine Water,* Vol. 11, No 4, pp 35-42.

Martin, C. D and Kaiser, P. K. (1984) Analysis of Rock Slopes with Internal Dilation, *Canadian Geotechnical Journal,* Vol. 21, No 4, pp 605-620

Martin, D.C. (1993) Time Dependent Deformation of Rock Slopes, *Unpublished PhD Thesis,* University of London, August, 1993.

McHugh, E. L., Jami, D., Long, D.G. and Sabine, C. (2006) Application of Ground-Based Radar to Mine Slope Monitoring, *National Institute for Occupational Safety and Health*, Investigation Report 9666, 86pp.

Mencl, V. (1966) Mechanics of Landslides with Non-circular Slip Surfaces with Special Reference to the Vaiont Slide, *Geotechnique*, Vol. 16 No 4, pp 329-337

Mercer, K. G. (2006) Investigation into the Time Dependent Deformation Behaviour and Failure Mechanisms of Unsupported Rock S lopes Based on the Interpretation of Observed Deformation Behaviour, *Unpublished PhD Thesis*, University of the Witwatersrand, Johannesburg, South Africa.

Meriam, J. L. (1980) Engineering Mechanisms, Static and Dynamic, John Wiley & Sons, New York, pp 2-3.

Montgomery, D. C., Peck, E. A., Vining, G. G. (2012) Introduction to Linear Regression, 5th ed. John Wiley & Sons, New Jersey, 642pp.

Mottie, G. (2008) Radar Flash, *Internal Report on Slope Monitoring at Klienkopje Open Cast Colliery*, Anglocoal, South Africa, pp 1-2.

Mufundirwa, A. Fujii, Y and Kodama, J (2010) A New Practical Method for Prediction of Geomechanical Failure-Time, *International Journal of Rock Mechanics and Mining Sciences*, Vol. 47, pp 1079-1090.

NASA. (2011) Glaciers and Ice Sheets in a Challenging Climate, Available at: http://www-radar.jpl.nasa.gov/glacier/ (Accessed 14 September, 2011)

New Vaal Colliery (2009a) Business plan and Two Year Forecast C2010 – C2012, Section 6.1, Section 4.2 and Section 5.1.

New Vaal Colliery (2009b) High-wall and Low-wall Monitoring Using the Radar, *Unpublished Report*, pp 2-3

Noon, D., Bellett, P. and Campbell, L. (2011) A New and Easy-to-Use Slope Radar Tool for Mine Production Crews, *Proceedings, Slope Stability 2011, International Symposium on Rock Slope Stability in Open Pit Mining and Civil Engineering,* Vancouver, Canada, pp N/A

Okagbue, C. O. (1987) Stability of Waste Rock Spoils in an Area Strip Mine – Geological and Geotechnical Considerations, *Journal of Earth Surface Processes and Landforms*, Vol. 12, pp 289-300.

Pavlovic, E. (1998) Principles of Numerical Modelling of Jointed Rock Mass, *Proceedings of the Third International Conference on Mechanics of Jointed and Faulted Rock,* H. Rossmanith (ed), MJFR-3/Vienna/Austria, pp 311-316.

Peltzer, G. (2010) Crustal Deformation Studies Using SAR Interferometry, Available at: http://www.radar.jpl.nasa-gov/insar4crust/ (Accessed 10 April 2010).

Petley, D. N., Mantovani, F., Bulmer, M. H. and Zamnnoni, A. (2005) The Use of Surface Monitoring Data for the Interpretation of Landslide Movement Patterns, *Geomorphology*, Vol. 66, pp 133-147.

Piteau, D. R. and Martin, D. C. (1982) Mechanics of Slope Failure, *Proceeding of the Third International Conference on Stability in Surface Mining*, C.O. Brawner (ed), AIME, Vancouver, pp 113-169.

Radbruch-Hall, D. H. (1978) Gravitational Creep of Rock Masses, B. Voight (ed) *Rockslides and Avalanches, 1,* Developments in Geotechnical Engineering, 14A, Elsevier, pp 607-657.

Reeves, B., Noon, D., Stickley, G. and Longstaff, D. (1997) Monitoring Rock Slope Deformation by Radar Interferometry, *Proceedings of the Workshop on Applications of Radio Science WARS'97,* A. Kulessa Edition, Australian Academy of Science, pp 119-123.

Reutech (2006a) Slope Monitoring, New Radar System Provides Accurate Slope Survey, Reutech Newsletter, Available at: http://www.rrs.co.za/news/MSR200serieslaunched.asp (Accessed 20 November 2008)

Reutech (2006b) MSR 300 Product Brochure, pp 15-16.

Reutech (2008) Movement and Surveying Radar Newsletter, Available at: http://www.rrs.co.za/news/documents/MSRNewsletter.pdf (Accessed 4 April 2009)

Reutech (2009) Slope Monitoring with the Movement and Surveying Radar (MSR), *personal communication with K. S. Osasan.*

Reutech (2011): Movement and Surveying Radar, Product Brochure, Available at: http://www.reutechmining.com/products/movement-surveying.htm (Accessed 30 September, 2011)

Rose, N. D. and Hungr, O. (2007) Forecasting Potential Rock Slope Failure in Open Pit Mines Using the Inverse-Velocity Method, *International Journal of Rock Mechanics and Mining Sciences,* Vol. 44, pp 308-320

Ryan, T. M., and Call, R. D. (1992) Applications of Rock Mass Monitoring for Stability Assessment of Pit Slope Failure, *Proceedings of the 33rd US Rock Mechanics Symposium,* Tillerson & Wawersik (eds) Santa Fe, New Mexico, Balkema, Rotterdam, pp 221-229.

Saito, M. and Uezawa, H. (1961) Failure of Soil due to Creep, *Proceedings of the 5th International Conference on Soil Mechanics and Foundation Engineering,* Vol. 1, pp 315-318.

Seegmiller, B. L. (2000) Coal Mine High-wall Stability, in Slope Stability in Surface Mining, W.A. Hustrulid, M.K. McCarter & D.J.A. Van Zyl (eds), Society for Mining, Metallurgy and Exploration (SME), Littleton, Co. pp 257-264.

Severin, J., Eberhardt, E., Leoni, L. and Fortin, S. (2011) Use of Ground Base Synthetic Aperture Radar to Investigate the Complex 3-D Kinematics of a Large Open Pit Slope, *Proceeding of the 12th International Congress on Rock Mechanics, Beijing,* Q, Qian and Y, Zhou (eds), Balkema, CRC, pp 730-731.

Shakesby, R. A. and Whitlow, J. R. (1991) Failure of a Mine Waste Dump in Zimbabwe: Causes and Consequences, *Environmental Geology and Water Science*, Vol. 18, No 2, pp 143-153

Sijing, W. (1981) On the Mechanism and Process of Slope Deformation in an Open Pit Mine, *Rock Mechanics*, Vol. 13, pp 145-156

Simmons, J. V. and Simpson, P. J. (2006) Composite Failure in Coal Measures, Rock Masses – Myths and Reality, *Journal of the Southern African Institute of Mining and Metallurgy*, Vol. 106, No 7, pp 459-669.

Singhroy, V. and Molch, K. (2004) Characterizing and Monitoring Rockslides from SAR Techniques, *Advances in Space and Research*, Vol. 33, pp 290-295.

Sjoberg, J. (2000) Failure Mechanisms for High Slopes in Hard Rock, in Slope Stability in Surface Mining, W.A. Hustrulid, M.K. McCarter & D.J.A. Van Zyl (eds), Society for Mining, Metallurgy and Exploration (SME), Littleton, Co. pp 71-79.

Sjoberg, J. (1996) Large Scale Stability in Open Pit Mining- A Review, *Technical Report*, Division of Rock Mechanics, Lulea University of Technology, Lulea, Sweden, 229 pp, pp 16-17.

Skolnik, M. (1990) Radar Handbook, 2nd Edition, New York, McGraw-Hill Inc. 1328pp

Stacey, P. (2009) Fundamentals of Slope Design, in guidelines for Open Pit Slope Design, Read, J. and Stacey, P. (eds), CSIRO Publishing, Collingwood, pp 1-14.

Stacey, T. R. (2007) Slope Stability in High Stress and Hard Rock Conditions, Keynote Address, *Proceedings of the International Symposium on Rock Slope Stability in Open Pit Mining and Civil Engineering*, Perth, Australia, Australian Centre for Geomechanics, pp 187-200.

Stacey, T. R. (2006) Considerations of Failure Mechanisms Associated with Rock Slope Instability and Consequences for Stability Analysis, *Journal of the South African Institute of Mining and Metallurgy*, Vol. 106, pp 485-493.

Stacey, T. R., Terbrugge, P. J., Keyter, G. J. and Xianbin, Y. (2003) A New Concept in Open Pit Slope Stability, and its Use in the Explanation of Two Slope Failures, *Proceedings of the Fifth Large Open Pit Mining Conference*, Kalgoorlie, Australia, pp 259-265.

Stead, D., Eberhardht., E. and Coggan, J. S. (2006) Developments in the Characterization of Complex Rock Slope Deformation and Failure Using Numerical Modelling Techniques, *Journal of Engineering geology*, Vol. 83, pp 217-235.

Stewart, D. H. and Reid, G. J. (1988) Geotechnical Pot-pourri, *CIM Bulletin*, pp 77-83

Ulusay, R., Gokceoglu, C., Sonmez, H. and Tuncay, E. (2001) Causes, Mechanism and Environmental Impacts of Instabilities at Himmetoglu Coal Mine and Possible Remedial Measures, *Environmental Geology*, Vol. 40 (6), pp 769-786.

University of Queensland (2002) Slope Stability Radar Goes Commercial, On-line news, University of Queensland, Australia, News Release, Available at: http://www.uq.edu.au/news/index (Accessed 4 February 2009).

Varnes, D.J. (1978) Slope Movement Types and Processes in Landslide, Analysis and Control, Transportation Research Board, Commission on Sociotechnical Systems, National Academy of Sciences, Washington D.C. Special Report 176.

Varnes, D. J. (1982) Time-deformation relations in creep to failure of earth materials, *Proceedings of the Seventh Southeast Asian Geotechnical Conference*, Hong Kong, Vol. 2, pp 107-130.

Vaziri, A., Moore, L. and Ali, H. (2010) Monitoring Systems for Warning Impending Failures in Slopes and Open Pit Mines, *Journal of Natural Hazards*, Vol. 55, No 2, pp 501-512.

Voight, B. (1988) A Method for prediction of Volcanic Eruptions, *Nature International Weekly Journal* Vol. 332, pp 125-130

Vyazmensky, A., Stead, D., Elmo, D. and Moss, A. (2010) Numerical Analysis of Block Caving-Induced Instability in Large Open Pit Slopes: A Finite Element/Discrete Element Approach, *Journal of Rock Mechanics and Rock Engineering*, Vol. 43, pp 21-39.

Wessels, S. D. N. and Naismith, W. A. (2005) Management of a Major Slope Failure at Nchanga Open Pit, Chingola, Zambia, *Proceedings of the Third Southern African Conference on Base Metals*, pp 391-406.

Wesseloo, J. and Dight, P. M. (2009) Rock Mass Damage in Hard Rock Open Pit Mine Slopes, *International Symposium on Rock Slope Stability in Open Pit and Civil Engineering*, Santiago, Chile, pp N/A.

Williams, P., Floyd, J., Chitombo, G. and Maton, T. (2009) Design Impementation, in Guidelines for Open Pit Slope Design, J. Read and P. Stacey (eds), CSIRO Publishing, pp 265-326.

Wyllie, D. C. and Mah, C. W. (2004) Rock Slope Engineering, Civil and Mining, 4th Edition, Spon Press, New York, 431 pp.

Xu, N., Tang, C., Li, H., Li, L., Ma, K., Shao, J. and Wu, J. (2011) Excavation-Induced Microseismicity: Microseismic Monitoring and Numerical Simulation, *Journal of Zhejiang University – Science*, Available at: www.zju.edu.cn/jzus/openiptxt.php (Accessed 30 September, 2011)

Yang, D. Y., Brouwer, K. J., Sheets, R. J., St. Louis, R. M. and Douglas, S. J. (2011) Large-Scale Slope Instability at the Gold Quarry Mine, Nevada, *Proceedings, Slope Stability 2011, International Symposium on Rock Slope Stability in Open Pit Mining and Civil Engineering,* Vancouver, Canada, pp N/A

Zavodni, Z. M. (2000) Time Dependent Movements of Open-Pit Slopes, in Slope Stability in Surface Mining, W.A. Hustrulid, M.K. McCarter & D.J.A. Van Zyl (eds), Society for Mining, Metallurgy and Exploration (SME), Littleton, Co. pp 81-87.

Zavodni, Z. M. and Broadbent, C.D. (1980) Slope Failure Kinematics, *Canadian Institute of Mining (CIM) Bulletin,* Vol. 73, pp 69-74.

Zhang, Q.,Wang, L., Zhang, X. Y., Huang, G. W., Ding, X. L., Dai, W. J. and Yang W. T. (2008) Application of Multi-Antenna GPS Technique in the stability Monitoring of Roadside Slopes. Landslide and Engineered Slopes, From Past to the Future, *Proceedings, 10th International Symposium on Landslides and Engineered Slopes,* Xi'an, China, pp 1367-1372.

Zindela, P. (2008) Movement and Surveying Radar (MSR) Applications at Anglo Coal New Vaal Colliery, *Anglo American Mining Conference 2008,* Session 11, Paper 37, pp 549-566

APPENDICES

APPENDIX 1

Kleinkopje Open-cast Coal Mine



Figure 1.1: Sinkhole resulting from old underground workings at Kleinkopje open-cast coal mine.



Figure 1.2: Stable high-wall found in 5 West pit at Kleinkopje open-cast coal mine.

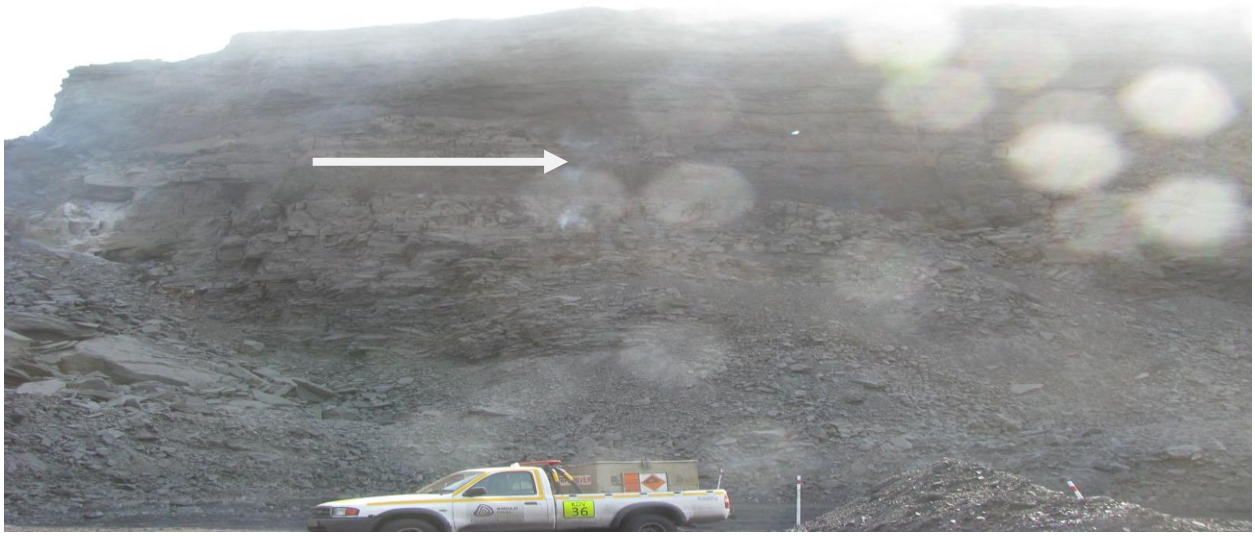


Figure 1.3: Highly fractured high-wall found in 2A pit at Kleinkopje open-cast coal mine.



Figure 1.4: Burning low-wall from spontaneous combustion at Kleinkopje open-cast coal mine.



Figure 1.5: Failed low-wall resulting from undercutting at Kleinkopje open-cast coal mine.

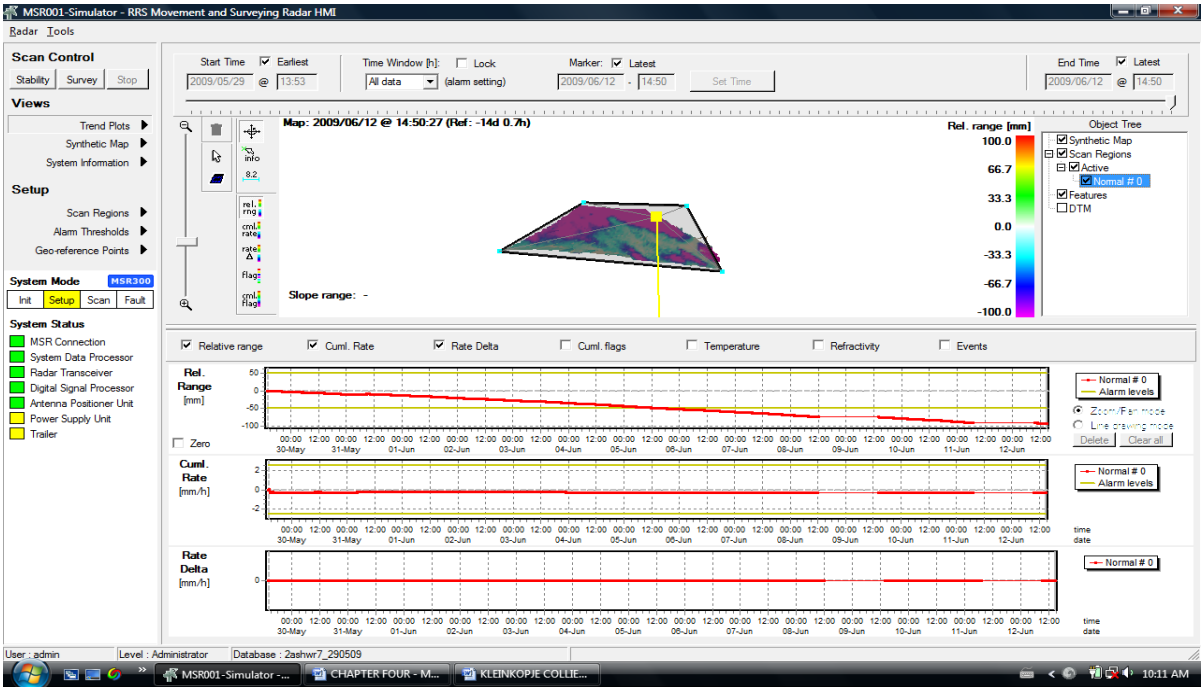


Figure 1.6: Typical print screen of monitored slope from the MSR.

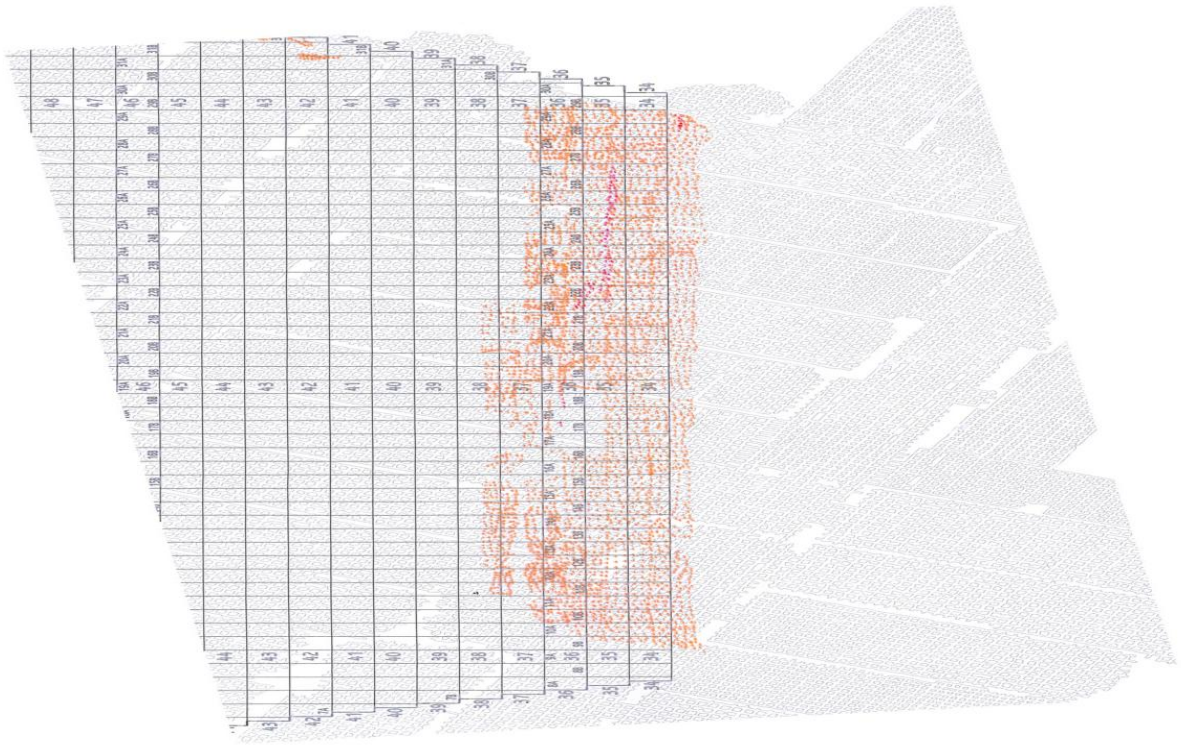


Figure 1.7: Plan of the old underground bord and pillar on number 2 seam in 2A Block.

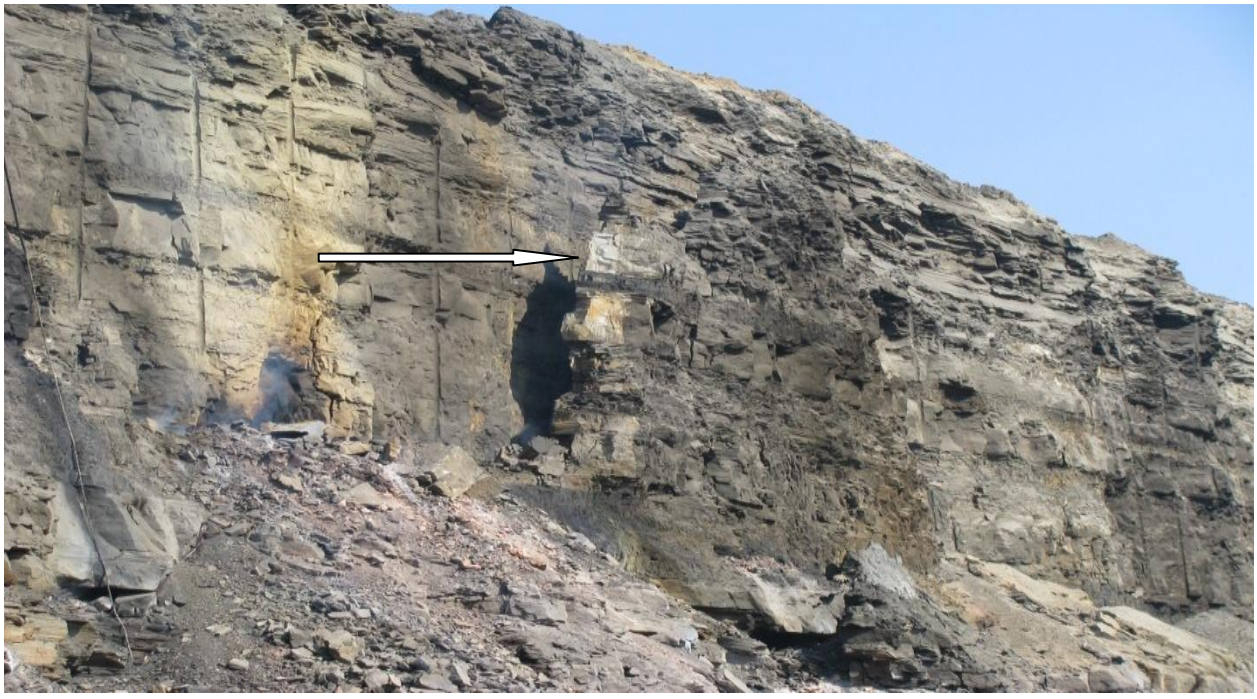


Figure 1.8: Dangerous overhang on high-wall at Kleinkopje open-cast coal mine.



Figure 1.9: Burning high-wall resulting from spontaneous combustion at Kleinkopje open-cast coal mine.



Figure 1.10: Burnt high-wall weakened by spontaneous combustion at Kleinkopje open-cast coal mine.

APPENDIX 2

New Vaal Open-cast Coal Mine



Figure 2.1: Stripping of heavy sand overburden at New Vaal coal mine

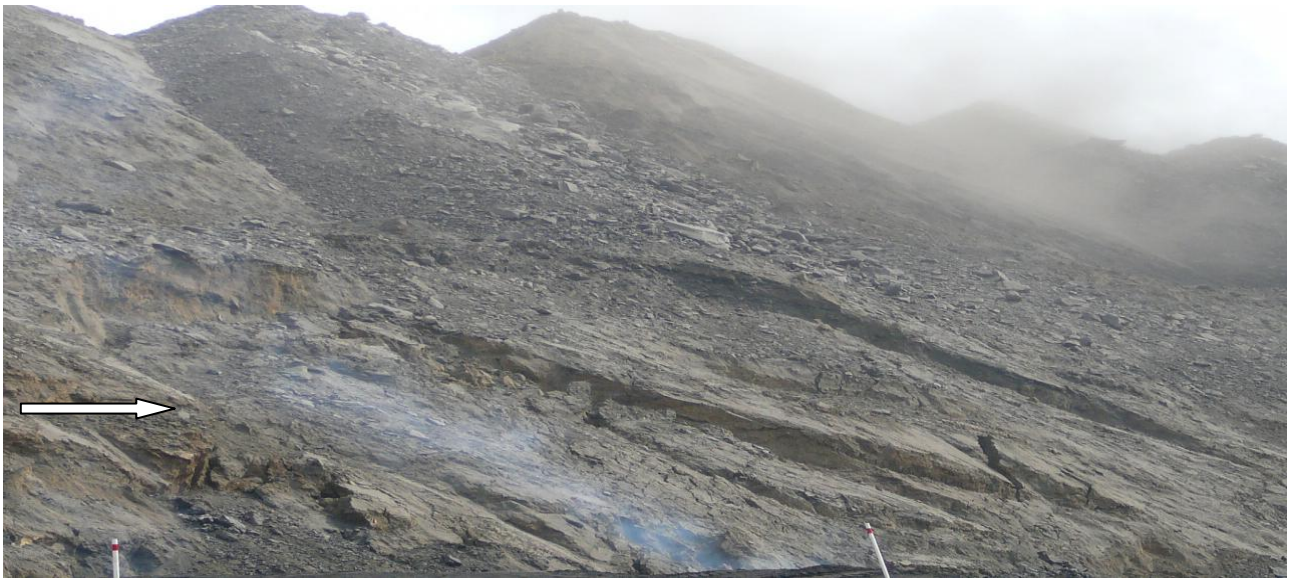


Figure 2.2: Roational failure on low-wall (spoil) at New Vaal Open-cast coal mine.

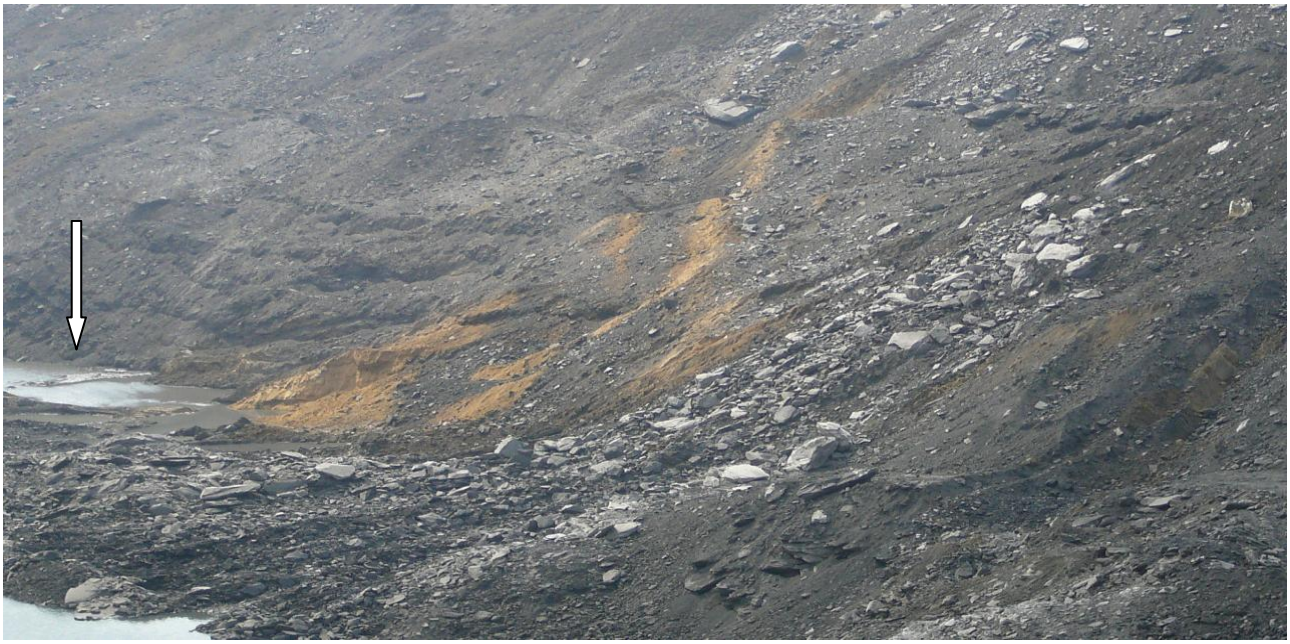


Figure 2.3: Pool of mine water beneath the low-wall at New Vaal Open-cast coal mine.

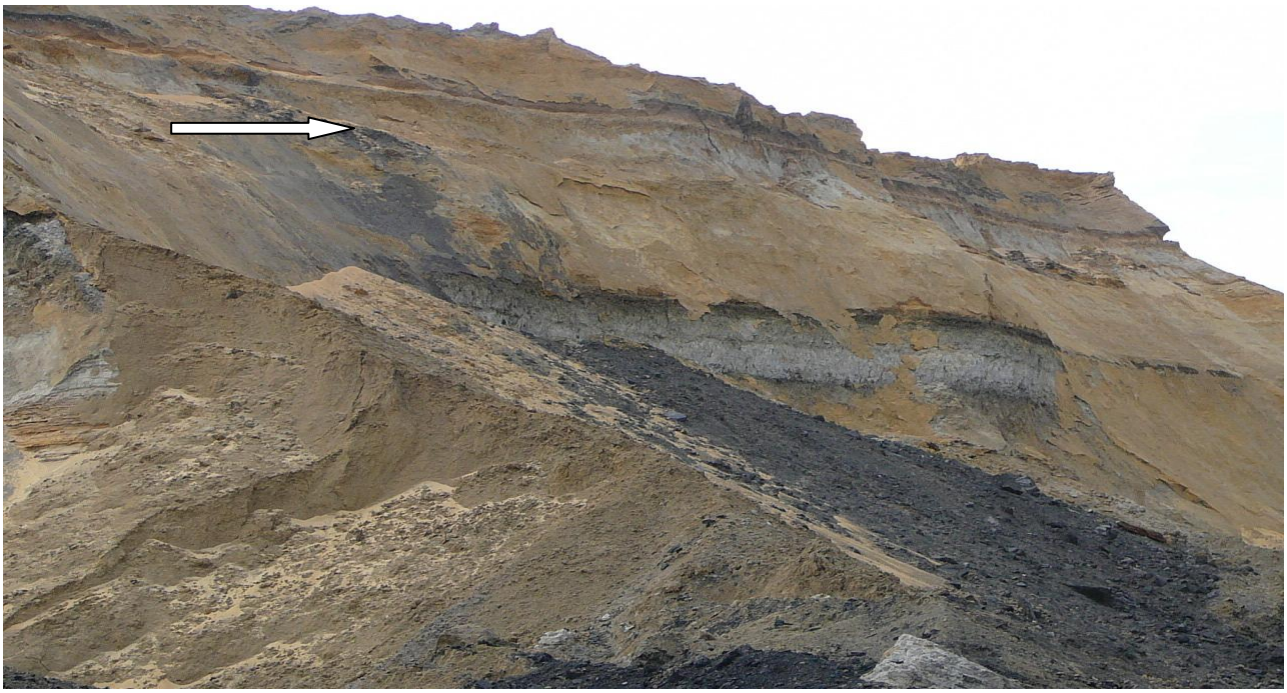


Figure 2.4: Unstable sand overburden at New Vaal Open-cast coal mine.



Figure 2.5: Typical MSR homepage.

APPENDIX 3

Mine Slope Displacement Records Used for Validation Tests

Appendix 3.1: Slope Displacement Data for Validation Test 1 (Copper Mine)

Date Time	P1	P2	P3	P4	P5	P6	P7	P8	P9	P10
8/5/2008 2:02	-4.9346	-16.5396	-8.6987	-8.0939	-10.4215	-7.1163	-8.0597	-7.8007	-6.2652	-1.0806
8/5/2008 2:06	-5.2759	-16.7734	-8.8613	-8.3648	-10.5222	-7.3391	-8.1153	-7.8226	-6.6699	-1.5603
8/5/2008 2:10	-4.9746	-16.5838	-9.1159	-7.5352	-10.1567	-6.9203	-7.7523	-7.4314	-6.3438	-1.2015
8/5/2008 2:14	-5.0065	-16.8191	-9.1741	-8.3521	-10.3956	-7.2242	-8.0984	-7.9797	-6.682	-1.5833
8/5/2008 2:18	-5.3059	-17.0736	-9.5076	-9.0137	-10.8846	-8.0262	-8.7243	-8.674	-7.1172	-2.1485
8/5/2008 2:22	-5.5219	-17.1798	-9.5191	-8.6809	-10.8394	-7.5639	-8.319	-7.9798	-6.8633	-1.8193
8/5/2008 2:26	-4.7667	-16.3377	-9.459	-7.4957	-10.1413	-6.706	-7.7721	-7.5772	-6.2471	-1.3097
8/5/2008 2:30	-5.5591	-17.7131	-10.2141	-9.268	-11.061	-8.1746	-8.6134	-8.5722	-6.9614	-1.9898
8/5/2008 2:34	-5.1768	-17.2956	-9.9274	-8.8088	-10.903	-7.5719	-7.9664	-7.8633	-6.6679	-1.7016
8/5/2008 2:38	-5.0173	-17.1786	-10.1202	-9.039	-11.0935	-7.7809	-8.3128	-8.1189	-7.0312	-1.9735
8/5/2008 2:42	-4.8468	-16.8279	-10.0234	-8.4287	-10.7912	-7.2853	-8.3813	-8.5258	-6.8313	-2.135
8/5/2008 2:46	-4.9526	-17.3658	-10.3349	-9.0456	-11.3102	-8.24	-8.4777	-8.6512	-6.7972	-1.9418
8/5/2008 2:50	-5.0436	-16.8409	-10.0197	-8.4686	-10.9316	-7.3588	-8.0544	-8.1138	-6.4747	-1.7691
8/5/2008 2:54	-4.8427	-16.6233	-9.8248	-8.1563	-10.5025	-7.2149	-8.0302	-7.8628	-6.4081	-1.5412
8/5/2008 2:58	-4.6204	-16.0991	-9.6395	-7.686	-10.2409	-6.9299	-7.7908	-7.575	-6.5853	-1.7722
8/5/2008 3:02	-3.9284	-15.5084	-8.954	-6.7126	-9.4031	-5.9087	-7.5773	-6.7573	-6.009	-1.1342
8/5/2008 3:06	-4.9251	-16.76	-9.5249	-8.2212	-9.9982	-7.03	-8.0821	-7.7876	-6.5085	-1.6617
8/5/2008 3:10	-5.4502	-17.7403	-10.1443	-9.4445	-10.4676	-7.8477	-8.7713	-8.8074	-7.1433	-2.244
8/5/2008 3:14	-4.4103	-16.0938	-9.1894	-7.3753	-9.7577	-6.7476	-8.0468	-7.9026	-6.4848	-1.4875
8/5/2008 3:18	-4.3762	-16.491	-9.1686	-7.4222	-9.7817	-6.8621	-8.113	-8.0171	-6.3453	-1.347
8/5/2008 3:22	-5.3697	-17.4114	-9.6677	-9.3183	-10.308	-7.9333	-8.7034	-8.8945	-6.9909	-2.0879
8/5/2008 3:26	-5.3666	-17.6749	-9.9424	-9.2401	-10.4919	-7.8553	-8.6891	-9.0335	-7.729	-2.5712
8/5/2008 3:30	-5.7438	-18.0808	-10.2232	-9.9984	-10.7548	-8.7983	-8.9865	-9.3642	-7.6396	-2.4947
8/5/2008 3:34	-5.2403	-17.5685	-9.9607	-9.1529	-10.6735	-8.0515	-8.9492	-9.0454	-7.5711	-2.4237
8/5/2008 3:38	-5.3402	-17.682	-9.9232	-9.2098	-10.6107	-8.0715	-9.241	-9.3856	-7.5676	-2.2814
8/5/2008 3:42	-5.3495	-17.7024	-9.877	-9.5767	-10.4411	-7.8366	-8.8596	-8.8863	-7.441	-2.4745
8/5/2008 3:46	-4.9555	-17.1472	-9.3386	-8.9256	-10.3945	-7.7514	-8.6322	-8.6317	-7.1978	-2.2133
8/5/2008 3:50	-4.4865	-16.6399	-8.9046	-8.3122	-10.1671	-7.3518	-8.6123	-8.4512	-7.0224	-1.9914
8/5/2008 3:54	-4.4531	-16.4767	-8.5055	-7.7974	-9.6468	-6.7028	-8.127	-7.7509	-6.8389	-1.8036
8/5/2008 3:58	-4.4778	-16.6462	-8.7782	-8.0264	-9.7415	-6.7927	-8.3177	-8.1161	-7.1071	-2.3404
8/5/2008 4:02	-4.626	-16.9849	-8.8551	-8.3368	-9.7184	-6.8962	-8.041	-7.7902	-6.701	-1.7093
8/5/2008 4:07	-4.7499	-17.39	-9.5715	-9.3119	-10.3257	-8.3005	-9.1591	-9.2903	-7.5287	-2.4325
8/5/2008 4:11	-5.1679	-17.8953	-10.0881	-9.7656	-10.6585	-8.4744	-9.6128	-9.8495	-8.0915	-3.0179
8/5/2008 4:15	-5.4877	-17.9386	-10.4386	-10.4296	-10.9227	-8.7205	-9.9023	-9.922	-8.1525	-3.0522
8/5/2008 4:19	-5.4309	-18.1846	-10.6676	-10.4524	-10.8857	-8.5885	-9.5597	-9.7392	-8.0517	-3.1894
8/5/2008 4:23	-5.7537	-18.2921	-10.4987	-10.0997	-10.9535	-8.8986	-9.9225	-10.1219	-7.8885	-3.098
8/5/2008 4:27	-5.6847	-17.6934	-10.1192	-9.7872	-10.6343	-8.1751	-9.4538	-9.4771	-7.7308	-2.8381
8/5/2008 4:31	-5.6899	-18.4413	-10.3583	-10.0291	-11.0696	-8.7641	-9.803	-9.8789	-7.7926	-2.9488

8/5/2008 4:35	-5.7384	-18.2536	-10.2396	-9.8848	-10.7372	-8.6167	-9.7394	-9.9391	-7.9402	-2.9732
8/5/2008 4:39	-4.7998	-17.0907	-9.7683	-8.8207	-9.0302	-7.2677	-9.0687	-9.0455	-7.1189	-2.2442
8/5/2008 4:43	-4.8111	-17.0333	-9.9402	-8.7946	-9.3009	-7.3974	-9.0089	-9.1819	-7.3377	-2.7702
8/5/2008 4:47	-4.7068	-17.379	-10.2062	-9.3645	-9.7441	-8.3076	-9.3142	-9.5595	-7.6512	-2.7572
8/5/2008 4:51	-5.232	-17.9419	-10.2606	-9.4011	-9.7771	-8.1521	-9.1356	-9.4025	-7.5328	-2.9352
8/5/2008 4:55	-4.6201	-17.6137	-10.1572	-9.4829	-9.6042	-8.2377	-8.8175	-8.9046	-7.1977	-2.5694
8/5/2008 4:59	-4.3274	-17.2387	-10.1196	-9.4121	-9.5235	-7.8108	-8.842	-8.8624	-7.272	-2.5699
8/5/2008 5:03	-5.1234	-17.6048	-10.2406	-9.8804	-9.5499	-8.1768	-8.9592	-9.062	-7.3927	-2.6144
8/5/2008 5:08	-4.7308	-17.3397	-9.8889	-9.0478	-9.1199	-7.5031	-8.4099	-8.5294	-7.0371	-2.3673
8/5/2008 5:12	-4.8334	-17.5742	-10.0715	-9.2118	-9.5064	-7.8436	-8.7699	-9.0284	-7.2059	-2.5525
8/5/2008 5:16	-4.6972	-17.5828	-9.9578	-8.559	-9.3169	-7.6043	-8.9624	-9.3336	-7.257	-2.8455
8/5/2008 5:20	-5.0532	-17.9209	-10.3509	-9.79	-9.6332	-8.191	-9.0603	-9.284	-7.3251	-3.0182
8/5/2008 5:24	-5.1242	-17.9112	-10.3886	-9.9322	-9.5617	-8.4752	-8.9609	-9.0864	-7.1292	-2.8614
8/5/2008 5:28	-4.4966	-17.2604	-10.0928	-8.9615	-8.793	-7.6211	-9.1588	-9.0815	-7.2415	-2.6864
8/5/2008 5:32	-4.2557	-16.7181	-9.8463	-8.4658	-8.7659	-7.2019	-8.6851	-8.8608	-7.0233	-2.4707
8/5/2008 5:36	-4.0581	-16.5606	-9.6735	-8.0742	-8.1745	-7.0435	-8.6331	-8.913	-7.4893	-2.5976
8/5/2008 5:40	-4.5832	-18.0591	-10.7248	-9.8846	-8.8726	-8.4997	-9.5401	-9.8612	-7.7311	-3.3384
8/5/2008 5:44	-4.3925	-17.5787	-10.514	-9.6122	-9.9894	-7.9237	-9.1688	-9.5597	-7.7107	-3.3289
8/5/2008 5:48	-5.0225	-18.3541	-11.1317	-10.6203	-10.7731	-9.0413	-9.9524	-10.5033	-8.2303	-3.7248
8/5/2008 5:52	-4.8827	-18.832	-11.0265	-10.7903	-10.9731	-9.6246	-10.2704	-10.7739	-8.4616	-4.0922
8/5/2008 5:56	-5.1468	-18.4573	-10.9486	-10.6702	-10.7082	-9.2518	-10.1344	-10.7274	-8.3589	-3.9463
8/5/2008 6:00	-4.9099	-18.3368	-10.9074	-10.6963	-10.6221	-9.0766	-9.8131	-10.6289	-8.5244	-3.9689
8/5/2008 6:04	-5.2523	-18.8585	-10.9523	-11.2035	-10.8116	-9.1441	-10.2143	-10.8312	-8.3353	-4.265
8/5/2008 6:08	-5.283	-18.8289	-11.1229	-11.404	-11.0425	-9.6038	-10.4837	-11.1752	-8.719	-4.2051
8/5/2008 6:12	-5.5112	-19.0477	-11.0336	-11.4815	-11.1326	-10.0549	-10.6835	-11.3802	-8.8405	-4.3159
8/5/2008 6:16	-5.0335	-18.529	-10.7228	-10.6002	-10.4191	-8.8678	-10.1014	-10.71	-8.0729	-3.9357
8/5/2008 6:20	-5.4077	-18.9606	-11.2461	-11.3078	-11.419	-9.9591	-10.7849	-11.4825	-8.7709	-4.7746
8/5/2008 6:24	-5.8608	-19.4757	-11.884	-12.0828	-11.3592	-10.5308	-11.0249	-11.7178	-9.3306	-4.8782
8/5/2008 6:28	-5.6374	-19.0419	-11.5732	-11.6675	-11.093	-9.8849	-10.9715	-11.6504	-8.7672	-4.7268
8/5/2008 6:32	-5.6322	-18.9724	-11.4591	-11.8065	-11.027	-9.9567	-11.044	-11.7896	-8.9007	-4.9666
8/5/2008 6:36	-5.6274	-19.1613	-11.5757	-12.1866	-10.8345	-10.4069	-11.0582	-11.7688	-8.8984	-5.1632
8/5/2008 6:40	-5.8108	-19.4909	-11.6742	-12.3499	-10.8842	-10.56	-11.237	-12.1133	-8.9394	-4.9743
8/5/2008 6:44	-5.8464	-19.3191	-11.9963	-12.5863	-11.1267	-10.7134	-11.2571	-12.0542	-8.901	-5.1317
8/5/2008 6:48	-5.9164	-19.451	-12.1522	-13.1579	-11.2482	-10.7893	-11.7527	-12.55	-9.3979	-5.4614
8/5/2008 6:52	-6.1138	-19.8877	-12.2512	-13.5119	-11.6978	-11.6425	-12.0297	-12.9211	-9.6567	-5.7197
8/5/2008 6:56	-6.1017	-19.8995	-12.3689	-13.2457	-11.4165	-11.1559	-11.9417	-12.8373	-9.4621	-5.7226
8/5/2008 7:00	-6.3269	-20.0497	-12.6157	-13.7328	-11.948	-11.779	-12.3251	-13.3032	-9.6068	-6.2024
8/5/2008 7:04	-6.3844	-20.096	-12.5521	-13.867	-11.8478	-11.8496	-12.5097	-13.7101	-9.8779	-6.1649
8/5/2008 7:08	-6.846	-20.5233	-12.9328	-14.5702	-12.1247	-12.194	-12.6977	-13.9381	-10.252	-6.6328
8/5/2008 7:12	-7.0009	-20.9376	-13.401	-15.113	-12.518	-12.5765	-13.0756	-14.37	-10.5336	-6.7649
8/5/2008 7:16	-6.6039	-20.1825	-12.8035	-14.5835	-12.346	-12.3665	-12.6851	-13.8026	-10.5252	-6.5368
8/5/2008 7:20	-6.7534	-20.4321	-12.9673	-14.5734	-12.3777	-12.3194	-12.871	-14.0574	-10.5225	-6.6652
8/5/2008 7:25	-7.2221	-20.7991	-13.4855	-15.5204	-12.934	-13.2278	-13.354	-14.5903	-10.8629	-6.928
8/5/2008 7:29	-7.1676	-20.8287	-13.2788	-15.35	-12.7209	-12.8261	-13.4767	-14.7609	-10.833	-7.0042

8/5/2008 7:33	-7.2664	-20.8683	-13.705	-15.4934	-12.7475	-12.8844	-13.2711	-14.563	-11.1963	-7.1404
8/5/2008 7:37	-6.9837	-20.6559	-13.2918	-15.1924	-12.8284	-13.1134	-13.3744	-14.5902	-10.9133	-7.1289
8/5/2008 7:41	-7.2473	-20.9428	-13.5167	-15.6669	-12.8127	-13.0438	-13.7985	-15.1188	-11.2964	-7.3373
8/5/2008 7:45	-7.7613	-21.2504	-13.6025	-16.0962	-12.8205	-13.449	-13.8698	-15.2439	-11.2237	-7.5402
8/5/2008 7:49	-7.9223	-21.2188	-13.8429	-16.2433	-12.8966	-13.7449	-14.1326	-15.733	-11.397	-7.6347
8/5/2008 7:53	-7.9098	-21.4968	-13.6009	-16.0354	-12.9496	-13.7586	-14.188	-15.8628	-11.0992	-7.7375
8/5/2008 7:57	-8.2441	-21.5899	-14.2922	-16.7769	-13.129	-14.0389	-14.6038	-16.3752	-11.4014	-7.8963
8/5/2008 8:01	-8.3351	-21.8735	-14.5756	-17.1052	-13.316	-14.3769	-14.9964	-16.8079	-11.5208	-8.1189
8/5/2008 8:05	-8.3678	-22.0036	-14.7235	-17.512	-13.1539	-14.3301	-14.8358	-16.4991	-11.8449	-8.168
8/5/2008 8:09	-8.2233	-21.9493	-14.2901	-16.9972	-13.1711	-14.2134	-14.6479	-16.38	-12.3359	-8.3228
8/5/2008 8:13	-8.6656	-22.6545	-15.0085	-18.036	-13.4125	-14.7353	-15.1258	-16.9687	-12.1194	-8.4636
8/5/2008 8:17	-8.78	-22.6529	-14.8559	-17.9215	-13.3243	-14.8298	-15.197	-17.0702	-12.2467	-8.6344
8/5/2008 8:21	-8.9636	-22.6083	-14.3726	-17.2888	-12.9225	-14.2986	-14.9387	-16.9011	-12.0588	-8.1206
8/5/2008 8:25	-8.8484	-22.9405	-14.5128	-18.1194	-13.6789	-15.4968	-15.3091	-17.2572	-12.2412	-8.9046
8/5/2008 8:29	-9.1538	-23.0232	-14.6614	-18.3207	-13.8125	-15.4021	-15.6268	-17.5462	-12.8156	-8.769
8/5/2008 8:33	-8.9552	-23.0346	-14.5873	-18.4158	-13.6274	-15.2886	-15.6986	-17.7899	-12.4666	-9.1228
8/5/2008 8:37	-8.9039	-22.8444	-14.4471	-18.1608	-14.2226	-15.6597	-15.6948	-17.6816	-12.622	-10.7076
8/5/2008 8:41	-9.4984	-23.6009	-15.0936	-19.2065	-14.2945	-15.8673	-16.1108	-18.2033	-13.0181	-11.5969
8/5/2008 8:45	-9.2555	-23.3016	-14.9096	-19.1184	-14.4817	-15.8727	-16.062	-18.201	-12.9738	-11.899
8/5/2008 8:49	-9.4511	-23.5544	-15.2155	-19.4417	-14.2312	-15.929	-16.3165	-18.4081	-12.8934	-12.3562
8/5/2008 8:53	-9.4814	-23.4327	-14.7022	-19.0948	-14.3074	-15.9407	-16.3247	-18.596	-12.8795	-12.5518
8/5/2008 8:57	-9.436	-23.4927	-14.8037	-19.0926	-14.2052	-15.7775	-15.9028	-17.918	-12.596	-12.6014
8/5/2008 9:01	-9.3995	-23.5017	-15.2234	-19.646	-14.6027	-16.3153	-16.796	-18.7413	-13.008	-13.4973
8/5/2008 9:05	-9.957	-24.0582	-15.8082	-20.0758	-15.415	-16.9224	-17.1234	-19.4281	-13.5063	-14.3659
8/5/2008 9:09	-10.0842	-24.3631	-15.2603	-20.2601	-15.6714	-16.751	-16.726	-18.9721	-12.8378	-14.1955
8/5/2008 9:13	-9.5188	-23.9593	-14.5905	-19.6494	-15.2763	-15.9551	-16.4326	-18.9493	-12.8618	-14.4408
8/5/2008 9:17	-9.8453	-23.9001	-13.9765	-19.5647	-15.3949	-16.0885	-16.7611	-19.1225	-12.9874	-14.8836
8/5/2008 9:21	-9.469	-24.2818	-14.0968	-20.0435	-16.0634	-16.6042	-17.3753	-19.9219	-12.9818	-15.2809
8/5/2008 9:25	-10.076	-25.2786	-14.6978	-21.2079	-17.491	-18.0988	-18.3962	-20.6422	-13.5965	-15.8543
8/5/2008 9:30	-10.0016	-25.1061	-14.6789	-21.0657	-17.0594	-17.5825	-17.6744	-19.951	-13.2793	-15.4027
8/5/2008 9:34	-10.2778	-25.5596	-15.0259	-21.8363	-16.9935	-18.0869	-17.7007	-19.3511	-13.0866	-15.4749
8/5/2008 9:38	-9.8641	-25.2562	-14.3339	-21.0899	-16.5713	-17.2176	-17.5594	-19.0482	-13.0085	-15.5646
8/5/2008 9:42	-9.6542	-24.6036	-14.0358	-20.6382	-16.4646	-17.115	-17.3036	-18.6842	-12.2147	-15.1829
8/5/2008 9:46	-9.9105	-24.9751	-13.9217	-21.0549	-16.5901	-17.4558	-17.7239	-19.2712	-12.421	-15.3862
8/5/2008 9:50	-9.6062	-24.8436	-13.8738	-21.093	-16.8202	-17.7203	-17.7864	-19.2765	-12.4776	-15.5782
8/5/2008 9:54	-9.7368	-24.6749	-13.7338	-20.88	-17.0027	-17.1654	-17.4672	-18.7814	-12.2423	-15.4135
8/5/2008 9:58	-9.5152	-24.8198	-13.6714	-21.2407	-16.8408	-17.8841	-18.0435	-18.7814	-12.5694	-16.2879
8/5/2008 10:02	-9.9251	-25.0722	-13.7621	-21.469	-17.01	-18.1497	-18.4351	-18.9163	-12.7136	-16.0964
8/5/2008 10:06	-9.6346	-24.8516	-13.5184	-21.4947	-17.0744	-18.0269	-18.3441	-18.9916	-12.4365	-16.6712
8/5/2008 10:10	-9.4622	-24.9734	-13.5798	-21.44	-16.8861	-17.956	-18.4321	-19.5106	-12.3605	-16.852
8/5/2008 10:14	-9.5298	-24.9004	-13.5546	-21.5556	-17.0792	-18.3149	-18.626	-20.0189	-12.6802	-16.852
8/5/2008 10:18	-9.7711	-25.0706	-13.7672	-21.6281	-16.9903	-18.2064	-18.713	-20.0028	-12.3334	-17.4846
8/5/2008 10:22	-9.7844	-25.0472	-13.9911	-21.8523	-17.1327	-18.7192	-19.0691	-20.1965	-12.538	-18.0599
8/5/2008 10:26	-9.8368	-25.0617	-14.0483	-21.7678	-17.108	-18.4667	-18.9415	-19.8925	-12.4349	-18.0713

8/5/2008 10:30	-9.8359	-25.1695	-14.1648	-22.0485	-17.4198	-18.8982	-19.5082	-19.8925	-12.8972	-18.0713
8/5/2008 10:34	-10.4592	-25.8565	-14.8682	-22.9097	-17.7921	-19.937	-19.957	-20.4243	-13.3985	-18.0713
8/5/2008 10:38	-10.0426	-24.9525	-14.0613	-21.852	-16.9877	-18.6725	-19.1257	-20.0779	-13.0574	-18.0713
8/5/2008 10:42	-9.9821	-25.0465	-14.1867	-21.854	-16.8018	-18.5913	-19.1713	-20.0906	-12.8059	-18.0713
8/5/2008 10:46	-9.1718	-24.4531	-13.5113	-21.1546	-16.3011	-17.6854	-18.5277	-19.0702	-12.595	-17.5255
8/5/2008 10:50	-9.8803	-25.0841	-13.9099	-21.9966	-16.8645	-18.7491	-19.1581	-20.6823	-14.6818	-17.5255
8/5/2008 10:54	-9.2041	-24.8352	-13.4205	-21.5919	-16.3195	-18.2511	-18.7133	-20.1951	-14.0126	-17.5255
8/5/2008 10:58	-9.4382	-25.3458	-14.0975	-22.5826	-16.6765	-19.1285	-19.3512	-20.1951	-14.715	-17.5255
8/5/2008 11:02	-9.8602	-25.5437	-14.1545	-22.8663	-17.0041	-19.4861	-19.5643	-20.1951	-14.8309	-17.5255
8/5/2008 11:06	-9.909	-25.5126	-14.1672	-22.8448	-17.1869	-19.703	-19.5114	-20.1951	-14.9323	-17.5255
8/5/2008 11:10	-9.5822	-24.6887	-13.5085	-22.191	-16.6765	-19.3278	-19.1451	-19.5084	-15.1252	-17.5255
8/5/2008 11:14	-9.5742	-25.0148	-13.3895	-22.6819	-16.167	-19.0172	-18.8804	-19.655	-14.7263	-17.5255
8/5/2008 11:18	-9.7985	-25.0649	-13.6979	-22.8738	-16.2971	-19.2734	-18.9292	-19.5217	-14.6516	-17.5255
8/5/2008 11:22	-10.1556	-25.3822	-14.2124	-23.5979	-16.0643	-19.9598	-19.4464	-20.0003	-14.9408	-17.5255
8/5/2008 11:26	-10.4482	-25.4125	-13.7214	-23.0771	-15.9615	-19.5514	-19.4459	-20.175	-14.9131	-17.47
8/5/2008 11:30	-10.7466	-25.4092	-13.8982	-23.4029	-16.2514	-19.9648	-19.8099	-19.8025	-15.0461	-17.47
8/5/2008 11:34	-10.4923	-25.1444	-13.7171	-23.1161	-16.0313	-19.5809	-19.7113	-19.5927	-14.5679	-17.47
8/5/2008 11:38	-10.7975	-25.3767	-14.2794	-23.6084	-16.3536	-19.86	-19.9343	-19.65	-14.682	-17.47
8/5/2008 11:43	-10.817	-24.9782	-13.64	-22.796	-16.1624	-19.6669	-20.047	-19.579	-14.6375	-21.3667
8/5/2008 11:47	-11.3766	-26.0927	-14.1212	-24.0816	-16.5918	-20.7415	-20.4271	-19.579	-15.1675	-21.3667
8/5/2008 11:51	-11.4476	-26.0443	-14.0275	-24.0608	-16.1816	-20.0816	-20.1541	-19.579	-14.8885	-21.3667
8/5/2008 11:55	-11.9399	-26.5898	-14.4361	-24.817	-16.4415	-21.1638	-20.619	-19.579	-15.12	-21.3667
8/5/2008 11:59	-11.1034	-25.7414	-13.956	-23.8683	-15.944	-20.2034	-20.573	-19.7733	-14.6891	-20.6545
8/5/2008 12:03	-11.5128	-25.896	-14.0807	-24.0914	-15.9059	-19.9644	-20.4183	-19.5977	-14.721	-21.2184
8/5/2008 12:07	-11.3425	-25.814	-14.093	-23.8504	-16.1972	-20.1323	-20.5433	-19.6811	-15.1094	-21.2184
8/5/2008 12:11	-11.0298	-25.4963	-13.9237	-23.4616	-15.8171	-19.6076	-20.3874	-19.5768	-14.8062	-21.2184
8/5/2008 12:15	-11.0575	-25.5251	-13.9061	-23.4614	-15.8699	-19.7339	-20.313	-19.7379	-14.9564	-22.1409
8/5/2008 12:19	-11.1486	-25.449	-14.127	-23.2526	-15.7091	-19.5362	-20.0668	-19.176	-14.1035	-22.1409
8/5/2008 12:23	-11.2316	-25.6173	-14.2305	-23.6215	-15.7892	-19.6745	-20.395	-19.7471	-14.4345	-22.1409
8/5/2008 12:27	-11.49	-26.1358	-14.7568	-24.1713	-16.0315	-19.9499	-20.8246	-20.2722	-14.6892	-21.9901
8/5/2008 12:31	-12.0427	-26.6172	-15.9479	-25.2124	-16.6507	-20.8358	-21.4276	-20.7981	-15.1659	-22.2087
8/5/2008 12:35	-11.7339	-26.2374	-15.3941	-24.4529	-16.2467	-20.4669	-21.0553	-20.4848	-14.9753	-22.3002
8/5/2008 12:39	-11.5499	-25.9804	-15.0831	-24.1606	-16.1517	-20.1196	-20.7011	-19.8104	-14.5306	-21.7052
8/5/2008 12:43	-11.9528	-26.3675	-15.762	-25.1711	-16.9892	-21.3357	-21.817	-21.1404	-15.3383	-22.1276
8/5/2008 12:47	-12.0847	-26.4222	-15.4602	-24.6212	-16.4659	-20.6731	-21.4208	-20.5316	-15.2831	-21.8637
8/5/2008 12:51	-12.1077	-26.9545	-16.2827	-25.5813	-16.7971	-21.4905	-21.7219	-20.9468	-15.6355	-22.0295
8/5/2008 12:55	-12.2637	-27.2369	-16.7624	-26.2469	-17.3207	-22.4197	-22.3442	-21.4816	-16.514	-22.2633

8/5/2008 12:59	-12.4566	-26.9666	-16.7319	-25.9604	-17.0682	-21.6706	-22.0108	-21.1106	-17.1445	-21.9564
8/5/2008 13:03	-12.0489	-26.2645	-15.9347	-25.0829	-16.6073	-21.1637	-21.4448	-20.4373	-16.7088	-21.847
8/5/2008 13:07	-12.1072	-26.2358	-16.0704	-24.9952	-16.5635	-20.9122	-21.4064	-20.2681	-16.3754	-21.7247
8/5/2008 13:11	-12.3428	-26.5106	-16.5803	-25.6024	-17.0612	-21.4211	-22.0493	-20.8641	-16.6933	-21.7247
8/5/2008 13:15	-12.6731	-26.7089	-16.7425	-25.8132	-17.2341	-21.5535	-22.2433	-20.6803	-16.7179	-22.1376
8/5/2008 13:19	-12.5647	-26.8589	-16.7458	-25.8599	-17.3372	-21.6297	-22.2134	-20.6063	-16.9428	-21.2576
8/5/2008 13:23	-12.3005	-26.2251	-16.2102	-25.0695	-16.7774	-20.8608	-21.5271	-19.7663	-16.4501	-20.4949
8/5/2008 13:27	-12.5181	-26.6385	-16.4308	-25.6312	-17.1424	-21.4111	-22.0262	-20.3795	-16.8935	-20.9924
8/5/2008 13:31	-13.1148	-26.975	-16.7812	-26.4459	-17.5545	-21.9376	-22.3311	-20.8852	-16.849	-20.9101
8/5/2008 13:35	-12.5356	-26.0895	-16.1909	-25.1992	-16.6686	-21.064	-21.606	-20.1266	-16.5705	-21.0646
8/5/2008 13:39	-12.4072	-26.1819	-16.6531	-26.1159	-17.2394	-21.5905	-22.3354	-20.7002	-17.0453	-21.4186
8/5/2008 13:43	-12.6486	-26.6851	-16.8332	-26.294	-17.5231	-21.9234	-22.6254	-21.0495	-17.1711	-21.4272
8/5/2008 13:47	-12.8856	-26.93	-16.7943	-26.7446	-17.6371	-22.172	-22.541	-20.8171	-17.2788	-21.5719
8/5/2008 13:51	-13.3932	-27.236	-16.5706	-27.2925	-17.7615	-22.4656	-22.779	-21.1196	-17.3228	-21.8846
8/5/2008 13:56	-13.1689	-26.9868	-16.0627	-26.9359	-17.4698	-22.217	-22.4362	-20.6935	-17.1112	-23.1347
8/5/2008 14:00	-13.0784	-26.7789	-15.7318	-26.7319	-17.2592	-22.0046	-22.2656	-20.571	-17.1752	-23.7135
8/5/2008 14:04	-13.712	-27.691	-16.5127	-27.9551	-18.1167	-23.0918	-23.0813	-21.4186	-17.7489	-24.1318
8/5/2008 14:08	-12.9918	-27.1418	-15.7222	-27.333	-17.5966	-22.6135	-22.5512	-21.2259	-17.6252	-24.1048
8/5/2008 14:12	-13.6279	-27.8612	-16.635	-28.8329	-18.8356	-23.9295	-23.7621	-22.0379	-18.3121	-24.7703
8/5/2008 14:16	-14.4464	-28.8468	-17.5356	-30.2457	-19.7877	-24.9264	-24.7545	-22.6706	-19.2569	-25.338
8/5/2008 14:20	-15.2709	-29.6054	-18.2159	-31.358	-20.4037	-25.697	-25.5969	-23.2644	-20.1587	-25.8785
8/5/2008 14:24	-15.4333	-29.5445	-18.3308	-31.4018	-20.5358	-26.0807	-26.1198	-23.7424	-20.5578	-26.2428
8/5/2008 14:28	-15.5676	-29.8181	-18.8775	-32.1298	-20.5914	-26.4177	-26.411	-23.8778	-20.6316	-26.352
8/5/2008 14:32	-16.6119	-30.5556	-19.5382	-33.1234	-20.9858	-27.5467	-26.8764	-24.5372	-20.851	-26.3796
8/5/2008 14:36	-16.7531	-30.8457	-19.7187	-33.6366	-21.2283	-28.0508	-27.3639	-25.0497	-21.1423	-26.7826
8/5/2008 14:40	-16.3159	-30.4142	-19.3559	-33.1455	-21.0115	-27.6606	-26.9163	-24.7519	-21.0035	-26.6215
8/5/2008 14:44	-16.7146	-30.6965	-19.5509	-33.5753	-21.023	-27.8246	-26.8814	-24.9277	-21.006	-26.6102
8/5/2008 14:48	-17.0604	-30.953	-19.8403	-34.1326	-21.3693	-28.3939	-27.2115	-25.2438	-21.5307	-26.8408
8/5/2008 14:52	-16.9283	-30.8903	-20.0176	-34.3563	-21.6725	-28.7869	-27.4348	-25.4473	-21.6473	-27.1314
8/5/2008 14:56	-16.6247	-30.6727	-19.9688	-34.2906	-21.7411	-28.8638	-27.5699	-25.5451	-21.8612	-27.3398
8/5/2008 15:00	-16.677	-30.6455	-19.8256	-34.3048	-21.7047	-28.6918	-27.1815	-25.2639	-21.7213	-27.0046
8/5/2008 15:04	-17.1003	-30.8885	-20.1213	-34.9521	-22.0088	-29.2306	-27.6935	-25.8428	-22.2021	-27.4109
8/5/2008 15:08	-17.2791	-30.9359	-20.4568	-35.322	-22.2053	-29.6818	-27.7684	-26.1881	-22.5016	-27.4938
8/5/2008 15:12	-17.5276	-30.8413	-20.4421	-35.341	-22.3662	-29.8966	-28.1422	-26.493	-22.7632	-27.7895
8/5/2008 15:16	-17.5011	-30.8072	-20.4185	-35.4546	-22.0214	-29.4734	-27.7192	-26.0468	-22.3004	-27.5311

8/5/2008 15:20	-18.6234	-31.6998	-21.3591	-37.5611	-23.3086	-31.7879	-29.0859	-27.4009	-23.8108	-28.7967
8/5/2008 15:24	-18.0889	-30.9324	-20.1084	-35.5319	-22.1612	-29.6745	-28.3916	-26.359	-22.7077	-28.3987
8/5/2008 15:28	-18.2447	-30.9291	-20.1769	-36.1153	-22.6036	-30.5099	-28.8411	-26.8973	-23.255	-28.86
8/5/2008 15:32	-19.1311	-31.754	-21.0642	-37.9856	-23.631	-32.4156	-30.059	-27.7747	-24.0176	-29.5287
8/5/2008 15:36	-18.5549	-30.8713	-20.2382	-36.5356	-22.8609	-30.8044	-29.1921	-26.7511	-23.382	-28.9926
8/5/2008 15:40	-18.9414	-30.9985	-20.4175	-36.9547	-23.1378	-31.4053	-29.6089	-27.3068	-23.4796	-29.3723
8/5/2008 15:44	-19.0282	-31.0852	-20.4813	-37.1809	-23.1164	-31.3482	-29.7542	-27.3013	-23.6067	-29.2842
8/5/2008 15:48	-19.0282	-31.2714	-20.982	-38.0306	-23.5479	-32.5199	-30.2107	-28.305	-24.5135	-30.1855
8/5/2008 15:52	-19.4581	-31.6801	-21.2002	-38.5774	-24.0105	-32.8716	-30.2262	-28.2296	-24.1982	-29.9124
8/5/2008 15:57	-19.1806	-31.3338	-21.1922	-38.3016	-23.8165	-32.6978	-30.225	-28.3414	-24.3317	-30.2642
8/5/2008 16:01	-19.0684	-31.1361	-21.0855	-38.3441	-23.7405	-32.7056	-30.3254	-28.2646	-23.9599	-30.1018
8/5/2008 16:05	-19.4801	-31.644	-21.4234	-39.0755	-24.4029	-33.862	-30.9998	-29.3307	-24.7493	-30.6787
8/5/2008 16:09	-19.121	-31.7502	-21.6385	-39.5988	-24.742	-34.7445	-31.506	-29.9413	-25.0817	-31.1285
8/5/2008 16:13	-19.2896	-31.6616	-21.502	-39.3163	-24.322	-34.211	-30.882	-29.5544	-24.868	-30.7961
8/5/2008 16:17	-19.1077	-31.488	-21.5653	-39.501	-24.3649	-34.3831	-30.8816	-29.7112	-24.9592	-30.8568
8/5/2008 16:21	-19.5876	-31.9057	-22.0696	-40.0654	-24.8606	-35.177	-31.4109	-30.2567	-25.2809	-31.3257
8/5/2008 16:25	-19.7735	-31.9068	-22.0987	-40.1506	-24.8622	-35.1077	-31.2122	-30.2201	-25.5791	-31.2876
8/5/2008 16:29	-19.6201	-31.7751	-21.8732	-40.0874	-24.8768	-35.2107	-31.2338	-30.3733	-25.623	-31.4119
8/5/2008 16:33	-19.8313	-31.6804	-22.0595	-40.2447	-24.9323	-35.422	-31.3568	-30.5665	-25.8205	-31.6335
8/5/2008 16:37	-21.4056	-32.1501	-22.6676	-41.099	-25.5576	-36.5413	-31.9561	-31.4947	-26.184	-32.0112
8/5/2008 16:41	-21.5757	-32.1284	-22.6698	-41.1762	-25.6942	-36.8039	-31.843	-31.7193	-26.7196	-32.2672
8/5/2008 16:45	-21.6085	-32.0152	-22.7167	-41.1905	-25.7546	-36.8173	-31.9755	-31.8341	-27.1882	-32.322
8/5/2008 16:49	-22.0278	-32.1346	-22.9388	-41.3665	-25.9027	-37.1232	-32.0897	-32.1526	-27.425	-32.5733
8/5/2008 16:53	-21.6461	-31.8198	-22.821	-41.2846	-25.8105	-36.8801	-31.8915	-32.0206	-26.5041	-32.4447
8/5/2008 16:57	-22.5788	-32.1743	-23.188	-41.7154	-26.0941	-37.6165	-32.3133	-32.7227	-27.1781	-32.8112
8/5/2008 17:01	-23.0614	-32.3968	-23.3415	-42.0631	-26.2477	-37.9475	-32.5575	-33.1609	-27.3196	-32.9632
8/5/2008 17:05	-23.6968	-32.8999	-24.0484	-43.0179	-26.9043	-39.3334	-33.2123	-34.5883	-27.9547	-33.6711
8/5/2008 17:09	-22.6852	-32.0195	-22.9394	-41.8032	-26.0554	-37.4989	-32.424	-32.8602	-27.0339	-32.8296
8/5/2008 17:13	-22.8253	-32.2574	-23.1229	-42.2954	-26.5031	-38.509	-32.9607	-33.857	-27.8627	-33.6055
8/5/2008 17:17	-22.9997	-32.3894	-23.4558	-42.6899	-26.6194	-38.8295	-33.0359	-33.9117	-27.7587	-33.5582
8/5/2008 17:21	-23.9316	-33.0918	-24.2247	-43.7896	-27.1706	-40.189	-33.6575	-35.4178	-28.736	-34.2937
8/5/2008 17:25	-23.625	-33.6193	-23.9588	-43.4561	-26.8726	-39.6929	-33.3801	-35.0743	-28.8001	-34.2015
8/5/2008 17:29	-23.6246	-33.5976	-24.194	-43.5384	-27.0312	-40.3804	-33.4463	-35.3177	-28.9381	-34.4048
8/5/2008 17:33	-24.2073	-34.2697	-24.897	-44.8466	-27.5747	-41.3835	-34.0259	-36.5163	-29.5858	-34.9177
8/5/2008 17:37	-24.3416	-34.1204	-24.6501	-44.5288	-27.3817	-40.8593	-33.7371	-36.0139	-29.3549	-34.7465

8/5/2008 17:41	-24.3697	-34.4123	-25.2698	-45.0815	-27.7088	-41.5977	-34.1409	-36.6746	-29.5752	-35.0575
8/5/2008 17:45	-24.628	-34.7649	-25.5459	-45.6183	-27.9882	-42.4222	-34.5136	-37.4241	-30.0176	-35.4564
8/5/2008 17:49	-24.7983	-34.8701	-25.653	-45.8731	-28.136	-42.6256	-34.6655	-37.7109	-30.2229	-35.7223
8/5/2008 17:54	-24.6977	-34.5587	-25.5176	-45.3999	-27.7639	-42.055	-34.3284	-36.9823	-29.7571	-35.3077
8/5/2008 17:58	-24.2163	-34.3971	-25.3932	-45.3483	-27.6425	-41.9374	-34.2628	-36.9648	-29.7986	-35.2813
8/5/2008 18:02	-24.1879	-34.6011	-25.4804	-45.9255	-27.8495	-42.8938	-34.6467	-37.8891	-30.1401	-35.7287
8/5/2008 18:06	-24.2189	-34.7027	-25.6811	-45.8894	-27.829	-42.6642	-34.4774	-37.8574	-30.2871	-35.7678
8/5/2008 18:10	-24.601	-35.0273	-25.9796	-46.401	-28.2986	-43.349	-35.0817	-38.7501	-30.5891	-36.074
8/5/2008 18:14	-24.5495	-34.8535	-26.0286	-46.496	-28.3275	-43.4864	-34.9658	-38.7483	-30.6311	-35.9447
8/5/2008 18:18	-24.4596	-35.2096	-26.1807	-46.9023	-28.6296	-44.0819	-35.5593	-39.3554	-30.8992	-36.3324
8/5/2008 18:22	-24.3738	-35.2623	-25.9686	-47.2212	-28.5109	-44.0184	-35.2256	-39.1317	-30.514	-35.9629
8/5/2008 18:26	-24.186	-35.1063	-26.1145	-46.8244	-28.3654	-43.7646	-35.2547	-39.1038	-30.697	-36.0405
8/5/2008 18:30	-24.7128	-35.6505	-27.0221	-47.9421	-29.8018	-45.2901	-36.4582	-40.0834	-31.6004	-36.7546
8/5/2008 18:34	-24.3297	-35.139	-27.0872	-47.3171	-29.4788	-44.5797	-35.7897	-39.5503	-31.2171	-36.3496
8/5/2008 18:38	-24.4525	-35.111	-27.2293	-47.3766	-29.4004	-44.588	-35.799	-39.4789	-31.1425	-36.0109
8/5/2008 18:42	-24.9656	-35.7298	-27.9817	-48.2966	-30.4557	-45.7699	-36.4241	-40.1725	-31.7202	-36.4684
8/5/2008 18:46	-25.0303	-35.7703	-27.9699	-48.3634	-30.483	-45.8872	-36.394	-40.1946	-31.7099	-36.4889
8/5/2008 18:50	-24.9214	-35.6557	-28.0974	-48.1618	-30.3047	-45.5999	-36.7323	-40.1237	-31.8402	-36.4197
8/5/2008 18:54	-25.0857	-35.8661	-28.308	-48.5056	-30.6007	-46.0822	-36.9585	-40.3033	-31.8937	-36.5145
8/5/2008 18:58	-25.4063	-36.1338	-28.5789	-49.0514	-31.1881	-46.7543	-37.3387	-40.7092	-32.3552	-36.8717
8/5/2008 19:02	-25.5903	-36.1748	-28.748	-49.2612	-31.3117	-47.2185	-37.6747	-40.9387	-32.4503	-37.0567
8/5/2008 19:06	-25.9971	-36.7099	-28.9385	-49.5673	-31.6547	-47.7721	-37.7387	-41.1026	-32.6198	-37.2808
8/5/2008 19:10	-25.96	-36.6246	-28.9166	-49.7814	-31.9656	-48.0459	-38.0305	-41.5072	-32.9367	-37.5381
8/5/2008 19:14	-26.1397	-36.5537	-28.9567	-49.7148	-31.5878	-47.9214	-37.9642	-41.4867	-33.066	-37.6967
8/5/2008 19:18	-26.5614	-38.0107	-29.5751	-50.7376	-32.5823	-48.9357	-38.6008	-42.404	-33.6134	-38.1176
8/5/2008 19:22	-26.813	-38.5469	-29.9476	-51.2071	-32.7384	-49.3299	-38.9462	-42.7808	-34.0118	-38.5063
8/5/2008 19:26	-26.9104	-38.9746	-30.2687	-51.5853	-33.164	-49.9147	-39.7647	-43.4301	-34.6501	-39.0634
8/5/2008 19:30	-27.28	-39.7981	-31.2251	-52.3446	-33.4041	-50.2907	-40.4179	-44.0853	-35.0239	-39.43
8/5/2008 19:34	-27.7137	-40.1033	-31.4715	-52.658	-33.5216	-51.353	-41.0661	-44.4266	-35.2393	-39.7333
8/5/2008 19:38	-27.5959	-40.3926	-31.6452	-52.954	-33.5155	-51.4021	-41.642	-44.8143	-35.5341	-40.1201
8/5/2008 19:42	-28.0323	-41.1615	-31.9927	-53.5865	-34.1746	-51.7327	-42.6629	-45.5639	-36.2677	-40.9548
8/5/2008 19:47	-28.5404	-41.5775	-32.338	-54.3248	-34.5487	-52.1397	-43.3701	-46.3677	-36.7035	-41.5291
8/5/2008 19:51	-29.7067	-42.8615	-33.0985	-55.6894	-35.2884	-53.4913	-44.5944	-47.7523	-37.7114	-42.455
8/5/2008 19:55	-30.1118	-43.3484	-33.8091	-56.5964	-35.7478	-54.4947	-46.15	-48.8093	-38.6719	-43.2692
8/5/2008 19:59	-30.5778	-44.2043	-34.6817	-57.5108	-36.3106	-54.7631	-46.8848	-49.8386	-39.4907	-44.1718
8/5/2008 20:03	-31.2867	-44.693	-35.6352	-58.1126	-37.2561	-55.4013	-47.7875	-51.0191	-39.9457	-45.014

8/5/2008 20:07	-31.2867	-46.5395	-36.0287	-58.9747	-38.6558	-56.3569	-48.644	-52.0402	-40.528	-46.0183

Appendix 3.2: Slope Displacement Data for Validation Test 2 (Ramp 12 High-wall, New Vaal open cast coal mine)

DATE	P1	P2	P3	P4	P5	P6	P7	P8	P9	P10
3/13/2008 13:26	-24.97	-19.57	-23.84	-25.65	-18.09	-21.91	-20.36	-19.34	-18.35	-23.84
3/13/2008 13:28	-26.05	-21.38	-24.99	-25.65	-19.78	-21.91	-22.54	-19.34	-20.17	-23.84
3/13/2008 13:30	-26.77	-22.56	-26.57	-25.65	-20.99	-22.95	-23.63	-23.08	-23.96	-25.36
3/13/2008 13:33	-28.59	-23.40	-27.89	-25.65	-22.47	-26.40	-25.01	-23.08	-26.22	-30.70
3/13/2008 13:35	-29.72	-24.39	-29.10	-26.63	-23.30	-27.51	-26.04	-24.16	-27.01	-31.69
3/13/2008 13:37	-30.52	-25.03	-29.90	-27.31	-24.23	-28.16	-26.94	-25.52	-27.01	-32.54
3/13/2008 13:40	-30.79	-25.66	-30.62	-27.96	-24.67	-28.82	-28.91	-26.19	-27.01	-33.17
3/13/2008 13:42	-31.37	-26.17	-31.43	-28.86	-25.62	-29.46	-29.83	-27.07	-28.81	-34.12
3/13/2008 13:44	-31.89	-26.95	-32.13	-29.34	-26.05	-29.90	-30.39	-27.98	-30.54	-34.67
3/13/2008 13:47	-32.31	-27.36	-33.13	-30.00	-26.24	-30.03	-30.78	-28.43	-31.18	-35.06
3/13/2008 13:49	-32.23	-27.55	-33.36	-30.38	-26.67	-30.46	-31.25	-29.00	-32.34	-35.53
3/13/2008 13:51	-32.76	-28.09	-33.98	-30.89	-27.02	-30.95	-31.60	-29.43	-32.68	-35.70
3/13/2008 13:54	-33.58	-28.20	-34.18	-31.06	-27.16	-31.04	-31.68	-29.63	-32.97	-35.89
3/13/2008 13:56	-33.81	-28.17	-34.49	-31.54	-27.50	-31.44	-32.23	-30.27	-34.13	-36.56
3/13/2008 13:58	-34.37	-28.81	-35.13	-32.19	-28.21	-32.02	-32.80	-30.75	-34.64	-37.02
3/13/2008 14:01	-34.72	-28.89	-35.16	-32.43	-28.10	-31.65	-32.79	-30.55	-34.59	-36.85
3/13/2008 14:03	-34.91	-29.12	-36.16	-32.73	-28.45	-32.10	-33.29	-31.06	-35.30	-37.51
3/13/2008 14:05	-35.47	-29.49	-36.55	-33.36	-29.04	-32.78	-34.10	-32.18	-36.25	-38.02
3/13/2008 14:08	-35.92	-29.93	-37.10	-33.29	-29.17	-33.16	-34.49	-32.59	-36.42	-38.58
3/13/2008 14:10	-36.16	-30.28	-37.41	-34.16	-29.99	-34.00	-35.06	-33.31	-37.13	-39.38
3/13/2008 14:12	-36.84	-31.01	-38.25	-34.59	-30.42	-34.38	-35.37	-33.73	-37.22	-40.04
3/13/2008 14:15	-37.01	-31.03	-38.62	-34.54	-30.63	-34.71	-35.66	-33.83	-38.32	-39.55
3/13/2008 14:17	-37.01	-31.53	-38.62	-35.25	-30.63	-35.87	-35.67	-33.83	-38.32	-41.36
3/13/2008 14:19	-37.01	-32.86	-38.62	-35.37	-31.09	-35.87	-35.67	-34.90	-41.85	-41.36
3/13/2008 14:22	-38.12	-34.21	-38.62	-35.37	-31.09	-38.03	-38.06	-35.76	-41.85	-41.36
3/13/2008 14:24	-39.31	-34.21	-38.62	-35.37	-31.09	-38.88	-39.26	-35.76	-44.58	-41.36
3/13/2008 14:27	-39.31	-35.07	-39.29	-35.37	-31.34	-39.62	-39.99	-38.11	-44.58	-45.25
3/13/2008 14:29	-39.31	-35.68	-39.96	-36.62	-31.94	-40.20	-41.29	-38.11	-44.58	-46.42
3/13/2008 14:31	-39.81	-37.12	-40.39	-36.56	-32.69	-41.23	-42.28	-39.04	-46.60	-46.42
3/13/2008 14:34	-39.81	-37.12	-41.18	-36.56	-34.57	-41.23	-43.32	-42.87	-46.60	-46.42
3/13/2008 14:36	-41.15	-37.12	-42.22	-39.92	-34.90	-42.24	-44.07	-45.13	-46.60	-47.39
3/13/2008 14:38	-44.82	-37.12	-43.37	-39.92	-35.63	-43.11	-44.79	-47.13	-47.70	-50.28
3/13/2008 14:41	-45.89	-37.12	-44.10	-39.92	-36.37	-44.18	-45.31	-48.51	-47.70	-50.49
3/13/2008 14:43	-46.89	-37.75	-44.92	-40.45	-36.99	-44.65	-46.19	-48.51	-47.70	-51.55
3/13/2008 14:45	-47.88	-38.31	-45.63	-40.97	-37.70	-45.25	-47.01	-48.99	-47.70	-51.55
3/13/2008 14:48	-48.92	-39.27	-46.68	-41.95	-38.70	-46.77	-47.84	-49.76	-48.90	-52.44
3/13/2008 14:50	-49.46	-39.81	-47.39	-42.36	-39.20	-47.29	-48.62	-50.42	-50.20	-53.68
3/13/2008 14:52	-49.92	-40.32	-47.89	-42.76	-39.57	-47.62	-49.14	-50.91	-50.84	-54.09

3/13/2008 14:55	-50.29	-40.81	-48.39	-43.42	-40.26	-48.37	-49.78	-51.71	-52.01	-54.81
3/13/2008 14:57	-51.06	-41.53	-49.22	-44.19	-41.05	-49.08	-50.38	-52.29	-52.01	-55.05
3/13/2008 14:59	-51.72	-42.14	-49.88	-44.68	-40.88	-49.60	-51.11	-53.05	-52.61	-55.94
3/13/2008 15:02	-52.31	-42.54	-50.40	-45.08	-41.16	-49.87	-51.31	-53.22	-52.66	-56.08
3/13/2008 15:04	-52.72	-42.80	-50.73	-45.48	-41.66	-50.30	-51.81	-53.85	-53.25	-57.54
3/13/2008 15:06	-53.30	-43.39	-51.30	-46.19	-42.16	-50.84	-52.24	-54.36	-53.83	-57.95
3/13/2008 15:09	-53.54	-43.74	-51.60	-46.40	-42.44	-51.06	-52.53	-54.62	-54.19	-58.24
3/13/2008 15:11	-53.82	-44.05	-51.90	-46.74	-42.81	-51.43	-53.00	-55.03	-54.62	-58.78
3/13/2008 15:13	-54.15	-44.48	-52.36	-47.05	-43.17	-51.85	-54.10	-55.57	-55.15	-59.43

Appendix 3.3: Slope Displacement Data for Validation Test 3 (Ramp 5 High-wall, Landau open cast coal mine)

DATE	P1	P2	P3	P4	P5	P6	P7	P8	P9	P10	P11
10/21/2007 11:53	-14.04	-17.86	-10.41	-13.52	-27.88	-14.78	-12.76	-19.48	-26.65	-18.10	-7.04
10/21/2007 11:55	-14.09	-18.10	-10.86	-13.54	-28.26	-15.30	-13.09	-19.42	-26.96	-17.84	-6.94
10/21/2007 11:58	-14.34	-18.48	-10.86	-13.96	-29.20	-15.79	-13.26	-19.61	-27.55	-18.13	-7.10
10/21/2007 12:00	-14.50	-18.94	-11.46	-14.08	-30.31	-16.50	-13.74	-19.53	-28.67	-18.02	-5.99
10/21/2007 12:03	-14.46	-19.25	-11.80	-14.00	-30.76	-17.26	-13.96	-19.76	-29.32	-18.02	-6.63
10/21/2007 12:05	-14.78	-19.91	-12.30	-14.20	-31.33	-18.10	-14.36	-19.65	-29.79	-18.02	-6.35
10/21/2007 12:08	-14.75	-20.19	-12.66	-14.24	-31.66	-18.73	-14.66	-20.12	-30.66	-18.02	-6.86
10/21/2007 12:11	-14.87	-20.44	-12.79	-14.44	-32.02	-19.08	-14.83	-20.19	-30.98	-19.90	-6.86
10/21/2007 12:13	-14.99	-20.58	-12.98	-14.40	-32.15	-19.30	-14.83	-20.51	-31.34	-20.50	-6.80
10/21/2007 12:16	-15.16	-20.90	-13.48	-14.44	-32.32	-19.49	-14.88	-20.34	-31.34	-20.50	-6.68
10/21/2007 12:18	-15.10	-20.87	-13.28	-14.65	-32.63	-19.83	-15.33	-20.73	-31.53	-21.00	-6.68
10/21/2007 12:21	-15.56	-21.41	-13.69	-14.88	-33.07	-20.33	-15.77	-20.38	-31.74	-20.41	-6.79
10/21/2007 12:23	-15.20	-21.18	-13.60	-14.77	-32.98	-20.28	-15.65	-20.69	-32.05	-20.41	-6.84
10/21/2007 12:26	-16.02	-22.03	-14.49	-15.53	-33.86	-21.09	-16.46	-21.07	-32.56	-20.41	-7.43
10/21/2007 12:29	-15.70	-21.74	-14.24	-15.15	-33.48	-20.75	-16.08	-20.79	-32.49	-20.41	-7.05
10/21/2007 12:31	-15.63	-21.65	-13.81	-15.22	-33.59	-20.84	-15.99	-20.77	-32.57	-20.92	-6.77
10/21/2007 12:34	-15.51	-21.55	-14.08	-15.11	-33.54	-20.78	-15.96	-21.29	-32.52	-20.88	-6.77
10/21/2007 12:36	-15.59	-21.58	-14.17	-14.77	-33.23	-20.44	-15.56	-20.24	-32.14	-20.88	-6.22
10/21/2007 12:39	-15.35	-21.39	-13.88	-14.56	-33.25	-20.48	-15.57	-20.99	-32.93	-21.35	-6.93
10/21/2007 12:42	-15.50	-21.67	-14.17	-15.23	-33.82	-21.07	-16.19	-20.79	-32.84	-20.86	-6.39
10/21/2007 12:44	-15.68	-22.00	-14.41	-15.27	-34.08	-21.35	-16.36	-20.99	-33.01	-20.88	-6.39
10/21/2007 12:47	-15.90	-22.12	-14.61	-15.52	-34.33	-21.58	-16.65	-21.49	-33.58	-21.50	-7.42
10/21/2007 12:49	-16.23	-22.46	-14.76	-15.61	-34.46	-21.72	-16.72	-21.22	-33.32	-21.13	-7.44
10/21/2007 12:52	-15.97	-22.27	-14.89	-15.53	-34.45	-21.61	-16.69	-20.92	-33.06	-20.89	-7.42
10/21/2007 12:54	-15.80	-22.05	-14.55	-15.44	-34.45	-21.68	-16.72	-21.09	-33.24	-20.94	-7.42
10/21/2007 12:57	-15.70	-21.94	-14.71	-15.32	-34.43	-22.00	-16.72	-21.25	-33.36	-21.68	-7.46
10/21/2007 13:00	-15.76	-22.07	-14.75	-15.48	-34.59	-21.93	-16.83	-21.30	-33.57	-21.84	-7.33
10/21/2007 13:02	-15.87	-22.28	-14.89	-15.46	-34.50	-21.91	-16.69	-21.27	-33.57	-21.83	-7.50
10/21/2007 13:05	-16.12	-22.47	-15.15	-15.64	-34.86	-22.22	-16.99	-21.57	-33.93	-22.22	-7.71
10/21/2007 13:07	-16.12	-22.48	-15.22	-15.64	-34.99	-22.45	-17.09	-21.59	-33.91	-22.29	-7.59

10/21/2007 13:10	-16.11	-22.53	-15.21	-15.75	-35.13	-22.61	-17.31	-21.62	-34.06	-22.58	-7.67
10/21/2007 13:12	-16.05	-22.51	-15.36	-15.58	-34.98	-22.57	-17.19	-21.84	-34.41	-22.92	-7.82
10/21/2007 13:15	-16.37	-22.87	-15.50	-15.82	-35.39	-22.94	-17.58	-21.18	-33.77	-22.09	-7.07
10/21/2007 13:18	-15.85	-22.36	-15.02	-15.32	-34.80	-22.43	-16.96	-21.07	-33.65	-22.13	-7.09
10/21/2007 13:20	-16.02	-22.68	-15.61	-15.70	-35.27	-23.43	-17.52	-20.95	-33.72	-22.64	-6.78
10/21/2007 13:23	-15.78	-22.67	-15.46	-14.94	-34.75	-23.22	-17.10	-21.10	-34.02	-22.64	-6.88
10/21/2007 13:25	-15.95	-22.97	-16.04	-15.37	-35.33	-24.21	-17.76	-21.44	-34.53	-23.19	-7.14
10/21/2007 13:28	-16.11	-23.38	-16.47	-15.93	-36.18	-25.81	-18.95	-21.46	-34.87	-24.85	-7.25
10/21/2007 13:30	-16.58	-24.47	-18.06	-16.12	-37.05	-27.81	-20.11	-21.95	-35.82	-26.38	-7.78
10/21/2007 13:33	-16.35	-24.59	-18.48	-15.94	-37.17	-28.63	-20.62	-21.96	-36.38	-27.16	-7.91
10/21/2007 13:36	-16.41	-25.25	-19.25	-16.03	-37.74	-30.26	-21.37	-22.00	-37.03	-28.34	-7.91
10/21/2007 13:38	-16.84	-26.05	-20.43	-16.29	-38.37	-31.40	-21.99	-22.30	-37.77	-29.01	-8.11
10/21/2007 13:41	-16.89	-26.38	-21.04	-16.42	-39.01	-32.05	-22.26	-22.24	-38.03	-29.98	-8.15
10/21/2007 13:43	-17.12	-26.92	-21.56	-16.58	-39.48	-32.93	-22.76	-22.49	-38.68	-30.92	-8.46
10/21/2007 13:46	-17.19	-27.22	-22.02	-16.80	-40.01	-33.85	-23.38	-22.58	-39.08	-30.38	-8.72
10/21/2007 13:49	-17.14	-27.33	-22.25	-16.64	-40.03	-34.11	-23.36	-22.56	-39.21	-31.40	-8.72
10/21/2007 13:51	-17.31	-27.66	-22.63	-16.84	-40.38	-34.62	-23.74	-22.71	-39.58	-31.84	-8.64
10/21/2007 13:54	-17.31	-27.75	-22.57	-16.70	-40.44	-34.75	-23.71	-22.51	-39.64	-31.88	-8.91
10/21/2007 13:56	-17.40	-27.92	-23.02	-16.79	-40.62	-35.11	-23.84	-22.93	-40.19	-31.88	-9.39
10/21/2007 13:59	-17.25	-27.90	-23.07	-16.66	-40.59	-35.25	-23.94	-22.61	-40.01	-31.88	-8.84
10/21/2007 14:01	-17.65	-28.40	-23.54	-17.08	-41.23	-36.24	-24.73	-22.65	-40.23	-32.94	-8.99
10/21/2007 14:04	-17.64	-28.64	-24.06	-17.34	-41.73	-37.50	-25.28	-23.24	-41.28	-34.64	-9.54
10/21/2007 14:07	-17.61	-28.85	-24.46	-17.12	-41.86	-38.24	-25.45	-23.23	-41.88	-39.06	-9.54
10/21/2007 14:09	-17.35	-28.83	-24.61	-17.01	-42.00	-38.72	-25.60	-22.90	-41.55	-39.99	-9.24
10/21/2007 14:12	-17.35	-29.21	-25.08	-16.78	-42.13	-39.79	-26.12	-23.05	-42.14	-41.70	-9.61
10/21/2007 14:14	-17.43	-29.97	-26.34	-16.73	-42.86	-42.77	-27.42	-22.98	-43.11	-41.70	-9.55
10/21/2007 14:17	-17.07	-30.65	-27.80	-16.84	-43.90	-45.29	-29.13	-22.78	-43.90	-46.93	-9.81
10/21/2007 14:19	-17.19	-31.21	-28.78	-17.10	-44.74	-47.31	-30.36	-23.19	-45.15	-50.06	-10.36
10/21/2007 14:22	-17.72	-32.78	-31.22	-17.28	-45.93	-50.82	-32.38	-23.00	-46.56	-50.06	-10.36
10/21/2007 14:25	-17.42	-33.12	-32.53	-16.81	-46.32	-52.27	-33.09	-23.18	-47.64	-50.06	-10.75

Appendix 3.4: Slope Displacement Data for Validation Test 4 (Mine name unknown**)**

DATE	P1	P2	P3	P4	P5	P6
2/12/2011 23:39	4.2968	0.0059	1.6728	-0.6902	-2.5116	-1.5201
2/12/2011 23:47	4.8334	-0.3407	1.5639	-0.6	-2.2114	-1.2804
2/12/2011 23:54	4.6871	-0.4098	1.3835	-0.2783	-1.9024	-0.712
2/13/2011 0:02	4.9998	-1.0425	1.3036	-0.1188	-2.0675	-0.7068
2/13/2011 0:09	4.8389	-1.2918	0.9626	-0.2521	-1.9599	-1.345
2/13/2011 0:17	4.7439	-1.013	0.7815	-0.3695	-2.8145	-1.7062
2/13/2011 0:24	4.8187	-1.3506	0.6542	-0.4622	-2.6521	-1.6553
2/13/2011 0:32	4.6332	-1.1608	0.4746	-0.3991	-3.1676	-2.3929
2/13/2011 0:39	4.4779	-1.6379	0.3379	-0.5895	-3.0778	-2.6281
2/13/2011 0:47	4.5249	-1.9236	0.2192	-0.5408	-3.1937	-2.7386
2/13/2011 0:54	4.5111	-1.8163	0.2095	-0.5027	-3.4756	-2.9962
2/13/2011 1:02	4.4232	-1.8398	0.1584	-0.5188	-3.9664	-3.4799
2/13/2011 1:09	4.2124	-2.0795	0.2154	-0.6867	-3.9894	-3.7266
2/13/2011 1:17	4.3934	-2.1421	0.0092	-0.6443	-4.0076	-3.9096
2/13/2011 1:24	4.3552	-2.1904	-0.0855	-0.7464	-4.1913	-4.9852
2/13/2011 1:32	4.3768	-1.9589	-0.2193	-0.7584	-4.1385	-5.9869
2/13/2011 1:39	4.2995	-2.1283	-0.4198	-0.9059	-5.1506	-6.3402
2/13/2011 1:47	4.385	-2.1322	-0.5562	-0.8493	-5.8107	-6.5464
2/13/2011 1:54	4.3755	-2.2464	-0.6108	-0.892	-5.6146	-6.6365
2/13/2011 2:02	4.2604	-2.3567	-0.7809	-0.9664	-6.4453	-7.7507
2/13/2011 2:09	4.2705	-2.2207	-0.7373	-0.913	-6.878	-8.6046
2/13/2011 2:17	4.173	-2.3065	-0.9005	-1.0775	-7.2695	-8.853
2/13/2011 2:24	4.1525	-2.2484	-0.9591	-1.039	-7.9508	-9.0344
2/13/2011 2:31	4.0644	-2.3102	-0.9807	-1.1371	-7.9754	-9.2354
2/13/2011 2:39	4.0134	-2.4871	-1.1353	-1.262	-7.756	-9.7705
2/13/2011 2:46	4.0865	-2.3252	-1.0525	-1.1845	-7.624	-10.2151
2/13/2011 2:54	4.0492	-2.352	-1.1475	-1.2481	-6.2066	-10.1969
2/13/2011 3:01	4.0855	-2.3214	-1.1809	-1.2036	-6.3304	-11.0684
2/13/2011 3:09	4.0169	-2.44	-1.2517	-1.3145	-7.0972	-12.0763
2/13/2011 3:16	4.0779	-2.3786	-1.3069	-1.2938	-7.9931	-13.5243
2/13/2011 3:24	3.9212	-2.5084	-1.4195	-1.3965	-8.7122	-12.9437
2/13/2011 3:31	3.9608	-2.4895	-1.4191	-1.3958	-9.2586	-13.377
2/13/2011 3:39	3.9972	-2.8492	-1.4854	-1.4281	-10.3528	-14.0547
2/13/2011 3:46	3.9674	-2.808	-1.5265	-1.4265	-10.4475	-15.1883
2/13/2011 3:54	3.9183	-2.8055	-1.5274	-1.4381	-10.5155	-16.1104
2/13/2011 4:01	3.9688	-2.7442	-1.5728	-1.5023	-10.3786	-16.3161
2/13/2011 4:09	3.8825	-2.842	-1.6407	-1.5635	-10.2812	-16.552
2/13/2011 4:16	3.8567	-2.9601	-1.7986	-1.7114	-10.1142	-16.4725
2/13/2011 4:24	3.856	-2.8724	-1.6665	-1.5473	-9.9197	-16.8526
2/13/2011 4:31	3.7087	-3.0769	-1.8858	-1.8428	-10.2029	-17.6726
2/13/2011 4:39	3.9931	-2.8404	-1.6916	-1.5545	-10.0294	-17.9837
2/13/2011 4:46	3.7629	-3.0623	-1.8922	-1.7557	-10.2669	-18.0243

2/13/2011 4:54	3.6553	-3.1309	-1.9783	-1.849	-10.2336	-18.0552
2/13/2011 5:01	3.7917	-3.0125	-1.9263	-1.758	-10.3237	-18.3343
2/13/2011 5:08	3.6812	-3.0616	-2.0774	-1.9486	-10.3833	-18.6801
2/13/2011 5:16	3.733	-3.0161	-2.0825	-1.8412	-10.4151	-18.8246
2/13/2011 5:23	3.7335	-3.019	-2.1064	-1.8802	-10.507	-19.5401
2/13/2011 5:31	3.6933	-2.994	-2.1167	-1.894	-10.5904	-20.1533
2/13/2011 5:38	3.6445	-2.9971	-2.287	-2.0088	-10.7109	-20.6405
2/13/2011 5:46	3.4906	-3.2314	-2.4873	-2.2446	-10.9487	-21.1542
2/13/2011 5:53	3.55	-3.2098	-2.3986	-2.1856	-10.8941	-21.4074
2/13/2011 6:01	3.7348	-3.0414	-2.3748	-2.0704	-10.8857	-21.8377
2/13/2011 6:08	3.5944	-3.1836	-2.4594	-2.1927	-10.8364	-22.2829
2/13/2011 6:16	3.6938	-3.0965	-2.4515	-2.1135	-10.8275	-22.4484
2/13/2011 6:23	3.5553	-3.2695	-2.6164	-2.2781	-11.0139	-23.1563
2/13/2011 6:31	3.6276	-3.2802	-2.7182	-2.2947	-11.0733	-23.7203
2/13/2011 6:38	3.687	-3.2702	-2.485	-2.2209	-10.9119	-23.9681
2/13/2011 6:46	3.6345	-3.3622	-2.5847	-2.1753	-11.019	-25.0235
2/13/2011 6:53	3.6811	-3.355	-2.7131	-2.2595	-11.2802	-25.3979
2/13/2011 7:01	3.7496	-3.5876	-2.7547	-2.3078	-11.5424	-26.078
2/13/2011 7:08	3.5691	-3.5191	-2.7107	-2.3029	-11.7205	-26.1945
2/13/2011 7:16	3.3954	-3.6035	-2.7369	-2.3524	-11.8395	-26.7153
2/13/2011 7:23	3.465	-3.5533	-2.7816	-2.22	-11.9008	-26.9444
2/13/2011 7:30	3.5989	-3.9653	-2.9772	-2.3614	-12.098	-27.9224
2/13/2011 7:38	3.6894	-3.6584	-2.9514	-1.9634	-12.2329	-28.3058
2/13/2011 7:45	3.5287	-3.6392	-2.7976	-2.009	-12.5993	-29.189
2/13/2011 7:53	3.2814	-3.9211	-2.5534	-2.2622	-13.6165	-29.8048
2/13/2011 8:00	3.142	-3.9085	-2.7732	-2.1734	-15.0581	-31.0637
2/13/2011 8:08	2.8781	-3.874	-2.9302	-2.2143	-15.2004	-34.7923
2/13/2011 8:15	3.0683	-3.9313	-3.0238	-2.2306	-15.7538	-36.3951
2/13/2011 8:23	2.5457	-4.2385	-3.2308	-2.3089	-15.5183	-37.5783
2/13/2011 8:30	1.8585	-4.2442	-3.692	-2.2317	-18.6408	-42.4103
2/13/2011 8:38	2.6234	-3.7707	-3.5882	-2.3253	-19.4257	-44.2451

APPENDIX 4

Slope Failure Prediction Model (SFPM)

(Saved as SFPM on the attached compact disc)